eCAM Evidence-Based Complementary and Alternative Medicine

Medicinal Plants and Natural Active Compounds for Diabetes and/or Obesity Treatment

Guest Editors: Hilal Zaid, Bashar Saad, Abbas A. Mahdi, Akhilesh K. Tamrakar, Pierre S. Haddad, and Fatma U. Afifi

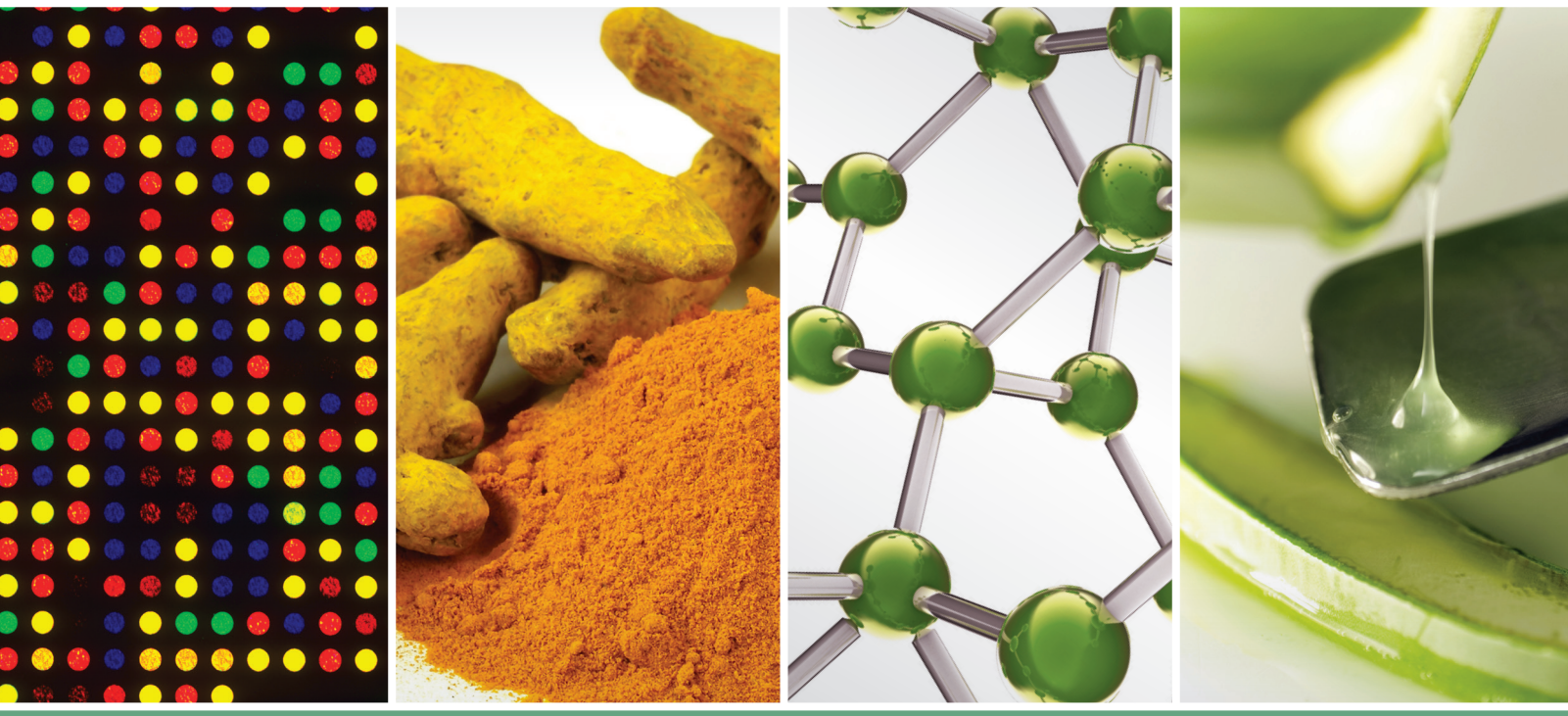

Medicinal Plants and Natural Active Compounds for Diabetes and/or Obesity Treatment

Evidence-Based Complementary and Alternative Medicine

Medicinal Plants and Natural Active Compounds for Diabetes and/or Obesity Treatment

Guest Editors: Hilal Zaid, Bashar Saad, Abbas A. Mahdi, Akhilesh K. Tamrakar, Pierre S. Haddad, and Fatma U. Afifi

Editorial Board

Contents

Hindawi Publishing Corporation
Evidence-Based Complementary and Alternative Medicine
Volume 2015, Article ID 469762, 2 pages
http://dx.doi.org/10.1155/2015/469762

Editorial

Medicinal Plants and Natural Active Compounds for Diabetes and/or Obesity Treatment

Hilal Zaid,[1,2] Bashar Saad,[1,2] Abbas A. Mahdi,[3] Akhilesh K. Tamrakar,[4] Pierre S. Haddad,[5] and Fatma U. Afifi[6]

[1]*Qasemi Research Center, Al-Qasemi Academy, P.O. Box 124, 30100 Baqa El-Gharbia, Israel*
[2]*Faculty of Arts and Sciences, Arab American University-Jenin, P.O. Box 240, Jenin, State of Palestine*
[3]*Department of Biochemistry, King George's Medical University, Lucknow 226003, India*
[4]*Division of Biochemistry, CSIR-Central Drug Research Institute, Lucknow 226031, India*
[5]*Department of Pharmacology, University of Montreal, Montreal, QC, Canada H3C 3J7*
[6]*Faculty of Pharmacy, University of Jordan, Amman 11942, Jordan*

Correspondence should be addressed to Hilal Zaid; hilal.zaid@aauj.edu

Received 7 October 2015; Accepted 8 October 2015

Diabetes has been recognized since ancient times, and its main symptoms were known by the increased thirst, frequent urination, and tiredness. Obesity is one of the major risk factors for a number of chronic diseases, especially type 2 diabetes (T2D), leading to increase in healthcare costs and decrease in life expectancy. Free fatty acids (FFA) represent a crucial link between obesity, inflammation, and insulin resistance and, as such, reduction in elevated plasma FFA should be an important therapeutic target in obesity and T2D. According to the World Health Organization (WHO), 35% of adults aged 20 and over were overweight in 2008, and 11% were obese. Moreover, T2D prevalence has increased from less than 10% in 1980 to more than 30% nowadays [1].

There are several types of glucose-lowering drugs [2], including insulin sensitizers (biguanides, metformin, and thiazolidinediones), insulin secretagogues (sulfonylureas, meglitinides), and α-glucosidase inhibitors (miglitol, acarbose). Most glucose-lowering drugs, however, may have side effects, such as severe hypoglycemia, idiosyncratic liver cell injury, lactic acidosis, permanent neurological deficit, digestive discomfort, headache, and dizziness [3, 4]. As a result, researchers are interested in finding more efficient medicines, with less side effects. Medicinal plant drug discovery provides important leads against various pharmacological targets including T2D and obesity.

With the dramatically increasing prevalence of obesity and T2D worldwide, there is an urgent need for new strategies to combat the growing epidemic of these metabolic diseases. Diet is an essential factor affecting the development of obesity and T2D and it can either prevent or accelerate metabolic diseases. In searching for preventative and therapeutic strategies, it is therefore advantageous to consider the potential of certain medicinal plants as well as herbal-based foods and their bioactive compounds to prevent/treat the pathogenic processes associated with these diseases. To date, the concept of antidiabetic and antiobesity medicinal plants is highlighted in textbooks and pharmaceutical pamphlets and has been reported in thousands of scientific publications. Yet, most of these publications report the activity of a crude extract without testing its chemical composition or identifying the active compound(s) or even its mechanism of action. We believe that natural novel drugs are now more achievable due to modern techniques for separation, structure elucidation, screening, and bio- and chemoinformatics. But whatever approach is used, the medicinal plant efficacy will be based on *in vitro* or *in vivo* bioassays.

This special issue on medicinal plants for the treatment of diabetes and obesity is a bird's eye view on up-to-date knowledge of promising traditional medicines and their active ingredients efficacy and mechanisms of action in treating obesity and T2D. Nine selected papers for publication in the present issue summarize the most recent knowledge and techniques to evaluate the medicinal plants and active compounds for their antidiabetic, antiobesity, and antioxidant

activity *in vitro* and *in vivo*. Manuscripts in this special issue cover several aspects of recent developments in the fields of (a) medicinal plants, buckwheat honey, and natural compounds preventing metabolic disorders (including T2D) *in vivo* and *in vitro*; (b) antioxidant and anti-inflammatory natural products; (c) phenolic compounds that show adipogenesis activity *in vitro*; (d) herbal pharmacotherapy and phytochemical studies *in vitro* and *in situ*; (e) examining the reliability of potential antioxidant substance based on the selected assays; (f) studies involving toxicology and pharmacological mechanisms of action of medicinal plants used *in vivo* and *in vitro*.

Acknowledgments

We are thankful to all contributors of this special issue for their valuable research papers. We are grateful to the reviewers for their constructive criticisms and timely response that made this special issue possible. Our sincere thanks and gratitude go to the Editorial Board of this journal for inviting us to edit this special issue.

Hilal Zaid
Bashar Saad
Abbas A. Mahdi
Akhilesh K. Tamrakar
Pierre S. Haddad
Fatma U. Afifi

References

[1] H. Zaid and B. Saad, "State of the art of diabetes treatment in Greco-Arab and islamic medicine," in *Bioactive Food as Dietary Interventions for Diabetes*, R. R. Watson and V. R. Preedy, Eds., pp. 327–335, Academic Press, San Diego, Calif, USA, 2013.

[2] P. Modi, "Diabetes beyond insulin: review of new drugs for treatment of diabetes mellitus," *Current Drug Discovery Technologies*, vol. 4, no. 1, pp. 39–47, 2007.

[3] Y. Cao and X.-M. Liu, "Should we still be concerned about the potential side effects of glucagon-like peptide-1 receptor agonists on thyroid C cells?" *Endocrine*, vol. 48, no. 1, pp. 47–52, 2015.

[4] J. Neustadt and S. R. Pieczenik, "Medication-induced mitochondrial damage and disease," *Molecular Nutrition and Food Research*, vol. 52, no. 7, pp. 780–788, 2008.

Hindawi Publishing Corporation
Evidence-Based Complementary and Alternative Medicine
Volume 2015, Article ID 987385, 10 pages
http://dx.doi.org/10.1155/2015/987385

Research Article

Buckwheat Honey Attenuates Carbon Tetrachloride-Induced Liver and DNA Damage in Mice

Ni Cheng,[1,2] Liming Wu,[3] Jianbin Zheng,[2] and Wei Cao[1,2]

[1] *Department of Food Science and Engineering, School of Chemical Engineering, Northwest University, 229 North TaiBai Road, Xi'an 710069, China*
[2] *Shaanxi Provincial Key Lab of Electroanalytical Chemistry, Institute of Analytical Science, Northwest University, 229 North TaiBai Road, Xi'an 710069, China*
[3] *Institute of Apicultural Research, Chinese Academy of Agricultural Science, Beijing 100093, China*

Correspondence should be addressed to Jianbin Zheng; zhengjb@nwu.edu.cn and Wei Cao; caowei@nwu.edu.cn

Received 1 March 2015; Revised 14 May 2015; Accepted 4 June 2015

Academic Editor: Abbas A. Mahdi

Buckwheat honey, which is widely consumed in China, has a characteristic dark color. The objective of this study was to investigate the protective effects of buckwheat honey on liver and DNA damage induced by carbon tetrachloride in mice. The results revealed that buckwheat honey had high total phenolic content, and rutin, hesperetin, and *p*-coumaric acid were the main phenolic compounds present. Buckwheat honey possesses super DPPH radical scavenging activity and strong ferric reducing antioxidant power. Administration of buckwheat honey for 10 weeks significantly inhibited serum lipoprotein oxidation and increased serum oxygen radical absorbance capacity. Moreover, buckwheat honey significantly inhibited aspartate aminotransferase and alanine aminotransferase activities, which are enhanced by carbon tetrachloride. Hepatic malondialdehyde decreased and hepatic antioxidant enzymes (superoxide dismutase and glutathione peroxidase) increased in the presence of buckwheat honey. In a comet assay, lymphocyte DNA damage induced by carbon tetrachloride was significantly inhibited by buckwheat honey. Therefore, buckwheat honey has a hepatoprotective effect and inhibits DNA damage, activities that are primarily attributable to its high antioxidant capacity.

1. Introduction

The liver plays important roles in metabolism, secretion, excretion, and biotransformation. In China, where liver disease is common, there are approximately 130 million individuals with hepatitis B virus, which may contribute to chronic hepatitis, cirrhosis, or liver cancer. Therefore, there has been an increasing interest in the treatment and prevention of liver disease. Oxidative stress, which is involved in the pathogenesis of liver diseases, leads to hepatic damage [1]. Antioxidants such as silymarin, tocopherol, and betaine have desirable effects in patients with liver disease [2–4].

Carbon tetrachloride (CCl_4) is one of the most widely used toxins for the experimental induction of liver damage in laboratory animals. The hepatotoxicity of CCl_4 stems from reductive dehalogenation products, such as trichloromethyl ($CCl_3^{\bullet}$) and trichloromethyl peroxyl ($CCl_3O_2^{\bullet}$) radicals [5], which can bind to proteins and lipids or remove a hydrogen atom from an unsaturated lipid, thereby initiating lipid peroxidation and contributing to liver damage [6]. In recent years, numerous studies have shown that polyphenol extract from natural products with high scavenging radical activity and strong reducing power could attenuate CCl_4-induced liver damage [7–9]. Our previous studies have also proven that bee pollen extract rich in phenolic compounds increases antioxidant potential in mice and protects against CCl_4-induced liver damage [10].

Buckwheat (*Fagopyrum esculentum* Moench), which is cultivated in several Asian and European counties, is an important source of nectar and pollen for bees. Buckwheat honey has a characteristic dark color and its antioxidant activity has been studied for more than 10 years. Pasini et al. [11] reported that there are 20 phenolic acids in buckwheat honey, including *p*-hydroxybenzoic and *p*-coumaric acids.

Phenolic antioxidants from buckwheat honey are bioavailable and increase the antioxidant activity of plasma. Gheldof et al. [12] reported that the serum antioxidant capacity determined by oxygen radical absorbance capacity (ORAC) was significantly increased following the consumption of buckwheat honey in water. However, *in vitro* serum lipoprotein oxidation and thiobarbituric acid reactive substances (TBARS) were not significantly affected following a single consumption of buckwheat honey. Therefore, long-term studies on oxidative stress-induced illnesses are necessary to investigate whether buckwheat honey has antioxidant-related health benefits. In this study, we assessed the antioxidant capacity of buckwheat honey in mice and evaluated its protection potential for attenuating CCl_4-induced liver and DNA damage.

2. Materials and Methods

2.1. Materials. Buckwheat honey was obtained from Shaanxi Bee Master Co., Ltd. (Xi'an, China). The pollen frequency (*Fagopyrum esculentum*) was approximately 61%. Buckwheat honey samples were stored at 4°C.

2.2. Chemicals and Reagents. Fluorescein disodium (FL), 1,1-diphenyl-2-picrylhydrazyl radical 2,2-diphenyl-1-(2,4,6-trinitrophenyl)hydrazyl (DPPH), 2,2′-azobis(2-amidinopropane)dihydrochloride (AAPH), dimethyl sulfoxide (DMSO), Trolox, and silymarin were obtained from Sigma-Aldrich (Steinheim, Germany). Agarose was purchased from BioRad (Hercules, CA, USA). Diagnostic kits for aspartate aminotransferase (AST), alanine aminotransferase (ALT), malondialdehyde (MDA), superoxide dismutase (SOD), glutathione peroxidase (GSH-Px), and protein were obtained from Nanjing Jiancheng Bioengineering Institute (Nanjing, China). Lymphocyte separation medium was purchased from Tianjin Hao Yang Biological Manufacture Co., Ltd. CCl_4, peanut oil, and other chemicals were acquired from Tianjin Kemiou Chemical Reagent Co. (Tianjin, China).

2.3. Antioxidant Assays

2.3.1. Total Phenolic Content (TPC) and HPLC Analysis. We used a modified Folin-Ciocalteu method to determine TPC in buckwheat honey [13]. Briefly, 0.2 mg of buckwheat honey was mixed with 1.0 mL of Folin-Ciocalteu reagent, allowed to stand at room temperature for 5 min, and mixed with 5 mL of 1 M Na_2CO_3. An hour later, absorbance was measured at 760 nm. TPC was expressed as the gallic acid equivalents per gram of buckwheat honey (mg GA/g).

The contents of individual phenols in buckwheat honey were estimated by HPLC-DAD analysis as proposed by Liang et al. [14]. An Agilent 1100 HPLC system (Agilent Technologies Deutschland, Waldbronn) equipped with a vacuum degasser, a quaternary solvent delivery pump, a manual chromatographic valve, a thermostated column compartment, and a diode-array detector (Agilent, Palo Alto, CA, USA) was used. The column was a Zorbax SB-C18 column (150 mm × 4.6 mm, 5.0 μm). The mobile phase adopted was methanol (A) and 0.15% aqueous acetic acid solution (B) (v/v) using a linear gradient elution of 5–15% A at 0–10 min, 15–35% A at 10–15 min, 35–55% A at 15–20 min, 55–65% A at 20–25 min, 65–80% A at 25–30 min, and 80% A at 30–35 min. The injected volume was 5 μL, and flow rate was 1.0 mL/min. The column was operated at 30°C. The diode-array detector was performed at 360 nm.

2.3.2. DPPH Radical Scavenging Activity. DPPH radical scavenging activity of buckwheat honey was assessed according to the method proposed by Wang et al. [15]. Briefly, different volumes of buckwheat honey (0.2 g/mL) were mixed with 4.0 mL of 0.1 mM DPPH radical solution. After adjusting the total volume to 10 mL, the mixture was mixed well and allowed to stand at room temperature for 30 min in the dark. Absorbance was measured at 517 nm. The DPPH radical scavenging activity was expressed as Trolox equivalents per gram of buckwheat honey (mg Trolox/g).

2.3.3. Ferrous Ion-Chelating Activity. The ferrous ion-chelating activity of buckwheat honey was measured by the method reported by Singh and Rajini with some modifications [16]. In this experiment, 50 μL of buckwheat honey (0.2 g/mL) was mixed with 50 μL of 1 mM iron vitriol and 20 μL of 1 mM ferrozine. The total volume was adjusted to 1 mL with methanol and incubated at room temperature for 10 min. The absorbance of the ferrozine-Fe^{2+} complex was measured at 562 nm. Ferrous ion-chelating activity was expressed as Na_2EDTA equivalents per gram of buckwheat honey (mg Na_2EDTA/g).

2.3.4. Ferric Reducing Antioxidant Power (FRAP). FRAP of buckwheat honey was assessed by the method reported by Benzie and Strain [17]. Buckwheat honey (0.3 mL at 0.2 mg/mL) was mixed with 4.0 mL of FRAP reagent (2.5 mL of 10 mM TPTZ solution in 40 mM HCl with 2.5 mL of 20 mM $FeCl_3$; 25 mL of 0.3 M acetate buffer, pH 3.6), mixed well and incubated at 37°C for 4 min. Absorbance was measured at 593 nm. FRAP was expressed as Trolox equivalents per gram of buckwheat honey (mg Trolox/g).

2.3.5. Animals and Study Design

(1) Animals. Male Kunming mice (18–22 g) were obtained from Xi'an Jiaotong University and housed in cages with six mice per cage. The animal ethical approval communication number is SCXK 2012-003. The animal experiments followed the guidelines and regulations of the State Committee of Science and Technology of the People's Republic of China.

After acclimatization to laboratory conditions for 7 d, the mice were randomly divided into four groups (12 mice/group). Control mice and CCl_4-treated mice were administered distilled water via gavage at 0.22 mL/10 g BW, twice daily for 10 weeks. According to the doses of honey and silymarin reported by Cheng et al. [18], the mice were administered 0.22 g/10 g BW of buckwheat honey and 0.5 mg/10 g BW of silymarin via gavage twice daily for 10 weeks. To investigate the serum antioxidant capacity after administration of buckwheat honey, the mice in the control

and honey groups were bled by cardiac puncture 2 h after the last administration. The blood samples were centrifuged at 3000 rpm for 15 min to obtain serum. The serum was used for serum lipoprotein oxidation and ORAC assays.

To investigate the protective effects of buckwheat honey on CCl_4-induced liver damage, all mice were continuously intragastrically administered distilled water, buckwheat honey, and silymarin for the next week. Two hours following the last administration, all mice (except control mice) were administered a CCl_4/peanut oil mixture (0.2 : 100, intraperitoneally, 0.1 mL/10 g BW); control mice received only peanut oil. Subsequently, the animals were fasted for 16 h and bled by cardiac puncture. Half of the blood samples were transferred to anticoagulant tubes for separating lymphocytes, and the other half were transferred to ordinary centrifuge tubes for serum collection.

(2) Serum Lipoprotein Oxidation. Serum lipoprotein oxidation was assessed by the method reported by Regnström et al. [19]. Serum samples from control and honey groups were diluted with phosphate buffer (10.1 mM Na_2HPO_4, 1.8 Mm KH_2PO_4, 27 mM KCl, and 138 mM NaCl) to 0.5%. Copper ions at 12 μmol/L were added to the diluted serum samples. Oxidation kinetics was determined at 234 nm every 20 minutes at 37°C. Diluted serum samples without copper were used as blanks. The area under the oxidation curve (AUC) was plotted and the percentage inhibition of serum lipoprotein oxidation was calculated according to the following equation:

$$\text{Inhibition (\%)} = \frac{\left(\text{AUC}_{\text{control}} - \text{AUC}_{\text{honey}}\right)}{\text{AUC}_{\text{control}}} \times 100, \quad (1)$$

where $\text{AUC}_{\text{control}}$ is the area under the oxidation curve for the control group serum samples and $\text{AUC}_{\text{honey}}$ is the area under the oxidation curve for the honey group serum samples.

(3) ORAC Assay. The ORAC assay was performed in 96-well plates and measured in a multifunctional plate reader (Infinite M200Pro, Switzerland) [20]. Serum samples from the control and honey groups were used in this assay. Analyses were performed in 75 mM sodium phosphate buffer (pH = 7.4) at 37°C. The excitation wavelength was 485 nm and the emission wavelength was 535 nm. FL was used as the substrate and AAPH was used for the production of peroxyl radicals. Briefly, 50 μL of 78 nM FL and 50 μL of 1% serum were transferred to 96-well plates. The blank consisted of 50 μL of phosphate buffer instead of serum. The mixture was preincubated at 37°C for 30 min before rapidly adding 25 μL of 221 mM AAPH solution. The plate was automatically shaken prior to each reading. Fluorescence was measured every 5 minutes. The assay was performed in triplicate, and the results were expressed as inhibition of the area under the curve (AUC) according to the following equation:

$$\text{Inhibition (\%)} = \frac{\left(\text{net AUC}_{\text{honey}} - \text{net AUC}_{\text{control}}\right)}{\text{net AUC}_{\text{control}}} \times 100, \quad (2)$$

where net $\text{AUC}_{\text{control}}$ = $\text{AUC}_{\text{control}}$ − $\text{AUC}_{\text{blank}}$; net $\text{AUC}_{\text{honey}}$ = $\text{AUC}_{\text{honey}}$ − $\text{AUC}_{\text{blank}}$.

(4) Comet Assay. The comet assay is the preferred technique for detecting DNA damage in single cells. In this study, lymphocytes isolated from control mice, CCl_4-treated mice, and honey mice were analyzed by the comet assay to assess the protective effects of buckwheat honey on CCl_4-induced DNA damage. Lymphocytes from silymarin mice were set as the positive reference. Following the methods proposed by Singh et al. [21] with slight modifications, lymphocytes were suspended in 0.15 M of phosphate buffer (pH 7.4) at a density of 1×10^5/mL. After fixing the lymphocytes on slides, the slides were immersed in lysis buffer (2.5 M NaCl, 100 mM EDTA, 1% N-lauroylsarcosine at pH 10, 10 mM Tris-HCl, 1% Triton X-100, and 10% dimethyl sulfoxide (DMSO)) for 2 h. Subsequently, the slides were immersed in electrophoresis buffer (1 mM EDTA and 300 mM NaOH, pH 13) for DNA unwinding. After 30 min, electrophoresis was run at 25 V (300 mA) for 20 min in the dark. All slides were treated with ethidium bromide and observed under a fluorescence microscope (Nikon 027012; Nikon, Tokyo, Japan). The results were scored and analyzed using an automated analysis system of the Comet Assay Software Project (CASP). At least 50 cells were scored from each slide. The degree of DNA damage was scored by determining the percentage of DNA in the tail (tail DNA %) and olive tail moment (OTM), defined as the fraction of tail DNA multiplied by the distance between the means of the head and tail:

$$\begin{aligned} \text{tail DNA\%} &= \left(\frac{\text{tail DNA}}{(\text{head DNA} + \text{tail DNA})}\right) \times 100, \\ \text{OTM} &= (\text{tail DNA\%}) \\ &\quad \times (\text{tail mean} - \text{head mean}). \end{aligned} \quad (3)$$

(5) Assessment of Liver Function. Serum was obtained following the centrifugation of blood samples at room temperature for 20 min at 3,000 rpm. Serum ALT and AST values were measured using commercially available diagnostic kits.

(6) Determination of MDA, SOD, and GSH-Px Activities. After the animals were sacrificed, livers were immediately excised. With the exception of a portion of the left lobe to be used for histopathological examination, the livers were homogenized in phosphate buffer (50 mM, pH 7.4) and centrifuged at 2,500 rpm for 20 min at 4°C. The MDA content, SOD, and GSH-Px activities along with protein levels in the supernatant were estimated according to commercially available diagnostic kits.

(7) Histopathological Examinations. A left lobe portion of the liver was incubated for 24 h in 10% neutral formalin solution. Based on standard procedures, we obtained 5 μm sections for histopathological studies using hematoxylin and eosin (H&E) staining.

2.4. Statistical Analysis. We analyzed the data in triplicate using SAS software version 8.1 (SAS Institute, Cary, NC,

Table 1: Phenolic compounds (mg/kg) and TPC (mg GA/g) of buckwheat honeys.

Phenolic compounds	Concentration
Gallic acid	2.02 ± 0.52
Protocatechuic acid	1.09 ± 0.34
Chlorogenic acid	0.56 ± 0.07
p-Coumaric acid	12.52 ± 1.92
Rutin	35.94 ± 3.76
Quercetin	1.97 ± 0.09
Hesperetin	23.76 ± 0.31
Galangin	2.38 ± 0.18
TPC	2.039 ± 0.03

Results presented in the table are expressed as means ± standard deviation (SD) for 3 replications.

Table 2: Antioxidant activities of buckwheat honey *in vitro*.

Antioxidant index	Results
DPPH radical scavenging activity	0.304 ± 0.02 (mg Trolox/g)
Ferrous ion-chelating activity	0.479 ± 0.01 (mg Na_2EDTA/g)
Ferric reducing antioxidant power	0.355 ± 0.05 (mg Trolox/g)

The results presented in the table were expressed as the mean values ± standard deviation (SD) for 3 replications.

USA). Tukey's posttest was used to assess statistical significance (P value < 0.05).

3. Results

3.1. Antioxidant Assay of Buckwheat Honey. To study the antioxidant activity, the TPC and individual phenolic compounds of buckwheat honey were determined, and the results are shown in Table 1 and Figure 1. The TPC of buckwheat honey was 2.04 mg GA/g. Four phenolic acids and four flavones were identified in buckwheat honey. Rutin, the most abundant phenolic compound, was measured at 35.94 mg/kg, followed by hesperetin (23.76 mg/kg) and *p*-coumaric acid (12.52 mg/kg).

The results of antioxidant activities of buckwheat honey *in vitro* are shown in Table 2. The DPPH radical scavenging activity is a widely used method to evaluate antioxidant capacity. The DPPH radical scavenging activity of buckwheat honey was 0.304 mg Trolox/g. The ferrous ion-chelating activity of buckwheat honey was 0.479 mg Na_2EDTA/g. The FRAP assay is often used to determine the antioxidant properties of foods based on their electron-donating capacity [22]. As shown in Table 2, the FRAP value of buckwheat honey was 0.355 mg Trolox/g, which is comparable to the values obtained in jujube honey, but lower than those obtained in cacao farm honey, mangrove honey, citrus honey, and a coconut grove honey in Mexico (48–152 mg Trolox/100 g) [23].

3.2. Buckwheat Honey Increased Serum Antioxidant Capacity in Mice. The administration of buckwheat honey (0.22 g/10 g BW, twice daily) for 10 weeks resulted in the inhibition

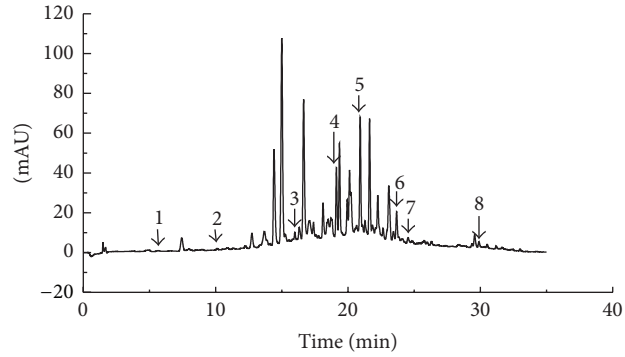

Figure 1: Chromatogram of the buckwheat honey using HPLC-DAD. Peaks: 1 = gallic acid; 2 = protocatechuic acid; 3 = chlorogenic acid; 4 = *p*-coumaric acid; 5 = rutin; 6 = quercetin; 7 = hesperetin; 8 = galangin.

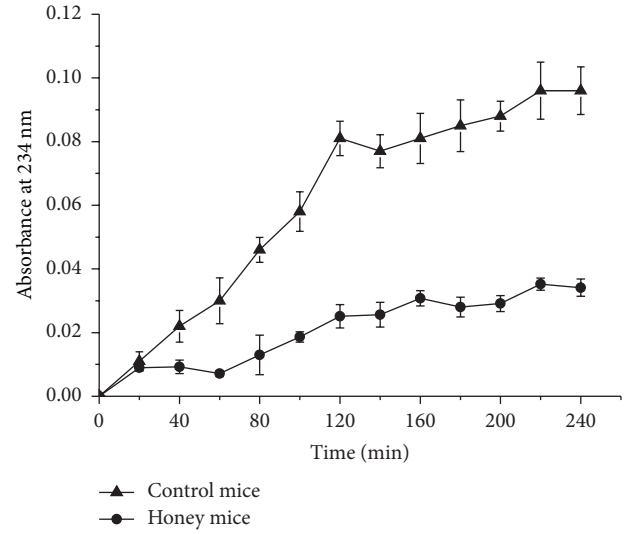

Figure 2: Effects of buckwheat honey on serum lipoprotein oxidation (absorbance values had been adjusted for the initial absorbance reading). Control mice were administered distilled water via gavage. Honey mice were administered buckwheat honey (0.22 g/10 g BW, twice daily for 10 weeks) via gavage.

of serum lipoprotein oxidation. Buckwheat honey inhibited serum lipoprotein oxidation by 65.71% (Figure 2). Serum ORAC is another method for measuring serum antioxidant capacity. As described in Figure 3, serum from honey-treated mice had a relatively high ORAC value, whereas serum from control mice had a relatively low ORAC value (27.19% lower than the former).

3.3. Buckwheat Honey Attenuated DNA Damage Induced by Carbon Tetrachloride. The protective effect of buckwheat honey on CCl_4-induced damage is shown in Figure 4. Based on the picture of lymphocytes in the CCl_4-treated group, a significant increase in the tail length of comet was observed. However, the lymphocyte from the mice administered honey and silymarin showed a similar decrease in the tail length of

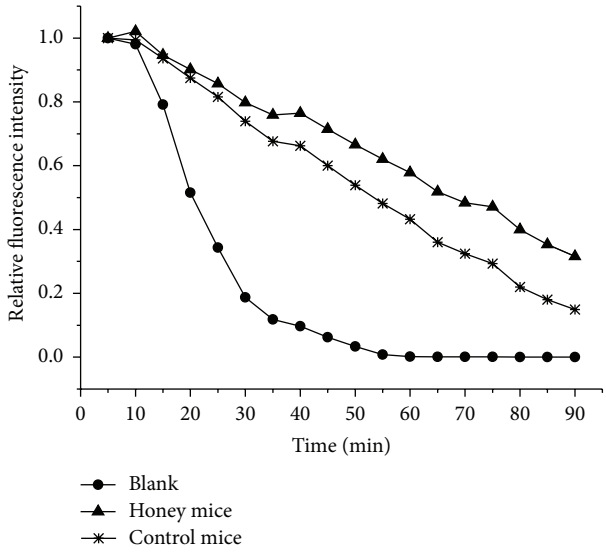

Figure 3: Effects of buckwheat honey on serum oxygen radical absorbance capacity (ORAC). Control mice were administered distilled water via gavage. Honey mice were administered buckwheat honey (0.22 g/10 g BW, twice daily for 10 weeks) via gavage. In the blank, PBS was used instead of serum.

comet. As shown in Figures 4(b) and 4(c), a similar variation was presented in mean tail DNA and OTM. The mean tail DNA and OTM in the CCl_4-treated group were 30.91% and 53.03%, respectively, whereas the mean tail DNA and OTM in the control group were 11.76% and 5.21%, respectively. Therefore, significant increases in the mean tail DNA and OTM of lymphocytes were associated with CCl_4 exposure ($P < 0.05$). Interestingly, pretreatment with buckwheat honey (0.22 g/10 g BW, twice daily) for 11 weeks decreased lymphocyte damage significantly ($P < 0.05$). Silymarin, as a positive reference, had super protective effect on DNA damage induced by CCl_4.

3.4. Buckwheat Honey Protected the Liver from Carbon Tetrachloride-Induced Damage. Serum ALT and AST activities were determined in this study and the results are shown in Figure 5. In the CCl_4-treated group, serum ALT and AST activities were 170.68 and 55.01 U/L, which were 15x and 1.52x higher than those of the control group, respectively ($P < 0.05$). In the honey and silymarin groups, serum ALT and AST activities were 11.12 and 27.77 U/L and 12.43 and 25.96 U/L, respectively. There were no significant differences in the hepatic enzyme activities between the control, honey, and silymarin groups. Therefore, buckwheat honey treatment (0.22 g/10 g BW, twice daily) for 11 weeks inhibited an increase in serum ALT and AST activity.

Hepatic MDA levels and GSH-Px and SOD activities were monitored in this study and the results are shown in Figure 6. A 54.90% increase of hepatic MDA was obtained in the CCl_4-treated group relative to the control mice. Pretreatment with buckwheat honey (0.22 g/10 g BW, twice daily) and silymarin (0.5 mg/10 g BW, twice daily) for 11 weeks significantly decreased hepatic MDA levels in the CCl_4-treated mice ($P < 0.05$) (Figure 6(a)). The activities of GSH-Px and SOD in CCl_4-treated mice decreased significantly compared to the control mice ($P < 0.05$; Figure 6(b)). Interestingly, pretreatment with buckwheat honey and silymarin significantly inhibited the decrease in GSH-Px and SOD activities induced by CCl_4 ($P < 0.05$).

The histological observations supported the results obtained from the enzyme assays. Liver sections from control mice showed regular cellular morphology (Figure 7(a)). However, liver sections from CCl_4-treated mice revealed extensive liver damage characterized by severe hepatocellular hydropic degeneration and necrosis around the central vein, dilated sinusoidal spaces, inflammatory cell infiltration, and ballooning degeneration (Figure 7(b)). Surprisingly, pretreatment with buckwheat honey remarkably ameliorated the hypertrophy of hepatocytes, inflammatory cell infiltration, ballooning degeneration, and dilated sinusoidal spaces (Figure 7(c)). The protective effect of buckwheat honey was similar to silymarin (Figure 7(d)).

4. Discussion

Phenolic compounds are present in plants and food products, including honey. Phenolic compounds possess powerful antioxidant capacity by acting as hydrogen donors to free radicals and as electron donors to metal ions [22]. According to previous studies, phenolic compounds are the main contributor to the antioxidant activity of honey. Moreover, the darker the honey, the stronger its antioxidant capability. Buckwheat honey is deemed the darkest honey in China. Therefore, a higher value of TPC (2.04 mg GA/g) was acquired in this study, which was significantly higher than that of seven honey samples from Slovenia, which ranged from 44.8 mg GA/kg in acacia honey to 241.4 mg GA/kg in fir honey [24]. Because phenolic hydroxyl can donate a hydrogen atom to reduce free radicals [25], the DPPH radical scavenging activity of buckwheat honey was higher than that reported in black locust honey (0.3 mmol Trolox/kg), goldenrod honey (0.2 mmol Trolox/kg), rapeseed honey (0.4 mmol Trolox/kg), and heather honey (0.6 mmol Trolox/kg) [26]. The ferrous ion-chelating activity represents another index of antioxidant activity in bioactive compounds because divalent transition metal ions play important roles in oxidation, such as by contributing to the formation of hydroxyl radicals and hydroperoxides via the Fenton reaction [27]. The ferrous ion-chelating activity of buckwheat honey was 0.479 mg Na_2EDTA/g, approximately 10x higher than that of jujube honey (37.59–53.04 mg Na_2EDTA/kg) [18]. The metal-chelating potential is strongly dependent on the arrangement of hydroxyls and carbonyl groups around the molecule [25]. Flavonoids such as rutin and hesperetin have been identified in buckwheat honey as the main phenolic compounds. Therefore, it is not difficult to understand why buckwheat honey has a high ferrous ion-chelating activity.

To investigate whether buckwheat honey could increase the antioxidant capacity of the mice, Cu^{2+}-induced oxidation of serum lipoprotein was determined. This method provides an indication of diene formation in lipoprotein fatty acids

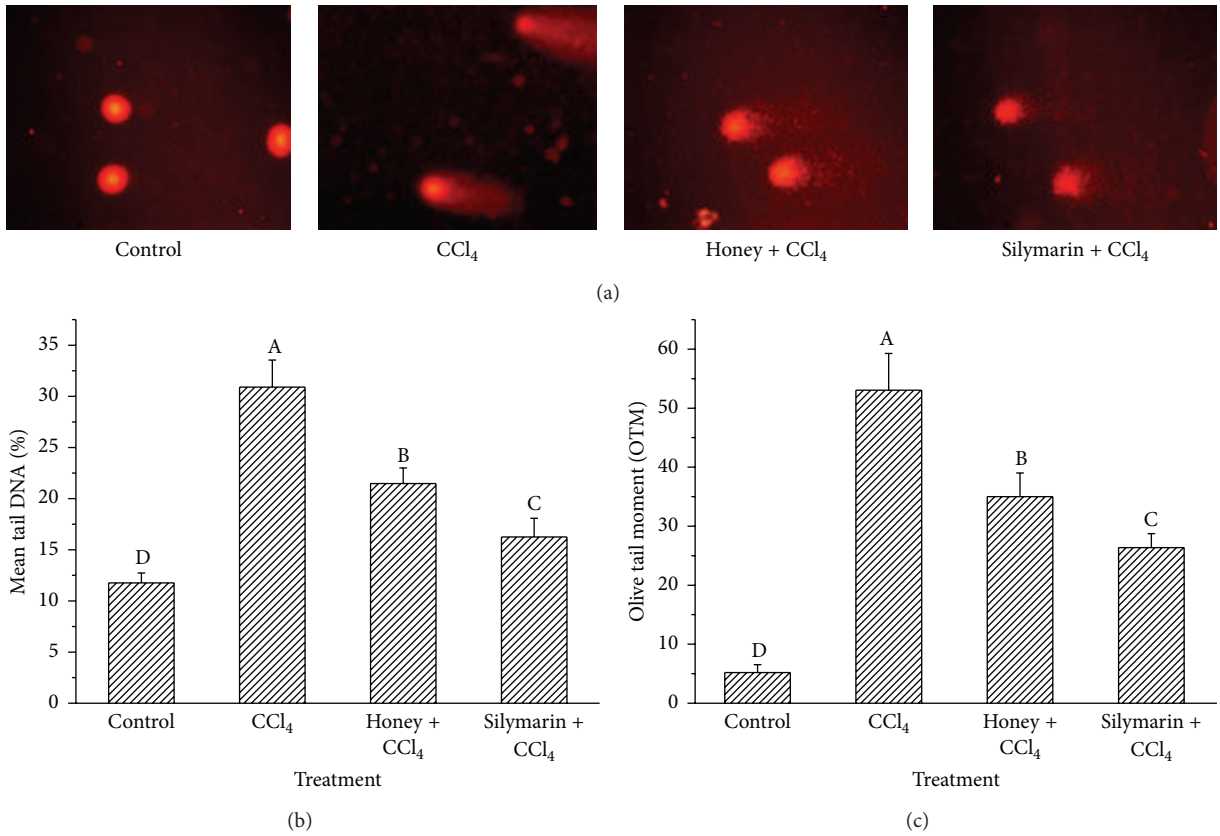

Figure 4: Effects of buckwheat honey on mice lymphocyte DNA damage induced by CCl_4 ((a) picture of lymphocyte DNA damage; (b) mean tail DNA%; (c): olive tail moment). Control: lymphocytes from control mice; CCl_4: lymphocytes from CCl_4-treated mice; honey + CCl_4: lymphocytes from mice administered buckwheat honey (0.22 g/10 g BW) twice daily for 11 weeks prior to CCl_4; silymarin + CCl_4: lymphocytes from mice administered silymarin (0.5 mg/10 g BW) twice daily for 11 weeks prior to CCl_4.

when exposed to Cu^{2+}. Diene formation is assessed by measuring changes in absorbance at 234 nm. High absorbance values correspond to diene formation as a result of serum lipoprotein oxidation, and low absorbance values correspond to inhibition of serum lipoprotein oxidation and, consequently, to high antioxidant activity [28]. The administration of buckwheat honey remarkably inhibited serum lipoprotein oxidation in this study. Phenolic compounds present in buckwheat honey inhibit oxidation of serum lipoproteins by acting as free radical scavengers or as metal-chelating agents [20]. Antioxidants are often added to foods to prevent the radical chain reactions of oxidation, and they act by inhibiting the initiation and propagation step, leading to termination of the reaction and a delay in the oxidation process [25, 29]. Therefore, buckwheat honey significantly inhibited the Cu^{2+}-induced oxidation of serum lipoprotein and increased the antioxidant capacity of mice. Serum ORAC is another method for measuring serum antioxidant capacity. This method, which incorporates FL as the fluorescent probe, is commonly used in biological samples and foods. The ORAC method is based on the inhibition of peroxyl-radical-induced oxidation initiated by the thermal decomposition of AAPH [20]. FL blocks the peroxyl-radical chain reaction process by donating hydrogen protons, thereby reducing the fluorescence intensity. Antioxidants can inhibit the decrease in fluorescence intensity by scavenging AAPH or by donating hydrogen protons, thereby blocking the free radical chain reaction [30]. Accordingly, buckwheat honey administered to mice for 10 weeks at 0.22 g/10 g BW increased the serum antioxidant activity.

Intraperitoneal administration of CCl_4 is a classic method used to induce oxidation and liver damage [7, 8]. Metabolites of CCl_4 include highly reactive free radicals, which initiate the chain reaction of lipid peroxidation, thereby affecting polyunsaturated fatty acids and phospholipids [31]. Lipid peroxidation affects the permeability of the mitochondria, endoplasmic reticulum, and plasma membranes, resulting in leakage of hepatic enzymes in the blood. Serum ALT and AST activities have been confirmed to be the most sensitive indicator of CCl_4-induced liver damage. Therefore, serum ALT and AST activities in the CCl_4-treated group were significantly higher than those of the control group. Interestingly, pretreatment with buckwheat honey inhibited the increase of serum ALT and AST activities induced by CCl_4. With increasing serum ALT and AST activities as a result of CCl_4-induced damage, lipid peroxidation products (e.g., MDA) accumulate in hepatic cells. Therefore, hepatic MDA levels were monitored in this study. As shown in Figure 6(a),

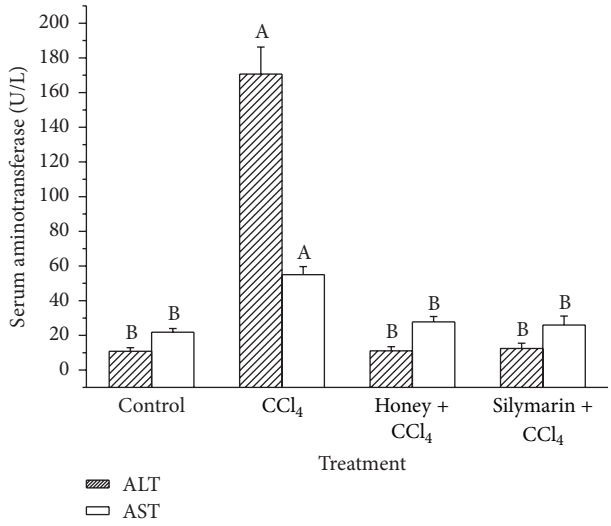

Figure 5: Effects of buckwheat honey on serum ALT and AST activities. Different lower case letters represent significant differences ($P < 0.05$). Mice in "control": distilled water plus peanut oil; mice in "CCl_4": distilled water plus CCl_4; mice in "honey + CCl_4": buckwheat honey (0.22 g/10 g BW) twice daily for 11 weeks plus CCl_4; mice in "silymarin + CCl_4": silymarin (0.5 mg/10 g BW) twice daily for 11 weeks plus CCl_4.

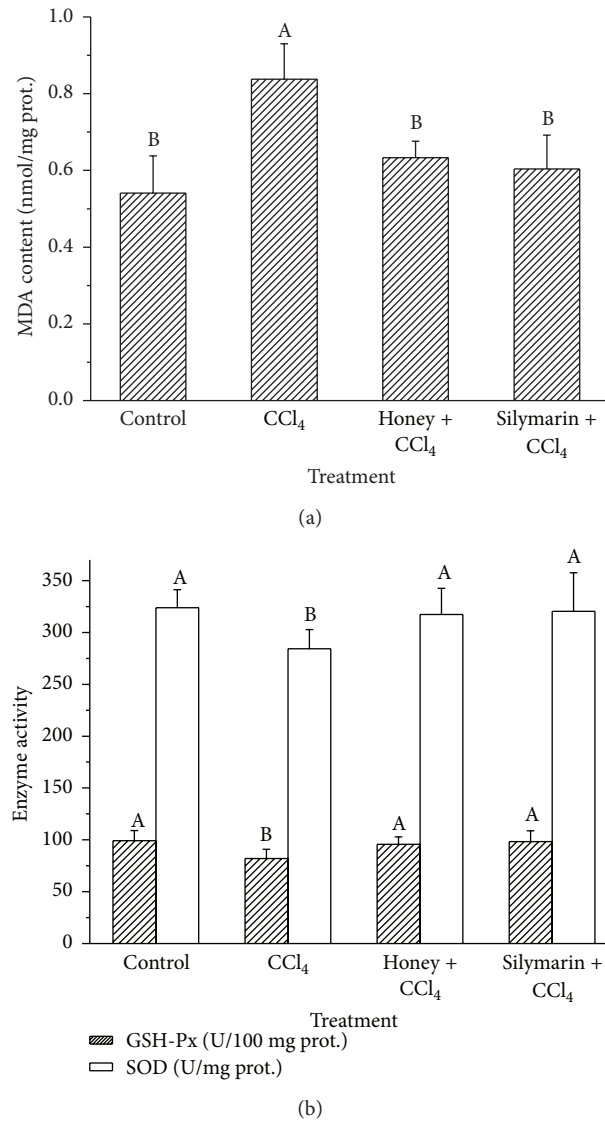

Figure 6: Effects of buckwheat honey on hepatic MDA content (a) and GSH-Px and SOD activities (b). Different lower case letters represent significant differences ($P < 0.05$). Mice in "control": distilled water plus peanut oil; mice in "CCl_4": distilled water plus CCl_4; mice in "honey + CCl_4": buckwheat honey (0.22 g/10 g BW) twice daily for 11 weeks plus CCl_4; mice in "silymarin + CCl_4": silymarin (0.5 mg/10 g BW) twice daily for 11 weeks plus CCl_4.

a 54.90% increase in hepatic MDA was obtained in the CCl_4-treated group relative to the control mice. Pretreatment with buckwheat honey and silymarin significantly decreased hepatic MDA levels in the CCl_4-treated mice. To delineate the mechanisms underlying the protective effects of buckwheat honey, the activities of hepatic antioxidant enzymes (e.g., GSH-Px and SOD) were determined. In this study, the activities of GSH-Px and SOD in the CCl_4-treated mice decreased significantly compared to those in the control mice ($P < 0.05$; Figure 6(b)). SOD is a critical endogenous antioxidant enzyme that prevents and neutralizes oxidative damage [32]. GSH-Px, which has both intracellular and extracellular antioxidant functions, catalyzes the reduction of hydrogen peroxide and hydroperoxides into nontoxic products [7]. When present in excess, lipid peroxides and reactive oxygen species can easily inactivate these antioxidant enzymes [33]. Therefore, the reduction in GSH-Px and SOD was attributed to an enhanced toxicity by CCl_4. Interestingly, pretreatment with buckwheat honey and silymarin significantly inhibited the decrease in GSH-Px and SOD activities induced by CCl_4 ($P < 0.05$). Meanwhile, histological observations further affirmed that administration with buckwheat honey significantly attenuates CCl_4-induced liver damage.

In the present study, eight phenolic compounds were identified in buckwheat honey, of which rutin and hesperetin are the majority. Rutin has been verified to exert renal-protective effects by inhibiting ROS and antioxidant activities [34]. Hesperetin has also been confirmed to protect against oxidative stress-related hepatic dysfunction [35]. In addition to rutin and hesperetin, there are some unidentified high content antioxidants in buckwheat, which may work together in creating these antioxidative and hepatoprotective effects. Silymarin, a high antioxidative flavonoid, has been used as a drug for human liver disease induced by oxidative stress for at least two decades [36]. Usually, it is used as a positive reference in many studies [9], including in this study on oxidative stress. Caffeic acid, unidentified in this study, was found to exist in buckwheat honey [11] and have the capability of preventing nickel-induced oxidative damage in rat livers [37]. Recently, inhibition of free radical-induced damage by antioxidant supplementation has become an attractive therapeutic strategy for reducing the risk of liver disease [7]. Polyphenol extracts from natural products such as apples, *Murraya koenigii* L., yam peel, and bee pollen have been

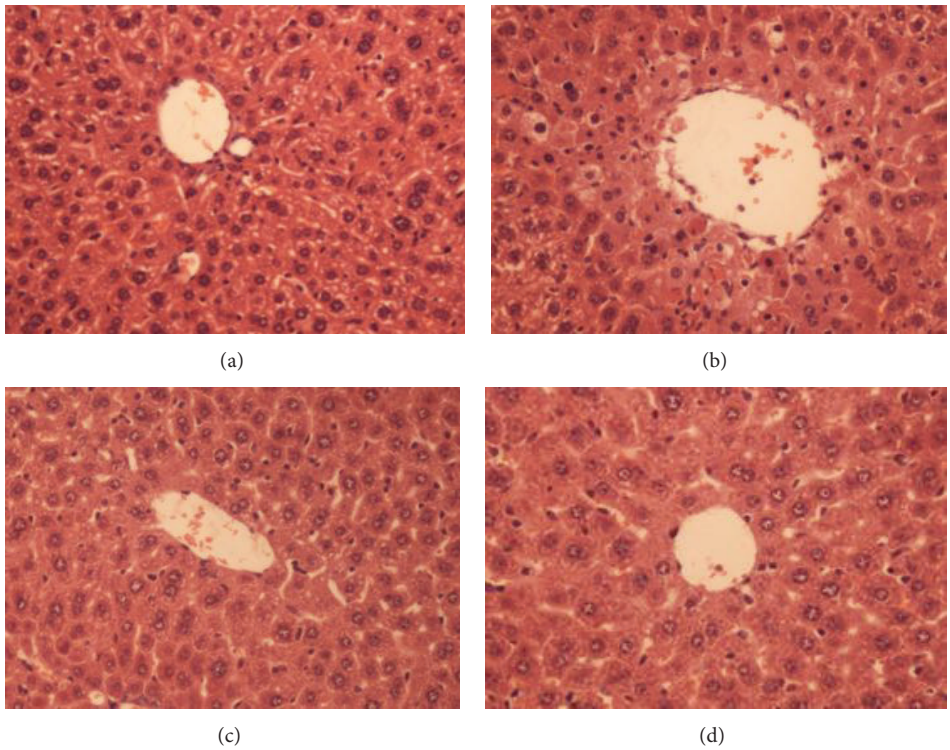

Figure 7: Effects of buckwheat honey on hepatic morphological analysis (×400 H&E): control mice (a), CCl_4-treated mice (b), and mice pretreated with buckwheat honey prior to CCl_4 (c) and with silymarin (d).

studied for their hepatoprotective effects [7, 9, 10]. The high levels of phenolic compounds in buckwheat honey reported in previous studies [13] were confirmed in this study. Additionally, buckwheat honey has free radical scavenging and ferrous ion-chelating properties. Moreover, CCl_4-induced DNA damage can be inhibited by the administration of buckwheat honey. Therefore, buckwheat honey, which has a free radical scavenging ability, reduces lipid peroxidation and increases antioxidant capacity, thereby attenuating CCl_4-induced liver damage in mice.

Additionally, another aim of this study was to assess whether buckwheat honey can attenuate CCl_4-induced DNA damage. Lymphocyte DNA damage induced by carbon tetrachloride was assessed by alkaline single cell gel electrophoresis, that is, the comet assay. This method is a rapid and sensitive technique for measuring and analyzing DNA damage in individual cells [38]. The more severe the cell damage, the higher the amount of tail DNA. Another parameter for DNA damage analysis is OTM, which is generally considered the main index of DNA damage because it provides information about the total DNA content in the tail as well as DNA migration from the comet-head. Thus, in the present experiment, OTM is taken into consideration for the interpretation of the data [39]. In the present study, increases in tail DNA and OTM induced by CCl_4 are shown in Figures 4(b) and 4(c). This demonstrated that the intraperitoneal administration of CCl_4 caused a significant rise in DNA damage in peripheral lymphocytes. This result could be attributed to the *in vivo* action of carbon tetrachloride metabolites, that is, trichloromethyl and/or trichloromethyl peroxy radicals, which pass from the liver to the circulatory system, or to the appearance of stimulated nuclear cells in circulation. According to Kujawska et al., oxidative damage to DNA increases by 33% in mice following intraperitoneal administration of CCl_4 [40]. On the other hand, Kadiiska et al. reported that CCl_4 did not increase DNA damage in rat blood leukocytes [41], which may be attributed to the dose and time of CCl_4 poisoning. In this study, a marked rise in tail DNA and OTM was obtained in mice treated with CCl_4. More importantly, pretreatment with antioxidants can inhibit the increase of mean tail DNA and OTM. This protection should be attributed to the phenolic compound existing in buckwheat honey, which could scavenge the free radicals produced in the metabolism of CCl_4 and thus attenuate the damage.

In conclusion, the results of this study demonstrated that buckwheat honey increased the antioxidant capacity and attenuated CCl_4-induced liver and DNA damage in mice. Buckwheat honey demonstrated high TPC, free radical scavenging capability, and ferric-reducing antioxidant properties. Pretreatment with buckwheat honey for 10 weeks in mice significantly increased serum antioxidant activities. Therefore, buckwheat honey exhibited hepatoprotective effects in mice. Additionally, pretreatment with buckwheat honey protected DNA from CCl_4-induced oxidation.

Conflict of Interests

The authors declare that there is no conflict of interests.

Acknowledgments

This work is financially supported by the National Natural Science Foundation of China (no. 31272510) and the China Agriculture Research System (no. CARS-45-KXJ10).

References

[1] J. Medina and R. Moreno-Otero, "Pathophysiological basis for antioxidant therapy in chronic liver disease," *Drugs*, vol. 65, no. 17, pp. 2445–2461, 2005.

[2] R. Saller, R. Meier, and R. Brignoli, "The use of silymarin in the treatment of liver diseases," *Drugs*, vol. 61, no. 14, pp. 2035–2063, 2001.

[3] P. Angulo, "Medical progress: nonalcoholic fatty liver disease," *The New England Journal of Medicine*, vol. 346, no. 16, pp. 1221–1231, 2002.

[4] J. Balkan, S. Öztezcan, M. Küçük, U. Çevikbaş, N. Koçak-Toker, and M. Uysal, "The effect of betaine treatment on triglyceride levels and oxidative stress in the liver of ethanol-treated guinea pigs," *Experimental and Toxicologic Pathology*, vol. 55, no. 6, pp. 505–509, 2004.

[5] W. J. Brattin, E. A. Glende Jr., and R. O. Recknagel, "Pathological mechanisms in carbon tetrachloride hepatotoxicity," *Journal of Free Radicals in Biology and Medicine*, vol. 1, no. 1, pp. 27–38, 1985.

[6] R. O. Recknagel, E. A. Glende Jr., J. A. Dolak, and R. L. Waller, "Mechanisms of carbon tetrachloride toxicity," *Pharmacology & Therapeutics*, vol. 43, no. 1, pp. 139–154, 1989.

[7] J. Y. Yang, Y. Li, F. Wang, and C. Wu, "Hepatoprotective effects of apple polyphenols on CCl_4-induced acute liver damage in mice," *Journal of Agricultural and Food Chemistry*, vol. 58, no. 10, pp. 6525–6531, 2010.

[8] Y.-H. Yeh, Y.-L. Hsieh, Y.-T. Lee, and C.-C. Hu, "Protective effects of *Geloina eros* extract against carbon tetrachloride-induced hepatotoxicity in rats," *Food Research International*, vol. 48, no. 2, pp. 551–558, 2012.

[9] Y.-H. Yeh, Y.-L. Hsieh, and Y.-T. Lee, "Effects of yam peel extract against carbon tetrachloride-induced hepatotoxicity in rats," *Journal of Agricultural and Food Chemistry*, vol. 61, no. 30, pp. 7387–7396, 2013.

[10] N. Cheng, N. Ren, H. Gao, X. Lei, J. Zheng, and W. Cao, "Antioxidant and hepatoprotective effects of *Schisandra chinensis* pollen extract on CCl_4-induced acute liver damage in mice," *Food and Chemical Toxicology*, vol. 55, pp. 234–240, 2013.

[11] F. Pasini, S. Gardini, G. L. Marcazzan, and M. F. Caboni, "Buckwheat honeys: screening of composition and properties," *Food Chemistry*, vol. 141, no. 3, pp. 2802–2811, 2013.

[12] N. Gheldof, X.-H. Wang, and N. J. Engeseth, "Buckwheat honey increases serum antioxidant capacity in humans," *Journal of Agricultural and Food Chemistry*, vol. 51, no. 5, pp. 1500–1505, 2003.

[13] V. R. Singelton, R. Orthifer, and R. M. Lamuela-Raventos, "Analysis of total phenols and other oxidation substrates and antioxidants by means of folin-ciocalteu reagent," *Methods in Enzymology*, vol. 299, pp. 152–178, 1999.

[14] Y. Liang, W. Cao, W.-J. Chen, X.-H. Xiao, and J.-B. Zheng, "Simultaneous determination of four phenolic components in citrus honey by high performance liquid chromatography using electrochemical detection," *Food Chemistry*, vol. 114, no. 4, pp. 1537–1541, 2009.

[15] B.-S. Wang, G.-J. Huang, H.-M. Tai, and M.-H. Huang, "Antioxidant and anti-inflammatory activities of aqueous extracts of *Schizonepeta tenuifolia* Briq," *Food and Chemical Toxicology*, vol. 50, no. 3-4, pp. 526–531, 2012.

[16] N. Singh and P. S. Rajini, "Free radical scavenging activity of an aqueous extract of potato peel," *Food Chemistry*, vol. 85, no. 4, pp. 611–616, 2004.

[17] I. F. F. Benzie and J. J. Strain, "The ferric reducing ability of plasma (FRAP) as a measure of 'antioxidant power': the FRAP assay," *Analytical Biochemistry*, vol. 239, no. 1, pp. 70–76, 1996.

[18] N. Cheng, B. Du, Y. Wang et al., "Antioxidant properties of jujube honey and its protective effects against chronic alcohol-induced liver damage in mice," *Food & Function*, vol. 5, no. 5, pp. 900–908, 2014.

[19] J. Regnström, K. Ström, P. Moldeus, and J. Nilsson, "Analysis of lipoprotein diene formation in human serum exposed to copper," *Free Radical Research*, vol. 19, no. 4, pp. 267–278, 1993.

[20] C. Lucas-Abellán, M. T. Mercader-Ros, M. P. Zafrilla, M. I. Fortea, J. A. Gabaldón, and E. Núñez-Delicado, "ORAC-fluorescein assay to determine the oxygen radical absorbance capacity of resveratrol complexed in cyclodextrins," *Journal of Agricultural and Food Chemistry*, vol. 56, no. 6, pp. 2254–2259, 2008.

[21] N. P. Singh, M. T. McCoy, R. R. Tice, and E. L. Schneider, "A simple technique for quantitation of low levels of DNA damage in individual cells," *Experimental Cell Research*, vol. 175, no. 1, pp. 184–191, 1988.

[22] T.-S. Chen, S.-Y. Liou, H.-C. Wu et al., "New analytical method for investigating the antioxidant power of food extracts on the basis of their electron-donating ability: comparison to the ferric reducing/antioxidant power (FRAP) assay," *Journal of Agricultural and Food Chemistry*, vol. 58, no. 15, pp. 8477–8480, 2010.

[23] Y. Ruiz-Navajas, M. Viuda-Martos, J. Fernández-López, J. M. Zaldivar-Cruz, V. Kuri, and J. Á. Pérez-Álvarez, "Antioxidant activity of artisanal honey from Tabasco, Mexico," *International Journal of Food Properties*, vol. 14, no. 2, pp. 459–470, 2011.

[24] J. Bertoncelj, U. Doberšek, M. Jamnik, and T. Golob, "Evaluation of the phenolic content, antioxidant activity and colour of Slovenian honey," *Food Chemistry*, vol. 105, no. 2, pp. 822–828, 2007.

[25] I. Gülçin, "Antioxidant activity of food constituents: an overview," *Archives of Toxicology*, vol. 86, no. 3, pp. 345–391, 2012.

[26] P. M. Kuś, F. Congiu, D. Teper, Z. Sroka, I. Jerković, and C. I. G. Tuberoso, "Antioxidant activity, color characteristics, total phenol content and general HPLC fingerprints of six Polish unifloral honey types," *LWT—Food Science and Technology*, vol. 55, no. 1, pp. 124–130, 2014.

[27] B. Halliwell, "Antioxidants in human health and disease," *Annual Review of Nutrition*, vol. 16, pp. 33–50, 1996.

[28] E. N. Frankel, J. Kanner, J. B. German, E. Parks, and J. E. Kinsella, "Inhibition of oxidation of human low-density lipoprotein by phenolic substances in red wine," *The Lancet*, vol. 341, no. 8843, pp. 454–457, 1993.

[29] F. Shahidi, P. K. Janitha, and P. D. Wanasundara, "Phenolic antioxidants," *Critical Reviews in Food Properties*, vol. 13, pp. 657–671, 1992.

[30] B. Ou, D. Huang, M. Hampsch-Woodill, J. A. Flanagan, and E. K. Deemer, "Analysis of antioxidant activities of common vegetables employing oxygen radical absorbance capacity (ORAC)

and ferric reducing antioxidant power (FRAP) assays: a comparative study," *Journal of Agricultural and Food Chemistry*, vol. 50, no. 11, pp. 3122–3128, 2002.

[31] L. W. D. Weber, M. Boll, and A. Stampfl, "Hepatotoxicity and mechanism of action of haloalkanes: carbon tetrachloride as a toxicological model," *Critical Reviews in Toxicology*, vol. 33, no. 2, pp. 105–136, 2003.

[32] I. N. Zelko, T. J. Mariani, and R. J. Folz, "Superoxide dismutase multigene family: a comparison of the CuZn–SOD (SOD1), Mn-SOD (SOD2), and EC-SOD (SOD3) gene structures, evolution, and expression," *Free Radical Biology and Medicine*, vol. 33, no. 3, pp. 337–349, 2002.

[33] Y.-S. Yang, T.-H. Ahn, J.-C. Lee et al., "Protective effects of *Pycnogenol* on carbon tetrachloride-induced hepatotoxicity in Sprague—Dawley rats," *Food and Chemical Toxicology*, vol. 46, no. 1, pp. 380–387, 2008.

[34] A. Korkmaz and D. Kolankaya, "Protective effect of rutin on the ischemia/reperfusion induced damage in rat kidney," *Journal of Surgical Research*, vol. 164, no. 2, pp. 309–315, 2010.

[35] L. Pari and K. Shagirtha, "Hesperetin protects against oxidative stress related hepatic dysfunction by cadmium in rats," *Experimental and Toxicologic Pathology*, vol. 64, no. 5, pp. 513–520, 2012.

[36] V. Kren and D. Walterová, "Silybin and silymarin—new effects and applications," *Biomedical Papers of the Medical Faculty of the University Palacký, Olomouc, Czechoslovakia*, vol. 149, no. 1, pp. 29–41, 2005.

[37] L. Pari and A. Prasath, "Efficacy of caffeic acid in preventing nickel induced oxidative damage in liver of rats," *Chemico-Biological Interactions*, vol. 173, no. 2, pp. 77–83, 2008.

[38] A. R. Collins, A. A. Oscoz, G. Brunborg et al., "The comet assay: topical issues," *Mutagenesis*, vol. 23, no. 3, pp. 143–151, 2008.

[39] R. R. Tice, E. Agurell, D. Anderson et al., "Single cell gel/comet assay: guidelines for in vitro and in vivo genetic toxicology testing," *Environmental and Molecular Mutagenesis*, vol. 35, no. 3, pp. 206–221, 2000.

[40] M. Kujawska, E. Ignatowicz, M. Murias, M. Ewertowska, K. Mikołajczyk, and J. Jodynis-Liebert, "Protective effect of red beetroot against carbon tetrachloride- and N-nitrosodiethylamine-induced oxidative stress in rats," *Journal of Agricultural and Food Chemistry*, vol. 57, no. 6, pp. 2570–2575, 2009.

[41] M. B. Kadiiska, B. C. Gladen, D. D. Baird et al., "Biomarkers of oxidative stress study II. Are oxidation products of lipids, proteins, and DNA markers of CCl_4 poisoning?" *Free Radical Biology and Medicine*, vol. 38, no. 6, pp. 698–710, 2005.

Hindawi Publishing Corporation
Evidence-Based Complementary and Alternative Medicine
Volume 2015, Article ID 651734, 11 pages
http://dx.doi.org/10.1155/2015/651734

Research Article

Bai-Hu-Jia-Ren-Shen-Tang Decoction Reduces Fatty Liver by Activating AMP-Activated Protein Kinase In Vitro and In Vivo

Hui-Kang Liu,[1,2] Tzu-Min Hung,[3] Hsiu-Chen Huang,[4] I-Jung Lee,[1] Chia-Chuan Chang,[5] Jing-Jy Cheng,[1] Lie-Chwen Lin,[1] and Cheng Huang[1]

[1]*National Research Institute of Chinese Medicine, Taipei 11221, Taiwan*
[2]*Ph.D. Program for the Clinical Drug Discovery from Botanical Herbs, Taipei Medical University, Taipei 11031, Taiwan*
[3]*Department of Medical Research, E-DA Hospital, Kaohsiung 82445, Taiwan*
[4]*Department of Applied Science, National Hsinchu University of Education, Hsinchu 30014, Taiwan*
[5]*School of Pharmacy, College of Medicine, National Taiwan University, Taipei 10051, Taiwan*

Correspondence should be addressed to Cheng Huang; chengh@nricm.edu.tw

Received 21 April 2015; Revised 14 July 2015; Accepted 11 August 2015

Academic Editor: Abbas A. Mahdi

Obesity and associated conditions, such as type 2 diabetes mellitus (T2DM) and nonalcoholic fatty liver disease (NAFLD), are currently a worldwide health problem. In Asian traditional medicine, Bai-Hu-Jia-Ren-Shen-Tang (BHJRST) is widely used in diabetes patients to reduce thirst. However, whether it has a therapeutic effect on T2DM or NAFLD is not known. The aim of this study was to examine whether BHJRST had a lipid-lowering effect using a HuS-E/2 cell model of fatty liver induced by palmitate and in a db/db mouse model of dyslipidemia. Incubation of HuS-E/2 cells with palmitate markedly increased lipid accumulation and expression of adipose triglyceride lipase (ATGL), which is involved in lipolysis. BHJRST significantly decreased lipid accumulation and increased ATGL levels and phosphorylation of AMP-activated protein kinase (AMPK) and its primary downstream target, acetyl-CoA carboxylase (ACC), which are involved in fatty acid oxidation. Furthermore, after twice daily oral administration for six weeks, BHJRST significantly reduced hepatic fat accumulation in db/db mice, as demonstrated by increased hepatic AMPK and ACC phosphorylation, reduced serum triglyceride levels, and reduced hepatic total lipid content. The results show that BHJRST has a lipid-lowering effect in the liver that is mediated by activation of the AMPK signaling pathway.

1. Introduction

Obesity and dysregulated insulin action in the liver are strongly associated and are currently a worldwide health problem [1]. Fatty liver, the initial stage of nonalcoholic fatty liver disease (NAFLD), is a common metabolic symptom [2] and is caused by an imbalance of lipid metabolism. NAFLD and type 2 diabetes mellitus (T2DM) frequently coexist, as they share the pathogenic abnormalities of excess adiposity and insulin resistance [3, 4]. Although the molecular mechanisms underlying fatty liver are not fully understood, dysregulation of hepatic lipid homeostasis caused by pathological conditions, such as reduced fatty acid oxidation, enhanced de novo lipogenesis, elevated hepatic fatty acid influx, and/or increased systemic insulin resistance, is thought to be important in its development [5]. Indeed, current therapies for fatty liver disease are aimed at reducing body weight and improving insulin sensitivity to alleviate the associated metabolic syndrome [6, 7].

The pathologic findings in NAFLD include accumulation of intracellular triglyceride in the parenchyma of the liver [8, 9]. Adipose triglyceride lipase (ATGL) and hormone-sensitive lipase (HSL) are the major triglyceride lipases in many tissues [10] and expression of both is decreased in the obese, insulin-resistant state, suggesting that insulin resistance is associated with impaired lipolysis [11, 12]. A large body of evidence indicates that AMP-activated protein kinase (AMPK) is important in regulating hepatic lipogenesis [13]. In the liver, activation of AMPK by phosphorylation of threonine 172 switches off fatty acid synthesis by increasing the phosphorylation and inactivation of acetyl-CoA carboxylase

(ACC) [14]. Some antidiabetic drugs, such as metformin and the thiazolidinediones, alleviate fatty liver in humans and rodents by downregulating lipid metabolism through AMPK activation [15]. Thus, AMPK represents an attractive target for therapeutic intervention in the treatment of fatty liver disorders [16, 17].

Bai-Hu-Tang (BHT), composed of Gypsum Fibrosum (Shi-Gao), Rhizoma Anemarrhenae (Zhi-Mu), Radix Glycyrrhizae Preparata (Zhi-Gan-Cao), and seed of *Oryza sativa* (Jing-Mi), is a traditional Chinese medicine described in the Chinese medicine book "Discussion of Cold Damage" ("Shang-Han-Lun" in Chinese), which has been used in China for over 1800 years. BHT potentiates insulin-stimulated glucose uptake in vitro [18]. The formula used in this study was Bai-Hu-Jia-Ren-Shen-Tang (BHJRST), which is an enhanced formula of BHT prepared by addition of Ginseng Radix (Ren-Shen). Traditionally, BHJRST is used to reduce thirst in diabetes patients and is the most common herbal formula prescribed by traditional Chinese medicine doctors for the treatment of type 2 diabetes mellitus (T2DM) in Taiwan [19]. Although BHJRST has been reported to have significant antihyperglycemic activity [20], it is not known whether it has a fat-lowering action.

In this study, we used a human hepatic cell line and an animal model to investigate the mechanisms responsible for the in vitro and in vivo effects of BHJRST on lipid metabolism. In the in vitro study, immortalized primary human hepatocytes, HuS-E/2 cells [21], which are phenotypically and functionally similar to primary hepatocytes, were used to established a fatty liver cell model. In in vivo experiments, db/db mice, which show dyslipidemia similar to that seen in patients with T2DM, were used as a model to study the pathogenesis and treatment of diabetic dyslipidemia [22].

2. Materials and Methods

2.1. Preparation of the BHJRST Formula and Single Remedy Extracts. Rhizome of Rhizoma Anemarrhenae (Zhi-Mu), Gypsum Fibrosum (Shi-Gao), root of Radix Glycyrrhizae Preparata (Zhi-Gan-Cao), seed of *Oryza sativa* (Jing-Mi), and root of Ginseng Radix (Ren-Shen) were mixed in a classical dosage ratio used in the Han Dynasty (6 parts by weight of Zhimu, 16 parts Shigao, 2 parts Gancao, 8 parts Jingmi, and 3 parts Renshen). To prepare the water extracts, 35 g of the mixture or the corresponding weight of each single ingredient (e.g., 6 g of Zhimu) was added to 400 mL of water and refluxed at 100°C for 1 h; then, the supernatant was collected, clarified by centrifugation at 1000 g for 10 min at 4°C, and either used directly as such in animal experiments or lyophilized and dissolved in DMSO for cell studies.

2.2. Confirmation of the Identity of the Ingredients by Microscopy. All the specimens were sliced manually by hand, fixed in a solution of 50% glycerin in water, and observed under a microscope (Carl Zeiss Inc., Germany) to confirm their identity.

2.3. HPLC Sample Preparation. Each lyophilized sample (5 mg) was dissolved in 5 mL of DMSO, ultrasonicated for 30 s, and then injected into solid-phase extraction tubes (Strata-X 33 μm Polymeric Reversed Phase, 200 mg/6 mL) (Phenomenex), which had been activated in advance by MeOH and equilibrated in distilled water. The tubes were then washed with distilled water, and the adsorbed materials were eluted with 10 mL of MeOH and filtered on a 0.45 μm filter (13 mm, Millex-GV, EMD Millipore) for HPLC analysis.

2.4. Reverse-Phase HPLC Chemical Fingerprint Analysis of BHJRST. All HPLC fingerprint analyses of the water extracts of BHJRST and the single remedies of BHJRST were performed on a HPLC instrument equipped with a Shimadzu 10A system controller (both from Shimadzu Corporation, Kyoto, Japan). The injection volume was 10 μL, the column was a Nacalai Cosmosil 5C_{18}-AR-II Waters (5 μm, 4.6 × 250 mm; Nacalai Tesque), the linear gradient was 10.0–90.0% B (A = MeOH, B = H_2O) in 60 min, detection was at 280 nm, and the flow rate was 0.8 mL/min.

2.5. Antibodies and Chemical Reagents. Antibodies against ATGL, AMPK, pACC (Ser 79), ACC, tubulin, or actin were obtained from Genetex, the anti-pAMPK (Thr 172) antibodies were from Millipore, and the horseradish peroxidase-conjugated anti-mouse or anti-rabbit IgG antibodies were from Jackson ImmunoResearch Laboratories Inc. Palmitate and Oil Red O were purchased from Sigma.

2.6. Cell Culture and Treatment. HuS-E/2 cells, kindly provided by Dr. Shimotohno (Kyoto University, Japan), were maintained as described previously in primary hepatocyte medium (PH medium) [DMEM with 25 mM glucose (Gibco) containing 20 mM HEPES, 10% fetal bovine serum, 15 μg/mL of L-proline, 0.25 μg/mL of insulin, 5×10^{-8} M dexamethasone, 44 mM $NaHCO_3$, 10 mM nicotinamide, 5 ng/mL of EGF, 0.1 mM Asc-2P, 100 IU/mL of penicillin, 100 μg/mL of streptomycin, 10 μg/mL of gentamicin, and 1 μg/mL of plasmocin] [21]. To induce fatty acid overload, HuS-E/2 cells at 70% confluence were cultured in glucose-free PH medium [made as above, but with glucose-free DMEM (Sigma)] and incubated with the indicated concentration of palmitate for 24 h. The palmitate used was provided in the form of a palmitate/BSA complex prepared as described previously [23]. To study the effect of BHJRST, the cells were incubated with various concentrations of palmitate and either BHJRST or a final concentration of 0.1% DMSO (vehicle) for the indicated time.

2.7. Cell Viability Assay. Cell viability was assessed using the 3-(4,5-dimethylthiazol-2-yl)-2,5-diphenyltetrazolium bromide (MTT) assay. MTT assay performed according to the manufacturer's suggestions (Sigma). HuS-E/2 cells were added to 96-well plates at a density of 1×10^4 cells per well in 100 μL of PH medium and allowed to attach for 18 h; then, the medium was changed to glucose-free PH medium containing different concentrations of BHJRST or 0.1% DMSO (vehicle control) and 0.1 mM palmitate for 24 h. They were then incubated with MTT for another 4 h at 37°C; then, the medium was removed and 100 μL of DMSO was added to each well. The absorbance of the samples was measured at 570 nm using a FlexStation 3 microplate reader (Molecular Devices).

2.8. Oil Red O Staining. To measure intracellular lipid content, HuS-E/2 cells in 6-well plates were stained using the Oil Red O method [24]. Briefly, the cells were fixed in 4% paraformaldehyde in phosphate-buffered saline (PBS) for 30 min at room temperature (23°C), stained with Oil Red O (stock solution, 3 mg/mL in isopropanol; working solution, 60% Oil Red O stock solution and 40% distilled water) for 1 h at room temperature, and then rinsed with water, and images were captured under a microscope. For quantitative analysis of cellular lipids, the cells were washed three times with ice-cold PBS, fixed with 10% formalin for 1 h, washed, stained with Oil Red O solution for 1 h at room temperature, and washed with water to remove nonbound dye; then, 1 mL of isopropanol was added to each well and the plate was shaken at room temperature for 5 min; then, the absorbance at 510 nm was read on a spectrophotometer.

2.9. Western Blot Analysis. After treatment, HuS-E/2 cells were harvested in lysis buffer (50 mM Tris-HCl, pH 8.0, 5 mM EDTA, 150 mM NaCl, 0.5% Nonidet P-40, 0.5 mM phenylmethylsulfonyl fluoride, and 0.5 mM dithiothreitol) and incubated for 30 min at 4°C; then, the samples were sonicated for 3 × 5 s with 15 s breaks and centrifuged at 12000 g for 10 min at 4°C. The protein concentrations of the supernatants were determined using a protein assay kit (Bio-Rad); then, equal amounts of total cellular protein (200 mg) were resolved by SDS-PAGE, transferred onto polyvinylidene difluoride membranes (Amersham Biosciences), and probed with primary antibody, followed by horseradish peroxidase-conjugated secondary antibody; then, bound antibody was visualized using enhanced chemiluminescence kits (Amersham Biosciences).

2.10. Total Lipid, Triglyceride, and Cholesterol Assay. For lipid determinations, cell homogenate, mouse serum, or mouse liver was extracted using a modified Bligh and Dyer procedure [25]. In brief, the sample was homogenized at room temperature with a mixture of chloroform-methanol-water (8 : 4 : 3) and the resulting mixture was shaken at 37°C for 1 h and then centrifuged at 1,000 g for 20 min at 4°C, and the supernatant was collected for lipid analysis. Triacylglycerol, total cholesterol, and total lipid levels were measured using enzymatic method kits from Randox Laboratories in accordance with the manufacturer's instructions.

2.11. Animal Experiments. Six- to 8-week-old male BKS.Cg-Lepr^{db}+/+Lepr^{db}/Jnarl (db/db) mice were purchased from The National Laboratory Animal Center, Taipei, Taiwan, and were housed at room temperature with controlled humidity and on a 12 h/12 h light/dark cycle (lights on at 7.00 a.m.) at the Animal Center of the National Research Institute of Chinese Medicine (NRICM), Taipei, Taiwan. The use of animals for this research was approved by the Animal Research Committee of the NRICM and all procedures followed The Guide for the Care and Use of Laboratory Animals (NIH publication, 85-23, revised 1996) and the guidelines of the Animal Welfare Act, Taiwan.

The mice were fed a standard diet (7.9% moisture, 22.9% crude protein, 5.4% crude fat, 6.2% crude ash, 3.4% crude fiber, and 54.2% nitrogen-free extract; Oriental Yeast Co., Ltd. data sheet) throughout the study, but, at the age of 12 weeks, they were divided into two groups which received either double-distilled water or BHJRST (900 mg/kg b.w. in double-distilled water) twice daily by gavage for 6 weeks. At 18 weeks, serum samples were collected prior to sacrifice and the liver was harvested for protein and lipid analysis.

2.12. Statistical Analysis. All values are expressed as the mean ± SD of the results from at least three separate experiments. One-way ANOVA followed by Dunnett's multiple comparison test was used to compare differences among groups of samples. Asterisks indicate that the values were significantly different from the control ($^{*}p < 0.05$; $^{**}p < 0.01$).

3. Results

3.1. Characterization of BHJRST. Ginseng-plus-Bai-Hu-Tang (BHJRST) is composed of five crude ingredients and the appearance and microscopic features of each of these were examined to confirm the identity of the ingredient (Figure 1(a)). HPLC pattern analysis, the so-called "fingerprint" method, was performed on the water extracts of BHJRST and three of the single ingredients (Figure 1(b)); analysis of the other two single ingredients, Gypsum Fibrosum (Shi-Gao) and seed of *Oryza sativa* (Jing-Mi), was not performed, as their active components are believed to be, respectively, inorganic ($CaSO_4$) or macromolecular (polysaccharides). The HPLC chromatogram of the extract prepared from BHJRST (Figure 1(b), top panel) showed three major peaks at 11.9, 24.4, and 32.6 min, corresponding to ginsenoside Rg3 from Ginseng Radix (Ren-Shen) (12.0 min), mangiferin from Rhizoma Anemarrhenae (Zhi-Mu) (24.6 min), and glycyrrhizic acid from Radix Glycyrrhizae Preparata (Zhi-Gan-Cao) (32.7 min).

3.2. A Fatty Liver Cell Model: A High Fat Environment Increases Intracellular Lipid Formation in HuS-E/2 Cells and Induces ATGL Expression. Fatty liver disease is mainly due to triglyceride accumulation in hepatocytes [26]. To determine whether liver cells esterify and deposit fatty acid as lipid droplets, HuS-E/2 immortalized human primary hepatocytes were incubated in glucose-free PH medium alone or containing 0.05–1 mM palmitate; then, intracellular lipid accumulation was measured using oil Red O staining. The results (Figures 2(a) and 2(b)) showed that HuS-E/2 cells exposed to palmitate showed a clear dose-dependent increase in lipid accumulation in the cytosol compared to the control, indicating that a cell model of steatosis was induced by palmitate. Incubation of HuS-E/2 cells with concentrations of palmitate lower than 0.25 mM did not affect cell viability, as demonstrated by the MTT assay (Figure 2(c)). Since ATGL is responsible for the catabolism of cellular lipid stores [12] and since we wanted conditions in which lipid could accumulate in the absence of ATGL overexpression, ATGL expression

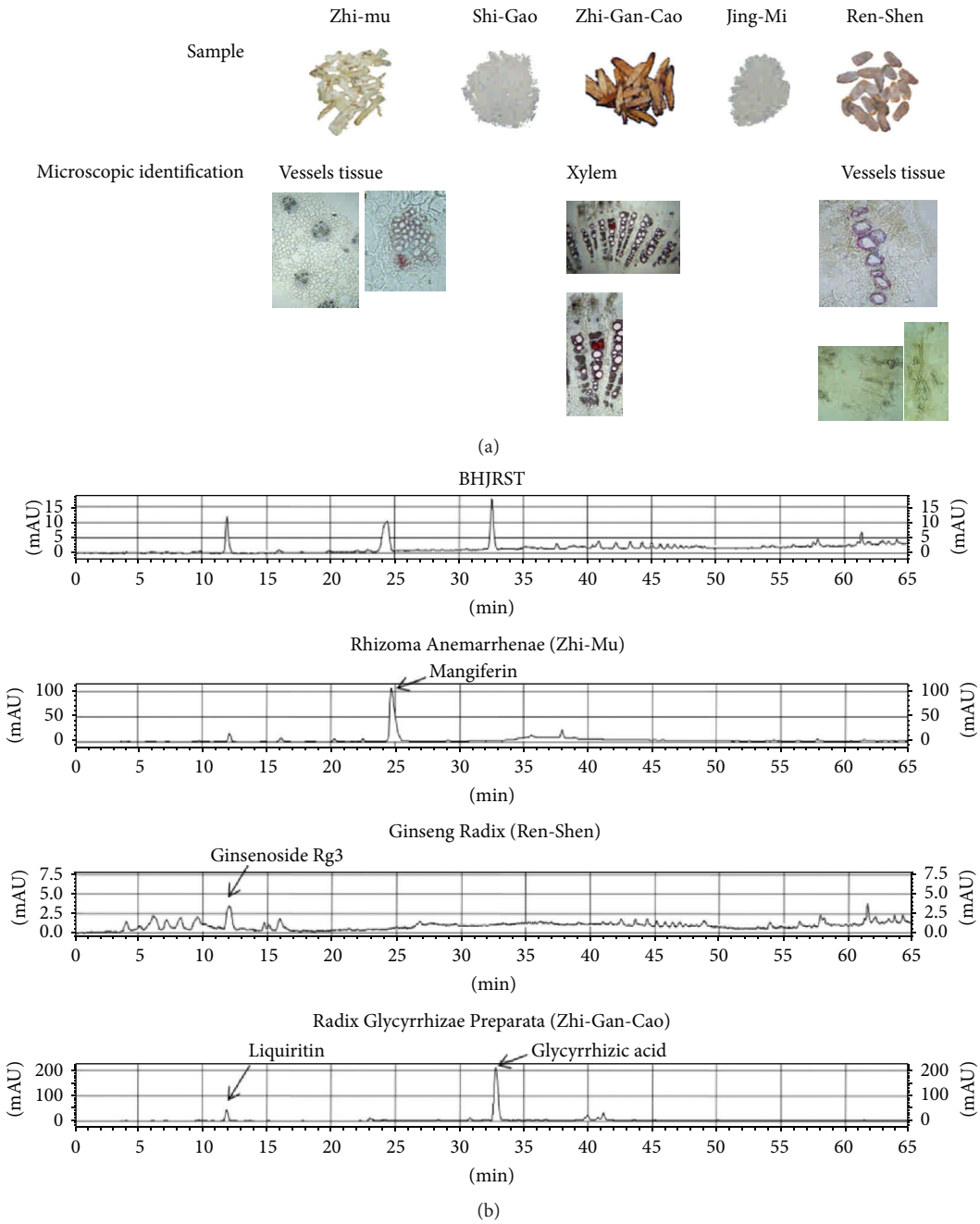

Figure 1: Characterization of BHJRST. (a) Confirmation of the identity of the ingredients. The macroscopic and microscopic appearance of the 5 ingredients used to prepare BHJRST was examined. (b) HPLC chromatograms of water extracts of BHJRST and three of the five single ingredients. Three major peaks were identified in the classical BHJRST formula (top panel) by comparison of their retention times with those of peaks in extracts of the single ingredients Rhizoma Anemarrhenae (Zhi-Mu), Ginseng Radix (Ren-Shen), or Radix Glycyrrhizae Preparata (Zhi-Gan-Cao).

was examined by western blotting in HuS-E/2 cells treated as above. As shown in Figure 2(d), ATGL expression was low when cells were incubated in glucose-free PH medium alone and was increased by treatment of cells with 0.25 mM palmitate for 24 h, but not by treatment with 0.1 mM palmitate. Thus, we established the parameters for a fatty liver cell model by incubating HuS-E/2 cells in high fat (0.1 mM palmitate) glucose-free PH medium.

3.3. Effect of BHJRST or Palmitate on Cell Survival. To examine the effect of BHJRST on cell viability, HuS-E/2 cells were incubated with glucose-free PH medium alone or containing 100–2000 μg/mL of BHJRST with or without 0.1 mM palmitate then an MTT assay was performed. As shown in Figure 3(a), BHJRST concentrations of 100, 250, or 500 μg/mL alone had no significant effect on viability, but a significant decrease was seen using concentrations of 1000 and

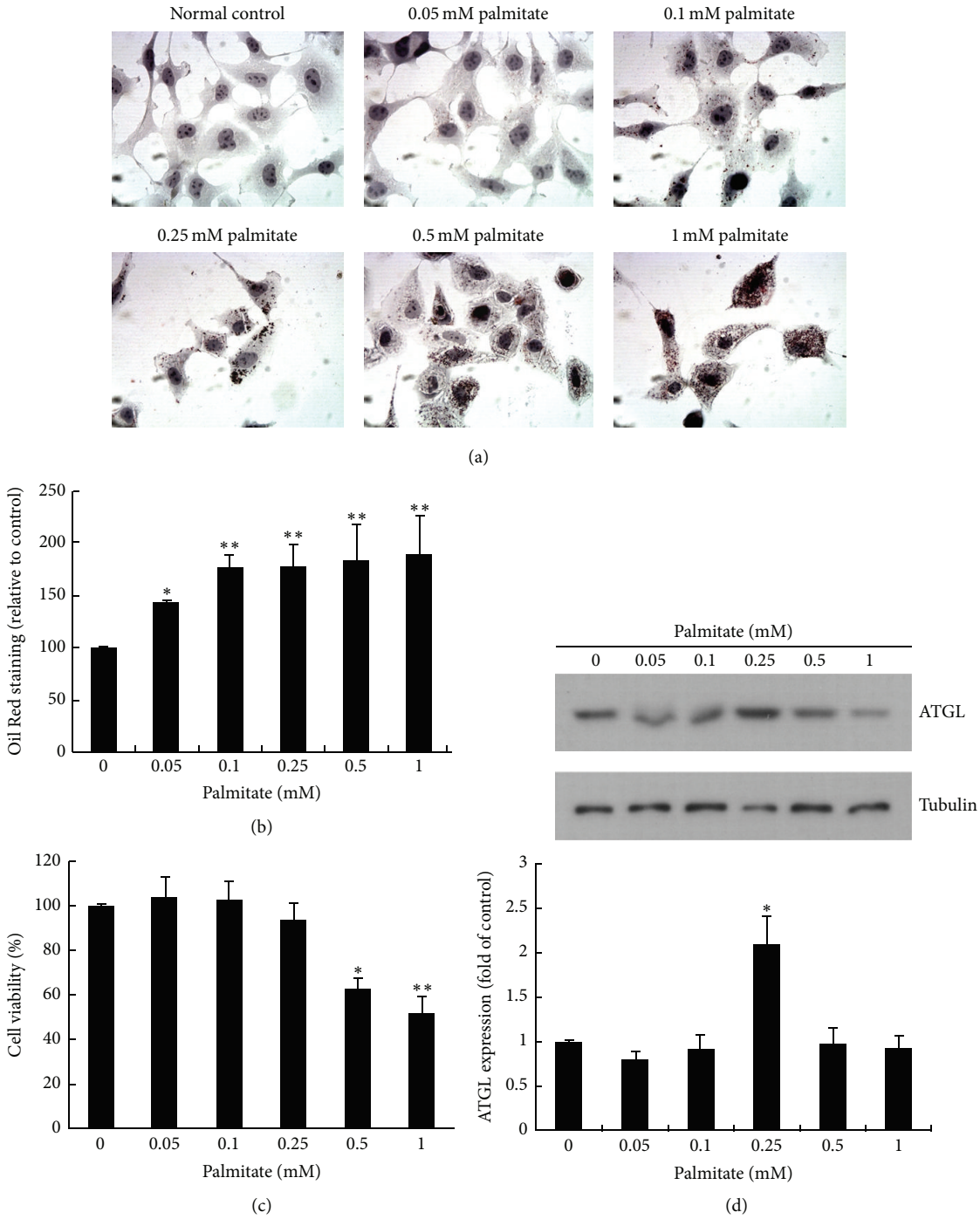

Figure 2: The fatty liver cell model—a high fat environment increases intracellular lipid formation in HuS-E/2 cells and induces ATGL expression. (a) Micrographs of HuS-E/2 cells incubated for 24 h in glucose-free PH medium with different concentrations of palmitate to simulate a high fat environment. Cells were stained with Oil Red O and observed under a microscope at 400x original magnification. (b) Quantitative analysis of lipid deposition in cells using Oil Red O staining. HuS-E/2 cells were treated with the indicated concentration of palmitate in glucose-free PH medium for 24 h. The data represent the mean ± SD for three independent experiments and are expressed as a percentage of the control value. (c) Cell viability in the high fat environment. HuS-E/2 cells were incubated with the indicated concentration of palmitate in glucose-free PH medium for 24 h as above; then, cell viability was determined using the MTT assay. The data represent the mean ± SD for three independent experiments and are expressed as a percentage of the control value. (d) Western blots showing ATGL and tubulin levels in HuS-E/2 cells incubated with the indicated concentration of palmitate in glucose-free PH medium for 24 h. The upper panel shows a representative result of those obtained in three experiments and the lower panel shows the quantitative analysis of ATGL expression normalized to that of tubulin and expressed as a fold value relative to the control value. The data represent the mean ± SD for three independent experiments. $^{*}p < 0.05$ and $^{**}p < 0.01$ versus control.

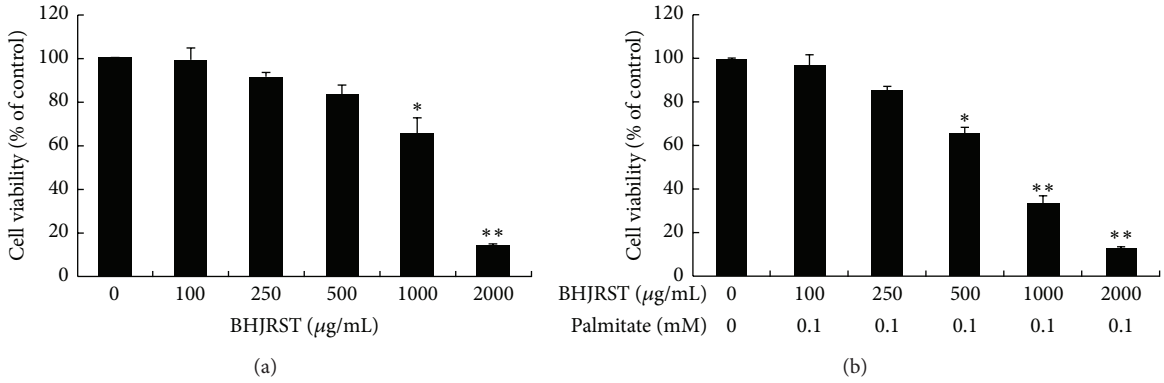

Figure 3: Effects of BHJRST on cell survival. Cells were cultured for 24 h in the presence of the indicated concentration of BHJRST alone (a) or together with 0 or 0.1 mM palmitate (b) in glucose-free PH medium; then, cell viability was measured using the MTT assay and expressed as a percentage of the value for untreated cells. The results are the mean ± SD for three independent experiments. $^{*}p < 0.05$ and $^{**}p < 0.01$ versus control.

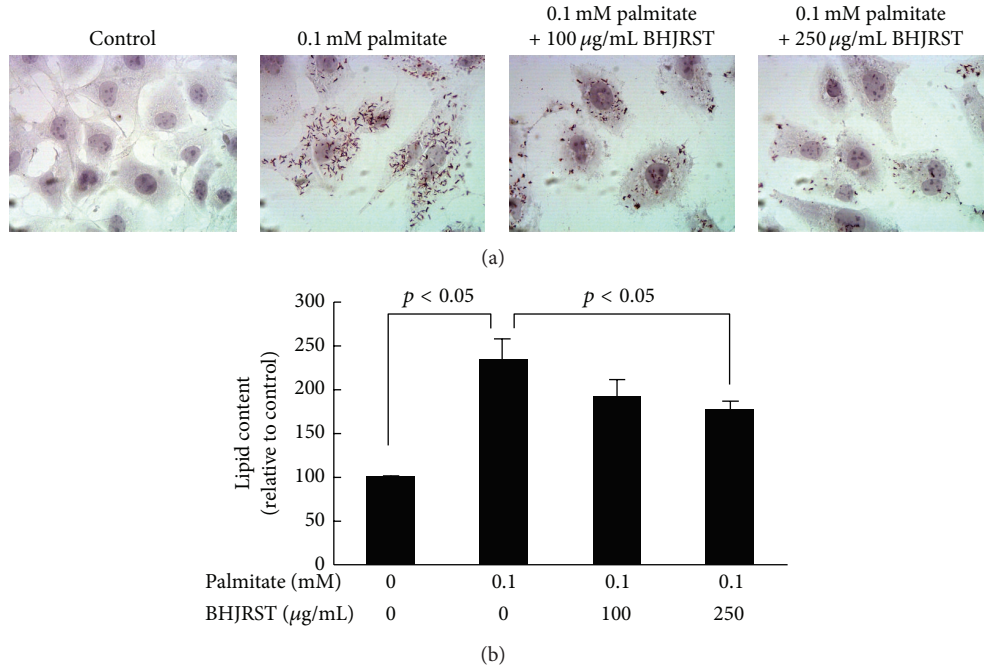

Figure 4: BHJRST inhibits palmitate-induced cellular lipid accumulation. (a) HuS-E/2 cells were treated with the indicated concentrations of BHJRST and palmitate in glucose-free PH medium for 24 h; then, images of the Oil Red O-stained cells were captured using a microscope at 400x original magnification. (b) HuS-E/2 cells were incubated for 24 h with the indicated concentrations of BHJRST and palmitate as above; then, quantitative analysis of lipid deposition in the Oil Red O-stained cells was performed. The data represent the mean ± SD for three independent experiments.

2000 μg/mL. Palmitate (0.1 mM) alone or in combination with 100 or 250 μg/mL of BHJRST also had no cytotoxic effect (Figure 3(b)). BHJRST concentrations of 100 and 250 μg/mL were therefore used in subsequent studies.

3.4. BHJRST Inhibits Palmitate-Induced Cellular Lipid Accumulation. To examine the ability of BHJRST to inhibit palmitate-induced lipid accumulation, HuS-E/2 cells were incubated in glucose-free PH medium alone or containing 0.1 mM palmitate with or without 100 or 250 μg/mL of BHJRST, then total lipid levels were measured by Oil Red O staining. As shown in Figure 4(a), treatment with 250 μg/mL of BHJRST significantly reduced palmitate-induced cellular lipid accumulation. These results were confirmed by quantification of the intracellular lipid content (Figure 4(b)).

3.5. BHJRST Stimulates AMPK Phosphorylation and ATGL Expression under High Fat Conditions. Having shown that BHJRST had an inhibitory effect on the palmitate-induced increase in hepatocyte lipid levels, the possible mechanisms responsible for this effect were assessed. Since AMPK responds to changes in cellular energy status [14] and has

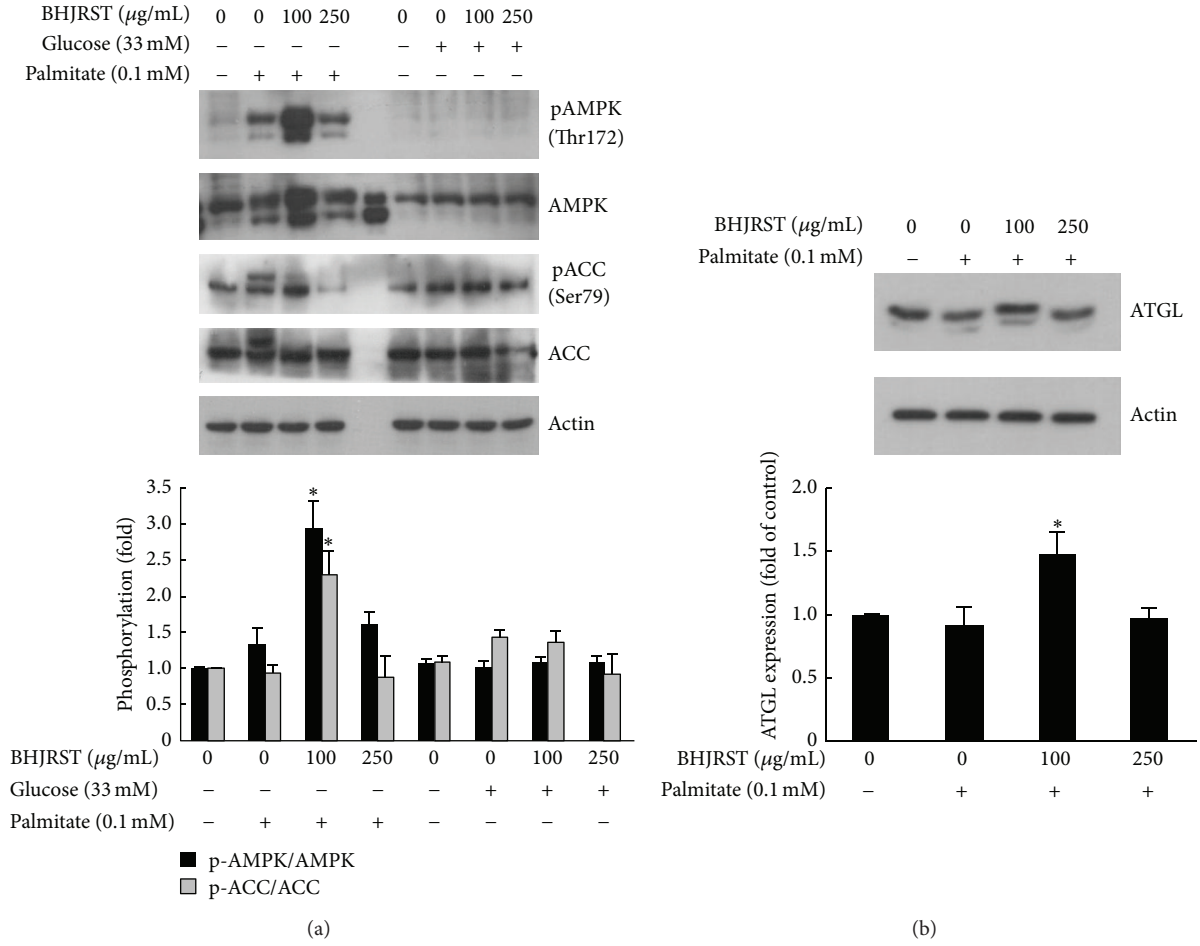

Figure 5: BHJRST stimulates AMPK phosphorylation and ATGL expression under high fat conditions. (a) HuS-E/2 cells were left untreated or were incubated for 24 h with or without 0.1 mM palmitate in glucose-free PH medium with or without BHJRST (100 or 250 μg/mL) (left section) or in PH medium containing 33 mM glucose with or without BHJRST (100 or 250 μg/mL) (right section); then, they were analyzed for phosphorylation of AMPK at Thr172 and ACC at Ser-79, total AMPK and ACC, and actin. Representative immunoblots are shown in the upper panel and the densitometric analysis of AMPK and ACC phosphorylation is shown in the lower panel; the results are the mean ± SD for three independent experiments for the intensity of the phosphorylated band divided by that for the "total" band expressed as a fold value of the control value. (b) Western blot analysis of the expression of ATGL and actin in untreated HuS-E/2 cells and cells incubated for 24 h with 0.1 mM palmitate and 0, 100, or 250 μg/mL of BHJRST as above. The upper panel shows a representative blot and the lower panel shows the quantitative analysis of ATGL expression normalized to actin levels and expressed as a fold value compared to the control value. The data represent the mean ± SD for three independent experiments. $^{*}p < 0.05$ versus control.

been suggested to play a crucial role in regulating fat metabolism in the liver, the effect of BHJRST on AMPK activation in HuS-E/2 cells was examined. Activation of AMPK, which correlates tightly with phosphorylation at Thr-172, and inactivation of its primary downstream target enzyme ACC by phosphorylation at Ser-79 were assessed by measuring phosphorylation at these sites by western blotting. To determine whether BHJRST increased phospho-AMPK levels, cells were incubated in glucose-free PH medium alone or containing 0.1 mM palmitate in the presence or absence of 100 and 250 μg/mL of BHJRST or in high glucose (33 mM) medium (glucose-free PH medium with 33 mM glucose added) in the presence or absence of 100 and 250 μg/mL of BHJRST. As shown in Figure 5(a), 100 μg/mL, but not 250 μg/mL, of BHJRST significantly increased AMPK phosphorylation at Thr-172 in fatty acid-overloaded HuS-E/2 cells, but not in high glucose-treated cells, and the increased AMPK phosphorylation was accompanied by a significant increase in ACC phosphorylation at Ser-79, indicating that BHJRST-induced activation of AMPK led to inhibition of ACC.

To determine whether BHJRST also induced ATGL expression in the high fat condition, cells were incubated in glucose-free PH medium alone or containing 0.1 mM palmitate with or without 100 or 250 μg/mL of BHJRST. As shown in Figure 5(b), treatment with 100 μg/mL, but not 250 μg/mL, of BHJRST increased ATGL protein levels in HuS-E/2 cells. These results show that, in vitro, AMPK activation by BHJRST increases ATGL expression under high fat conditions.

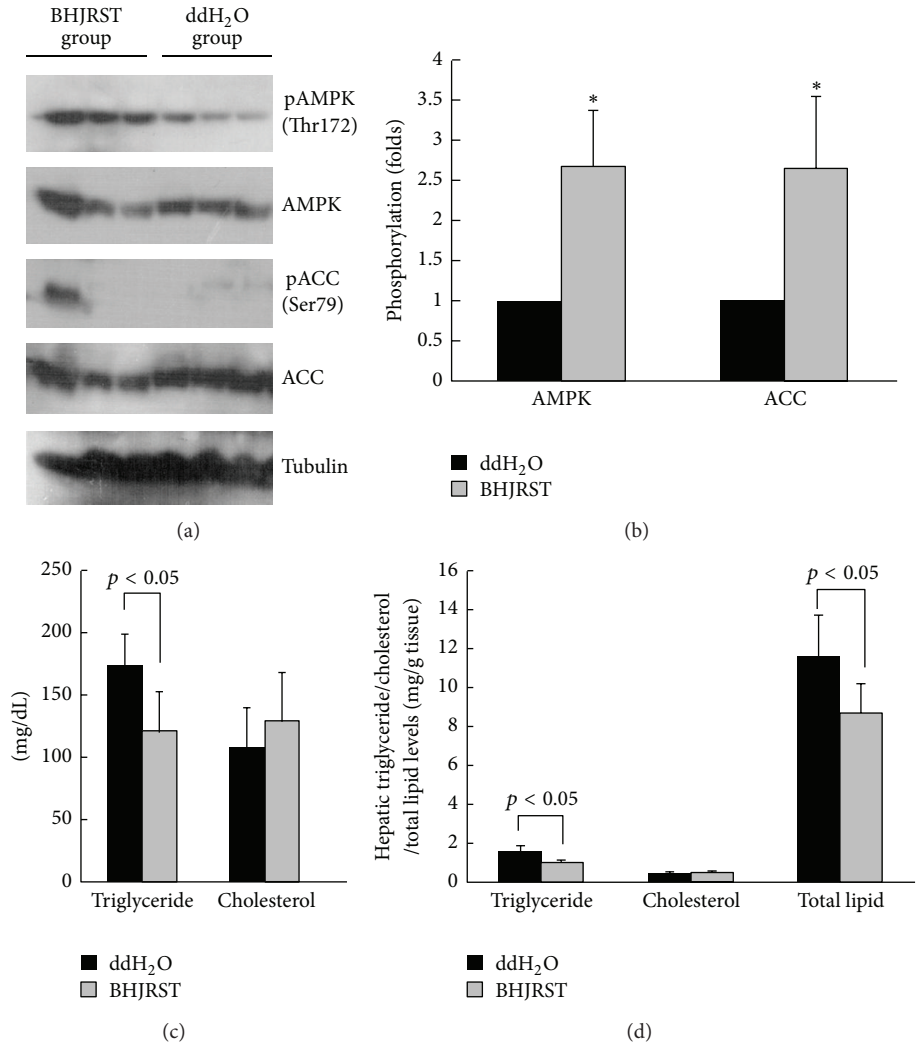

Figure 6: BHJRST treatment of db/db mice stimulates AMPK phosphorylation and reduces liver lipid accumulation. Animals (5 per group) were given BHJRST or double-distilled water ($n = 5$) twice daily by gavage for 6 weeks; then, they were euthanized for analysis of liver tissues and serum, as described in Section 2. (a) Representative immunoblots of liver for phosphorylation for AMPK and ACC, total AMPK and ACC, and tubulin. (b) Densitometric analysis of phosphorylation of AMPK and ACC levels. The results are the mean ± SD for the intensity of the phosphorylated band divided by that for the "total" band expressed as a fold value of the control value. (c) Serum triglyceride and cholesterol levels. The data represent the mean ± SD. (d) Hepatic triglyceride, cholesterol, and total lipid levels. The data represent the mean ± SD. In (b–d), the p value compared to the control group is shown either as a value or as $^{*}p < 0.05$.

3.6. BHJRST Treatment Stimulates AMPK Phosphorylation and Reduces Liver Lipid Accumulation in db/db Mice. The db/db mouse has high plasma levels of triglyceride and cholesterol and is a good model for diabetic dyslipidemia [22]. To examine whether BHJRST treatment could prevent liver lipid accumulation in vivo, we administered BHJRST (900 mg BHJRST/kg) or double-distilled water (control) twice daily by gavage for 6 weeks to male db/db mice fed a standard diet. Consistent with the upregulated AMPK phosphorylation seen in vitro, as shown in Figures 6(a) and 6(b), BHJRST treatment resulted in significantly increased AMPK phosphorylation at The-172 in liver tissue lysates and also in significantly increased ACC phosphorylation at Ser-79. To test the effects of BHJRST on lipid homeostasis, we next measured serum and hepatic lipid levels. Figure 6(c) shows that the BHJRST-treated group had significantly lower serum levels of triglyceride compared to the controls, while Figure 6(d) shows that BHJRST administration also resulted in decreases of 40.4% in hepatic triglyceride levels and 25.5% in hepatic total lipid levels. Together, these data suggest that BHJRST induces activation of AMPK, which translates into inhibition of ACC and leads to a decrease in hepatic fatty acid synthesis and lipid accumulation.

4. Discussion

Fatty liver is characterized by increased levels of hepatocellular lipids and is frequently associated with steatohepatitis and hepatocellular injury, which eventually can result in severe liver damage, including bridging fibrosis and cirrhosis [27].

Current treatment strategies aim to improve insulin resistance by weight loss and exercise, improving insulin sensitivity by the use of insulin-sensitizing agents (e.g., pioglitazone) and reducing oxidative stress by the use of antioxidants, such as vitamin E. Some Chinese medicines with hypolipidemic, antidiabetic, and antiobesity effects have been used by traditional Chinese medicine doctors for over a thousand years. However, their therapeutic mechanism remains unclear. Bai-Hu-Jia-Ren-Shen-Tang (BHJRST) is one of the most common herbal medicines used to treat T2DM patients in Taiwan [19]. These findings prompted us to ask whether BHJRST could reduce the hepatic fat accumulation associated with obesity and to determine the mechanisms responsible for the therapeutic effect of BHJRST in fatty liver disease. Here, we report the new finding that BHRST inhibits cellular lipid accumulation through activation of AMPK. In the liver, the AMPK complex, an evolutionally conserved serine/threonine heterotrimer kinase complex [28], is emerging as a possible target molecule for antiobesity therapy, as its activation results in increased fatty acid oxidation and decreased lipid synthesis [29]. In addition, inactivation of ACC reduces the synthesis of malonyl-CoA and activates fatty acid oxidation [30].

BHJRST is an enhanced formula in which Ginseng Radix (Ren-Shen) is added to the Bai-Hu-Tang (BHT) formula. Traditionally, BHJRST, but not BHT, is used to decrease thirst in diabetes patients. In a recent study, a water extract of ginseng root was found to have a fat-lowering action in vivo [31]. Ginsenoside Rb1 (Rb1), a compound extracted from ginseng root, has a glucose-lowering action in vitro [32] and significantly reduces body weight, improves glucose tolerance, and enhances insulin action in high fat diet-induced obese rats [33]. In our study, we found that if the content of Gypsum Fibrosum (Shi-Gao) in BHJRST was reduced from 16 g to 10 g, the concentrations of ginsenoside Rg3 and mangiferin in the final extract were reduced, as shown by HPLC analysis (data not shown), suggesting that Gypsum Fibrosum (Shi-Gao) may help in dissolving these ingredients.

Normal human hepatocytes are the ideal system in which to study the liver-specific metabolism of lipid, but when cultured in vitro, they proliferate poorly and divide only a few times. The most common cell line used to study liver lipid metabolism is the hepatoma-derived HepG2 cell line, but there is concern about its use, as it was derived from liver tissue with differentiated hepatocellular carcinoma and is probably genetically distinct from primary hepatocytes. In this study, we used the HuS-E/2 cell line, which was derived from normal hepatocytes and has been shown to be phenotypically and functionally similar to primary hepatocytes [21, 34]. We investigated the ability of BHJRST to prevent fat deposition using an HuS-E/2 cell model of fatty liver induced by palmitate and found that 0.1 mM palmitate resulted in marked fat accumulation, as demonstrated by Oil Red O staining (Figure 2), and that coaddition of 100 μg/mL of BHJRST significantly reduced the amount of accumulated lipid (Figure 4), without having a cytotoxic effect (Figure 3). In addition, treatment with 100 μg/mL of BHJRST increased phosphorylation of AMPK and ACC and upregulated ATGL protein expression in HuS-E/2 cells (Figure 5). Thus, we demonstrated that HuS-E/2 cells develop palmitate-induced hepatic lipid accumulation and that BHJRST has a protective effect associated with a significant increase in hepatic AMPK activation and hepatic ATGL expression.

Animal models of fatty liver disease can arise as a result of induced genetic mutation and most published studies have employed the leptin-resistant (db/db) mouse [35]. In this study, we used db/db mice and showed that BHJRST also activated AMPK and reduced ACC activation and lipid levels in vivo (Figure 6). These results were confirmed by quantification of intracellular triglyceride and total lipid levels. We suggest that AMPK and ACC are the critical components involved in the BHJRST-induced inhibition of lipid synthesis in the db/db mice liver, implying a role of BHJRST in energy balance control by modulating lipid biosynthesis. It has been demonstrated that AMPK increases glucose transporter 4 (GLUT 4) transposition and GLUT 4 gene transcription in muscle and liver [36], suggesting a possible mechanism by which BHJRST modulates homoeostasis of lipid and carbohydrate metabolism in living cells.

ATGL is important for basal lipolysis and is responsible for the first step in the breakdown of fat. Regulation of ATGL expression is impaired with age and could contribute to the observed increased difficulty in metabolizing lipids [37]. It is the rate-limiting enzyme in triglyceride hydrolysis, which produces free fatty acids, which are released into the medium and do not accumulate in cells [10]. The findings agree with the fact that calorie restriction and exercise can be used to treat nonalcoholic fatty liver disease, as both activate AMPK. Our data are in agreement with the reports of Reid et al. and Caimari et al. showing that an increase in ATGL levels results in decreased hepatic lipogenesis and liver triglyceride accumulation and secretion.

Palmitate, a lipotoxic fatty acid, increases oxidative stress and ROS production and induces insulin resistance in hepatocytes [38]. Indeed, it has been shown that ROS levels are increased in patients and mice with clinical conditions associated with insulin resistance, such as obesity and T2DM, that palmitate treatment of cultured adipocytes induces cellular oxidative stress and ROS generation, and that a decrease in ROS production in obese mice contributes to a reduction in palmitate-induced lipid accumulation [39]. It will be very interesting to examine whether BHJRST is an antioxidant and can lower ROS production.

In summary, we have demonstrated that activation of the AMPK signaling pathway plays a critical role in the inhibitory effect of BHJRST on lipid metabolism in vitro and in vivo. These findings provide molecular evidence for the use of BHJRST as therapy for the management of fatty liver diseases. Unraveling the molecular mechanisms by which BHJRST controls energy balance by modulating lipid biosynthesis will provide new insights into the pathogenesis of these diseases and open avenues for novel therapeutic strategies.

Abbreviations

ACC: Acetyl-CoA carboxylase
AMPK: AMP-activated protein kinase
ATGL: Adipose triglyceride lipase
BHJRST: Bai-Hu-Jia-Ren-Shen-Tang

NAFLD: Nonalcoholic fatty liver disease
PH medium: Primary hepatocyte medium
T2DM: Type 2 diabetes mellitus.

Conflict of Interests

The authors declare that there is no conflict of interests regarding the publication of this paper.

Acknowledgments

This work was supported by Research Grants MOST102-2320-B-077-004-, MOST100-2313-B-134-001-MY3, and MOST103-2313-B-134-001-MY3 from the Ministry of Science and Technology, Taiwan, and Grants NRICM102-DBCM-06-F3, MOHW103-NRICM-C-305-122106, and MOHW103-NRICM-C-305-122606 from the National Research Institute of Chinese Medicine, Taiwan.

References

[1] W. Dunn, R. Xu, D. L. Wingard et al., "Suspected nonalcoholic fatty liver disease and mortality risk in a population-based cohort study," *The American Journal of Gastroenterology*, vol. 103, no. 9, pp. 2263–2271, 2008.

[2] C. Postic and J. Girard, "Contribution of de novo fatty acid synthesis to hepatic steatosis and insulin resistance: lessons from genetically engineered mice," *Journal of Clinical Investigation*, vol. 118, no. 3, pp. 829–838, 2008.

[3] H. C. Masuoka and N. Chalasani, "Nonalcoholic fatty liver disease: an emerging threat to obese and diabetic individuals," *Annals of the New York Academy of Sciences*, vol. 1281, no. 1, pp. 106–122, 2013.

[4] B. W. Smith and L. A. Adams, "Nonalcoholic fatty liver disease and diabetes mellitus: pathogenesis and treatment," *Nature Reviews Endocrinology*, vol. 7, no. 8, pp. 456–465, 2011.

[5] S. Parekh and F. A. Anania, "Abnormal lipid and glucose metabolism in obesity: implications for nonalcoholic fatty liver disease," *Gastroenterology*, vol. 132, no. 6, pp. 2191–2207, 2007.

[6] L. A. Adams and P. Angulo, "Treatment of non-alcoholic fatty liver disease," *Postgraduate Medical Journal*, vol. 82, no. 967, pp. 315–322, 2006.

[7] V. Nobili, M. Manco, R. Devito et al., "Lifestyle intervention and antioxidant therapy in children with nonalcoholic fatty liver disease: a randomized, controlled trial," *Hepatology*, vol. 48, no. 1, pp. 119–128, 2008.

[8] E. M. Brunt, "Histopathology of non-alcoholic fatty liver disease," *Clinics in Liver Disease*, vol. 13, no. 4, pp. 533–544, 2009.

[9] C. Carter-Kent, L. M. Yerian, E. M. Brunt et al., "Nonalcoholic steatohepatitis in children: a multicenter clinicopathological study," *Hepatology*, vol. 50, no. 4, pp. 1113–1120, 2009.

[10] B. N. Reid, G. P. Ables, O. A. Otlivanchik et al., "Hepatic overexpression of hormone-sensitive lipase and adipose triglyceride lipase promotes fatty acid oxidation, stimulates direct release of free fatty acids, and ameliorates steatosis," *Journal of Biological Chemistry*, vol. 283, no. 19, pp. 13087–13099, 2008.

[11] J. W. E. Jocken, D. Langin, E. Smit et al., "Adipose triglyceride lipase and hormone-sensitive lipase protein expression is decreased in the obese insulin-resistant state," *The Journal of Clinical Endocrinology & Metabolism*, vol. 92, no. 6, pp. 2292–2299, 2007.

[12] R. Zechner, P. C. Kienesberger, G. Haemmerle, R. Zimmermann, and A. Lass, "Adipose triglyceride lipase and the lipolytic catabolism of cellular fat stores," *Journal of Lipid Research*, vol. 50, no. 1, pp. 3–21, 2009.

[13] B. B. Kahn, T. Alquier, D. Carling, and D. G. Hardie, "AMP-activated protein kinase: ancient energy gauge provides clues to modern understanding of metabolism," *Cell Metabolism*, vol. 1, no. 1, pp. 15–25, 2005.

[14] D. G. Hardie, "AMP-activated/SNF1 protein kinases: conserved guardians of cellular energy," *Nature Reviews Molecular Cell Biology*, vol. 8, no. 10, pp. 774–785, 2007.

[15] G. Zhou, R. Myers, Y. Li et al., "Role of AMP-activated protein kinase in mechanism of metformin action," *Journal of Clinical Investigation*, vol. 108, no. 8, pp. 1167–1174, 2001.

[16] G. Schimmack, R. A. DeFronzo, and N. Musi, "AMP-activated protein kinase: role in metabolism and therapeutic implications," *Diabetes, Obesity and Metabolism*, vol. 8, no. 6, pp. 591–602, 2006.

[17] B. Viollet, M. Foretz, B. Guigas et al., "Activation of AMP-activated protein kinase in the liver: a new strategy for the management of metabolic hepatic disorders," *Journal of Physiology*, vol. 574, no. 1, pp. 41–53, 2006.

[18] C.-C. Chen, C.-Y. Hsiang, A.-N. Chiang, H.-Y. Lo, and C.-I. Li, "Peroxisome proliferator-activated receptor gamma transactivation-mediated potentiation of glucose uptake by Bai-Hu-Tang," *Journal of Ethnopharmacology*, vol. 118, no. 1, pp. 46–50, 2008.

[19] C.-Y. Huang, Y.-T. Tsai, J.-N. Lai, and F.-L. Hsu, "Prescription pattern of Chinese herbal products for diabetes mellitus in Taiwan: a population-based study," *Evidence-Based Complementary and Alternative Medicine*, vol. 2013, Article ID 201329, 10 pages, 2013.

[20] I. Kimura, N. Nakashima, Y. Sugihara, C. Fu-Jun, and M. Kimura, "The antihyperglycaemic blend effect of traditional Chinese medicine byakko-ka-ninjin-to on alloxan and diabetic KK-CA(y) mice," *Phytotherapy Research*, vol. 13, no. 6, pp. 484–488, 1999.

[21] H. H. Aly, K. Watashi, M. Hijikata et al., "Serum-derived hepatitis C virus infectivity in interferon regulatory factor-7-suppressed human primary hepatocytes," *Journal of Hepatology*, vol. 46, no. 1, pp. 26–36, 2007.

[22] K. Kobayashi, T. M. Forte, S. Taniguchi, B. Y. Ishida, K. Oka, and L. Chan, "The db/db mouse, a model for diabetic dyslipidemia: molecular characterization and effects of western diet feeding," *Metabolism: Clinical and Experimental*, vol. 49, no. 1, pp. 22–31, 2000.

[23] S. P. Cousin, S. R. Hügl, C. E. Wrede, H. Kajio, M. G. Myers Jr., and C. J. Rhodes, "Free fatty acid-induced inhibition of glucose and insulin-like growth factor I-induced deoxyribonucleic acid synthesis in the pancreatic β-cell line INS-1," *Endocrinology*, vol. 142, no. 1, pp. 229–240, 2001.

[24] J. L. Ramírez-Zacarías, F. Castro-Muñozledo, and W. Kuri-Harcuch, "Quantitation of adipose conversion and triglycerides by staining intracytoplasmic lipids with Oil red O," *Histochemistry*, vol. 97, no. 6, pp. 493–497, 1992.

[25] E. G. Bligh and W. J. A. Dyer, "A rapid method of total lipid extraction and purification," *Canadian Journal of Biochemistry and Physiology*, vol. 37, no. 8, pp. 911–917, 1959.

[26] V. Zámbó, L. Simon-Szabó, P. Szelényi, É. Kereszturi, G. Bánhegyi, and M. Csala, "Lipotoxicity in the liver," *World Journal of Hepatology*, vol. 5, no. 10, pp. 550–557, 2013.

[27] B. A. Neuschwander-Tetri and S. H. Caldwell, "Nonalcoholic steatohepatitis: summary of an AASLD single topic conference," *Hepatology*, vol. 37, no. 5, pp. 1202–1219, 2003.

[28] D. G. Hardie, "AMPK and SNF1: snuffing out stress," *Cell Metabolism*, vol. 6, no. 5, pp. 339–340, 2007.

[29] C.-L. Lin, H.-C. Huang, and J.-K. Lin, "Theaflavins attenuate hepatic lipid accumulation through activating AMPK in human HepG2 cells," *Journal of Lipid Research*, vol. 48, no. 11, pp. 2334–2343, 2007.

[30] J. D. McGarry and N. F. Brown, "The mitochondrial carnitine palmitoyltransferase system. From concept to molecular analysis," *European Journal of Biochemistry*, vol. 244, no. 1, pp. 1–14, 1997.

[31] L. Shen, Y. Xiong, D. Q.-H. Wang et al., "Ginsenoside Rb1 reduces fatty liver by activating AMP-activated protein kinase in obese rats," *Journal of Lipid Research*, vol. 54, no. 5, pp. 1430–1438, 2013.

[32] S. Park, I. S. Ahn, D. Y. Kwon, B. S. Ko, and W. K. Jun, "Ginsenosides Rb1 and Rg1 suppress triglyceride accumulation in 3T3-L1 adipocytes and enhance beta-cell insulin secretion and viability in min6 cells via PKA-dependent pathways," *Bioscience, Biotechnology and Biochemistry*, vol. 72, no. 11, pp. 2815–2823, 2008.

[33] Y. Xiong, L. Shen, K. J. Liu et al., "Antiobesity and antihyperglycemic effects of ginsenoside Rb1 in rats," *Diabetes*, vol. 59, no. 10, pp. 2505–2512, 2010.

[34] H.-C. Huang, C.-C. Chen, W.-C. Chang, M.-H. Tao, and C. Huang, "Entry of hepatitis B virus into immortalized human primary hepatocytes by clathrin-dependent endocytosis," *Journal of Virology*, vol. 86, no. 17, pp. 9443–9453, 2012.

[35] Q. M. Anstee and R. D. Goldin, "Mouse models in non-alcoholic fatty liver disease and steatohepatitis research," *International Journal of Experimental Pathology*, vol. 87, no. 1, pp. 1–16, 2006.

[36] R. Burcelin, V. Crivelli, C. Perrin et al., "GLUT4, AMP kinase, but not the insulin receptor, are required for hepatoportal glucose sensor-stimulated muscle glucose utilization," *The Journal of Clinical Investigation*, vol. 111, no. 10, pp. 1555–1562, 2003.

[37] A. Caimari, P. Oliver, and A. Palou, "Impairment of nutritional regulation of adipose triglyceride lipase expression with age," *International Journal of Obesity*, vol. 32, no. 8, pp. 1193–1200, 2008.

[38] S. Nakamura, T. Takamura, N. Matsuzawa-Nagata et al., "Palmitate induces insulin resistance in H4IIEC3 hepatocytes through reactive oxygen species produced by mitochondria," *The Journal of Biological Chemistry*, vol. 284, no. 22, pp. 14809–14818, 2009.

[39] S. Furukawa, T. Fujita, M. Shimabukuro et al., "Increased oxidative stress in obesity and its impact on metabolic syndrome," *The Journal of Clinical Investigation*, vol. 114, no. 12, pp. 1752–1761, 2004.

Hindawi Publishing Corporation
Evidence-Based Complementary and Alternative Medicine
Volume 2015, Article ID 859048, 11 pages
http://dx.doi.org/10.1155/2015/859048

Research Article

Oxidative Stress Type Influences the Properties of Antioxidants Containing Polyphenols in RINm5F Beta Cells

Nathalie Auberval,[1] Stéphanie Dal,[1] William Bietiger,[1] Elodie Seyfritz,[1] Jean Peluso,[2] Christian Muller,[2] Minjie Zhao,[3] Eric Marchioni,[3] Michel Pinget,[1,4,5] Nathalie Jeandidier,[1,4,5] Elisa Maillard,[1] Valérie Schini-Kerth,[5] and Séverine Sigrist[1]

[1] *UMR DIATHEC, EA 7294, Centre Européen d'Etude du Diabète, Université de Strasbourg, Fédération de Médecine Translationnelle de Strasbourg, boulevard René Leriche, 67200 Strasbourg, France*
[2] *UMR 7200 Laboratoire d'Innovation Thérapeutique, Faculté de Pharmacie, Université de Strasbourg, 67 400 Illkirch, France*
[3] *Chimie Analytique des Molécules Bioactives (CAMBA), Institut Pluridisciplinaire Hubert Curien (UMR 7178 CNRS/UDS), 74 route du Rhin, 67400 Illkirch, France*
[4] *Departement d'Endocrinologie, Diabète, Maladies Métaboliques, Pôle NUDE, Hôpitaux Universitaires de Strasbourg (HUS), 67 000 Strasbourg, France*
[5] *UMR 7175 CNRS, Pharmacologie et Physico-Chimie, Faculté de Pharmacie, Université de Strasbourg, 67 400 Illkirch, France*

Correspondence should be addressed to Séverine Sigrist; s.sigrist@ceed-diabete.org

Received 11 February 2015; Accepted 4 June 2015

Academic Editor: Akhilesh K. Tamrakar

The *in vitro* methods currently used to screen bioactive compounds focus on the use of a single model of oxidative stress. However, this simplistic view may lead to conflicting results. The aim of this study was to evaluate the antioxidant properties of two natural extracts (a mix of red wine polyphenols (RWPs) and epigallocatechin gallate (EGCG)) with three models of oxidative stress induced with hydrogen peroxide (H_2O_2), a mixture of hypoxanthine and xanthine oxidase (HX/XO), or streptozotocin (STZ) in RINm5F beta cells. We employed multiple approaches to validate their potential as therapeutic treatment options, including cell viability, reactive oxygen species production, and antioxidant enzymes expression. All three oxidative stresses induced a decrease in cell viability and an increase in apoptosis, whereas the level of ROS production was variable depending on the type of stress. The highest level of ROS was found for the HX/XO-induced stress, an increase that was reflected by higher expression antioxidant enzymes. Further, both antioxidant compounds presented beneficial effects during oxidative stress, but EGCG appeared to be a more efficient antioxidant. These data indicate that the efficiency of natural antioxidants is dependent on both the nature of the compound and the type of oxidative stress generated.

1. Introduction

Oxidative stress can be defined as an imbalance between pro- and antioxidants and is often associated with free radical [1] overproduction and/or defective physiological defence mechanisms resulting in the cell being overwhelmed with oxidizing radicals [2]. This phenomenon involves reactive oxygen species [3], such as superoxide anion (O_2^{-}) [4], hydroxyl radical ($OH^{\bullet}$) [1], singlet oxygen ($^1O_2$), and hydrogen peroxide (H_2O_2) [5]. High concentrations of ROS can cause lipid peroxidation, protein oxidation or denaturation, nuclear acid oxidation, and many other macromolecular changes that can lead to serious cellular damage [6]. Such ROS-related damage has been identified to occur in numerous diseases, including metabolic syndrome, diabetes, multiple types of cancer, Alzheimer's disease, and cardiovascular diseases.

Further, obesity, hyperglycemia, and hyperlipidemia have also been shown to promote oxidative stress through elevated ROS production [7], which is likely due to the higher occurrence of mitochondrial dysfunction and superoxide production that has been associated with fat accumulation [8]. Under normal conditions, enzymatic defence mechanisms [9], such

as scavenging by superoxide dismutase [10] and glutathione peroxidase, are active in most types of cells to degrade ROS and prevent cellular damage. However, the antioxidant defence system functioning in insulin producing beta cells, which have been linked to both diabetes and obesity, is known to be very weak [1, 11, 12], making these beta cells highly sensitive to oxidative stress, which can lead to cell death and disease [5]. Notably, the prevention of ROS-related beta cell destruction using antioxidant compounds has been identified to be an effective strategy to delay the onset of diabetes [10, 13, 14].

In fact, several dietary plants that have pharmacological properties shown to prevent apoptosis induced by oxidative stress are under investigation as treatment options for diabetes [9, 15]. Some of these plants appear to utilize antioxidant mechanisms related to their rich flavonoid (polyphenols family) content. The unique chemical structures and redox properties of these polyphenols [16] allow them to scavenge free radicals as well as chelate transition metals and inhibit prooxidant enzymes, such as inducible nitric oxide synthase (iNOS) in macrophages [17]. For example, tea catechins, especially epigallocatechin gallate (EGCG), appear to have antiobesity and antidiabetic properties [11, 18], and the beneficial effects of red wine polyphenols (RWPs) in diabetics have been widely documented [19]. RWPs are qualitatively and quantitatively rich in polyphenols, particularly anthocyanins, flavonol, and stilbene. In general, polyphenols are characterized by antioxidant activity and *in vitro* studies have shown that they act as radical peroxyl scavengers [20]. However, most of these *in vitro* studies were performed using a single model of stress, such as hypoxanthine/xanthine oxidase (HX/XO) [21] or H_2O_2 [22, 23], whereby HX/XO was a direct supplier in O_2^-, while H_2O_2 activated NADPH oxidase or NOS which produce O_2^-. In diabetes, in addition to $O_2^{-\bullet}$, generated by chronic hyperglycemia [4], other types of ROS are produced during insulin resistance and hyperinsulinism development [24]. Therefore, a single model of oxidative stress does not reflect the full complexity of this disease. In more relevant studies, oxidative stress was induced by multiple mechanisms using cytokines [25], alloxan [26], or streptozotocin [9, 27]. Notably, STZ is an NO donor and induces the formation of several kinds of ROS (e.g., $O_2^{-\bullet}$, H_2O_2, $OH^\bullet$, and peroxynitrite; Szkudelski, 2001) as well as DNA alkylation and tricarboxylic citric acid (TCA) cycle inhibition, all of which lead to cell damage and death. Thus, STZ can be used to induce multiple levels of oxidative stress in order to more appropriately mimic that which occurs during diabetes *in vivo*.

Obviously the oxidative stress observed during diabetes is complex, and the screening of antioxidant compounds cannot be reduced to the use of a single chemical stress. It is therefore important to validate the antioxidant properties of each antioxidant treatment compound, such as the RWPs, using both simple (single) and complex (multiple) oxidative mechanisms. The aim of this study was to create three *in vitro* models of oxidative stress (one with single radicals produced by HX/XO and two with more complex oxidative reactions using H_2O_2 and STZ) in order to assess the antioxidant efficiencies of a RWP extract and a purified extract of EGCG.

2. Materials and Methods

2.1. Cell Line. Rat insulinoma clone m5F (RINm5F) [28] cells were purchased from the American Type Culture Collection (ATCC, Manassas, USA). Cells were cultivated in Roswell Park Memorial Institute (RPMI-1640) medium supplemented with 10% fetal bovine serum (FBS; Sigma, St. Louis, USA) and 1% antibiotic-antimycotic (ABAM; Gibco, Invitrogen, Grand Island, USA). Cells were grown in a humidified 5% CO_2 atmosphere at 37°C and trypsinized at 80% confluence using 0.05% trypsin EDTA (Sigma). Medium was refreshed every 48 hours.

2.2. Antioxidant Molecules. The RWP extract used in this study was generously given by Dr. M. Moutounet (National Institute of Agronomic Research, Montpellier, France). Red wine phenolic extract dry powder was obtained from French red wine (Corbières AOC) and analyzed by Dr. P.-L. Teissedre (Département d'Oenologie, Bordeaux, France). The extract was prepared as previously described [29]: briefly, phenolic compounds were adsorbed on a preparative column and, then, alcohol desorbed; the alcoholic eluent was gently evaporated; the concentrated residue was lyophilized and finely sprayed to obtain the phenolic extract dry powder. One liter of red wine produced 2.9 g of phenolic extract, which contained 471 mg/g of total phenolic compounds expressed as gallic acid. Phenolic levels in phenolic extract were measured by HPLC. The extract contained 8.6 mg/g catechin, 8.7 mg/g epicatechin, dimers (B1: 6.9 mg/g, B2: 8.0 mg/g, B3: 20.7 mg/g, and B4: 0.7 mg/g), anthocyanins (malvidin-3-glucoside: 11.7 mg/g, peonidin-3-glucoside: 0.66 mg/g, and cyanidin-3-glucoside: 0.06 mg/g), and phenolic acids (gallic acid: 5.0 mg/g, caffeic acid: 2.5 mg/g, and caftaric acid: 12.5 mg/g).

A stock solution of this RWP extract was prepared by diluting 10 mg/mL in a 1 : 1 mixture of distilled water and 100% ethanol. The EGCG extract was a pure form of green tea Teavigo (DSM Nutritional Product, Gland, Switzerland). To confirm its purity, Teavigo was analysed using chromatographic separation on a octadecylsilyl silica gel LC column (l: 0.125 mm; d: 4; 0 mm; Thermo Scientific, France) with spherical particles. Mobile phase consisted of water : formic acid (0.1%, phase A) and methanol : formic acid (0.1%, phase B). A split system was used allowing the HPLC eluate to enter the MS detector at a flow rate of 0.2 mL/min. The injection volume was 20 μL. UV spectral data were acquired at 275 nm (the chromatogram was presented in Supplementary Material available online at http://dx.doi.org/10.1155/2015/859048). The extract was prepared at a 10 mg/mL stock solution concentration which was then diluted in 1× phosphate-buffered saline (PBS), pH 7.4 (Gibco, Invitrogen) as previously described [18]. Cells were cultured for 48 hours before all treatments. The antioxidant compounds (200 to 1000 pg/mM for the EGCG and 100 to 1000 μg/mL for the RWPs) were added to cells seeded in 96-well treated microplates (BD Falcon, Franklin Lakes, USA) at 30,000 cells/well and incubated for 1 hour. The toxicity of the EGCG and RWP extracts was then assessed as described below.

2.3. Oxidative Stress Induction and Protective Effects of EGCG and RWPs. Oxidative stress was induced in the RINm5F cells with (1) H_2O_2 using a 33% daily prepared solution [30] that was diluted with culture medium to multiple concentrations (1, 10, 25, and 40 μmol/L); (2) a mixture of various HX (mmol/L) to XO (mU/mL) ratios (0.05/2, 0.2/8, 0.25/10, and 0.3/12) isolated from butter milk [22]; and (3) a 40 μmol/L solution of STZ prepared in 0.1 mol/L citrate buffer solution, pH 4.2 (27, 25, and 40 μmol/L, prepared in pH 4.2 citrate buffer solution (0.1 mol/L)) [27]. All products were purchased from Sigma.

To evaluate the toxicity of the EGCG and RWP antioxidants alone, various concentrations (EGCG at 200, 500, and 1000 μg/mL; RWPs at 10, 50, 100, 150, and 200 μg/mL) were added to stressed and unstressed cells and incubated for 1 hour.

2.4. MTS Assay. Cell viability was assessed by measuring the mitochondrial activity with the CellTiter 96 AQueous One Solution Cell Proliferation Assay from Promega Corporation (Madison, USA). After treatment, 100 μL of culture medium containing 20 μL of 3-(4,5-dimethylthiazol-2-yl)-5-(3-carboxymethoxyphenyl)-2-(4-sulfophenyl)-2H-tetrazolium (MTS) was added. Cells were incubated for 2 hours at 37°C, in 5% CO_2, and the absorbance was measured at 490 nm with a Metertech 960 microplate reader (Metertech Inc., Taipei, Taiwan). The quantity of the formazan product was directly proportional to the mitochondrial activity related to number of living cells. Results are expressed as the percentage of cell viability compared to the appropriate negative controls.

2.5. Flow Cytometry

2.5.1. Caspase 8. Oxidative stress often affects the cells very quickly, making it difficult to identify the primary apoptotic effects of the ROS. Therefore, the expression and/or activity of initiator caspases, such as caspase 8 [31], are often used to study apoptosis in this context as they reflect the initial effects of oxidative stress. Here, the activity of caspase 8 was determined by flow cytometry using fluorescent inhibitor of activated caspase 8 (caspase 8 FAM; Millipore, Guava Technologies, Hayward, CA). Briefly, cells were seeded in 96-well treated microplates (BD Falcon, Franklin Lakes, USA) at 30,000 cells/well. After treatment, fresh medium supplemented with 10 μL of caspase inhibitor was added. After mixing, plates were incubated for 1 hour at 37°C and centrifuged for 5 minutes at 300 ×g. Cells were then resuspended and 200 μL of 7-aminoactinomycin D (7′AAD) was added and incubated for 10 minutes at room temperature in the dark before analysis. A Guava Easycyte microcapillary flow cytometer (Millipore) was used with laser excitation at 488 nm in order to detect caspase 8 FAM emission at 517 nm with carboxyfluorescein [6] according to the manufacturer's instructions. For each assay, 200 cellular events were collected. Results were analysed with CytoSoft software (Guava Technologies Inc., Hayward, CA, USA) and are expressed as the percentage of stained cells.

2.5.2. ROS Production. Cells were seeded in 24-well treated microplates (BD Falcon, Franklin Lakes, USA) at 500,000 cells/well. After treatment, 500 μL of fresh medium supplemented with 2′,7′-dichlorofluorescein diacetate (DCFH-DA; Sigma) at final concentration of 5 μM [32] was added. DCFH-DA is deacetylated by a membrane esterase, forming DCFH, which is then transformed by intracellular H_2O_2 to a fluorescent molecule [28]. Cells were incubated for 1 hour and then trypsinized. After centrifugation during 10 minutes (500 ×g), pellets were dissolved with 500 μL PBS and 200 μL of the cell solution was transferred to 96-well treated microplates. The suspended cells were then treated with 10 μL of propidium iodide [11] for 15 minutes and assayed for fluorescence by flow cytometry at 530 nm. Assays were analyzed with CytoSoft software and the results are expressed as a percentage of ROS production (DCF-labelled cells) compared to the appropriate negative controls.

2.6. Antioxidant Enzyme Expression: Catalase (CAT) and Manganese Superoxide Dismutase (MnSOD). Protein extracts were prepared from the treated cells using lysis buffer containing 20 mM Tris ultrapure pH 8 (Euromedex, Mundolsheim, France), 137 mM NaCl (Sigma), 1% Igepal CA-630 (Sigma), 31 mM phenyl methyl sulfonide fluoride (Eurobio, Les Ulis, France), and 10% glycerol (Sigma) with protease inhibitor Complete Mini 1X (Roche, Indianapolis, USA). The protein content of each was measured using the methods of Bradford [33].

A 50 μg aliquot of the total protein was then separated on 4–12% Bis-Tris Criterion XT Precast Gels (Bio-Rad), transferred to 0.45 μm nitrocellulose membranes (Bio-Rad), and detected with the following primary antibodies: anti-catalase produced in mouse (Sigma) or anti-MnSOD produced in rabbit (Sigma), each diluted to $1/1000^e$, as well as a $1/5000^e$ dilution of anti-β-actin monoclonal antibody produced in mouse. All antibodies were diluted in blocking buffer from the WesternBreeze Chemiluminescent Kit (Invitrogen, Grand Island, USA) overnight at 4°C. Secondary antibody solution (anti-mouse (1/2000) or anti-rabbit (1/4000) coupled to alkaline phosphatase) was incubated with the membranes for 30 minutes with continuous rotation as described in the kit. Membranes were then exposed with a Bio-Rad Chemi-Doc XRS System for 600 seconds, and the captured images were analysed using Quantity One software. Expression of CAT and MnSOD proteins was normalized to the quantity of β-actin and expressed as a percentage compared to the appropriate negative controls.

2.7. Statistical Analysis. Samples were assayed at least three times for each test and the results are given as the mean ± standard error (SEM). Data were analysed with one-way analysis of variance [34] when designated using the Statistica program (Statsoft©, Créteil, France). Treatment differences were subjected to Fischer's test with a 95% significance ($P < 0.05$) threshold.

3. Results

3.1. Cellular Effects of Various Oxidative Stressors. We first screened the cell viability following treatment with multiple

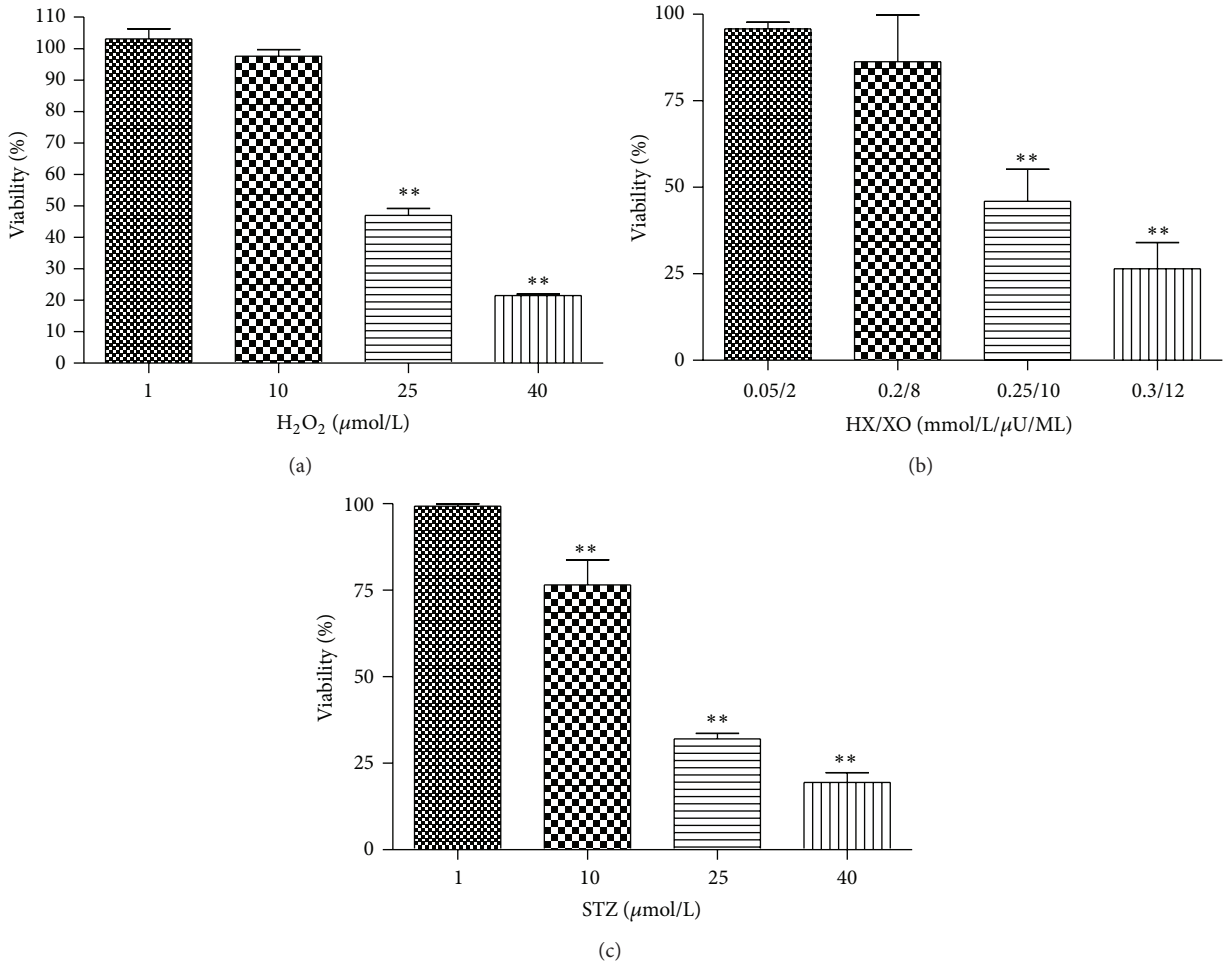

Figure 1: Effects of H_2O_2 (a), HX/XO (b), and STZ (c) on RINm5F cell viability. Values are given as the mean ± SEM for three different experiments. $n = 6$; $^{*}P < 0.05$ and $^{**}P < 0.01$ compared to the control cells.

concentrations of each oxidative molecule to determine the concentration of each that induced RINm5F cell death in at least 50% of the culture (Figure 1). H_2O_2 appears to induce a significant decrease in cell viability at concentrations above 25 μmol/mL ($P < 0.01$), with the lowest number of viable cells reaching 21.4 ± 0.5% at the 40 μmol/mL concentration (Figure 1(a)). Further, a ratio of 0.25 mmol/L of HX and 10 mU/mL of XO was sufficient to induce a significant loss of cell viability, resulting in only 45.9 ± 9.2% of the cells being viable at this ratio ($P < 0.01$) (Figure 1(b)). Finally, even though the 10 mmol/L concentration of STZ induced a significant decrease in cell viability, leaving only 76.5 ± 0.7% of the cells ($P < 0.01$), a more marked reduction of cell viability similar to that of the other oxidants was observed at 25 mmol/L, which resulted in only 32 ± 1.6% of the cells remaining alive in the culture ($P < 0.01$) (Figure 1(c)). Concentrations that induced a loss greater than 50% (25 μmol/L of H_2O_2, a ratio of 0.25 mmol/L of HX and 10 mU/mL of XO, and 25 mmol/L of STZ) were the sole concentrations used in the subsequent analyses to study the antioxidant properties of the EGCG and RWP extracts.

3.2. Antioxidant Toxicity Assessment. The potential toxicity of each antioxidant extract on the unstressed RINm5F cells was evaluated by measuring the cell viability in the presence of different concentrations of EGCG and RWPs (Figure 2). RWPs appear to have no effect on cell viability until reaching a concentration of 500 μg/mL, at which point the number of viable cells drops to 92.4 ± 14.7% (not significant). A dose-dependent decreasing trend in cell viability was also observed around this concentration; however, this decrease was not significant until the RWP concentration reached 1000 μg/mL ($P < 0.05$) (Figure 2(a)). In contrast, EGCG was observed to induce a significant increase in cell viability at the 500 μg/mL (152 ± 26%, $P < 0.01$) and 1000 μg/mL (233.5 ± 13.0%, $P < 0.01$) concentrations (Figure 2(b)).

3.3. Effects of EGCG and RWPs during H_2O_2-Induced Oxidative Stress. RWPs were shown to reduce the loss of RINm5F cell viability induced by H_2O_2 oxidative stress (Figure 3(a)) in a dose-dependent manner starting at a concentration of 50 μg/mL (32.4 ± 1.8%, $P < 0.01$) and reaching a maximum level at 200 μg/mL (73.9 ± 3.5%, $P < 0.01$), the highest

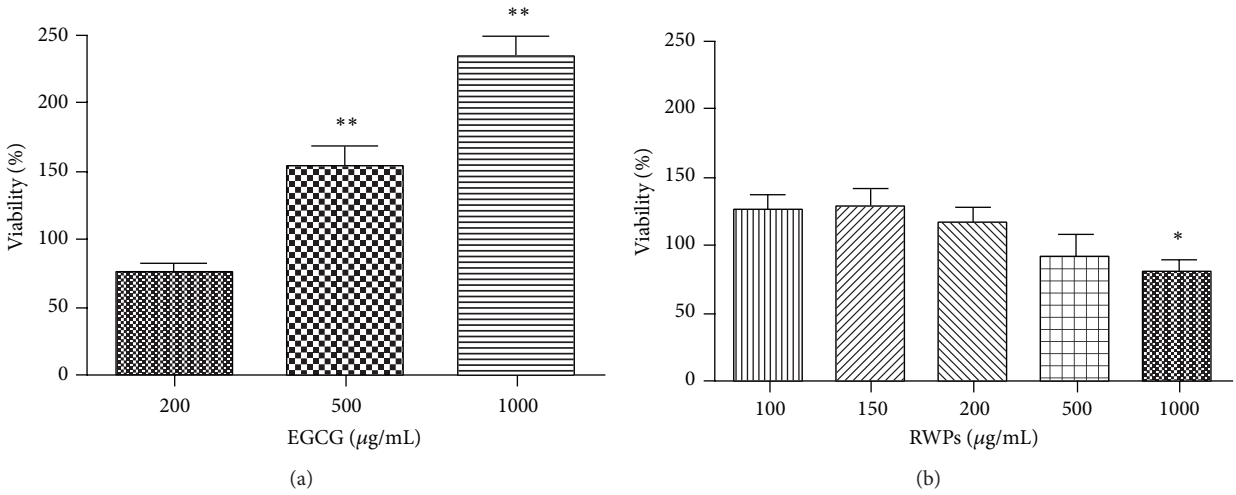

Figure 2: Effects of RWPs (a) and EGCG (b) on RINm5F cell viability. Values are given as the mean ± SEM for three different experiments. $n = 6$; $^{*}P < 0.05$ and $^{**}P < 0.01$ compared to the control cells.

concentration used in this study. Further, 500 μg/mL of EGCG was sufficient to significantly improve cell viability after oxidative stress (82.3 ± 6.2%, $P < 0.01$) (Figure 3(b)). This effect again appeared to be dose-dependent, with the cell viability being completely restored and enhanced at an EGCG concentration of 1000 μg/mL (110 ± 8.9%, $P < 0.01$).

The antioxidant properties of RWPs and EGCG were also confirmed by measuring apoptosis through the evaluation caspase 8 expression using 150 μg/mL of RWPS and 500 μg/mL of EGCG. Both antioxidants appear to reduce the significant increase in caspase 8 activation observed during H_2O_2-induced oxidative stress back to levels similar to the unstressed control cells ($P < 0.01$). Surprisingly, the significant increase in ROS production observed during H_2O_2 oxidative stress was not reduced by the RWP extract; it actually appeared to induce an increase in ROS production, going from 11.1±2.1% to 19.2±1.9% ($P < 0.01$). On the other hand, EGCG extract significantly reduced ROS production during oxidative stress. In terms of antioxidant enzyme expression during H_2O_2-induced oxidative stress, MnSOD (Figure 3(e)) and CAT protein expression (Figure 3(f)) was comparable to that of the unstressed control cells. Further, MnSOD protein expression was significantly reduced by RWPs during oxidative stress ($P < 0.05$), while CAT protein expression was reduced using EGCG ($P < 0.01$).

3.4. Effects of EGCG and RWPs on HX/XO-Induced Oxidative Stress. The significant decrease RINm5F cell viability observed during HX/XO-induced oxidative stress was significantly increased when 200 μg/mL of RWP was added, but the percentage of viable cells did not exceed 40.2±1.9% ($P < 0.01$) (Figure 4(a)). The efficiency of EGCG to improve the viability of stress cells was similar to that observed for RWPs at the 200 μg/mL concentration (43.1±3.8%), although this was not significant (Figure 4(b)). However, at higher concentrations EGCG was able to significantly increase cell viability from 16.5 ± 2.1% in the stressed control cells to 88.5 ± 7.4% at 500 μg/mL ($P < 0.01$) and over 100% at the 1000 μg/mL concentration.

Further, the 150 μg/mL and 500 μg/mL concentrations of RWPs and EGCG, respectively, were then used to study their antioxidant properties during HX/XO-induced oxidative stress. It appears that these concentrations of RWPs and EGCG significantly reduce caspase 8 cleavage during HX/XO-induced oxidative stress ($P < 0.05$ and $P < 0.01$, resp.; Figure 4(c)), bringing the caspase 8 activity back down to levels similar to the unstressed control cells. Moreover, both antioxidants significantly reduced the ROS production as well (Figure 4(d)). Notably, only EGCG was observed to increase the protein expression of MnSOD (Figure 4(e)) and CAT (Figure 4(f)) during HX/XO-induced oxidative stress.

3.5. Effects of EGCG and RWPs on STZ-Induced Oxidative Stress. The significant decrease in cell viability during STZ-induced oxidative stress was slightly opposed by 200 μg/mL of RWPs, which significantly increased the number of viable cells to a mere 50.6±0.5% ($P < 0.01$). Similarly, a 1000 μg/mL concentration of EGCG was needed to significantly increase the cell viability during STZ-induced oxidative stress (60 ± 14%, $P < 0.05$) (Figure 5(b)). For further investigation of the antioxidant properties of the RWPs and EGCG extracts during this type of oxidative stress, we focused on the 200 μg/mL and 1000 μg/mL concentrations of RWPs and EGCG, respectively.

Notably, caspase 8 activation was not observed to increase during STZ-induced oxidative stress; the addition of either of the antioxidants did not significantly change these levels compared to the unstressed or stressed control cells (Figure 5(c)). However, the production of ROS was significantly increased during STZ-induced stress and only EGCG treatment caused a significant reduction of this induced ROS production ($P < 0.05$; Figure 5(d)). The unaltered MnSOD (Figure 5(e)) and CAT (Figure 5(f)) protein expression during STZ-induced oxidative stress was also only affected by the addition of EGCG.

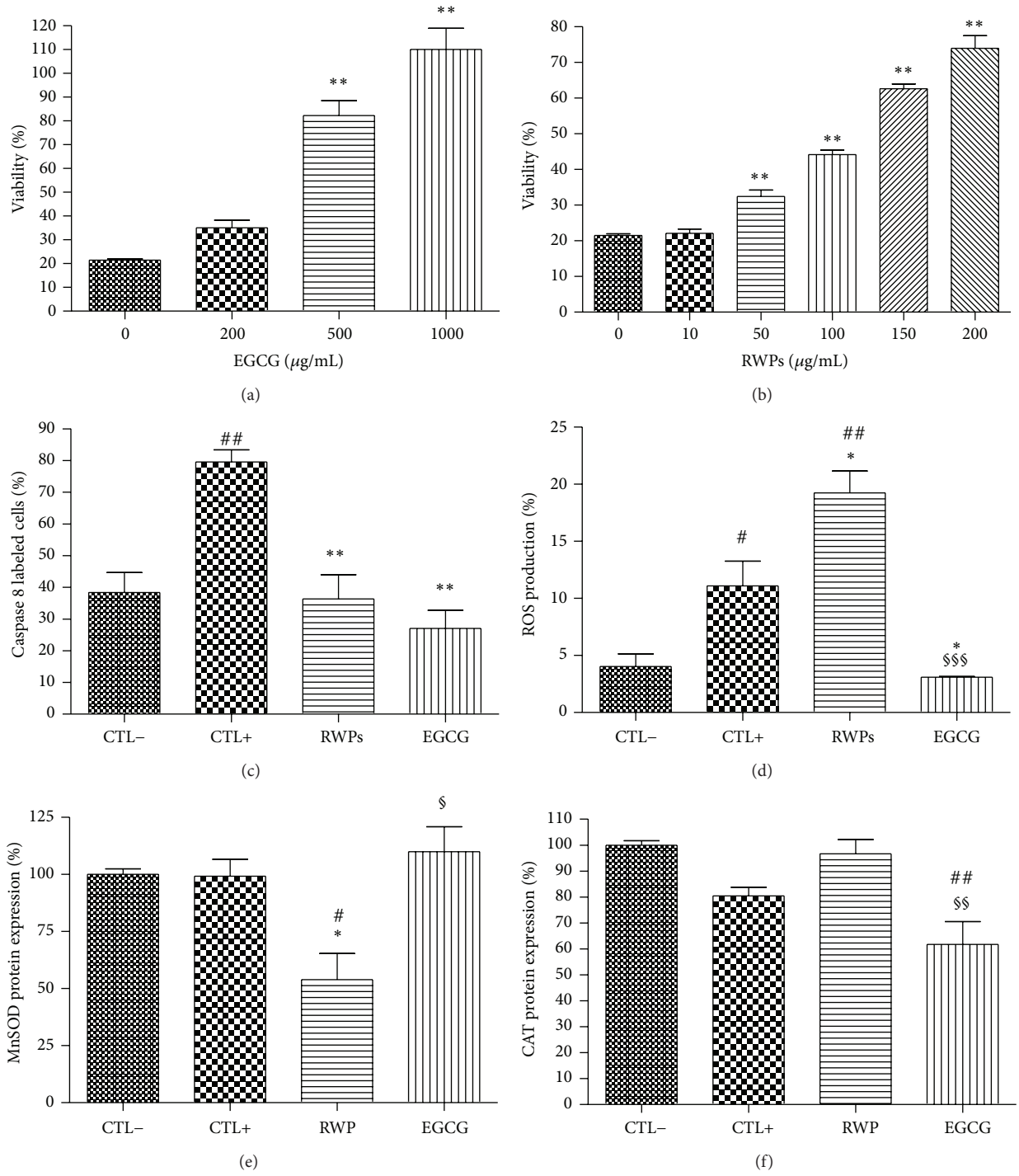

Figure 3: Effects of the antioxidants RWPs and EGCG on cell viability (a, b), caspase 8 activity/apoptosis (c), ROS production (d), MnSOD expression (e), and CAT expression (f) during H_2O_2-induced oxidative stress. Values are given as the mean ± SEM for three different experiments. $n = 6$; $^{*}P < 0.05$ and $^{**}P < 0.01$ compared to the unstressed control cells (CTL−); $^{\#}P < 0.05$, $^{\#\#}P < 0.01$ compared to the stressed control cells (CTL+); $^{\S}P < 0.05$, $^{\S\S}P < 0.01$, and $^{\S\S\S}P < 0.001$ compared to the stressed cells treated with RWPs.

4. Discussion

In the present study, we sought to accurately determine the antioxidant properties of two specific natural compounds, RWPs and EGCG. In doing so, we have demonstrated that antioxidant properties depend not only on the nature of the compound itself, but also on the type of oxidative stress induced. These data show, for the first time, that using one

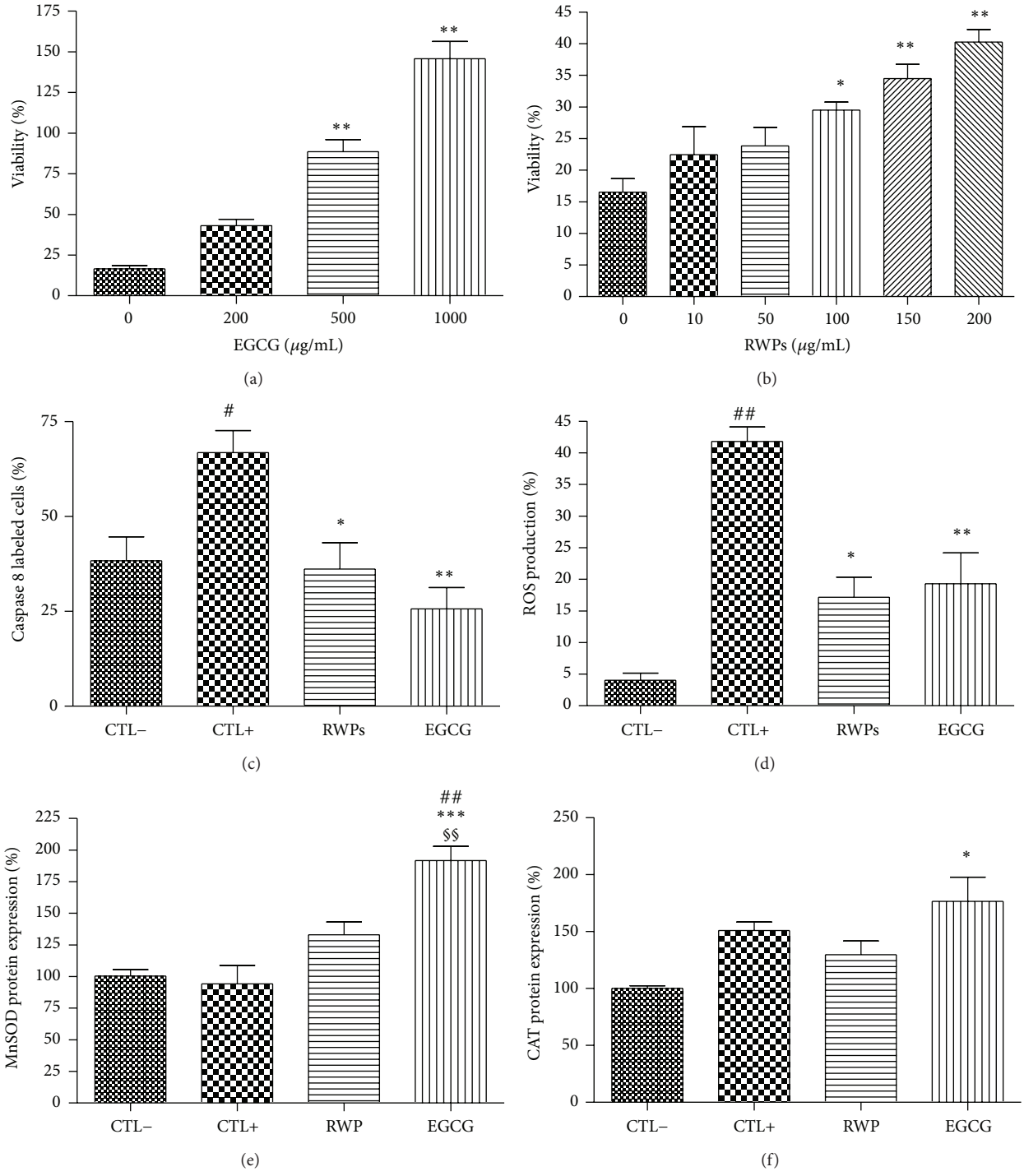

Figure 4: Effects of the antioxidants RWPs and EGCG on cell viability (a, b), caspase 8 activity/apoptosis (c), ROS production (d), MnSOD expression (e), and CAT expression (f) during HX/XO-induced oxidative stress. Values are given as the mean ± SEM for three different experiments. $n = 6$; $^{*}P < 0.05$, $^{**}P < 0.01$, and $^{***}P < 0.001$ compared to the unstressed control cells (CTL−); $^{\#}P < 0.05$, $^{\#\#}P < 0.01$ compared to the stressed control cells (CTL+); $^{\S\S}P < 0.01$ compared to the stressed cells treated with RWPs.

model of oxidative stress is not sufficient to make meaningful conclusions concerning the action of an antioxidant, particularly in regard to disease-related oxidative stress.

Complex mechanisms related to glucose autoxidation and hyperinsulinism, which increase ROS production, have been identified in diabetes [5]. Further, the increased level of ROS has been associated with beta cell apoptosis, which, in time, induces insulin dependence [34, 35]. In order to decrease beta cell oxidative stress, nutraceutical approaches have been developed focusing on the screening of plant extract [36–38].

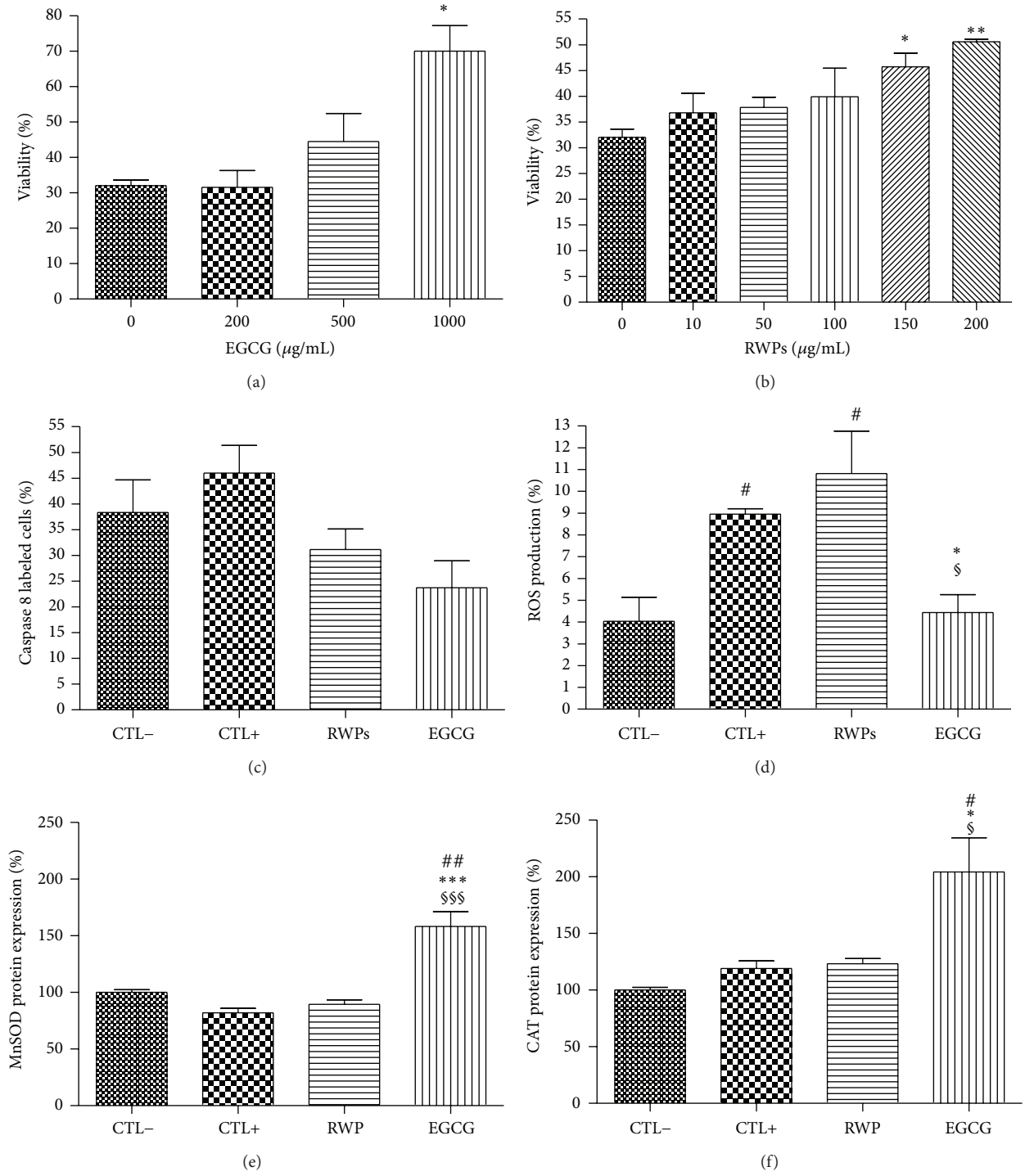

Figure 5: Effects of the antioxidants RWPs and EGCG on cell viability (a, b), caspase 8 activity/apoptosis (c), ROS production (d), MnSOD expression (e), and CAT expression (f) during STZ-induced oxidative stress. Values are given as the mean ± SEM for three different experiments. $n = 6$; $^{*}P < 0.05$, $^{**}P < 0.01$, and $^{***}P < 0.001$ compared to the unstressed control cells (CTL−); $^{\#}P < 0.05$, $^{\#\#}P < 0.01$ compared to the stressed control cells (CTL+); $^{\S}P < 0.05$, $^{\S\S\S}P < 0.001$ compared to the stressed cells treated with RWPs.

For the initial screening, the efficiency of the bioactive compounds in the plant is currently validated *in vitro* using a single type of oxidative stress [27, 39–41]. Here, in order to provide a comprehensive overview of ROS generated in diabetes, we have utilized three models of oxidative stress to screen our bioactive compounds.

Not surprisingly, the level of cell death induced by each type of oxidative stress studied was similar. However, the level

of ROS produced in the cells was found to be higher in the HX/XO model compared to the others. In fact, our data show that there is no correlation between ROS production and the level of cell death, indicating that cell viability alone is not an accurate marker of the oxidative stress response in a cell or tissue. This is in contrast to several previous studies that have linked oxidative stress to cell viability [3, 26, 28]. Notably, the conclusions in these studies were all based on single models of oxidative stress. We chose to measure ROS production in parallel with other markers of the cellular stress response, such as changes in SOD and CAT expression as well as the caspase 8 activity in the cells, in order to evaluate the full effect of the oxidant. According to these results, the cellular defence mechanisms, characterised by SOD and CAT expression, were more activated by the HX/XO-induced stress, which is correlated to the higher level of ROS. Thus, we suggest that antioxidant enzymes likely play a crucial role in cell protection following the introduction of oxidative stress, particularly because the cell viability was comparable to the other conditions as previously described [21, 40]. This phenomenon in the HX/XO experiments could also be explained by the type of radical generated. In fact, the stress induced by H_2O_2 and STZ was more complex (ROS generation via NADPH oxidase activation and/or NO synthase) compared to that generated by HX/XO (direct ROS provider), which may result in the latter inducing the cell's response to stress earlier or more efficiently. Additional work is necessary to further elucidate the differing effects caused by the various free radicals.

Using the three stress models outlined here in conjunction with parallel investigations of ROS generation and cellular defence mechanisms to screen bioactive compounds also provided more detailed information on the cellular stress response. For example, in these experiments, EGCG appeared to be a better antioxidant for the three types of different stresses induced, with a decrease in ROS production and an activation of MnSOD and CAT expression, whereas RWPs were shown to be efficient only on the strongest stress (HX/XO) and even then only had a limited influence on antioxidant enzyme expression. Thus, the use of multiple types of free radical stress indicates that EGCG is likely the most efficient scavenger [26] and pharmacological treatment [37] investigated in this study. This is corroborated by a previous study that demonstrated the neuroprotective effects of EGCG involving inhibition of the Fenton reaction and upregulation of several antioxidant enzymes, such as superoxide dismutase and catalase, resulting in the attenuation of oxidative stress [42]. In contrast, the antioxidant properties of RWPs seem to be solely related to scavenging during severe changes in oxidative stress. Moreover, our study suggests that RWPs may be both antioxidant and prooxidant because we observed an increase of ROS production when RPWs were added during H_2O_2 oxidative stress. It is well known [43] that polyphenols extract could autoxidize and produce more hydrogen peroxide. In our study, we have demonstrated in this condition that RWPs have no impact on SOD or CAT protein expression but other protective mechanisms could be activated like the stimulation of CAT and SOD activity or a direct action glutathione or thioredoxin. Notably, while we sought to use the same concentration of compound (pure or extract) for both RWPs and EGCG, the composition of these compounds made this impractical. Using HPLC [29], it appears that the raw RWP extract also contains several flavonoids (epicatechin, catechin, and gallic acid) but is found at concentrations that are 100 times less than that of the pure EGCG used in this study. This composition could explain the relatively low efficiency of RWPs shown here. In contrast, the pure EGCG extract was able to activate antioxidant pathways through several mechanisms, which could be due to the high concentration of the flavonoids present.

Regardless of the composition of the compounds, if only one oxidative stress model had been used or only one ROS or cell death assay had been performed, then it is unlikely that the complex nature of these antioxidants would have been uncovered. Therefore, we believe that the sole use of one model or one assay to validate the efficiency of bioactive compounds in the current literature [30, 32] greatly limits the scope and conclusions of these studies. Further, a more precise determination of cell death, ideally using additional apoptosis signalling pathways, like additional caspase activation, antiapoptotic Bcl-xL, and proapoptotic Bax expression [27, 37], as well as further analysis of oxidation-related enzymes could also be utilized to expand our current analysis. Additional work is necessary to determine the full functionality of our multitype oxidative stress model in testing the antioxidant properties of other compounds.

5. Conclusion

Here, we have demonstrated that the level of ROS generated by different oxidative stresses was variable and a drug screening using a single kind of stress can introduce bias in the estimation of the antioxidant properties of a compound. Therefore, a combination of several stresses and several cellular and molecular approaches would provide a more accurate experimental text to determine if the compound is an efficient antioxidant. This *in vitro* model also more accurately mimics the *in vivo* biological situation, which will help avoid unnecessary spending of money and time when transitioning a bioactive antioxidant treatment from the context of cell culture to clinical validation. Taken together, this study provides a much needed method for the comprehensive assessment of antioxidants for the treatment of oxidative stress-related diseases.

Abbreviations

7′AAD: 7-Aminoactinomycin D
ABAM: Antibiotic-antimycotic
CAT: Catalase
DCF: Dichlorofluorescein
DCFH-DA: 2′,7′-Dichlorofluorescein-diacetate
DNA: Deoxyribonucleic acid
EDTA: Ethylenediaminetetraacetic acid
EGCG: Epigallocatechin gallate
FAM: Carboxyfluorescein
FBS: Fetal bovine serum
HX/XO: Hypoxanthine/xanthine oxidase

iNOS: Inducible NO synthase
MnSOD: Manganese superoxide dismutase
NO: Nitric oxide
PBS: Phosphate-buffered saline
RINm5F: Rat pancreatic cell line
ROS: Reactive oxygen species
RWPs: Red wine polyphenols
SEM: Standard error of the mean
SOD: Superoxide dismutase
STZ: Streptozotocin
TCA: Tricarboxylic citric acid.

Conflict of Interests

The authors declare that there is no conflict of interests regarding the publication of this paper.

Acknowledgments

The authors would like to express their gratitude to "Vaincre le Diabète" and ASDIA (Assistance Service DIAbete) for partially funding this project.

References

[1] K. Grankvist, S. L. Marklund, and I. B. Taljedal, "CuZn-superoxide dismutase, Mn-superoxide dismutase, catalase and glutathione peroxidase in pancreatic islets and other tissues in the mouse," *Biochemical Journal*, vol. 199, no. 2, pp. 393–398, 1981.

[2] H. Sies, "Role of reactive oxygen species in biological processes," *Klinische Wochenschrift*, vol. 69, no. 21–23, pp. 965–968, 1991.

[3] S. R. Sampson, E. Bucris, M. Horovitz-Fried et al., "Insulin increases H_2O_2-induced pancreatic beta cell death," *Apoptosis*, vol. 15, no. 10, pp. 1165–1176, 2010.

[4] A. Y. Andreyev, Y. E. Kushnareva, and A. A. Starkov, "Mitochondrial metabolism of reactive oxygen species," *Biochemistry*, vol. 70, no. 2, pp. 200–214, 2005.

[5] S. Lenzen, "The mechanisms of alloxan- and streptozotocin-induced diabetes," *Diabetologia*, vol. 51, no. 2, pp. 216–226, 2008.

[6] A. Favier, "Oxidative stress in human diseases," *Annales Pharmaceutiques Francaises*, vol. 64, no. 6, pp. 390–396, 2006.

[7] K. Fisher-Wellman and R. J. Bloomer, "Macronutrient specific postprandial oxidative stress: relevance to the development of insulin resistance," *Current Diabetes Reviews*, vol. 5, no. 4, pp. 228–238, 2009.

[8] M. D. Brand, A. L. Orr, I. V. Perevoshchikova, and C. L. Quinlan, "The role of mitochondrial function and cellular bioenergetics in ageing and disease," *British Journal of Dermatology*, vol. 169, no. 2, pp. 1–8, 2013.

[9] M. Latha, L. Pari, S. Sitasawad, and R. Bhonde, "Scoparia dulcis, a traditional antidiabetic plant, protects against streptozotocin induced oxidative stress and apoptosis in vitro and in vivo," *Journal of Biochemical and Molecular Toxicology*, vol. 18, no. 5, pp. 261–272, 2004.

[10] C. Gökkuşu, Ş. Palanduz, E. Ademoğlu, and S. Tamer, "Oxidant and antioxidant systems in niddm patients: influence of vitamin E supplementation," *Endocrine Research*, vol. 27, no. 3, pp. 377–386, 2001.

[11] H. P. Ammon, R. Hägele, N. Youssif, R. Eujen, and N. El-Amri, "A possible role of intracellular and membrane thiols of rat pancreatic islets in calcium uptake and insulin release," *Endocrinology*, vol. 112, no. 2, pp. 720–726, 1983.

[12] S. Lenzen, J. Drinkgern, and M. Tiedge, "Low antioxidant enzyme gene expression in pancreatic islets compared with various other mouse tissues," *Free Radical Biology and Medicine*, vol. 20, no. 3, pp. 463–466, 1996.

[13] R. Hägerkvist, S. Sandler, D. Mokhtari, and N. Welsh, "Amelioration of diabetes by imatinib mesylate (Gleevec): role of beta-cell NF-kappaB activation and anti-apoptotic preconditioning," *The FASEB Journal*, vol. 21, no. 2, pp. 618–628, 2007.

[14] S. M. Virtanen and A. Aro, "Dietary factors in the aetiology of diabetes," *Annals of Medicine*, vol. 26, no. 6, pp. 469–478, 1994.

[15] R. A. Kinloch, J. M. Treherne, L. M. Furness, and I. Hajimohamadreza, "The pharmacology of apoptosis," *Trends in Pharmacological Sciences*, vol. 20, no. 1, pp. 35–42, 1999.

[16] C. Rice-Evans, "Plant polyphenols: free radical scavengers or chain-breaking antioxidants?" *Biochemical Society symposium*, vol. 61, pp. 103–116, 1995.

[17] A. Sarkar and A. Bhaduri, "Black tea is a powerful chemopreventor of reactive oxygen and nitrogen species: comparison with its individual catechin constituents and green tea," *Biochemical and Biophysical Research Communications*, vol. 284, no. 1, pp. 173–178, 2001.

[18] Y.-H. Kao, H.-H. Chang, M.-J. Lee, and C.-L. Chen, "Tea, obesity, and diabetes," *Molecular Nutrition and Food Research*, vol. 50, no. 2, pp. 188–210, 2006.

[19] R. Rodrigo, A. Miranda, and L. Vergara, "Modulation of endogenous antioxidant system by wine polyphenols in human disease," *Clinica Chimica Acta*, vol. 412, no. 5-6, pp. 410–424, 2011.

[20] C. Sandoval-Acuña, J. Ferreira, and H. Speisky, "Polyphenols and mitochondria: an update on their increasingly emerging ROS-scavenging independent actions," *Archives of Biochemistry and Biophysics*, vol. 559, pp. 75–90, 2014.

[21] S. Lortz and M. Tiedge, "Sequential inactivation of reactive oxygen species by combined overexpression of SOD isoforms and catalase in insulin-producing cells," *Free Radical Biology and Medicine*, vol. 34, no. 6, pp. 683–688, 2003.

[22] C. Moriscot, M. J. Richard, M. C. Favrot, and P. Y. Benhamou, "Protection of insulin-secreting INS-1 cells against oxidative stress through adenoviral-mediated glutathione peroxidase overexpression," *Diabetes and Metabolism*, vol. 29, no. 2 I, pp. 145–151, 2003.

[23] R. Zhang, Q. Zhang, J. Niu et al., "Screening of microRNAs associated with Alzheimer's disease using oxidative stress cell model and different strains of senescence accelerated mice," *Journal of the Neurological Sciences*, vol. 338, no. 1-2, pp. 57–64, 2014.

[24] A. Ceriello and E. Motz, "Is oxidative stress the pathogenic mechanism underlying insulin resistance, diabetes, and cardiovascular disease? The common soil hypothesis revisited," *Arteriosclerosis, Thrombosis, and Vascular Biology*, vol. 24, no. 5, pp. 816–823, 2004.

[25] K.-B. Kwon, J.-H. Kim, Y.-R. Lee et al., "Amomum xanthoides extract prevents cytokine-induced cell death of RINm5F cells through the inhibition of nitric oxide formation," *Life Sciences*, vol. 73, no. 2, pp. 181–191, 2003.

[26] K. M. Ramkumar, A. S. Lee, K. Krishnamurthi et al., "*Gymnema montanum* H. Protects against alloxan-induced oxidative stress

and apoptosis in pancreatic β-cells," *Cellular Physiology and Biochemistry*, vol. 24, no. 5-6, pp. 429–440, 2009.

[27] S. A. Kalekar, R. P. Munshi, and U. M. Thatte, "Do plants mediate their anti-diabetic effects through anti-oxidant and anti-apoptotic actions? An in vitro assay of 3 Indian medicinal plants," *BMC Complementary and Alternative Medicine*, vol. 13, article 257, 2013.

[28] K. Dembele, K. H. Nguyen, T. A. Hernandez, and B. L. G. Nyomba, "Effects of ethanol on pancreatic beta-cell death: interaction with glucose and fatty acids," *Cell Biology and Toxicology*, vol. 25, no. 2, pp. 141–152, 2009.

[29] C. Auger, B. Caporiccio, N. Landrault et al., "Red wine phenolic compounds reduce plasma lipids and apolipoprotein B and prevent early aortic atherosclerosis in hypercholesterolemic golden Syrian hamsters (*Mesocricetus auratus*)," *Journal of Nutrition*, vol. 132, no. 6, pp. 1207–1213, 2002.

[30] A. Mira, A. Tanaka, Y. Tateyama, R. Kondo, and K. Shimizu, "Comparative biological study of roots, stems, leaves, and seeds of *Angelica shikokiana* Makino," *Journal of Ethnopharmacology*, vol. 148, no. 3, pp. 980–987, 2013.

[31] C. H. Kim and Y.-M. Yoo, "Melatonin induces apoptotic cell death via p53 in LNCaP cells," *Korean Journal of Physiology and Pharmacology*, vol. 14, no. 6, pp. 365–369, 2010.

[32] L. Liu and S.-Y. Wang, "Protective effects of paeoniflorin against aβ25-35-induced oxidative stress in PC12 cells," *Zhongguo Zhong Yao Za Zhi*, vol. 38, no. 9, pp. 1318–1322, 2013.

[33] M. M. Bradford, "A rapid and sensitive method for the quantitation of microgram quantities of protein utilizing the principle of protein-dye binding," *Analytical Biochemistry*, vol. 72, no. 1-2, pp. 248–254, 1976.

[34] V. Z. Lankin, M. V. Ivanova, G. G. Konovalova, A. K. Tikhaze, A. I. Kaminnyi, and V. V. Kukharchuk, "Effect of β-hydroxy-β-methylglutaryl coenzyme a reductase inhibitors and antioxidant vitamins on free radical lipid oxidation in rat liver," *Bulletin of Experimental Biology and Medicine*, vol. 143, no. 4, pp. 414–417, 2007.

[35] P. P. Singh, F. Mahadi, A. Roy, and P. Sharma, "Reactive oxygen species, reactive nitrogen species and antioxidants in etiopathogenesis of diabetes mellitus type-2," *Indian Journal of Clinical Biochemistry*, vol. 24, pp. 324–342, 2009.

[36] U. Karunakaran and K.-G. Park, "A systematic review of oxidative stress and safety of antioxidants in diabetes: focus on islets and their defense," *Diabetes and Metabolism Journal*, vol. 37, no. 2, pp. 106–112, 2013.

[37] S.-H. Lee, S.-M. Kang, S.-C. Ko, M.-C. Kang, and Y.-J. Jeon, "Octaphlorethol A, a novel phenolic compound isolated from Ishige foliacea, protects against streptozotocin-induced pancreatic beta cell damage by reducing oxidative stress and apoptosis," *Food and Chemical Toxicology*, vol. 59, pp. 643–649, 2013.

[38] M. Á. Martín, S. Ramos, I. Cordero-Herrero, L. Bravo, and L. Goya, "Cocoa phenolic extract protects pancreatic beta cells against oxidative stress," *Nutrients*, vol. 5, no. 8, pp. 2955–2968, 2013.

[39] L. A. Flores-López, M. Díaz-Flores, R. García-Macedo et al., "High glucose induces mitochondrial p53 phosphorylation by p38 MAPK in pancreatic RINm5F cells," *Molecular Biology Reports*, vol. 40, no. 8, pp. 4947–4958, 2013.

[40] V. Nadithe, D. Mishra, and Y. H. Bae, "Poly(ethylene glycol) cross-linked hemoglobin with antioxidant enzymes protects pancreatic islets from hypoxic and free radical stress and extends islet functionality," *Biotechnology and Bioengineering*, vol. 109, no. 9, pp. 2392–2401, 2012.

[41] F. M. M. Paula, S. M. Ferreira, A. C. Boschero, and K. L. A. Souza, "Modulation of the peroxiredoxin system by cytokines in insulin-producing RINm5F cells: down-regulation of PRDX6 increases susceptibility of beta cells to oxidative stress," *Molecular and Cellular Endocrinology*, vol. 374, no. 1-2, pp. 56–64, 2013.

[42] O. Weinreb, T. Amit, S. Mandel, and M. B. H. Youdim, "Neuroprotective molecular mechanisms of (−)-epigallocatechin-3-gallate: a reflective outcome of its antioxidant, iron chelating and neuritogenic properties," *Genes and Nutrition*, vol. 4, no. 4, pp. 283–296, 2009.

[43] J. Zhu, W. J. M. van de Ven, T. Verbiest et al., "Polyphenols can inhibit furin *in vitro* as A result of the reactivity of their auto-oxidation products to proteins," *Current Medicinal Chemistry*, vol. 20, no. 6, pp. 840–850, 2013.

Hindawi Publishing Corporation
Evidence-Based Complementary and Alternative Medicine
Volume 2015, Article ID 492458, 7 pages
http://dx.doi.org/10.1155/2015/492458

Research Article

Adipogenic Activity of Wild Populations of *Rhododendron groenlandicum*, a Medicinal Shrub from the James Bay Cree Traditional Pharmacopeia

Michel Rapinski,[1,2] Lina Musallam,[1,3] John Thor Arnason,[1,4] Pierre Haddad,[1,3] and Alain Cuerrier[1,2]

[1] *Canadian Institutes of Health Research Team in Aboriginal Antidiabetic Medicines, Université de Montréal, Montréal, QC, Canada H3C 3J7*
[2] *Institut de Recherche en Biologie Végétale, Jardin Botanique de Montréal, Université de Montréal, 4101 Sherbrooke Est, Montréal, QC, Canada H1X 2B2*
[3] *Natural Health Products and Metabolic Diseases Laboratory, Department of Pharmacology, Université de Montréal, Montréal, QC, Canada H3C 3J7*
[4] *Centre for Research in Biotechnology and Biopharmaceuticals, Department of Biology, University of Ottawa, Ottawa, ON, Canada K1N 6N5*

Correspondence should be addressed to Pierre Haddad; pierre.haddad@umontreal.ca
and Alain Cuerrier; alain.cuerrier@umontreal.ca

Received 20 March 2015; Accepted 25 May 2015

Academic Editor: Nunziatina De Tommasi

The traditional medicinal plant, Labrador tea (*Rhododendron groenlandicum* (Oeder) Kron & Judd; Ericaceae), present in the pharmacopoeia of the Cree of Eeyou Istchee, has shown glitazone-like activity in the 3T3-L1 adipogenesis bioassay. This activity has been attributed to phenolic compounds, which have been shown to vary in this plant as a function of insolation parameters. The goal of this study was to determine if these changes in phenolic content were pharmacologically significant. Leaves were harvested in 2006 throughout the James Bay region of Northern Quebec and ethanol extracts were tested *in vitro* using the 3T3-L1 murine cell line adipogenesis bioassay. This traditional medicinal plant was found active in the assay. However, there was no detectable spatial pattern in the accumulation of intracellular triglycerides, suggesting that such patterns previously observed in the phenolic profile of Labrador tea were not pharmacologically significant. Nonetheless, a reduction in the adipogenic activity was observed and associated with higher concentrations of quercetin for which selected environmental variables did not appropriately explain its variation.

1. Introduction

In a previous study on the phytochemistry of the North American medicinal plant, *Rhododendron groenlandicum* (Oeder) Kron & Judd (Ericaceae), Labrador tea, we found the concentration of biologically active compounds to vary in Northern Quebec's Hudson and James Bay region [1]. Labrador tea is a common species in Canada's boreal forest. More importantly, it is a popular medicinal plant found in the traditional pharmacopoeia of indigenous populations from the Algonquian, Salish, Wakashan, Tsimshian, and Eskimo-Aleut linguistic families [2–9].

In ethnobotanical studies conducted in six communities of the Cree Nation of Eeyou Istchee (CEI), we found *R. groenlandicum* to be the top-ranked plant species used for the treatment of symptoms associated with type 2 diabetes (T2D) [10–13]. The inherent cultural relevance of this species to CEI traditional medicine (CTM) warrants further investigation into its antidiabetic potential.

The CIHR Team on Antidiabetic Aboriginal Medicines (CIHR-TAAM), formed through collaborative work between CEI communities, the Cree Board of Health and Social Services of James Bay (CBHSSJB), and Canadian academic researchers, has screened many of the multiple plants

present in the CEI pharmacopoeia [14–17]. Of these, *R. groenlandicum* was shown to possess *in vitro* glitazone-like activity comparable to rosiglitazone in an adipogenic assay measuring the lipid accumulation in differentiating 3T3-L1 preadipocytes [14].

The antidiabetic drug rosiglitazone induces an increase in the sensitivity to insulin, acting as a PPARγ receptor agonist [18]; the expression of this transcription factor is particularly implicated in the differentiation of adipocytes [19–22] and in insulin sensitivity [18]. Hence, it plays a critical role in the pathogenesis of T2D. The action of PPARγ results in an improvement in the absorption of fatty acids in differentiated adipocytes which store them as triglycerides (TG) [18]. Adipocytes therefore provide storage for fatty substances that would otherwise accumulate in tissues such as skeletal muscle and liver, thereby contributing to metabolic disorders such as insulin resistance [22].

The pharmacological activity of *R. groenlandicum* has been attributed to phenolic compounds [14, 16, 23]. Bioassay-guided fractionation using adipogenesis of 3T3-L1 murine cells confirmed that specific phenolics are the most active compounds [24]. In developing culturally appropriate approaches to treating T2D in the CEI communities, the variation of these compounds in *R. groenlandicum* has important implications in ensuring the quality control of traditional medicinal plants or to develop standardized natural health products (NHPs).

In this study, we assessed possible variations in the antidiabetic potential of *R. groenlandicum*. Our objective was to determine if the phytochemical variations observed in the species' phenolic profile are biologically significant. We evaluated the *in vitro* pharmacological activity of crude extracts from various localities using the adipogenesis bioassay and hypothesized that high concentrations of phenolic compounds would result in a stronger adipogenic activity.

2. Materials and Methods

2.1. Sampling, Extraction, and Phytochemical Analysis. The sampling, extraction, and analytical methods for phytochemical identification and quantification are thoroughly described in Rapinski et al. [1], which reports on the phytochemistry of *R. groenlandicum*. A subsample, selected randomly, of previously reported samples was used in this *in vitro* study.

Briefly, mature leaves were sampled during the summer of 2006 around the communities of Mistissini, Nemaska, Eastmain, Wemindji, and Whapmagoostui, thus covering much of the northsouth gradient in Eeyou Istchee. Five accessions, each containing leaves from multiple individual plants, were collected within a 50 km radius around each community and selected for this study. Samples were air-dried and preserved in paper bags at room temperature.

Samples were milled through a Wiley Mill at 40 mesh and extracted overnight in 25 mL/g of 80% EtOH by orbital shaking at room temperature at 250 RPM. The pellet was extracted overnight in 15 mL 80% EtOH. An aliquot (1 mL) of the pooled supernatants (adjusted to 50.0 mL in a volumetric flask) was prepared for High Performance Liquid Chromatography coupled with Diode Array Detector (HPLC-DAD). The leftover crude extracts were dried using a speedVac; the trace water was removed by lyophilization using SuperModulo freeze dryer and the dehydrated extracts were stored at −80°C.

Finally, 10 μL of each extract aliquot was injected through an autosampler and detected by DAD at 290 nm, bandwidth 4, reference off. The separations were performed on a Luna C18 column (250 × 4.6 mm, 5 μM particle size). Peak identification was undertaken by cochromatographic comparison of the spectral data adopted in our in-house metabolomics spectral library [23]. A standard curve was constructed by injection of serially diluted marker compounds in methanol. The quantification was based on peak area. The quantitation of putatively identified quercetin-glycosides was achieved based on calibration curve of quercetin-3-galactoside. Each sample was analyzed in triplicate and averaged to account for instrumental variation.

2.2. Cell Culture. 3T3-L1 murine preadipocyte cells were grown to confluence in 24-well plates in DMEM proliferation medium containing 10% FBS. Media were changed every 2 days. At 24 h after confluence (day 0), cells were induced to differentiate with a short-term differentiation medium of DMEM supplemented with 10% FBS, 1 μM DMX, 250 μM IBMX, and 500 nM insulin. After 48 h, the media were replaced with DMEM containing 10% FBS and 500 nM insulin for long-term differentiation. Cells were differentiated for a total of 5 days with media change every 2 days. *Rhododendron groenlandicum* crude extracts (75 μg/mL) and rosiglitazone (10 μM; positive control) were dissolved in DMSO and added to the cells as of day 0 of differentiation. The final concentration of DMSO was kept at 0.1% throughout the differentiation period.

2.3. Adipogenesis. We measured intracellular TG content at day 5 of differentiation using the AdipoRed reagent according to the manufacturer's instructions. Methods have been previously described in Spoor et al. [14] and Harbilas et al. [16]. In short, wells containing adipocytes were washed twice with phosphate-buffered saline (PBS) before 1 mL of PBS containing 30 μL of AdipoRed reagent was added to each well and incubated for 15 minutes at room temperature. AdipoRed becomes fluorescent when partitioned in a hydrophobic compartment, namely, intracellular triglycerides (TG). The fluorescence of each well was measured with a Wallac Victor2 fluorimeter (Perkin-Elmer, Saint-Laurent, QC) at an excitation wavelength of 485 nm and an emission wavelength of 572 nm. The results were reported as percentage of the vehicle control, 0.1% DMSO.

2.4. Cell Lines, Chemicals, Biochemicals, and Standards. For the identification and quantification of phenolic markers, (+)-catechin (**1**), chlorogenic acid (**2**), (−)-epicatechin (**3**), *p*-coumaric acid (**4**), rutin (**5**), quercetin-3-galactoside (**6**), quercetin-3-glucoside (**7**), quercetin-3-rhamnoside (**12**), myricetin (**13**), and quercetin (**14**) were purchased from Sigma-Aldrich (Oakville, Ontario, Canada) and Extrasynthese (Genay, France). HPLC grade water, acetonitrile, and

formic acid (99% purity) were purchased from Sigma-Aldrich.

For cell culture and adipogenesis, preadipocyte 3T3-L1 cell line was purchased from the American Type Culture Collection (ATCC; Manassas, VA). Dexamethasone (DMX), bovine pancreatic insulin, 3-isobutyl-1-methylxanthine (IBMX), and Dimethyl sulfoxide (DMSO) were purchased from Sigma-Aldrich (Oakville, ON). Rosiglitazone was obtained from Alexis Biochemicals (Hornby, ON).

Dulbecco's Modified Eagle Medium (DMEM), fetal bovine serum (FBS), and bovine calf serum (NCS) were from Wisent Inc. (Saint-Bruno, QC). AdipoRed reagent was purchased from Cambrex Bio Science Walkersville Inc. (Walkersville, MD).

2.5. Environmental Data. Annual estimates of bioclimatic variables, namely, annual temperature range, corresponding to our sampling year and long-term estimates for insolation variables were provided by the Canadian Forest Services of Natural Resources Canada [25]. Long-term estimates were derived from multidecade meteorological data collected from 1971 to 2000 [26, 27].

2.6. Statistical Analysis. To reduce interassay variation, TG content was normalized relative to each assay's vehicle control, 0.1% DMSO, set at 100%. *Rhododendron groenlandicum* and rosiglitazone always induced significant increases in activity as verified by the fact that the 95% confidence interval of the mean activity (quadruplicate determinations) did not include the 100% adipogenic activity reference ($p < 0.05$). Differences between communities were analyzed by one-way analysis of variance. The relationships between TG content and compounds were analyzed by multiple and simple linear regressions. To represent the adipogenic activity of *R. groenlandicum* and the quantified compounds, principal components analysis (PCA) was performed on the matrix of these compounds using the correlation matrix. Individual samples were scored onto the PCA axes and represented with the vectors for each compounds. TG content was subsequently projected as a supplementary variable onto the principal components in order to interpret the dimensions of variability. In doing so, the calculation of distances between each of the samples and the construction principal components depends only on their phytochemical profile. Using the transition formulae described by Lê et al. [28], the coordinates for TG content are calculated using the original eigenvalues. Finally, we partitioned the variation in the adipogenic activity of *R. groenlandicum* between the two sets of variables: compounds and environmental factors. This was done using a partial-redundancy analysis (partial-RDA) approach [29, 30]. All analyses were performed using R statistical language [31]. Results are reported as means ± SD and statistical significance is set at $\alpha = 0.05$.

3. Results and Discussion

The phytochemistry of the same *R. groenlandicum* accessions has already been described and discussed in greater length in Rapinski et al. [1]. Here, we present the results of a subsample of 2006 accessions in the adipogenesis bioassay.

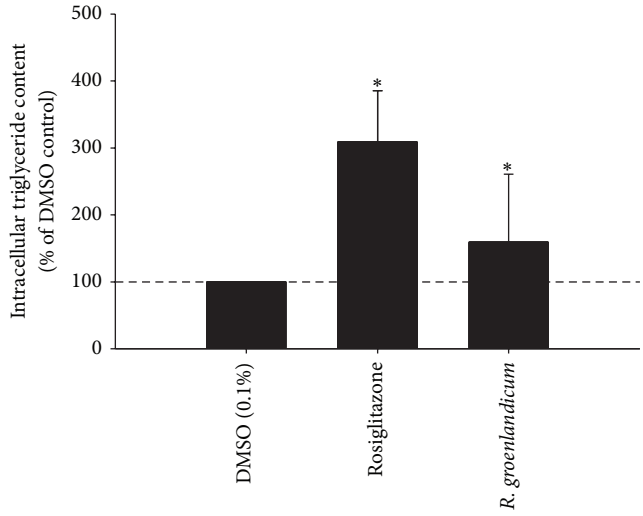

Figure 1: Effect of *R. groenlandicum* crude leaf extracts from Northern Quebec on lipid accumulation. Intracellular triglyceride content was measured by AdipoRed fluorescence, in live 3T3-L1 murine adipocytes incubated with plant extracts for 5 days after differentiation. Means ± SD ($n = 4$ for rosiglitazone, $n = 100$ for *R. groenlandicum*) are normalized to the vehicle control (0.1% DMSO). Asterisk (∗) indicates significant differences with respect to the DMSO control at $\alpha = 0.05$.

The glitazone-like activity of *R. groenlandicum* to increase the accumulation of intracellular TG in 3T3-L1 adipocytes was measured at day 5 of differentiation. Extracts increased adipogenesis, with an average content of TG of 159.0% that of DMSO (Figure 1) and a 95% confidence interval of 138.8–179.1% of DMSO. The adipogenic activity of *R. groenlandicum* was roughly half of the positive control, rosiglitazone. This is lower than what has previously been reported for this species. Spoor et al. [14] reported the stimulation of adipogenesis to be comparable to rosiglitazone, while later determinations measured an activity representing two-thirds that of the antidiabetic drug [24]. With few exceptions (Figure 2), our results nonetheless confirm the adipogenic potential of this species. It is important to consider the fact that previous determinations of activity were carried out using extracts prepared from large quantities of source material (large number of individual plants) collected a few years prior to the material used in the present studies. Hence, interindividual variations were absent and different climatic conditions may have prevailed. This can explain, at least in part, the differences in adipogenic potential observed between the studies.

There were no statistically distinct spatial patterns detected in the pharmacological activity of *R. groenlandicum*. None of the communities sampled possessed accessions which significantly increased intracellular TG more than the others ($p = 0.348$, Figure 3). We have previously found that biologically active phenolics were greater in collections made around the communities of Nemaska, Eastmain, and Wemindji [1]. The adipogenic activity of *R. groenlandicum*

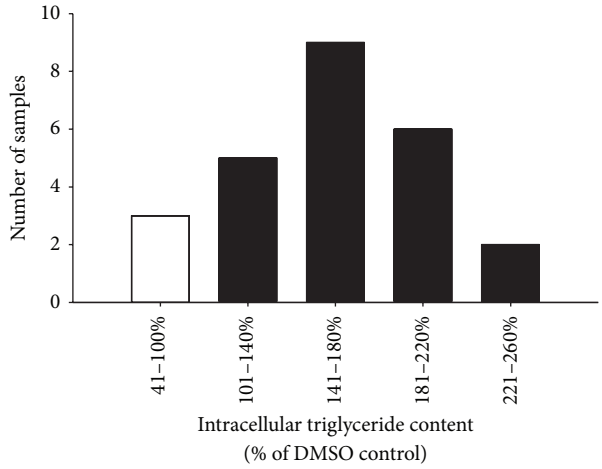

Figure 2: Frequency distribution of the adipogenic activity from 25 samples of *R. groenlandicum* leaves collected throughout Northern Quebec. Intracellular triglyceride content was measured by AdipoRed fluorescence, in live 3T3-L1 murine adipocytes incubated with plant extracts for 5 days after differentiation. Triglyceride content was normalized to the vehicle control (0.1% DMSO). Samples with content levels below 100% (in white) were considered inhibitory and decreased lipid accumulation.

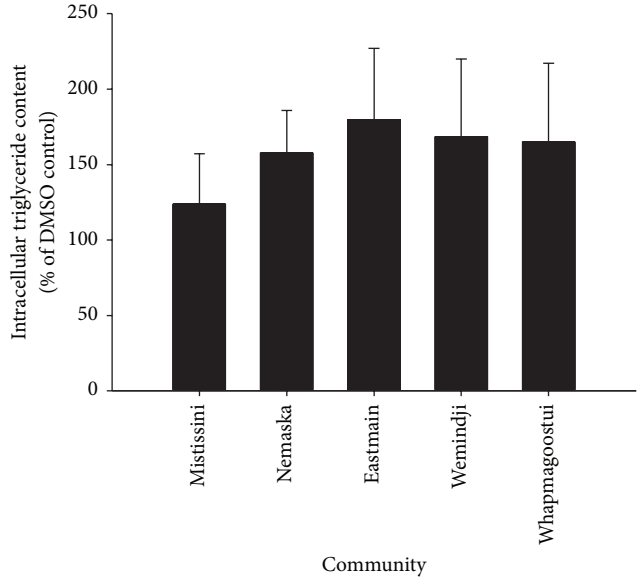

Figure 3: Effect of *R. groenlandicum* crude leaf extracts prepared from accessions collected around five communities in Northern Quebec on lipid accumulation. Intracellular triglyceride content was measured by AdipoRed fluorescence, in live 3T3-L1 murine adipocytes incubated with plant extracts for 5 days after differentiation. Means ± SD ($n = 5$) are normalized to the vehicle control (0.1% DMSO). There were no significant differences between communities ($p = 0.348$).

followed a similar trend, as can be observed in Figure 3, although statistical significance of a polynomial relationship was not achieved ($p = 0.170$), possibly due to high variability. This suggests that variations in the phytochemical profiles, observed in Rapinski et al. [1], may be pharmacologically relevant, but further studies will be necessary to confirm this point.

Indeed, we found that quantified compounds explained considerable variability obtained in this species' pharmacological activity ($p = 0.0279$, $R^2_{adj} = 0.491$). The distribution of *R. groenlandicum* samples based on their phytochemical profile was reconstructed into a reduced three-dimensional space, which represented 69.92% of the samples' variation over three statistically constructed principal components, or axes (Figure 4). Each principal component, from the first to the third, respectively, explained 35.99% ($\lambda_1 = 3.96$), 22.97% ($\lambda_2 = 2.53$), and 10.96% ($\lambda_3 = 1.20$) of the variation. The direction and proximity of arrows for some major markers suggest that these are highly correlated (Figure 4). When projecting intracellular TG onto this plot, it did not appear to be well correlated with the bulk of these markers, many of which were found near a 90° angle from it, thus indicating week or null correlations. One of the only markers for which a significant relationship with TG appears to exist is quercetin (Figures 4(b) and 4(c)). This suggests that, out of all the compounds assessed, variations in the adipogenic activity of *R. groenlandicum* are most vulnerable to changes in the content of quercetin found in the crude extracts. Figure 5 further illustrates the linear correlation ($p = 0.0458$, $R^2 = 0.162$) whereby the adipogenic activity of *R. groenlandicum* decreases as the concentration of quercetin in the sample increases. This is consistent with observations from our own group [24] where pure quercetin was found to inhibit adipogenesis in a dose-dependent manner. The activity of quercetin is well studied and has also been consistently shown by others to be a potent inhibitor of adipocyte differentiation and adipogenesis [18, 32–34].

Our results suggest that while the geographical location does not appear to have a statistically significant impact on the adipogenic activity of crude extracts of localized *R. groenlandicum* samples, variations in active compounds do explain a significant proportion of variability in pharmacological activity. We have shown that annual temperature ranges and insolation parameters, such as solar radiation, could significantly explain some of the variation in the species' phenolic compounds [1]. Although we did not find in this study that these environmental variables could significantly explain the variation in TG content ($p = 0.150$, $R^2_{adj} = 0.162$), we found, nonetheless, that they explained an important proportion of the variation in the phytochemical profiles of *R. groenlandicum*, which could significantly explain TG content (nontestable; see Table 1, Figure 6). Indeed, variation partitioning of TG content with both phytochemical and environmental variables indicates that while the relationship with compounds was statistically significant ($p = 0.0279$, $R^2_{adj} = 0.491$), their unique contribution to explaining TG content no longer was when the contribution of environmental variables, albeit small, was taken into account and removed ($p = 0.0619$, $R^2_{adj} = 0.424$).

This confirms the caveat that environmental variables play an underlying role in affecting the content of biologically active compounds. Conversely, quercetin, the only significant

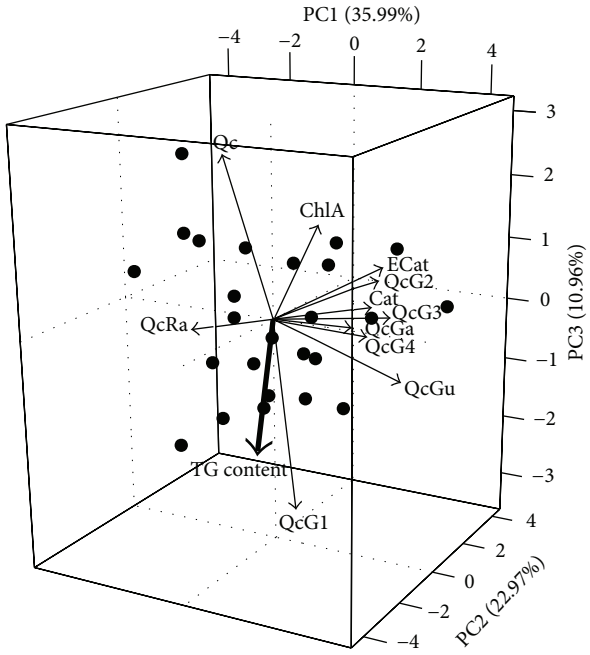

Figure 4: Principal component analysis biplot of 11 phenolic compounds in *R. groenlandicum* leaves. Solid lines represent relative loadings of these variables on axes 1, 2, and 3. TG content (bold arrow) was selected as a supplementary variable and plotted onto principal components generated from the phytochemical markers. Scores for individual samples are represented by symbols for the communities of Mistissini (▲), Nemaska (●), Eastmain (■), Wemindji (◆), and Whapmagoostui (▼). Abbreviations represent compounds as follows: (+)-catechin: Cat; chlorogenic acid: ChlA; (−)-epicatechin: ECat; quercetin-3-galactoside: QcGa; quercetin-3-glucoside: QcGu; quercetin-glycoside 1: QcG1; quercetin-glycoside 2: QcG2; quercetin-glycoside 3: QcG3; quercetin-glycoside 4: QcG4; quercetin-3-rhamnoside: Qc-Ra; and quercetin: Qc.

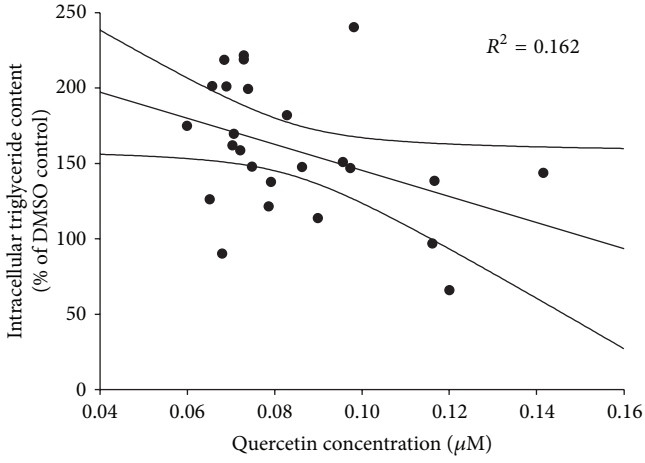

Figure 5: Intracellular triglycerides content of 3T3-L1 murine adipocytes exposed to 75 μg/mL of *R. groenlandicum* leaf extracts collected from various locations. Quercetin concentrations in crude extract were significantly and negatively associated with the species' adipogenic activity ($p = 0.0458$). Triglyceride contents are normalized to the vehicle control (0.1% DMSO).

Table 1: Variation partitioning of the adipogenic activity of *R. groenlandicum* leaf extracts explained by the content in biologically active compounds (compounds) and the effect of bioclimatic variables (environment). Fraction [*a*] corresponds to the unique contribution of compounds once the environment has been taken into account, whereas fraction [*c*] represents the reverse. Fraction [*b*] represents the shared portion, or overlap, between the effect of compounds and environment. The variation (R^2_{adj}) of each fraction is represented in Figure 6. Asterisk (∗) indicates significant fractions at $\alpha = 0.05$.

Fractions	R^2_{adj}	p
$[a + b]$ = compounds	0.491	0.0279*
$[b + c]$ = environment	0.109	0.150
$[a + b + c]$ = compounds + environment (full model)	0.534	0.0437*
$[a]$ = compounds|environment	0.424	0.0619
$[b]$ = shared	0.0668	Not testable
$[c]$ = environment|compounds	0.0424	0.302
$[d]$ = unexplained (residuals)	0.466	Not testable

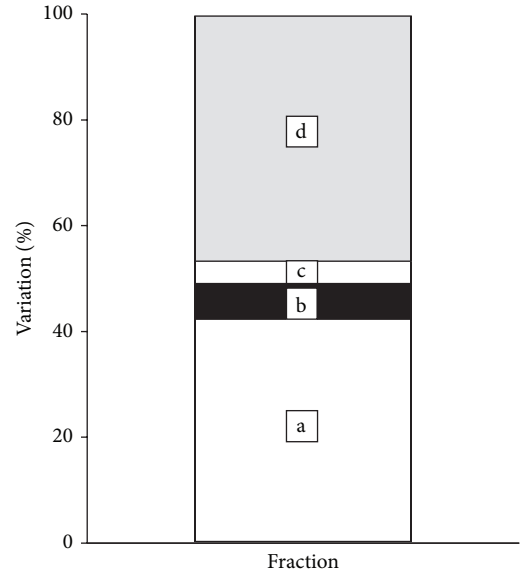

Figure 6: Variation partitioning of the adipogenic activity of *R. groenlandicum* leaf extracts explained by the content in biologically active compounds and the effect of bioclimatic variables. *a* = compounds|environment, *b* = shared component, *c* = environment|compounds, and *d* = unexplained (see Table 1 for more details). The full model, fraction $[a + b + c]$, as well as the model including compounds only, fraction $[a + b]$, was significant at $\alpha = 0.05$.

compound related to changes in the adipogenic activity of *R. groenlandicum*, was not found to be strongly associated with environmental variables [1]. This may hence explain why the portion of variation those environmental variables contribute to the model, and more specifically to the content of biologically active compounds, which best explains the variation in TG content, is considerably small (Table 1, Figure 6).

On the other hand, our results provide support for the hypothesis that synergistic interactions may occur between

compounds. For instance, the inhibitory action of *Hibiscus sabdariffa* (Malvaceae) was greater than the sum of its parts when polyphenols had been fractionated, isolated, and tested individually [35]. More importantly, in bioassay-guided fractionation experiments, the activity of crude Labrador tea extracts was higher than that of each active compound tested individually [24]. Finally, quercetin and resveratrol, together, decreased lipid accumulation considerably more than each of these used separately at the same dose [34].

Many of the compounds quantified in this paper have shown adipogenic activity in some form or another. Quercetin-3-glucoside has been found toxic to adipocytes at relatively low concentration (50 μM) but was not found to affect adipogenic activity [33]. Quercetin-3-rhamnoside has been found inactive at low concentrations yet inhibited adipogenesis at high concentrations and chlorogenic acid has also been found to inhibit intracellular triglycerides accumulation [33]. Content variations of some of these, particularly (+)-catechin and (−)-epicatechin, have been explained by environmental variables [1]. Although the individual effect of these compounds was not detected in our study, it does not undermine the role they may play when found in a cocktail of substances.

4. Conclusion

We have previously shown that latitude acted as a marker for the impact of environmental variables on phytochemical concentrations [1]. Therefore, a trend could possibly exist between abiotic factors and concentration of targeted secondary metabolites, but a larger sample size might be needed to detect it. There may also be other environmental, climatic, and even biotic factors that were not taken into account, which explain the changes in quercetin content. These may better explain the ecophysiological processes affecting the antidiabetic potential of *R. groenlandicum*. Increase in the adipogenic potential of this traditional medicine was associated primarily with lower concentrations of quercetin, but the cause for its variation will require further investigation. Nonetheless, our results do not provide enough evidence to justify the idea that specific accessions of Labrador tea may have reproducibly better adipogenic potential than others along a latitudinal gradient. Conversely, our study implies that random harvesting of *R. groenlandicum* in the Eeyouch territory of Northern Quebec should not have a major impact on the quality of traditional preparations or NHPs made from this plant.

Conflict of Interests

The authors declare that there is no conflict of interests regarding the publication of this paper.

Acknowledgments

This work was supported by the Canadian Institutes of Health Research (CIHR) Team Grant (CTP-79855) to Pierre S. Haddad, J. T. Arnason, and Alain Cuerrier and discovery grant to J. T. Arnason as well as funding from the Natural Sciences and Engineering Research Council (NSERC), Canada's Northern Internship program, and Network Environments for Aboriginal Health Research (NEAHR) to M. Rapinski. Special thanks are due to the Elders of the Eeyou Istchee Cree Nations of Mistissini, Nemaska, Waskaganish, Eastmain, Wemindji, and Whapmagoostui for sharing their traditional knowledge and allowing us to collect medicinal plants from their lands with the purpose of bridging indigenous knowledge and contemporary science. The authors also thank the Cree Board of Health and Social Services of James Bay for their constant support, as well as A. Léger, N. Roy, A. Downing, Y. Tendland, B. Walsh-Roussel, C. H Ta, D. Vallerand, N. Shang, and M. Ouchfoun for helping out with field and lab work. Special recognition is due to Jonathan Ferrier who also provided comments, ideas, and support. Finally, thanks are due to S. Daigle and P. Legendre for statistical advice.

References

[1] M. Rapinski, R. Liu, A. Saleem, J. T. Arnason, and A. Cuerrier, "Environmental trends in the variation of biologically active phenolic compounds in Labrador tea, *Rhododendron groenlandicum*, from northern Quebec, Canada," *Botany*, vol. 92, no. 11, pp. 783–794, 2014.

[2] T. Arnason, R. J. Hebda, and T. Johns, "Use of plants for food and medicine by Native Peoples of Eastern Canada," *Canadian Journal of Botany*, vol. 59, no. 11, pp. 2189–2325, 1981.

[3] R. A. Zieba, *Healing and Healers among the Northern Cree*, University of Manitoba, 1990.

[4] E. V. Siegfried, *Ethnobotany of the Northern Cree of Wabasca/Desmarais*, University of Calgary, 1994.

[5] R. J. Marles, C. Clavelle, L. Monteleone et al., *Aboriginal Plant Use in Canada's Northwest Boreal Forest*, Natural Resources Canada, Edmonton, Canada, 2008.

[6] A. Cuerrier and Elders of Kangiqsujuaq, *The Botanical Knowledge of the Inuit of Kangiqsujuaq*, Avataq Cultural Institute, Inukjuak, Canada, 2011.

[7] A. Cuerrier and Elders of Kangiqsualujjuaq, *The Botanical Knowledge of the Inuit of Kangiqsualujjuaq, Nunavik*, Avataq Cultural Institute, Inukjuak, Canada, 2011.

[8] A. Cuerrier, Elders of Umiujaq, and Elders of Kuujjuarapik, *The Botanical Knowledge of the Inuit of Umiujaq and Kuujjuarapik, Nunavik*, Avataq Cultural Institute, Inukjuak, Canada, 2011.

[9] A. Cuerrier and L. Hermanutz, *Our Plants... Our Land. Plants of Nain and Torngat Mountains Basecamp and Research Station (Nunatsiavut)*, Institut de Recherche en Biologie Végétale, Montreal, Canada; Memorial University of Newfoundland, St. John's, Canada, 2012.

[10] M.-H. Fraser, *Ethnobotanical Investigation of Plants Used for the Treatment of type 2 Diabetes by Two Cree Communities in Québec: Quantitative Comparisons and Antioxidant Evaluation*, McGill University, 2006.

[11] C. Leduc, J. Coonishish, P. Haddad, and A. Cuerrier, "Plants used by the Cree Nation of Eeyou Istchee (Quebec, Canada) for the treatment of diabetes: a novel approach in quantitative ethnobotany," *Journal of Ethnopharmacology*, vol. 105, no. 1-2, pp. 55–63, 2006.

[12] A. Downing, *Inter and Intra-Specific Differences in Medicinal Plant Use for the Treatment of Type II Diabetes Symptoms by the Cree Elders of Eeyou Istchee (QC)*, Université de Montréal, 2010.

[13] M. Rapinski, *Ethnobotanique de la Nation crie d'Eeyou Istchee et variation géographique des plantes médicinales antidiabétiques*, Université de Montréal, 2012.

[14] D. C. A. Spoor, L. C. Martineau, C. Leduc et al., "Selected plant species from the Cree pharmacopoeia of northern Quebec possess anti-diabetic potential," *Canadian Journal of Physiology and Pharmacology*, vol. 84, no. 8-9, pp. 847–858, 2006.

[15] M.-H. Fraser, A. Cuerrier, P. S. Haddad, J. T. Arnason, P. L. Owen, and T. Johns, "Medicinal plants of Cree communities (Québec, Canada): antioxidant activity of plants used to treat type 2 diabetes symptoms," *Canadian Journal of Physiology and Pharmacology*, vol. 85, no. 11, pp. 1200–1214, 2007.

[16] D. Harbilas, L. C. Martineau, C. S. Harris et al., "Evaluation of the antidiabetic potential of selected medicinal plant extracts from the Canadian boreal forest used to treat symptoms of diabetes: part II," *Canadian Journal of Physiology and Pharmacology*, vol. 87, no. 6, pp. 479–492, 2009.

[17] C. S. Harris, L.-P. Beaulieu, M.-H. Fraser et al., "Inhibition of advanced glycation end product formation by medicinal plant extracts correlates with phenolic metabolites and antioxidant activity," *Planta Medica*, vol. 77, no. 2, pp. 196–204, 2011.

[18] X.-K. Fang, J. Gao, and D.-N. Zhu, "Kaempferol and quercetin isolated from *Euonymus alatus* improve glucose uptake of 3T3-L1 cells without adipogenesis activity," *Life Sciences*, vol. 82, no. 11-12, pp. 615–622, 2008.

[19] P. A. Grimaldi, "The roles of PPARs in adipocyte differentiation," *Progress in Lipid Research*, vol. 40, no. 4, pp. 269–281, 2001.

[20] J. B. Hansen and K. Kristiansen, "Regulatory circuits controlling white versus brown adipocyte differentiation," *The Biochemical Journal*, vol. 398, no. 2, pp. 153–168, 2006.

[21] O. A. MacDougald and S. Mandrup, "Adipogenesis: forces that tip the scales," *Trends in Endocrinology & Metabolism*, vol. 13, no. 1, pp. 5–11, 2002.

[22] E. D. Rosen and O. A. MacDougald, "Adipocyte differentiation from the inside out," *Nature Reviews Molecular Cell Biology*, vol. 7, no. 12, pp. 885–896, 2006.

[23] A. Saleem, C. S. Harris, M. Asim et al., "A RP-HPLC-DAD-APCI/MSD method for the characterisation of medicinal Ericaceae used by the Eeyou Istchee Cree First Nations," *Phytochemical Analysis*, vol. 21, no. 4, pp. 328–339, 2010.

[24] M. Ouchfoun, *Validation des effets antidiabétiques de Rhododendron groenlandicum, une plante médicinale des Cri de la Baie James, dans le modèle in vitro et in vivo: élucidation des mécanismes d'action et identification des composés actifs*, Université de Montréal, 2011.

[25] LAAS, GLFC, CFS et al., *Selected Modeled Climate Data for Point Locations*, LAAS, Sault Ste. Marie, Canada, 2014.

[26] D. W. McKenney, J. H. Pedlar, K. Lawrence, K. Campbell, and M. F. Hutchinson, "Beyond traditional hardiness zones: using climate envelopes to map plant range limits," *BioScience*, vol. 57, no. 11, pp. 929–937, 2007.

[27] D. McKenney, P. Papadopol, K. Lawrence et al., "Customized spatial climate models for Canada," 2007.

[28] S. Lê, J. Josse, and F. Husson, "FactoMineR: an R package for multivariate analysis," *Journal of Statistical Software*, vol. 25, no. 1, pp. 1–18, 2008.

[29] D. Borcard, P. Legendre, and P. Drapeau, "Partialling out the spatial component of ecological variation," *Ecology*, vol. 73, no. 3, pp. 1045–1055, 1992.

[30] A. Méot, P. Legendre, and D. Borcard, "Partialling out the spatial component of ecological variation: questions and propositions in the linear modelling framework," *Environmental and Ecological Statistics*, vol. 5, no. 1, pp. 1–27, 1998.

[31] R Core Team, *R: A Language and Environment for Statistical Computing*, 2014, http://www.r-project.org/.

[32] K. Iwashtta, K. Yamaki, and T. Tsushida, "Effect of flavonoids on the differentiation of 3T3-L1 adipocytes," *Food Science and Technology Research*, vol. 7, no. 2, pp. 154–160, 2001.

[33] C.-L. Hsu and G.-C. Yen, "Effects of flavonoids and phenolic acids on the inhibition of adipogenesis in 3T3-L1 adipocytes," *Journal of Agricultural and Food Chemistry*, vol. 55, no. 21, pp. 8404–8410, 2007.

[34] J.-Y. Yang, M. A. Della-Fera, S. Rayalam et al., "Enhanced inhibition of adipogenesis and induction of apoptosis in 3T3-L1 adipocytes with combinations of resveratrol and quercetin," *Life Sciences*, vol. 82, no. 19-20, pp. 1032–1039, 2008.

[35] M. Herranz-López, S. Fernández-Arroyo, A. Pérez-Sanchez et al., "Synergism of plant-derived polyphenols in adipogenesis: perspectives and implications," *Phytomedicine*, vol. 19, no. 3-4, pp. 253–261, 2012.

Hindawi Publishing Corporation
Evidence-Based Complementary and Alternative Medicine
Volume 2015, Article ID 501272, 9 pages
http://dx.doi.org/10.1155/2015/501272

Research Article

Erchen Decoction Prevents High-Fat Diet Induced Metabolic Disorders in C57BL/6 Mice

Bi-Zhen Gao,[1,2] Ji-Cheng Chen,[3] Ling-Hong Liao,[1,2] Jia-Qi Xu,[1] Xiao-Feng Lin,[1] and Shan-Shan Ding[1,2]

[1] *Fujian University of Traditional Chinese Medicine, Fujian 350122, China*
[2] *Fujian Key Laboratory of TCM Health State, Fujian University of Traditional Chinese Medicine, Fujian 350122, China*
[3] *Department of Endocrinology, Quanzhou City Hospital of Traditional Chinese Medicine, Fujian 362002, China*

Correspondence should be addressed to Bi-Zhen Gao; gbz688@163.com

Received 12 July 2015; Accepted 3 September 2015

Academic Editor: Pierre S. Haddad

Erchen decoction (ECD) is a traditional Chinese medicine prescription, which is used in the treatment of obesity, hyperlipidemia, fatty liver, diabetes, hypertension, and other diseases caused by retention of phlegm dampness. In this study we investigated the potential mechanism of ECD, using metabolism-disabled mice induced by high-fat diet. Body weight and abdominal circumference were detected. OGTT was measured by means of collecting blood samples from the tail vein. Blood lipid levels and insulin were measured using biochemical assay kit. Real-time PCR was used to measure the CDKAL1 gene expression and western blot was used to measure the protein expression. Through the research, it was found that ECD showed markedly lower body weight and abdominal circumference than those in the HFD group. Consistently, we observed that ECD significantly improved glucose tolerance, promoted the secretion of insulin and decreased the level of TG, TC level. Meanwhile, we observed significantly increased CDKAL1 mRNA and protein level in the ECD group. Therefore, we speculate that the potential molecular mechanism of ECD is to promote the CDKAL1 expression, ameliorate islet cell function, and raise insulin levels to regulate the metabolic disorder.

1. Introduction

Erchen decoction (ECD) is a common Traditional Chinese Medicine prescription, which was first recorded in a classic clinical Traditional Chinese Medicine (TCM) book titled The Taiping Huimin Heji Jufang, and it is a basic prescription of the treatment in drying dampness and resolving phlegm and is used in the treatment of a variety of diseases caused by retention of phlegm dampness. In the clinical application of TCM, ECD is used extensively in the treatment of obesity, hyperlipidemia, fatty liver, diabetes, hypertension, and other diseases caused by retention of phlegm dampness [1–4]. It has been reported that the phlegm dampness tends to be concentrated in the metabolic syndrome people [5, 6]. At present, metabolic syndrome (MS) refers to the clinical syndrome gathered by diabetes, hyperlipidemia, and hypertension, which takes the insulin resistance as the basis and central obesity as the main performance. In the past decades, MS has attracted attention due to its higher and higher incidence related to changes of people's life style in China. It is shown in studies that ECD [7, 8] could improve the fatty deposits, reduce blood lipid, lower body mass index and blood glucose, improve the glycolipid metabolic disorder, and so on. It is found in animal experiments that ECD could reduce the blood glucose and blood lipid in mice fed with high-fat diet and increase insulin sensitivity [9, 10]. It also has the function of reducing the atherosclerosis index and antiatherosclerosis [11]. Despite multiple treatment effects observed, the molecular mechanism of ECD in regulating metabolism disorder is still unclear.

CDKAL1 is located on chromosome 6, 6P22.3, and its full length is 37 kb. The mRNA of CDKAL1 is highly expressed in the bone, muscle, pancreas, and brain tissues in the human body. In recent years, part of the study shows that CDKAL1 is a mammalian methylthiotransferase that catalyzes the 2-methylthio (ms2) modification of N6-threonylcarbamoyladenosine (t6A) to produce 2-methylthio-N6-threonylcarbamoyladenosine (ms2t6A) at position 37 of

tRNALys (UUU) [12]. The ms2 modification of tRNALys (UUU) stabilises the interaction with its cognate codons, allowing for efficient translation. CDKAL1 induces insulin secretion through induction of precise protein translation of insulin [13]. Clinical studies and animal studies have suggested that ECD can promote the secretion of insulin. In this study, we would like to explore the molecular mechanisms of ECD in treatment of MS by observing its effect on the expression of CDKAL1 in mice fed with high-fat diet.

2. Materials and Methods

2.1. Drug Preparation and Diet. ECD comprises four Chinese herbs: *Pericarpium Citri Reticulatae* (9 g), *Rhizoma Pinelliae* (9 g), *Poria* (6 g), and *Radix Glycyrrhizae* (3 g). The dosage is determined according to the book of The Taiping Huimin Heji Jufang. All herbs were purchased from Guoyi Hospital affiliated to Fujian University of TCM. Herbal decoction was prepared in accordance with conventional TCM decocting methods. (1) Place all herbs in a cooking pot (porcelain) with 500 mL water; (2) boil the herbs with highest heat after 30 minutes of soak; (3) reduce heat and simmer for 20 minutes; (4) transfer the liquid by filtration; (5) add water and boil the remaining, and then repeat (3) and (4) one more time to make a second dose of medicine; and (6) mix the two doses in a glass pot and concentrate solution by the rotary evaporation apparatus. The final concentrated decoction is 50 mL. ECD, metformin, and simvastatin were administered at a dose of 10 mL/kg/d (pure solution), which was approximately 12 times of the standard dose in practice, according to the dose-equivalence equation between mice and humans [14]. The high-fat diet (HFD) contained 34.9% fat (60% of calories), 26.3% carbohydrates (20% of calories), and 26.2% protein (20% of calories) as well as fiber, vitamins, and minerals with total calorific value 21924 kJ/kg (D12492, Research Diets, New Brunswick, NJ, USA). The ordinary diet (NFD) contained 5% fat, 23% protein, and 53% carbohydrate with total calorific value 25 kJ/kg (Shanghai Slac Laboratory Animal Company, Shanghai, China).

2.2. Animals and Interventions. SPF animals (male C57BL/6J mice, 20 g ± 2 g) were obtained from Shanghai Slac Laboratory Animal Company (Shanghai, China). Mice were housed in an SPF, temperature (24°C ± 2°C) and humidity controlled (55%± 10%) room with a 12-hour light-dark cycle (commencing with light at 08:00) in the animal experiment center of Fujian University of TCM. The experimental protocol was approved by the Fujian University of TCM Ethics Committee for the use of experimental animals (number 2014-004). Animals were randomized into 2 groups: the normal group (NFD, $n = 8$), fed ordinary diet, and the high-fat diet group (HFD, $n = 32$), fed high-fat diet. After 10 weeks, the mice in the HFD group were randomized into 4 groups: the model group (HFD, $n = 8$), the Erchen decoction group (ECD, $n = 8$), the metformin group (MFN, $n = 8$, each mouse is given 0.3 g/kg metformin), and the simvastatin group (SVN, $n = 8$, each mouse is given 2 mg/kg simvastatin). Every group, respectively, gives corresponding drug by gavage orally for 4 weeks. All mice could eat and drink ad libitum. Body weight and abdominal circumference were recorded every 2 weeks.

2.3. Intraperitoneal Glucose Tolerance Test. At week 10, week 12, and the end of the treatment, mice were fasted overnight (12 h). The baseline glucose values (0 min), prior to injection of glucose (1 g/kg body weight), were measured by means of collecting blood samples from the tail vein. Additional blood samples were collected at regular intervals (30, 60, and 120 min) for glucose tolerance tests.

2.4. Serum Chemistry Analysis. The mice were fasted overnight and anesthetized. Blood samples were collected from the retroorbital sinuses of each group. Serum triglyceride (TG), total cholesterol (TC), HDL cholesterol (HDL-c), and LDL cholesterol (LDL-c) were measured using biochemical assay kit according to the manufacturer's instruction (Nanjing Jiancheng Bioengineering Institute, Nanjing, China). Serum insulin was measured using an ELISA kit according to the manufacturer's instruction (Shanghai Westang Bio-Tech Co. Ltd., Shanghai, China).

2.5. Real-Time PCR for mRNA Analysis. Total RNA was extracted from liver subcutaneous adipose and visceral adipose tissues using Trizol reagent (TaKaRa, Otsu, Japan). First-strand complementary DNA (cDNA) was generated by reverse transcriptase, with random primers (TaKaRa, Otsu, Japan). The sequences of the primers are described in Table 1. To evaluate the mRNA expression of CDKAL1 in the liver subcutaneous adipose and visceral adipose tissues, real-time PCR was performed using a SYBR Green master mix kit (TaKaRa, Otsu, Japan) according to the manufacturer's instructions on the Mastercycler ep realplex4S real-time PCR system (Eppendorf, Hamburg, Germany). The cDNA was denatured at 95°C for 10 min followed by 40 cycles of PCR (95°C, 15 s; 60°C, 60 s). The $2^{-\Delta\Delta Ct}$ method [15] was used to determine relative amounts of product, and data are presented as fold change, using β-actin as an endogenous control.

2.6. Protein Isolation and Western Blotting. The liver subcutaneous adipose and visceral adipose tissues of every group were homogenized in liquid nitrogen, and whole-cell protein was extracted by using lysate buffer containing proteinase inhibitor (Beyotime Biotechnology, Shanghai, China). Protein concentration was quantified spectrophotometrically by using BSA protein assay kit (Beyotime Biotechnology, Shanghai, China). Protein samples were separated by PAGE using 10% SDS-polyacrylamide gels. Samples were transferred to polyvinylidene fluoride membrane and blocked with 5% milk. The membrane was incubated with a rabbit anti-CDKAL1 primary antibody (1 : 500, Abcam, Cambridge, England) overnight at 4°C and followed by the secondary antibody (against rabbit, Beyotime Biotechnology, Shanghai, China) for 1 h at 37°C. The primary antibodies including mouse anti-β-actin (1 : 1000, Sigma, America) were similar. Lastly, each protein band was detected using enhanced

Table 1: List of primers.

Gene	Forward primer	Reverse primer
CDKAL1	ATCGGGGTTCAGCAGATAGAT	TCTTCGGCAAATCCAGTCGAG
β-actin	GGCTGTATTCCCCTCCATCG	CCAGTTGGTAACAATGCCATGT

chemiluminescence (ECL, Beyotime Biotechnology, Shanghai, China). The densitometric values were measured with Gel-Pro Analyzer.

2.7. Statistical Analysis. Data analyses were performed using the statistical program SPSS 19.0. All data were presented as means ± SE. Independent-samples t-test was performed to compare two groups. ANOVA was performed to compare multiple groups. Differences were considered as significant, $P < 0.05$, or not significant, $P > 0.05$.

3. Results

3.1. ECD Reduces the Body Weight and Abdominal Circumference in Mice Fed with High-Fat Diet. In order to explore ECD effects on body weight and abdominal circumference in high-fat mice, body weight and abdominal circumference were recorded every 2 weeks. Since the second week, the HFD group was significantly higher than the NFD group regarding body weight and abdominal circumference ($P < 0.01$) (Figures 1(a) and 1(b)). After the medication intervention, the body weight and abdominal circumference in the ECD and SVN groups were markedly lower than in the HFD group ($P < 0.01$) which also lost more weight and abdominal circumference than the MFN group at week 12 ($P < 0.01$). In addition, the body weight and abdominal circumference in the MFN group were significantly lower than in the HFD group at week 14 ($P < 0.05$) (Figures 1(c) and 1(d)).

3.2. ECD Improves the Glucose Tolerance in Mice Fed with High-Fat Diet. We used the glucose tolerance test to explore the change of blood glucose. After high-fat feeding, the glucose tolerance was markedly lower in the HFD group ($P < 0.01$) (Figure 2(b)). After the medication intervention, fasting blood glucose significantly decreased in the ECD and MFN groups compared to the HFD group ($P < 0.01$); meanwhile, there was no significant difference between the ECD, MFN, and NFD groups at week 14 ($P > 0.05$). For the glucose tolerance, compared with the HFD group, the ECD group was significantly improved at week 12 and week 14 ($P < 0.05$), and the MFN and SVN groups were significantly improved at week 14 ($P < 0.05$) (Figures 2(c) and 2(d)).

3.3. ECD Improves the Level of Insulin and Reduces Blood Lipid Levels. We surmised that the ECD can possibly improve the glucose tolerance by changing the insulin levels. Later on, the study found that the insulin levels of the ECD, MFN, and SVN groups were significantly higher than the HFD group ($P < 0.05$), and the effect of MFN was better than that of ECD; the difference was statistically significant ($P < 0.05$) (Figure 2(a)). Compared with the NFD group, TC, TG, HDL-c, and LDL-c in the HFD group were higher, and the difference was statistically significant ($P < 0.01$); TC and TG in the ECD, MFN, and SVN groups decreased significantly compared to the HFD group ($P < 0.01$); LDL-c of the MFN and SVN groups decreased significantly compared to the HFD group ($P < 0.05$); HDL-c of the SVN group decreased significantly compared to the HFD group ($P < 0.01$). In addition, the SVN group was markedly lower than the ECD group regarding the level of HDL-c and LDL-c ($P < 0.05$). Meanwhile, compared with the MFN group, the level of LDL-c in the SVN group was significantly lower ($P < 0.01$) (Figure 2(e)).

3.4. ECD Increased the Expression of CDKAL1 in the Liver Visceral Adipose and Subcutaneous Adipose Tissues. To explore the mechanisms by which ECD regulate the metabolic disorder in high-fat mice, the expressions of CDKAL1 mRNA and protein were tested. The study found that the expression of CDKAL1 mRNA and protein in the HFD group decreased significantly in the liver, visceral adipose and subcutaneous adipose tissues ($P < 0.01$). In the liver tissues, the expressions of CDKAL1 mRNA and protein in the ECD, MFN, and SVN groups were significantly higher than that of the HFD group ($P < 0.05$); meanwhile, the MFN group was markedly higher than the SVN group ($P < 0.05$). Indeed, the MFN group was significantly higher than the ECD group regarding the expression of protein ($P < 0.01$) (Figures 3(a) and 4(a)). In visceral adipose and subcutaneous adipose tissue, compared with HFD group, the expression of mRNA and protein significantly elevated in the ECD group ($P < 0.01$), and the expression of protein significantly elevated in the MFN group ($P < 0.01$). In addition, the ECD group was markedly higher than the MFN group regarding the expression of mRNA ($P < 0.05$). Compared with the HFD and MFN groups, the expression of mRNA and protein markedly elevated in the SVN group ($P < 0.05$); meanwhile, the SVN group was significantly higher than the ECD group regarding the expression of protein ($P < 0.05$) (Figures 3(b), 3(c), 4(b), and 4(c)).

4. Discussion

The retention of phlegm dampness is considered to be an important factor in the metabolic disorders related diseases in the TCM theory. And according to the TCM theory, the high-fat diet causes the spleen and stomach impairment and then leads to the accumulation of grease in the body, and finally the excess grease induces the retention of phlegm dampness [16]. We fed the mice with the high-fat diet; after 2 weeks, the body weights and abdominal circumference of the mice increased significantly and the obvious abdominal obesity appeared. At the same time, the mice had significantly elevated blood glucose, impaired glucose tolerance, and lipid metabolism

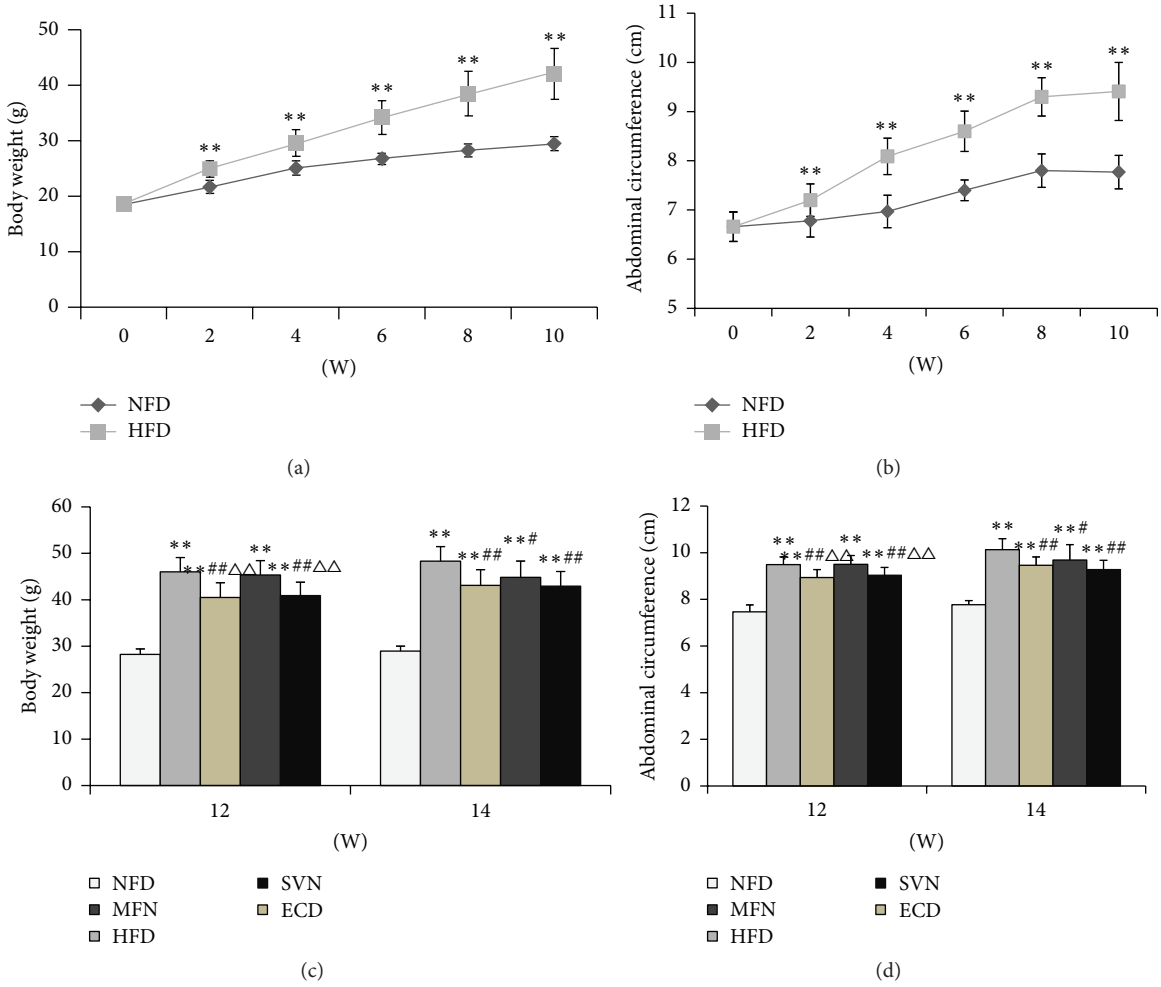

Figure 1: The changes of body weight and abdominal circumference: (a) body weight (weeks 0–10); (b) abdominal circumference (weeks 0–10); (c) body weight (weeks 12 and 14); and (d) abdominal circumference (weeks 12 and 14); $^{**}P < 0.01$, versus the NFD group; $^{\#}P < 0.05$, $^{\#\#}P < 0.01$, versus the HFD group; $^{\triangle\triangle}P < 0.01$, versus the MFN group.

disorders. All of these symptoms are consistent with the pathological diagnosis of metabolic syndrome. Therefore, it is considered that the mice fed with high-fat diet can induce the model of the retention of phlegm dampness in MS.

A series of TCM studies have indicated that [5, 6] the retention of phlegm dampness is one of main TCM pathological factors of MS, which runs through the whole disease development process. As the basic prescription of the treatment in drying dampness and resolving phlegm, ECD showed a good effect in the treatment of MS. It was found in the animal experiments [17, 18] that ECD could reduce blood glucose, regulate lipid metabolism, and reduce the expression of IR, IRS-1, and Cav-1, so as to improve insulin resistance. Also ECD can decrease the NF-κB excessive activation and inhibit the adipose tissue low-grade inflammation in MS model of rats [19]. Another study carried out in rats fed with HFD also showed that ECD can reduce AST, ALT, and APN and remit the pathological changes of liver tissue [20]. In our study, it was observed that ECD can significantly reduce the body weight and abdominal circumference in mice fed with high-fat diet, improve glucose tolerance, promote the secretion of insulin and reduce the level of blood lipid, and also promote the expression of CDKAL1 mRNA and protein.

MS refers to the clinical syndrome gathered by abnormal glucose metabolism, hypertension, and lipid metabolism disorder, which takes the insulin resistance as the basis [21] and central obesity as the main performance [22]. When the insulin secretion decreased and the blood glucose increased, the apoB100 saccharification happened and then resulted in the decline of the LDL clearance by apoB receptor-mediated in liver cells and the increase in LDL-c. While the MS is in the presence of insulin resistance, the liver synthesis, and secretion of VLDL, TG is increasing, and the clearance decreases, so as to produce hyperlipidemia. It is found in this study that ECD can significantly decrease the body weight and abdominal circumference in mice fed with high-fat diet, and it is surmised that it reduces the weight and improves abdominal obesity by reducing abdominal fat accumulation. At the same time in this study, ECD improves the OGTT and decreases the TG and TC. So it is surmised

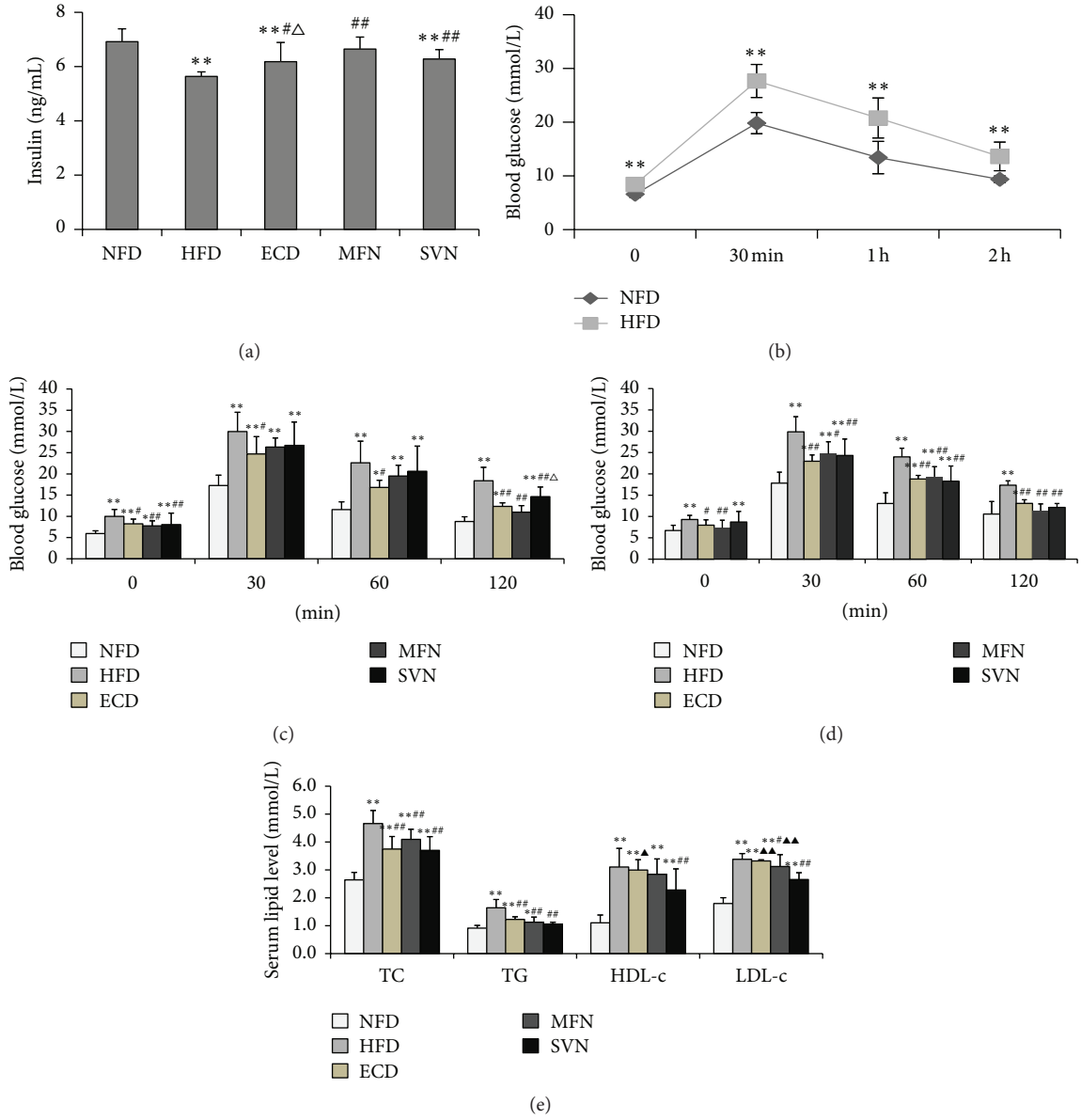

Figure 2: ECD improve insulin level, OGTT, and lipid accumulation: (a) insulin level; (b) OGTT (week 10); (c) OGTT (week 12); (d) OGTT (week 14); and (e) lipid levels; $^{*}P < 0.05$, $^{**}P < 0.01$, versus the NFD group; $^{\#}P < 0.05$, $^{\#\#}P < 0.01$, versus the HFD group; $^{\triangle}P < 0.05$, versus the MFN group; $^{\blacktriangle}P < 0.05$, $^{\blacktriangle\blacktriangle}P < 0.01$, versus the SVN group.

that ECD can reduce blood glucose through the promotion of insulin secretion and result in the improvement of the apoB saccharification, so as to improve the insulin resistance and reduce the secretion of VLDL and TG in liver, ultimately improving hyperlipidemia.

It was reported that the ms2t6A modification of tRNALys (UUU) by CDKAL1 is required for the accurate translation of AAA and AAG codons. The human insulin gene contains 2 Lys (AAG) codons. One of the Lys residues is located at the cleavage site between the C-peptide and A chain of insulin. And it was confirmed that the defects of CDKAL1 in β-cell easily misread this Lys codon by ms2t6A modification-deficient tRNALys (UUU) which results in the misfolding or miscleavage of proinsulin and leads to decrease in insulin secretion and impairment of glucose regulation eventually [13, 23]. It has been reported that CDKAL1 risk allele carriers display an insulin secretory defect that is concomitant with higher levels of proinsulin [24], while some studies have shown that CDKAL1 can also promote the generation of ATP and control the insulin release within the first phase of pancreatic β-cells [25, 26], which has also been confirmed in the study of gene knockout mice [13]. The first phase insulin secretion is important to reduce the postprandial blood glucose, which can inhibit the production of endogenous glucose and inhibit the increase of postprandial blood glucose levels, and participate in the occurrence of high blood glucose after meal. Another animal study suggested that CDKAL1 gene deletion is accompanied by modestly impaired

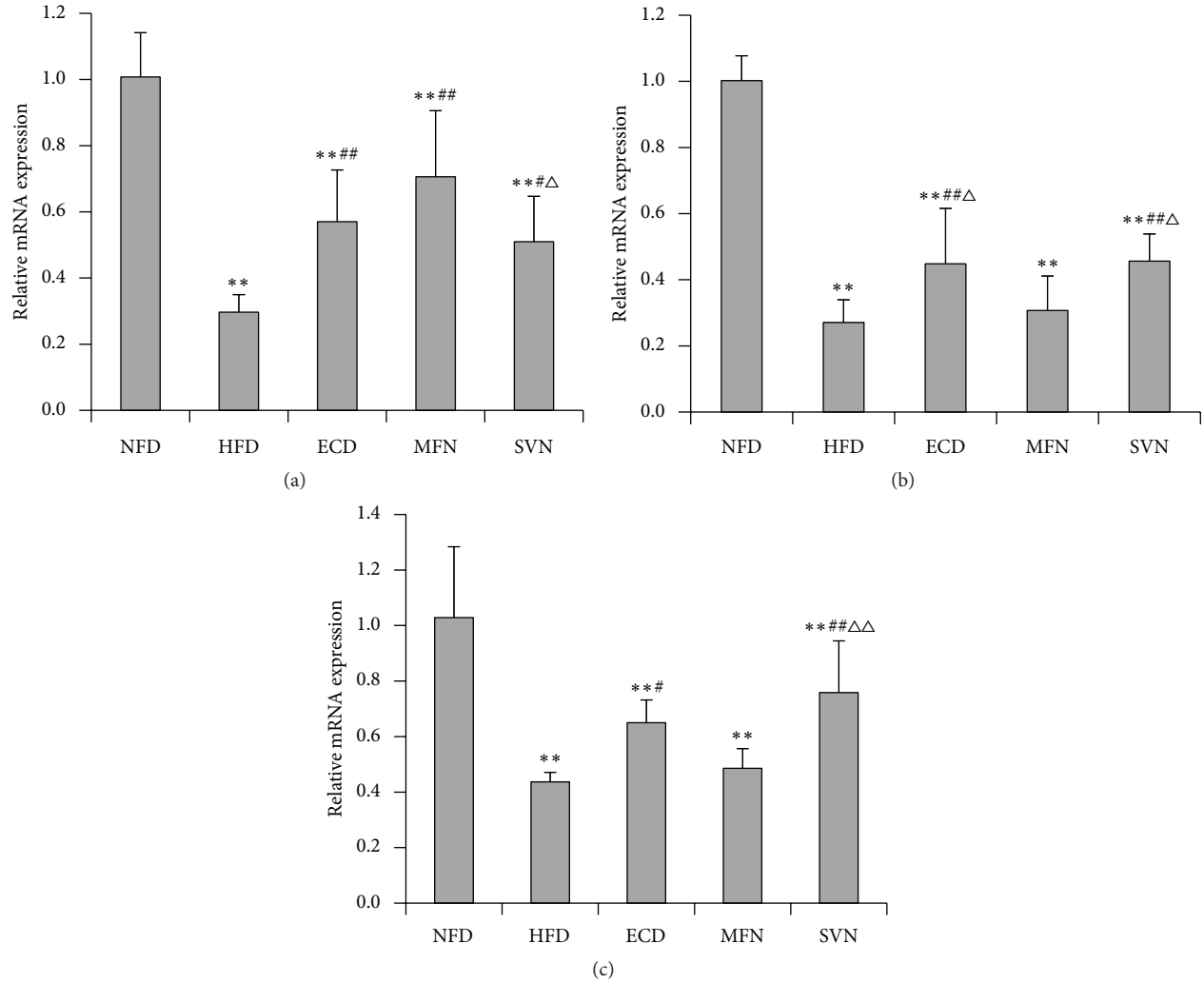

Figure 3: The mRNA expression of CDKAL1: (a) liver tissue; (b) visceral adipose tissue; and (c) subcutaneous adipose tissue; $^{**}P < 0.01$, versus the NFD group; $^{\#}P < 0.05$, $^{\#\#}P < 0.01$, versus the HFD group; $^{\triangle}P < 0.05$, $^{\triangle\triangle}P < 0.01$, versus the MFN group.

insulin secretion and longitudinal fluctuations in insulin sensitivity during high-fat feeding in mice. CDKAL1 may affect such compensatory mechanisms regulating glucose homeostasis through interaction with diet [27]. Additionally, several genome-wide association analyses identified that CDKAL1 multiple single nucleotide polymorphism loci were associated with human susceptibility of type 2 diabetes [28–32]. Thus far, several human studies have indicated that the risk variant of CDKAL1 is associated with reduced insulin secretion [26, 33–36].

In this study, the expressions of CDKAL1 mRNA and protein in the liver visceral adipose and subcutaneous adipose tissues of mice were significantly downregulated after being induced by high-fat diet. And after the treatment of ECD, the expressions of CDKAL1 mRNA and protein in the liver visceral adipose and subcutaneous adipose tissues of mice increased significantly. At the same time, it is found in this study that the insulin secretion in mice is reduced after inducement by the high-fat diet, and ECD can promote mouse insulin secretion. These observations suggested that ECD can increase the expression of CDKAL1 to promote the secretion of insulin, which can improve glucose metabolism.

There are several limitations in the present study. Above all, although ECD can promote the expression of CDKAL1, the mechanism of how ECD triggered the increase of CDKAL1 was still unclear. Also why ECD can regulate lipid metabolism and how ECD can adjust lipid metabolism have not been investigated in our study.

In summary, ECD has good therapeutic effects on the metabolic disorders induced by high-fat diet in mice, including reducing body weight and abdominal circumference, improving glucose tolerance, and regulating glucose and lipid metabolism. At the same time, it was observed to improve the function of islet cell by regulating the expression of CDKAL1, so as to promote the secretion of insulin. This research preliminarily studied the potential mechanism of ECD from the blood biochemical levels and the expression of CDKAL1, and further research on other related mechanisms and related pathways should be taken to provide a more effective basis for the clinical application of ECD.

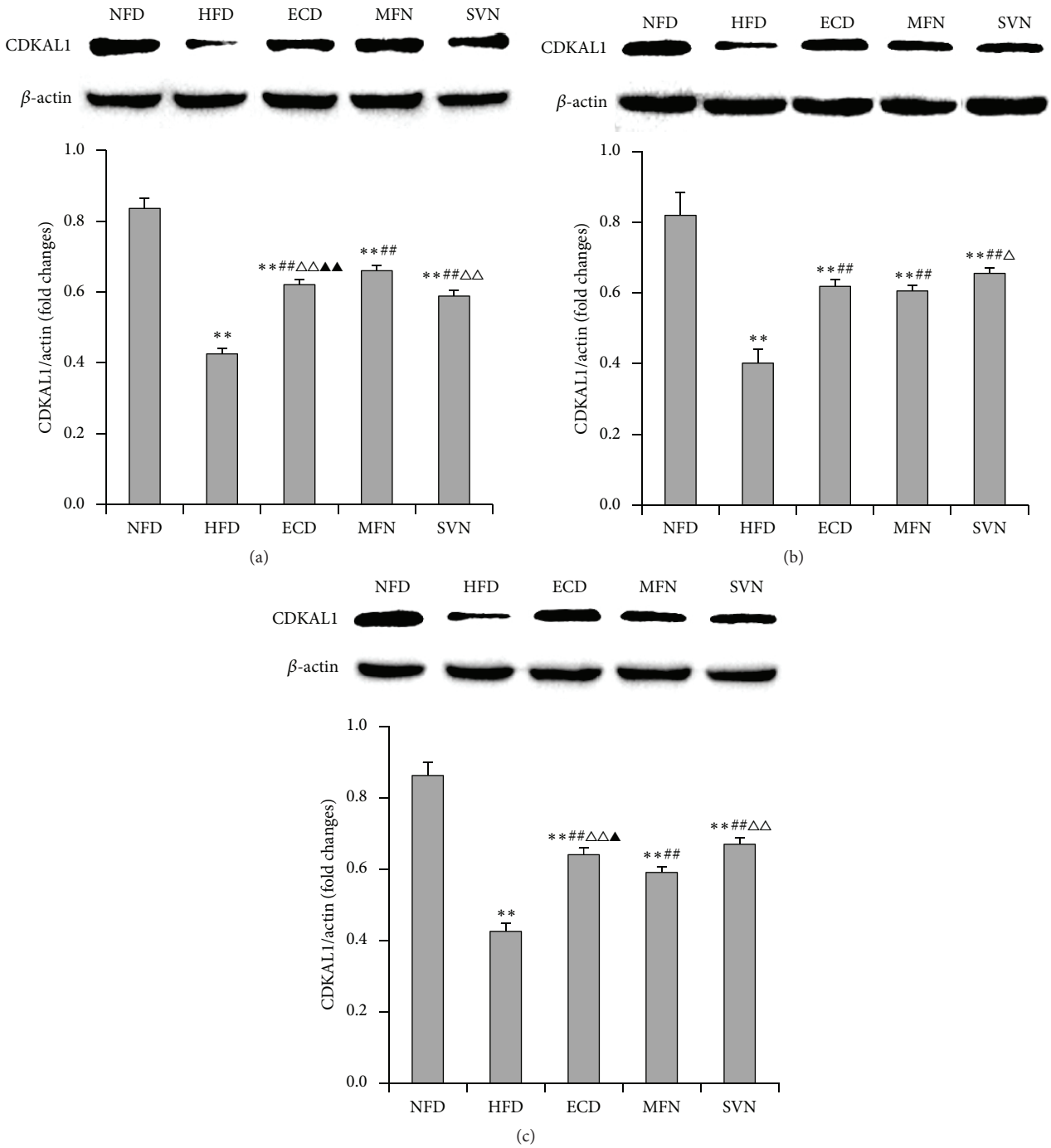

Figure 4: The protein expression of CDKAL1: (a) liver tissue; (b) visceral adipose tissue; and (c) subcutaneous adipose tissue; $^{**}P < 0.01$, versus the NFD group; $^{\#\#}P < 0.01$, versus the HFD group; $^{\triangle}P < 0.05$, $^{\triangle\triangle}P < 0.01$, versus the MFN group; $^{\blacktriangle}P < 0.05$, $^{\blacktriangle\blacktriangle}P < 0.01$, versus the SVN group.

Abbreviations

ALT: Almandine aminotransferase
ApoB100: Apolipoprotein B100
APN: Aminopeptidase
AST: Aspartate aminotransferase
CDKAL1: CDK5 Regulatory Subunit Associated Protein 1 Like 1
HDL-C: High-density lipoprotein cholesterol
LDL-C: Low-density lipoprotein cholesterol
MS: Metabolic syndrome
OGTT: Oral glucose tolerance test
TC: Total cholesterol
TCM: Traditional Chinese Medicine
TG: Triglyceride
VLDL: Very low-density lipoprotein.

Conflict of Interests

The authors report no conflict of interests.

Authors' Contribution

Bi-Zhen Gao and Ji-Cheng Chen have equally contributed to this paper.

Acknowledgments

This study was supported by the National Natural Science Foundation of China (no. 81273666), Traditional Chinese Medicine Scientific Research of Fujian Province (no. wztn201309), and Key Project of Fujian Education Department (no. JA12166).

References

[1] Q. Fu, "Clinical research on senile hypertension combined treatment of traditional Chinese and western medicine," *China Journal of Traditional Chinese Medicine and Pharmacy*, vol. 28, no. 9, pp. 2802–2803, 2013.

[2] H. Z. Chen, G. M. Wei, Y. H. Dong et al., "Effects of Shenlin Baizu San and Erchen decoction and acupuncture on insulin resistance in type 2 diabetes mellitus," *Clinical Journal of Chinese Medicine*, vol. 6, no. 19, pp. 1–3, 2014.

[3] F. T. Gao and S. S. Liu, "Clinical observation on Erchen decoction for the treatment of hyperlipidemia," *Guide of China Medicine*, vol. 11, no. 5, pp. 287–288, 2013.

[4] T. Y. Luo, "Experience of Huangqi Jianzhong decoction and Erchen decoction in treating hyperlipidaemia," *Journal of Practical Traditional Chinese Internal Medicine*, vol. 28, no. 5, pp. 128–129, 2014.

[5] H. P. Xiong, C. D. Li, B. Z. Gao, and H. Gan, "Study on relationship of pathology of phlegm syndrome of TCM with blood sugar, insulin and insulin resistance in metabolic syndrome," *China Journal of Traditional Chinese Medicine and Pharmacy*, vol. 25, no. 5, pp. 763–765, 2010.

[6] H. P. Xiong, C. D. Li, B. Z. Gao et al., "TCM risk factors of metabolic syndrome," *China Journal of Traditional Chinese Medicine and Pharmacy*, vol. 25, no. 11, pp. 1858–1859, 2010.

[7] F. M. Pan and Z. Gui, "Clinical observation of Erchen decoction on treatment of 42 cases in nonalcoholic fatty liver disease," *Journal of Yangtze University (Natural Science Edition) Medicine V*, vol. 7, no. 4, pp. 13–14, 2010.

[8] X. P. Hong, "Clinical observation of Erchen decoction on treatment of 60 cases in metabolic syndrome," *Zhejiang Journal of Traditional Chinese Medicine*, vol. 46, no. 5, article 343, 2011.

[9] S. S. Ding, J. Kang, L. Y. Zhang et al., "Effect of Erchen decoction on blood fat and insulin resistance in rats fed a high-fat diet," *Medical Innovation of China*, vol. 11, no. 15, pp. 22–24, 2014.

[10] X. J. Xie, J. Xu, Y. M. Li et al., "Effects of the Chinese medicine, modified Erchen decoction, on the lipid metabolism and hepatocyte morphology in ApoE-/- mice," *Chinese Journal of Comparative Medicine*, vol. 25, no. 4, pp. 44–47, 2015.

[11] Z. H. Wang, X. M. Ji, Z. C. Wu et al., "Therapeutic effect of Cangbai Erchen decoction on aorta ICAM1 in metabolic syndrome rats," *Chinese Archives of Traditional Chinese Medicine*, vol. 31, no. 6, pp. 1243–1245, 2013.

[12] S. Arragain, S. K. Handelman, F. Forouhar et al., "Identification of eukaryotic and prokaryotic methylthiotransferase for biosynthesis of 2-methylthio-N^6-threonylcarbamoyladenosine in tRNA," *The Journal of Biological Chemistry*, vol. 285, no. 37, pp. 28425–28433, 2010.

[13] F.-Y. Wei, T. Suzuki, S. Watanabe et al., "Deficit of tRNALys modification by Cdkal1 causes the development of type 2 diabetes in mice," *The Journal of Clinical Investigation*, vol. 121, no. 9, pp. 3598–3608, 2011.

[14] C. X. Chen, *Pharmacology of Traditional Chinese Medicine*, Shanghai Scientific and Technical Publishers, Shanghai, China, 2006.

[15] K. J. Livak and T. D. Schmittgen, "Analysis of relative gene expression data using real-time quantitative PCR and the $2^{-\Delta\Delta C_T}$ method," *Methods*, vol. 25, no. 4, pp. 402–408, 2001.

[16] T. Y. Wu, B. Z. Gao, S. Lin et al., "Impacts of different herbal formulas on blood lipid in insulin resistance model rats," *World Journal of Integrated Traditional and Western Medicine*, vol. 4, no. 7, pp. 470–472, 2009.

[17] S. Ding, J. Kang, L. Y. Zhang et al., "Effect of Erchen decoction on insulin resistance and related gene expression in rats fed a high-fat diet," *Guangming Journal of Chinese Medicine*, vol. 29, no. 9, pp. 1833–1836, 1833.

[18] S. S. Ding, L. Y. Zhang, J. Kang et al., "Effect of Erchen decoction on lipid metabolism and Caveolin-1 expression in rats fed a high-fat diet," *Lishizhen Medicine and Materia Medica Research*, vol. 25, no. 9, pp. 2060–2062, 2014.

[19] Z. H. Wang and Z. C. Wu, "Effect of Cangbai Erchen decoction on the expression of NF-κb in metabolic syndrome rats," *Shandong Journal of Traditional Chinese Medicine*, vol. 31, no. 8, pp. 594–596, 2012.

[20] H. Y. Wang, Q. Yang, C. J. Liao et al., "Effect of Erchen decoction and Taohong Siwu decoction on nonalcoholic fatty liver disease rats," *Journal of Guangzhou University of Traditional Chinese Medicine*, vol. 30, no. 5, pp. 713–717, 2013.

[21] E. Kim, "Insulin resistance at the crossroads of metabolic syndrome: systemic analysis using microarrays," *Biotechnology Journal*, vol. 5, no. 9, pp. 919–929, 2010.

[22] S. Mottillo, K. B. Filion, J. Genest et al., "The metabolic syndrome and cardiovascular risk: a systematic review and meta-analysis," *Journal of the American College of Cardiology*, vol. 56, no. 14, pp. 1113–1132, 2010.

[23] F.-Y. Wei and K. Tomizawa, "Functional loss of Cdkal1, a novel tRNA modification enzyme, causes the development of type 2 diabetes," *Endocrine Journal*, vol. 58, no. 10, pp. 819–825, 2011.

[24] A. S. Dimas, V. Lagou, A. Barker et al., "Impact of type 2 diabetes susceptibility variants on quantitative glycemic traits reveals mechanistic heterogeneity," *Diabetes*, vol. 63, no. 6, pp. 2158–2171, 2014.

[25] M. Ohara-Imaizumi, M. Yoshida, K. Aoyagi et al., "Deletion of CDKAL1 affects mitochondrial ATP generation and first-phase insulin exocytosis," *PLoS ONE*, vol. 5, no. 12, Article ID e15553, 2010.

[26] L. M. 'T Hart, A. M. Simonis-Bik, G. Nijpels et al., "Combined risk allele score of eight type 2 diabetes genes is associated with reduced first-phase glucose-stimulated insulin secretion during hyperglycemic clamps," *Diabetes*, vol. 59, no. 1, pp. 287–292, 2010.

[27] T. Okamura, R. Yanobu-Takanashi, F. Takeuchi et al., "Deletion of CDKAL1 affects high-fat diet-induced fat accumulation and glucose-stimulated insulin secretion in mice, indicating

relevance to diabetes," *PLoS ONE*, vol. 7, no. 11, Article ID e49055, 2012.

[28] H. Ryoo, J. Woo, Y. Kim, and C. Lee, "Heterogeneity of genetic associations of CDKAL1 and HHEX with susceptibility of type 2 diabetes mellitus by gender," *European Journal of Human Genetics*, vol. 19, no. 6, pp. 672–675, 2011.

[29] F. Peng, D. Hu, C. Gu et al., "The relationship between five widely-evaluated variants in CDKN2A/B and CDKAL1 genes and the risk of type 2 diabetes: a meta-analysis," *Gene*, vol. 531, no. 2, pp. 435–443, 2013.

[30] Y. Mansoori, A. Daraei, M. Naghizadeh, and R. Salehi, "Significance of a common variant in the *CDKAL1* gene with susceptibility to type 2 diabetes mellitus in Iranian population," *Advanced Biomedical Research*, vol. 4, no. 1, pp. 45–51, 2015.

[31] K. U. Jyothi and B. M. Reddy, "Gene-gene and gene-environment interactions in the etiology of type 2 diabetes mellitus in the population of Hyderabad, India," *Meta Gene*, vol. 5, pp. 9–20, 2015.

[32] S. Al-Sinani, N. Woodhouse, A. Al-Mamari et al., "Association of gene variants with susceptibility to type 2 diabetes among Omanis," *World Journal of Diabetes*, vol. 6, no. 2, pp. 358–366, 2015.

[33] M. J. Groenewoud, J. M. Dekker, A. Fritsche et al., "Variants of CDKAL1 and IGF2BP2 affect first-phase insulin secretion during hyperglycaemic clamps," *Diabetologia*, vol. 51, no. 9, pp. 1659–1663, 2008.

[34] A. Stančáková, T. Kuulasmaa, J. Paananen et al., "Association of 18 confirmed susceptibility loci for type 2 diabetes with indices of insulin release, proinsulin conversion, and insulin sensitivity in 5,327 nondiabetic Finnish men," *Diabetes*, vol. 58, no. 9, pp. 2129–2136, 2009.

[35] S.-M. Ruchat, C. E. Elks, R. J. F. Loos et al., "Association between insulin secretion, insulin sensitivity and type 2 diabetes susceptibility variants identified in genome-wide association studies," *Acta Diabetologica*, vol. 46, no. 3, pp. 217–226, 2009.

[36] J. Mei, S. Liao, Y. Liu et al., "Association of variants in CDKN2A/2B and CDKAL1 genes with gestational insulin sensitivity and disposition in pregnant Han Chinese women," *Journal of Diabetes Investigation*, vol. 6, no. 3, pp. 295–301, 2015.

Hindawi Publishing Corporation
Evidence-Based Complementary and Alternative Medicine
Volume 2015, Article ID 687690, 9 pages
http://dx.doi.org/10.1155/2015/687690

Research Article

Effects of Soothing Liver and Invigorating Spleen Recipes on the IKKβ-NF-κB Signaling Pathway in Kupffer Cells of Nonalcoholic Steatohepatitis Rats

Xiang-Wen Gong, Yong-Jian Xu, Qin-He Yang, Yin-Ji Liang, Yu-Pei Zhang, Guan-Long Wang, and Yuan-Yuan Li

Department of Traditional Chinese Medicine, Medical College of Jinan University, 601 Huangpu Road West, Guangzhou, Guangdong 510632, China

Correspondence should be addressed to Qin-He Yang; tyangqh@jnu.edu.cn

Received 16 February 2015; Revised 19 May 2015; Accepted 31 May 2015

Academic Editor: Bashar Saad

This study investigates the effect of soothing liver and invigorating spleen recipes on steatohepatitis examining the IKKβ-NF-κB signaling pathway in KCs of NASH rats. SD male rats were randomly divided into 8 groups, and the NASH model was induced by a high-fat diet (HFD). After 26 weeks, liver tissue was examined in H&E stained sections and liver function was monitored biochemically. KCs were isolated by Seglen's method, with some modifications. The mRNA and protein expression of the IKKβ-NF-κB signaling pathway components was examined by quantitative PCR and Western blotting. The results show that the high-fat diet induced NASH in the rats, and the soothing liver recipe and invigorating spleen recipe decreased the levels of TNF-α, IL-1, and IL-6 in KCs, as well as inhibiting the mRNA and protein expression of the IKKβ-NF-κB signaling pathway components. In conclusion, the experiment indicated the importance of the IKKβ-NF-κB signaling pathway in KCs for the anti-inflammatory effects of the soothing liver and invigorating spleen recipes.

1. Introduction

Nonalcoholic fatty liver disease (NAFLD) encompasses a spectrum of diseases ranging from simple hepatic steatosis to the aggressive condition, nonalcoholic steatohepatitis, whereas NASH is an aggressive liver disease which leads to advanced fibrosis, cirrhosis, and even hepatic failure [1]. NAFLD is also a strong independent predictor of cardiovascular disease and may play a central role in the cardiovascular risks of the metabolic syndrome [2]. Epidemiological studies suggest that NAFLD has become the most common cause of chronic liver disease worldwide among children and adolescents, with a prevalence in the west of approximately 15~35% [3]. The overall prevalence of NAFLD in China was 20.09% (17.95~22.31%) [4]. Hence, studies of the prevention and treatment of NAFLD are important.

Because the pathogenesis of NAFLD is incompletely characterized, there is no consensus regarding the most effective and appropriate pharmacologic therapy [5]. Herbal treatment for NAFLD has received increasing attention in recent decades due to its wide availability, minimal side effects, proven therapeutic mechanisms, and benefits [6]. Evidence-based medicine supports this point of view [7]. Based on TCM theory, liver stagnation and spleen deficiency were principal pathogenesis of NAFLD. Following the principles of "prescription-syndrome correspondence," the important treatment would be soothing liver and invigorating spleen recipes [8]. Clinical and experiment studies showed that soothing liver and invigorating spleen recipes could effectively treat NAFLD [9, 10].

The soothing liver recipe (Chaihu-Shugan-San) is a classical formula from "Jingyue Quanshu" that was written by Jingyue Zhang, a famous Ming dynasty physician, in China in 1640 A.D. The invigorating spleen recipe (Shen-ling-bai-zhu-San) is also a famous classical formula recorded in "Taiping Huimin Heji Ju Fang" that was written by the Imperial

Medical Bureau of the Song Dynasty in 1078 A.D. The invigorating spleen recipe is recognized in the widely used official Chinese Pharmacopoeia. According to TCM theory, the soothing liver recipe dredges liver qi and enhances blood circulation and is prescribed mainly for liver qi stasis. The invigorating spleen recipe invigorates the spleen and stomach qi, which it is mainly used to restore. Chaihu-Shugan-San and Shen-ling-bai-zhu-San have a significant effect on dredging by the liver and spleen deficiency.

IKKβ-NF-κB is an important redox-sensitive and proinflammatory transcription factor that plays a critical role in the regulation of a variety of genes important in cellular responses [11]. Our previous study showed that rats fed a high-fat diet for 16 weeks developed NAFLD and that I kappa B kinase β (IKKβ), phospho-IKKβ (p-IKKβ), and nuclear factor-κB (NF-κB) were highly expressed in their KCs, implying a relationship between NAFLD and the IKKβ-NF-κB pathway [12]. We next asked whether rats fed a HFD for 26 weeks would develop NASH and, in this paper, we study the effects of soothing liver and invigorating spleen recipes on inflammatory markers and proteins involved in IKKβ-NF-κB p65 pathway in KCs to explore some of the underlying mechanisms involved. To explore the evolution of the pathology, we also examined the inflammatory changes that accompany NAFLD at different periods.

2. Materials and Methods

2.1. Preparation of Soothing Liver and Invigorating Spleen Recipes. The soothing liver recipe is composed of seven Chinese herbs: Bupleuri radix, Citri reticulatae pericarpium, Chuanxiong Rhizoma, Cyperi Rhizoma, Bitter Orange Aurantii Fructus, Paeonia lactiflora Pall, and Glycyrrhizae radix, in a traditional dose ratio of 6 : 6 : 5 : 5 : 5 : 5 : 3. The invigorating spleen recipe includes Dolichos lablab, Atractylodes macrocephala Koidz, Poria cocos (Schw.) Wolf, Glycyrrhizae radix, Platycodi radix, Sulphur, Panax ginseng C. A. Mey, Amomum villosum Lour, Dioscorea opposita Thunb, and Semen Coicisin a ratio of 5 : 5 : 5 : 5 : 4 : 3 : 3 : 3 : 2 : 2. The integrated recipe is a mixture of CSGS and SLBZ in a 1 : 1 ratio. All Chinese medicines were purchased as formula granules from Shenzhen Sanjiu Medical Co., Ltd. (1005001S). The formula granules were dissolved in distilled water and stored at −4°C in a refrigerator.

2.2. Animals. 120 SD rats (6 weeks old, 200 g ± 20 g) were obtained from the Laboratory Animal Research Center of Guangzhou University of Traditional Chinese Medicine (China, Animal License Key no. 0107792; License no. SCXK (Yue) 2008–0020). The use of animals in this study was approved by the Ethics Committee of Medical College of Jinan University. The rats were separately housed in the Animal Administration Laboratory, Jinan University, at a controlled temperature (24°C ± 2°C) and humidity (70% ± 10%) with a 12 h light and 12 h dark cycle, with free access to food and water.

2.3. Grouping and Modeling. After 7 d for adaptation, the rats were randomly divided into 8 groups, each of 15 rats (liver samples were taken from 9 rats of each group and KCs were isolated from the remaining 6). The groups comprised normal, model, low-dose soothing liver recipe (L-SLG), high-dose soothing liver recipe (H-SLG), low-dose invigorating spleen recipe (L-ISG), high-dose invigorating spleen recipe (H-ISG), low-dose integrated recipe (L-IG), and high-dose integrated recipe (H-IG) group. NASH was reproduced in our rats by our previously reported method [13] with some minor modifications. The normal group of rats had free access to a normal chow diet, and the model group of rats were fed a HFD composed of regular chow 88%, axungia porci 10%, cholesterol 1.5%, and bile salt 0.5%. All recipes were given by gastrogavage [14] at 8 am at 1 mL/100 g body weight for the low-dose groups (equivalent to the human dose) and 3 times this volume for the high-dose groups. Rats in the normal and model groups were fed with the same dose of distilled water once daily at 8:00 am. All treatments lasted for 26 weeks.

2.4. Histopathological Examination of Liver Tissue. Rats were anesthetized by intraperitoneal injection of 3% pentobarbital (0.2 mL/100 g body weight) and a portion (approximately 1 cm × 1 cm × 0.5 cm) of liver approximately 0.5 cm from the edge of the right hepatic lobule was removed and paraffin-embedded for sectioning and hematoxylin-eosin (H&E) staining. The steatosis, fibrosis, and inflammation of NASH were identified by light microscopy.

2.5. Biochemical Test in Serum. Liver tissues were placed in isopropanol and homogenized with a TissueLyser-II homogenizer, centrifuged at 3000 ×g, 4°C for 10 min, when the clear supernatants were collected. Levels of alanine aminotransferase (ALT), aspartate aminotransferase (AST), and the AST/ALT ratio in the serum were determined with automatic biochemical analyzer.

2.6. Separation and Identification of KCs. KCs were isolated and identified from 6 rats in each group as previously described [15], and some modifications were made. After rats were anesthetized, the liver was perfused in situ with 200 mL 0.5 mmol/L Ethylene Glycol Tetraacetic Acid (EGTA) in D-Hanks at 20 mL/min, 37°C, until the color of the liver changed into amber. Then the liver was transferred to a culture dish and was perfused ex situ with 0.03% collagenase IV in Hanks, which contained 5 mmol/L calcium ions and was preheated to 37°C, at 20 mL/min in a recirculating fashion for 15 min. The liver was then placed in 10 mL RPMI-1640 culture medium containing 10% fetal calf serum (FBS). The capsule and fibrous tissue were removed, and the remaining tissue was cut into small pieces. After the obtained liver homogenate was filtered through a 200 μm and 300 μm nylon mesh, the cell suspension was centrifuged at 350 rpm, 4°C, for 3 min and clear supernatant was collected in another tube and centrifuged at 1050 rpm, 4°C, for 10 min. The cell pellet was subsequently resuspended in RPMI-1640 containing 10% FBS.

Table 1: Primer sequences, annealing temperatures, and length of products in real-time PCR.

Gene	Forward	Backward
GAPDH	GATCCCGCTAACATCAAATG	GAGGGAGTTGTCATATTTCTC
IKKβ	GAGAAGAAAGTGCGGGTGATTTACT	GAGCCTCACCACCTCTTCTACTTT
NF-κB	GTGGGCAAGCACTGTGAGGA	TCATCCGTGCTTCCAGTGTTTC

Then some 15 mL centrifuge tubes were carefully laid into 2.5 mL 24% Nycodenz working solution at the bottom, 2.5 mL 11% Nycodenz working solution in the middle layer, and 2.5 mL the cell suspension at the top. Then it was centrifuged at 2500 rpm, 4°C, for 15 min. KCs cloud appearance between the 11% Nycodenz layer and 24% Nycodenz layer was collected into another 15 mL tube, resuspended in GBSS, and then centrifuged twice at 1050 rpm, 4°C, for 15 min. The cell pellet was then resuspended and seeded on a culture dish at a density of 2–5 $\times$ 10^6 cells/mL with RPMI-1640 containing 10% FBS and incubated in a 5% CO_2 atmosphere for 30 min at 37°C. By further using adhesion purification, KC purity was improved, and cell viability was tested by trypan blue dye exclusion.

2.7. Determination of Inflammatory Cytokines in KCs. KCs from each group were isolated and identified. The cells were then centrifuged, washed 3 times in PBS, adjusted to 1 $\times$ 10^6/mL, and sonicated at 4°C for 15 min at 10000 rpm. Clear supernatants were used for the cytokine measurements. TNF-α, IL-1, and IL-6 were measured by enzyme-linked immunosorbent assay (ELISA) using ShangHai ExCell Biotechnology Co., Ltd. (China) kits: 24122012-002 for TNF-α, ZGAHBZAB01 for IL-1, and ZIBIBZAB02 for IL-6.

2.8. Determination of IKKβ and NF-κB p65 mRNA Expression in KCs. Total RNA was extracted from KCs using TRIZOL Reagent. The integrity of each RNA sample was evaluated by agarose gel electrophoresis, its purity and concentration were assayed, and then the total RNA was reverse transcribed to cDNA. Using the gene sequences for IKKβ, NF-κB p65, and glyceraldehyde-3-phosphate dehydrogenase (GAPDH) in Genebank, the primers were designed and synthesized by Shanghai Generay Biological Engineering Co., Ltd. GAPDH was used as the reference gene. The reaction conditions were as follows: ① predenaturation for 10 s at 95°C, ② denaturation for 5 s at 95°C, ③ GAPDH 55°C, IKKβ 60°C, NF-κB 62°C, renaturation for 20 s, ④ extension for 40 s at 60°C, ②–④ being repeated 39 times, and ⑤ analysis of the solubility curve, 72°C to 95°C for 5–10 s. After the reaction was finished, the results were analyzed using Opticon Monitor 3.1 software, and the $2^{-\Delta\Delta Ct}$ formula was used for relative quantification (Table 1).

2.9. Analysis of IKKβ, p-IKKβ, and NF-κB p65 Protein Expression in KCs. The IKKβ, p-IKKβ, NF-κB p65, and GAPDH proteins in KCs were measured by Western blotting. GAPDH was used as an internal control. KCs were lysed in RIPA lysis buffer and centrifuged at 12000 rpm for 5 min at 4°C, when the supernatants were collected. The concentration of supernatant protein was determined by a BCA protein assay. Protein preparations were subjected to 10% SDS-PAGE and transferred to a polyvinylidene difluoride (PVDF) membrane. After transfer, the membrane was blocked in 5% skim milk in Tris-Buffered Saline Tween-20 (TBST) and incubated overnight at 4°C with specific primary antibodies. The IKKβ antibody (no. 0002), anti-phosphor-IKKβ antibody (no. 0013), NF-κB p65 antibody (no. 0006), and GAPDH antibody were purchased from Cell Signaling Technology (USA). Then, horseradish peroxidase (HRP) conjugated goat-anti-rabbit antibody was added and incubated at room temperature for 1 h. After being washed for three times in TBST, the PVDF membrane was put into developer and exposed to X-ray film. The films were scanned and analyzed by a gel image processing system.

2.10. Statistical Analysis. Statistical analyses were performed by using SPSS 13.0. The values were presented as the mean ± standard. One-way analysis of variance (one-way ANOVA) and Tukey's test were used to determine the statistical significance of the differences. P values less than 0.05 were considered significant.

3. Results

3.1. Histopathological Changes. Sections were stained with H&E staining. As shown in Figure 1, hepatocyte nuclei were blue, and cytoplasm was uniformly red-stained, with less or no adipose hollow space. The hepatic lobule and liver rope both had clear structures and regular arrangement. There was no point necrosis or soakage of inflammatory cell soakage. In the model group, the central vein and portal area appeared as a diffuse adipose hollow space. Hepatocytes had obvious tumefaction or enlargement or even ballooning. Substantial adipose hollow space was observed in the cytoplasm. Some small hollow spaces were converted into a larger space. The narrow hepatic sinusoidal and disorder liver rope were observed. It was difficult to find the normal hepatocytes. Inflammatory infiltrates were found in the hepatic lobule and portal areas are scant. Compared with the model group, the structure arrangement, morphological features, macrovesicular lipid droplets, ballooning, inflammatory infiltrates, and spots necrosis improved by various degrees in all drug therapy groups. H-IG had the most significant impact on liver tissue histopathology.

3.2. Changes of ALT, AST, and AST/ALT in Serum. The ALT results showed no differences between the normal and model groups, and there were no obvious differences in the serum ALT levels of the treatment groups ($P > 0.05$). The

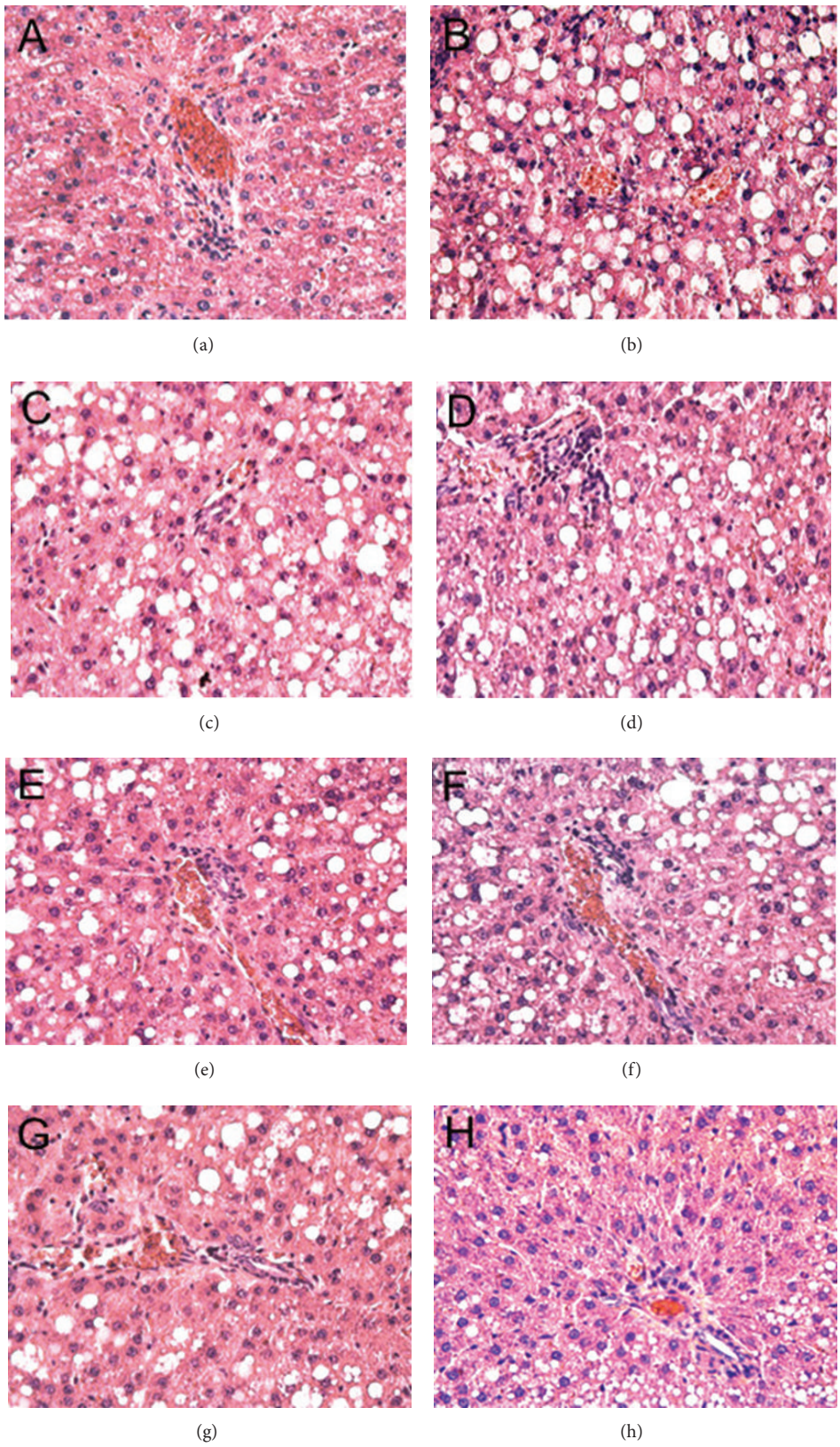

Figure 1: Histological changes of liver sections in different groups (HE stain ×200). (a) Normal group, (b) model group, (c) L-SLG, (d) H-SLG, (e) L-ISG, (f) H-ISG, (g) L-IG, and (h) H-IG.

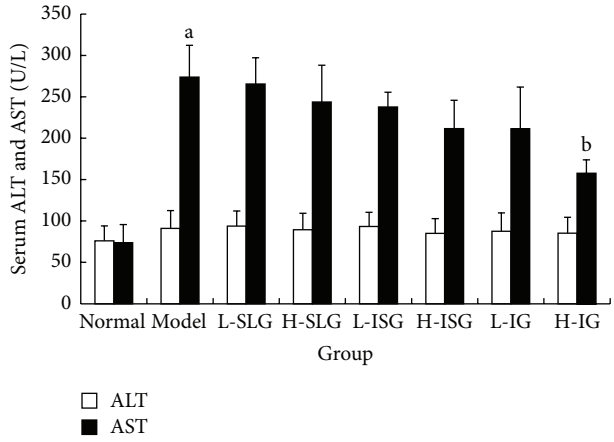

Figure 2: Levels of ALT and AST in serum were determined. Rats were fed with normal chow diet or HFD with or without CSS and SLBZS for 26 weeks. The values were expressed as mean ± S.E.M. 9 rats per group. [a]$P < 0.01$ versus normal group; [b]$P < 0.01$ versus model group.

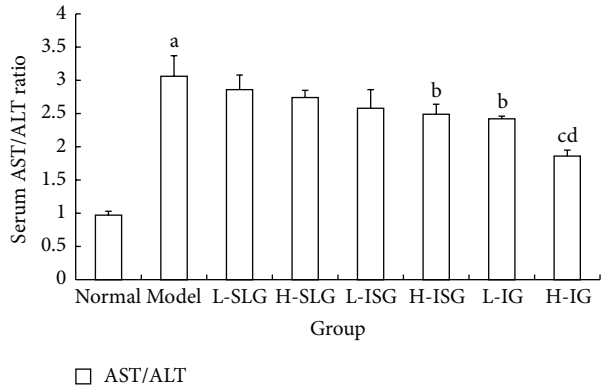

Figure 3: AST/ALT ratio in serum was computed. Rats were fed with normal chow diet or HFD with or without CSS and SLBZS for 26 weeks. The values were expressed as mean ± S.E.M. 9 rats per group. [a]$P < 0.01$ versus normal group; [b]$P < 0.05$, [c]$P < 0.01$ versus model AST/ALT; [d]$P < 0.01$ versus L-SLG, H-SLG, L-ISG, H-IS, and L-IG.

serum AST level and AST/ALT ratio of the model group were obviously increased ($P < 0.01$) compared with normal group. Compared with model group, the H-IG group had a significantly decreased level of AST ($P < 0.05$). The AST/ALT ratios of the H-SG, H-IG, and L-IG were all decreased ($P < 0.01$, $P < 0.05$), as shown in Figures 2 and 3.

3.3. The Population, Purity, and Viability of KCs. KCs were isolated from 6 rats in each group by collagenase perfusion as described. After 3 h incubation at 37°C, the cells were washed 3 times with PBS and nonadherent cells were washed off. The KCs viability was >95% (as tested by trypan blue dye exclusion). The purity of KCs was 91.21% (as assessed by flow cytometry method using a Lysozyme antibody), as shown in Figures 4 and 5.

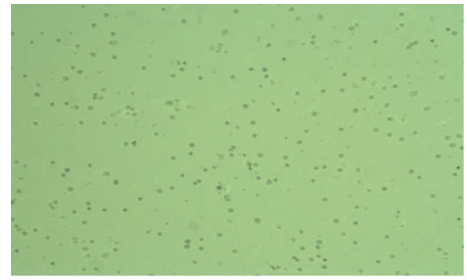

Figure 4: Isolated rat KCs cultured for 3 h (×100).

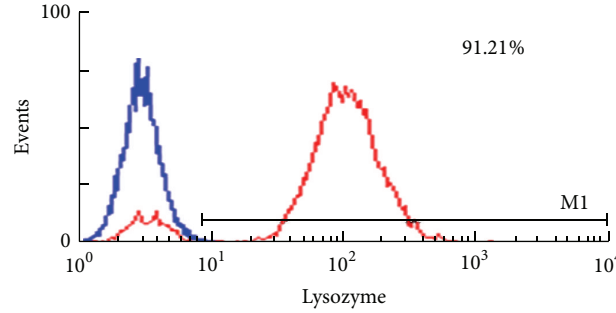

Figure 5: The purity of KCs identified by flow cytometer. Isolated rat KCs positive for lysozyme were more than 91.21%.

3.4. Changes of Inflammatory Cytokines in KCs. Higher levels of TNF-α, IL-1, and IL-6 were observed in KCs of the model group compared with those of the normal group ($P < 0.01$). Compared with the model group, the H-ISG, H-IG, and L-IG groups showed significant decreases in TNF-α and IL-6 ($P < 0.01$ or $P < 0.05$), and the H-ISG and H-IG had clearly lower levels of IL-1 ($P < 0.01$ or $P < 0.05$). The results showed that the high dose of both the invigorating spleen recipe and integrated recipes reduced the TNF-α, IL-1, and IL-6 levels of liver inflammatory cytokine in rats with NASH induced by HFD, as shown in Figure 6.

3.5. The IKKβ and NF-κB Expression in KCs. Compared with the normal rats, the levels of IKKβ and NF-κB mRNA in KCs of the model group increased 20.56-fold and 16.29-fold, ($P < 0.01$). The H-CG, H-SG, H-IG, and L-IG treated animals had lower expression levels of IKKβ and NF-κB mRNA than the model rats ($P < 0.01$, $P < 0.05$). The expression levels of IKKβ and NF-κB mRNA in the H-IG were obviously lower than those of the H-SG and L-IG ($P < 0.05$), as shown in Table 2.

3.6. Expression of IKKβ, p- IKKβ, and NF-κB p65 Proteins in KCs. To explore the mechanism of the anti-inflammatory effect of soothing liver and invigorating spleen recipes in the KCs of NASH rats, we assayed three important proteins, IKKβ, p-IKKβ, and NF-κB, which participate importantly in the NF-κB p65 signaling pathway to an inflammatory response, as shown in Figure 7(a). The expression levels of IKKβ, p- IKKβ, and NF-κB p65 in the model group were significantly higher than those in the normal control group ($P < 0.01$, Figure 7(b)). Compared to the model group, the

Table 2: Expression of IKKβ and NF-κB mRNA in KCs ($\overline{x} \pm s$, $n = 6$).

	$2^{-\Delta\Delta CT}$ IKKβ Rel. to control	$2^{-\Delta\Delta CT}$ NF-κB p65Rel. to control
Normal	1 (0.25–4.09)	1 (0.39–2.65)
Model	20.56 (4.56–34.05)[a]	16.29 (2.77–48.16)[a]
L-SLG	17.99 (1.89–30.69)	14.43 (2.33–31.12)
H-SLG	14.34 (3.51–23.43)[b]	10.39 (2.15–22.31)[b]
L-ISG	15.63 (7.31–28.05)	12.07 (7.06–15.78)
H-ISG	10.32 (3.83–23.91)[c]	9.15 (4.43–27.10)[c]
L-IG	12.09 (4.75–20.11)[b]	9.85 (2.56–18.90)[b]
H-IG	6.55 (1.80–14.83)[cd]	4.76 (0.55–12.47)[cd]

Expression of IKKβ and NF-κB mRNA in KCs was determined by Q-PCR. Rats were fed with normal chow diet or HFD with or without CSS and SLBZS for 26 weeks. The values were expressed as mean ± S.E.M. of 6 rats per group. [a]$P < 0.01$ versus normal group; [b]$P < 0.05$, [c]$P < 0.01$ versus model group, [d]$P < 0.01$ versus H-ISG and L-IG group.

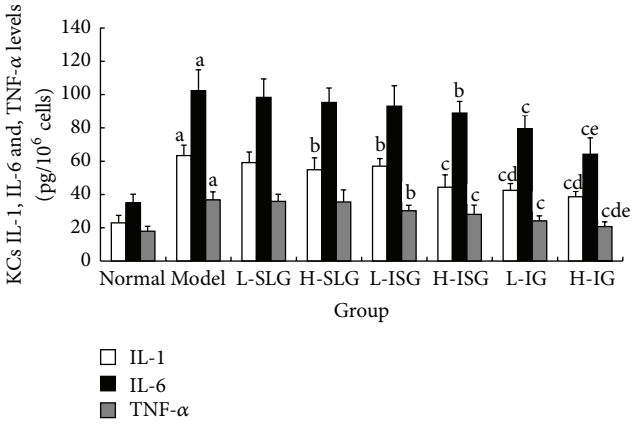

Figure 6: Related inflammatory cytokines of IL-1, IL-6, and TNF-α in KCs were determined by ELISA. Rats were fed with normal chow diet or HFD with or without CSS and SLBZS for 26 weeks. The values were expressed as mean ± S.E.M. 6 rats per group. [a]$P < 0.01$ versus normal group; [b]$P < 0.05$, [c]$P < 0.01$ versus model group; [d]$P < 0.01$ compared with H-SLG; [e]$P < 0.01$ compared with L-ISG.

expression levels of IKKβ, p- IKKβ, and NF-κB p65 were reduced in all treatment groups ($P < 0.01$, $P < 0.05$). We found that IKKβ, p-IKKβ, and NF-κB p65 protein expression was inhibited in the H-IG more than in the H-CG, L-CG, H-SG, and L-SG (Figure 7(b)).

4. Discussion

In our previous study, a rat model of NASH was established using 16 weeks of HFD, so as to resemble the pathogenesis of NASH in humans more closely. In this study, we showed by H&E staining that NASH was successfully established. In the model group, the central vein and portal areas appeared as diffuse adipose hollow spaces. The hepatocytes had obvious tumefaction, enlargement, or even ballooning. The H&E staining also suggested that the different treatments affected the NAFLD to different degrees, with the H-IG superior to other groups.

Past studies indicated that the ALT and AST are the most useful tools for diagnosis of the chronic liver disease. Beyond these tools, the ALT/AST ratio is a prognostic parameter in patients with liver injury [16]. If hepatocytes are badly damaged and their cytoplasm and mitochondria are destroyed, AST is released into the blood and its level increases more than that of ALT, so the AST/ALT ratio increases [17]. The AST/ALT ratio has therefore become an important index for the diagnosis of NAFLD [18]. In this study, the serum AST levels and AST/ALT ratios were obviously increased ($P < 0.05$). We speculate that liver injury already exists in NAFLD rats. Combining the H&E staining and liver function tests, we can see that the liver has sustained serious damage from inflammation. We now show that a high dose of integrated recipes protects against liver injury and moderates NASH progression ($P < 0.05$). TCM theory attributes the abnormalities in the 26 weeks' HFD-induced NASH rats to liver stagnation and spleen deficiency. Therefore, the effects of the soothing liver recipe and the invigorating spleen recipe were superior to other classical formulas.

KCs are resident hepatic macrophages that account for 80–90% of the total number of fixed tissue macrophages of the body [19]. KCs eliminate and detoxify microorganisms, endotoxins, and degenerated cells, as well as possessing other functions [20]. Therefore, KCs play an important role in liver physiological homeostasis and are intimately involved in the liver's response to infection, toxins, and various other stresses through the expression and secretion of soluble inflammatory mediators [21, 22]. KCs are associated with the proinflammatory response and produce associated cytokines such as IL-1β, IL-12, IL-23, and TNF-α. Cytokines act as protective mediators for the recovery of normal liver function. However, excessive activation of KCs may aggravate liver damage [23, 24]. According to the two-hit hypothesis, the second hit is an exacerbating factor such as an inflammatory cytokine. Previous studies show that inflammatory KCs play a key role in NASH [25]. In this paper, the expression of IL-6 and TNF-α was significantly increased in KC supernatants from the model group ($P < 0.01$) while the levels in the supernatants of the low- and high-dose integrated recipes were significantly lower than the other groups ($P < 0.01$, $P < 0.05$). These findings suggest that increases in liver TNF-α, IL-1, and IL-6 may aggravate hepatic inflammation, necrosis, and fibrosis and that the high dose of the invigorating spleen and integrated recipes may have a favorable effect on the inflammatory reaction in the steatotic liver.

As everyone knows, excessive inflammatory cytokines such as TNF-α, IL-1, and/or IL-6 exacerbated liver injury and promoted NASH progression in different ways [26]. The mechanisms involved remain unclear, though many reports implicate the NF-κB signal pathway. To elucidate the regulatory mechanisms in the NF-κB signaling pathway and the anti-inflammatory effects of the soothing liver and invigorating spleen recipes further, we examined the expression and levels of several proteins closely related to the signal

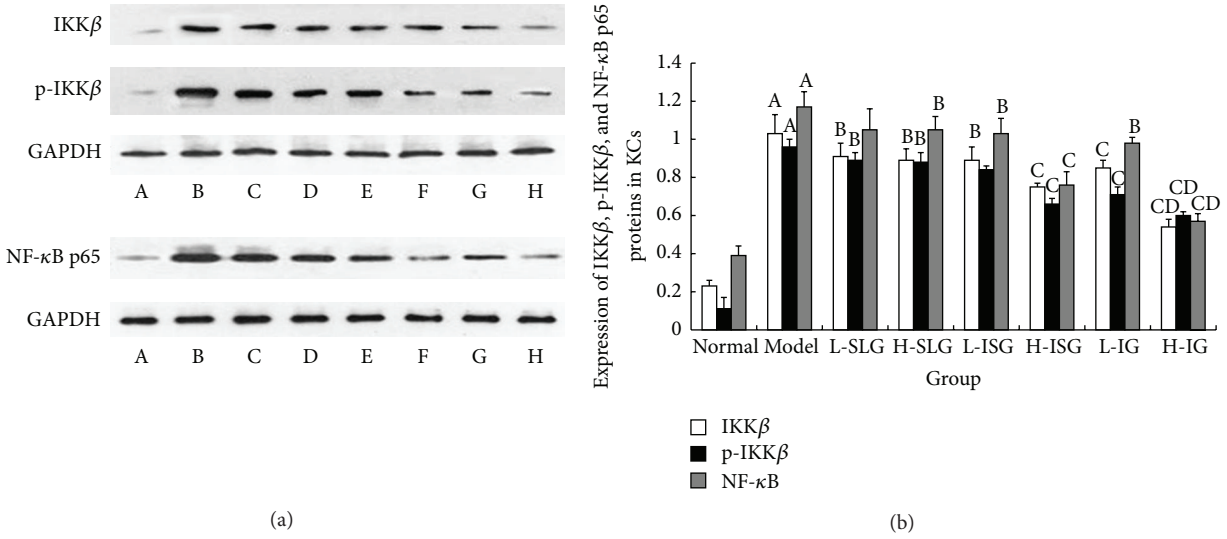

Figure 7: (a) Western blot of IKKβ, p-IKKβ, and NF-κB p65 proteins in KCs. A: normal group; B: model group; C: L-SLG; D: H-SLG; E: L-ISG; F: H-ISG; G: L-IG; H: H-IG. (b) Expression of IKKβ, p-IKKβ, and NF-κB p65 proteins in KCs. Rats were fed with normal chow diet or HFD with or without CSS and SLBZS for 26 weeks. The values were expressed as mean ± S.E.M. 6 rats per group. $^{A}P < 0.01$ versus normal group; $^{B}P < 0.05$, $^{C}P < 0.01$ versus model group; $^{D}P < 0.01$ versus L-SLG, H-SLG, L-ISG, H-IS, and L-IG.

transduction in the NF-κB pathway of KCs from NASH rats [27].

The IKKβ-NF-κB p65 signaling pathway is an important regulator of inflammatory gene transcription involved in many chronic inflammatory diseases. In NASH, different activators of the IKKs-IκB-NF-κB p65 signaling pathway in KCs regulate the synthesis of downstream inflammatory mediators. Possible pathways are reviewed in and include [28–31] (1) LPS captured by LPS-binding protein (LBP), with the LPS-LBP complex then interacting with the membrane form of CD14 on the surface of KCs. TLR4 serves as the LPS receptor and binds MyD88 to activate IRAK-1 or IRAK-4, leading to downstream activation of the IKKs-I Kb-NF-κB signaling pathway. (2) The TNF receptor combined with its related apoptosis structural domain protein TRADD interacts with the TNFR-2 pathway through ubiquitinated receptor interacting protein RIP and finally forms the RNFR complex with IKKγ, which leads to activation of the IKKs-IκB-NF-κB signaling pathway. During hepatic steatosis, inflammation, and fibrosis, hepatic NF-κB is highly expressed, though IKKβ/NF-κB pathway activation is inhibited. These findings suggest that it may be possible to delay the occurrence of inflammation and liver steatosis and insulin resistance (IR). (3) A previous study showed that, in IRF3 gene-knockout mice, activation of the IKKβ/NF-κB signaling pathway caused severe inflammation of the liver IR and fatty degeneration.

Traditional Chinese medicine has received increasing attention as an alternative source of treatments for a variety of diseases [32]. According to TCM theory, NAFLD belongs to the Gan-Pi and Gan-Zhu. Epidemiological researches showed that the syndrome of stagnation of liver qi and spleen deficiency is one of the most common syndromes of NAFLD in china, and the proportion is 34.7%. This study suggested the clinical characteristics of Chinese NAFLD population in contemporary [33]. Therefore, the syndrome of stagnation of liver qi and spleen deficiency has become the most important syndrome in expert consensus document of NAFLD [34]. According to Chinese medicinal chemistry, the principal active components of Senlinbaizhu Powder and Chaihushugan Powder include: ferulic acid, ginsenoside, paeoniflorin, naringin, hesperidin, meranzin hydrate, neohesperidin, albiflorin, and atractylenolide, together with other drug ingredients [35, 36]. At the same time, Chinese medicinal pharmacology has demonstrated that Chaihu-Shugan-San and Shen-ling-bai-zhu-San have inhibitory activities on oxidative stress [37], lipid peroxidation, and inflammatory reactions [38]. Beyond that, naringin, hesperidin, ferulic acid, and other active ingredients have some anti-inflammatory effects [36, 37]. Our results show that soothing liver and invigorating spleen recipes can protect the liver from inflammatory injury caused by an HFD, that the release of IL-1, IL-6, and TNF-α was significantly reduced, and that the downregulation of IL-1, IL-6, and TNF-α might be due to different degrees of inhibitory expression of IKKβ, p-IKKβ, and NF-κB. A previous study showed that the soothing liver and invigorating spleen recipes could regulate the expression and activation of the interacting protein of IKKβ-NF-κB signaling pathway of KCs in NASH rats, reducing the release of inflammatory mediators (IL-6, TNF-α, and IL-1) in KCs and, ultimately, ameliorating inflammatory damage. Consequently, a combination of the soothing liver and invigorating spleen recipes could have a significant anti-inflammatory effect, which might be closely related to their effects on the NF-κBp65 signaling pathway.

5. Conclusion

In conclusion, this study showed that the release of inflammatory factors such as IL-1, TNF-α, and IL-6 by KCs was significantly increased by a HFD and that the IKKβ-NF-κBp65 signaling pathway maybe the effective target for the soothing liver and invigorating spleen recipes.

Conflict of Interests

All of the authors of this paper declare that they have no direct financial relation with the commercial identities mentioned in this paper. And all of the authors declare that they have no competing interests.

Authors' Contribution

Xiang-Wen Gong and Yong-Jian Xu contributed equally to this work.

Acknowledgment

The present work was supported by a Grant (no. 30973694) from the Natural Science Foundation of China.

References

[1] B. A. Elkhader and M. Z. Mahmoud, "Prevalence of non-alcoholic fatty liver among adults in Khartoum-Sudan: epidemiological survey," *Journal of American Science*, vol. 9, no. 6, pp. 62–66, 2013.

[2] H. Lu, H. Liu, F. Hu, L. Zou, S. Luo, and L. Sun, "Independent association between nonalcoholic fatty liver disease and cardiovascular disease: a systematic review and meta-analysis," *International Journal of Endocrinology*, vol. 2013, Article ID 124958, 7 pages, 2013.

[3] S. Berardis and E. Sokal, "Pediatric non-alcoholic fatty liver disease: an increasing public health issue," *European Journal of Pediatrics*, vol. 173, no. 2, pp. 131–139, 2014.

[4] Z. Li, J. Xue, P. Chen, L. Chen, S. Yan, and L. Liu, "Prevalence of nonalcoholic fatty liver disease in mainland of China: a meta-analysis of published studies," *Journal of Gastroenterology and Hepatology*, vol. 29, no. 1, pp. 42–51, 2014.

[5] W. Tomeno, M. Yoneda, K. Imajo et al., "Emerging drugs for non-alcoholic steatohepatitis," *Expert Opinion on Emerging Drugs*, vol. 18, no. 3, pp. 279–290, 2013.

[6] J. Xiao, K. F. So, E. C. Liong, and G. L. Tipoe, "Recent advances in the herbal treatment of non-alcoholic fatty liver disease," *Journal of Traditional and Complementary Medicine*, vol. 3, no. 2, pp. 88–94, 2013.

[7] K.-Q. Shi, Y.-C. Fan, W.-Y. Liu, L.-F. Li, Y.-P. Chen, and M.-H. Zheng, "Traditional Chinese medicines benefit to nonalcoholic fatty liver disease: a systematic review and meta-analysis," *Molecular Biology Reports*, vol. 39, no. 10, pp. 9715–9722, 2012.

[8] J. R. Liu and X. N. Zhu, "Pathogenesis and therapy summary of traditional Chinese with medicine nonalcoholic fatty liver disease," *Journal of Luzhou Medical College*, vol. 37, no. 6, pp. 640–641, 2014.

[9] J. X. Li, Y. L. Wang, M. Liu et al., "Treatment of nonalcoholic steatohepatitis by Jianpi Shugan Recipe: a multi-center, randomized, controlled clinical trial," *Chinese Journal of Integrated Traditional and Western Medicine*, vol. 34, no. 1, pp. 15–19, 2014.

[10] L. Zeng and G. G. Sheng, "The effect of Shuganjianpi and Huatanhuoxue formula on mitochondrial membrane liquidity and membrane potential level of cell model with non-alcoholic fatty liver disease," *Chinese Journal of Integrated Traditional and Western Medicine on Liver Diseases*, vol. 22, no. 6, pp. 360–362, 2012.

[11] J. Xiao, C. T. Ho, E. C. Liong et al., "Epigallocatechin gallate attenuates fibrosis, oxidative stress, and inflammation in non-alcoholic fatty liver disease rat model through TGF/SMAD, PI3 K/Akt/FoxO1, and NF-kappa B pathways," *European Journal of Nutrition*, vol. 53, no. 1, pp. 187–199, 2014.

[12] B. Wei, Q.-H. Yang, W.-J. Wang, and C.-F. Hu, "Effects of Shugan Jian-pi prescriptions on expression of IKKβ at mRNA and protein levels in liver tissues of rats with non-alcoholic steatohepatitis," *Chinese Journal of Pathophysiology*, vol. 28, no. 8, pp. 1448–1454, 2012.

[13] Q.-H. Yang, S.-P. Hu, Y.-P. Zhang et al., "Effect of berberine on expressions of uncoupling protein-2 mRNA and protein in hepatic tissue of non-alcoholic fatty liver disease in rats," *Chinese Journal of Integrative Medicine*, vol. 17, no. 3, pp. 205–211, 2011.

[14] X. Y. Shi, *Experimental Zoology of Modern Medicine*, People's Military Medical Press, Beijing, China, 1st edition, 2000.

[15] G. F. Feng, Q. H. Yang, W. J. Wang et al., "Simultaneously isolation and identification of hepatocytes and Kupffer cells from nonalcoholic steatohepatitis rat," *Guangdong Medical Journal*, vol. 33, no. 1, pp. 40–43, 2012.

[16] K. M. Surapaneni and M. Jainu, "Pioglitazone, quercetin and hydroxy citric acid effect on hepatic biomarkers in Non Alcoholic Steatohepatitis," *Pharmacognosy Research*, vol. 6, no. 2, pp. 153–162, 2014.

[17] R. Kawamoto, K. Kohara, T. Kusunoki, Y. Tabara, M. Abe, and T. Miki, "Alanine aminotransferase/aspartate aminotransferase ratio is the best surrogate marker for insulin resistance in non-obese Japanese adults," *Cardiovascular Diabetology*, vol. 11, article 117, 2012.

[18] S. Fuyan, L. Jing, C. Wenjun et al., "Fatty liver disease index: a simple screening tool to facilitate diagnosis of nonalcoholic fatty liver disease in the Chinese population," *Digestive Diseases and Sciences*, vol. 58, no. 11, pp. 3326–3334, 2013.

[19] E. Liaskou, D. V. Wilson, and Y. H. Oo, "Innate immune cells in liver inflammation," *Mediators of Inflammation*, vol. 2012, Article ID 949157, 21 pages, 2012.

[20] G. Kolios, V. Valatas, and E. Kouroumalis, "Role of Kupffer cells in the pathogenesis of liver disease," *World Journal of Gastroenterology*, vol. 12, no. 46, pp. 7413–7420, 2006.

[21] P. J. Murray and T. A. Wynn, "Protective and pathogenic functions of macrophage subsets," *Nature Reviews Immunology*, vol. 11, no. 11, pp. 723–737, 2011.

[22] H. W. Zimmermann, C. Trautwein, and F. Tacke, "Functional role of monocytes and macrophages for the inflammatory response in acute liver injury," *Frontiers in Physiology*, vol. 3, article 56, 2012.

[23] X. Kong, N. Horiguchi, M. Mori, and B. Gao, "Cytokines and STATs in liver fibrosis," *Frontiers in Physiology*, vol. 3, article 69, 2012.

[24] Z. Papackova, E. Palenickova, H. Dankova et al., "Kupffer cells ameliorate hepatic insulin resistance induced by high-fat

diet rich in monounsaturated fatty acids: the evidence for the involvement of alternatively activated macrophages," *Nutrition & Metabolism*, vol. 9, article 22, 2012.

[25] G. C. Farrell, D. van Rooyen, L. Gan, and S. Chitturi, "NASH is an inflammatory disorder: pathogenic, prognostic and therapeutic implications," *Gut and Liver*, vol. 6, no. 2, pp. 149–171, 2012.

[26] H. Tilg, "The role of cytokines in non-alcoholic fatty liver disease," *Digestive Diseases*, vol. 28, no. 1, pp. 179–185, 2010.

[27] J. Zhao, H. Zheng, Y. Liu et al., "Anti-inflammatory effects of total alkaloids from Rubus alceifolius Poir. on non-alcoholic fatty liver disease through regulation of the NF-κB pathway," *International Journal of Molecular Medicine*, vol. 31, no. 4, pp. 931–937, 2013.

[28] Y. Shirai, H. Yoshiji, R. Noguchi et al., "Cross talk between toll-like receptor-4 signaling and angiotensin-II in liver fibrosis development in the rat model of non-alcoholic steatohepatitis," *Journal of Gastroenterology and Hepatology*, vol. 28, no. 4, pp. 723–730, 2013.

[29] G. Ramakrishna, A. Rastogi, N. Trehanpati, B. Sen, R. Khosla, and S. K. Sarin, "From cirrhosis to hepatocellular carcinoma: new molecular insights on inflammation and cellular senescence," *Liver Cancer*, vol. 2, no. 3-4, pp. 367–383, 2013.

[30] H. L. Wright, B. Chikura, R. C. Bucknall, R. J. Moots, and S. W. Edwards, "Changes in expression of membrane TNF, NF-κB activation and neutrophil apoptosis during active and resolved inflammation," *Annals of the Rheumatic Diseases*, vol. 70, no. 3, pp. 537–543, 2011.

[31] X.-A. Wang, R. Zhang, Z.-G. She et al., "Interferon regulatory factor 3 constrains IKKβ/NF-κB signaling to alleviate hepatic steatosis and insulin resistance," *Hepatology*, vol. 59, no. 3, pp. 870–885, 2014.

[32] J.-K. Luo, H.-J. Zhou, J. Wu, T. Tang, and Q.-H. Liang, "Electroacupuncture at Zusanli (ST36) accelerates intracerebral hemorrhage-induced angiogenesis in rats," *Chinese Journal of Integrative Medicine*, vol. 19, no. 5, pp. 367–373, 2013.

[33] H. F. Wei, G. Ji, and L. J. Xin, "Preliminary research on nonalcoholic fatty liver syndrome classification," *Liaoning Journal of Traditional Chinese Medicine*, vol. 29, no. 11, pp. 655–656, 2002.

[34] S. S. Zhang, Q. G. Li, and J. X. Li, "Diagnosis and treatment of traditional Chinese Medicine Consensus on nonalcoholic fatty liver disease," *Beijing Zhong Yi Yao*, vol. 29, no. 2, pp. 83–86, 2011.

[35] W. Shu-ling, J. Wei, and G. Xiao-ling, "HPLC characteristics of aqueous extract of Chaihu Shugan Powder and determination of marks," *Chinese Traditional Patent Medicine*, vol. 34, no. 12, pp. 2384–2388, 2012.

[36] W.-L. Li, Q.-C. Dai, Y.-B. Ji, Z. Sun, J. Du, and J. Bai, "Investigation of chemical composition and sources of Bazhentang by HPLC-ESI/MS," *Chinese Pharmaceutical Journal*, vol. 44, no. 21, pp. 1622–1626, 2009.

[37] Y. You, Y. H. Liu, and S. L. Gao, "Effect and mechanism of Shenling Baizhu San on the murine model of inflammatory bowel disease induced by dextran sodium sulfate in mice," *Journal of Experimental Traditional Medical Formulae*, vol. 18, no. 5, pp. 136–140, 2012.

[38] Z.-H. Li, J. Wang, Y.-W. Wang, R.-L. Cai, J. Sun, and M.-G. Ye, "Effect of Shenlingbaizhu powder on serum levels of EGF, SOD and MDA in ulcerative colitis rats with syndrome of dampness stagnancy due to spleen deficiency," *World Chinese Journal of Digestology*, vol. 20, no. 5, pp. 410–413, 2012.

Hindawi Publishing Corporation
Evidence-Based Complementary and Alternative Medicine
Volume 2015, Article ID 980345, 8 pages
http://dx.doi.org/10.1155/2015/980345

Research Article

Deepure Tea Improves High Fat Diet-Induced Insulin Resistance and Nonalcoholic Fatty Liver Disease

Jing-Na Deng,[1,2,3] Juan Li,[4] Hong-Na Mu,[1,2,3,5] Yu-Ying Liu,[1,2,3] Ming-Xia Wang,[1,2,3] Chun-Shui Pan,[1,2,3] Jing-Yu Fan,[1,2,3] Fei Ye,[4] and Jing-Yan Han[1,2,3,5]

[1] *Tasly Microcirculation Research Center, Peking University Health Science Center, Beijing 100191, China*
[2] *Key Laboratory of Microcirculation, State Administration of Traditional Chinese Medicine of the People's Republic of China, Beijing 100191, China*
[3] *Key Laboratory of Stasis and Phlegm, State Administration of Traditional Chinese Medicine of the People's Republic of China, Beijing 100191, China*
[4] *Institute of Materia Medica, Chinese Academy of Medical Science and Peking Union Medical College, Beijing 100050, China*
[5] *Department of Integration of Chinese and Western Medicine, School of Basic Medical Sciences, Peking University, Beijing 100191, China*

Correspondence should be addressed to Fei Ye; yefei@imm.ac.cn and Jing-Yan Han; hanjingyan@bjmu.edu.cn

Received 26 March 2015; Revised 24 June 2015; Accepted 25 June 2015

Academic Editor: Akhilesh K. Tamrakar

This study was to explore the protective effects of Deepure tea against insulin resistance and hepatic steatosis and elucidate the potential underlying molecular mechanisms. C57BL/6 mice were fed with a high fat diet (HFD) for 8 weeks to induce the metabolic syndrome. In the Deepure tea group, HFD mice were administrated with Deepure tea at 160 mg/kg/day by gavage for 14 days. The mice in HFD group received water in the same way over the same period. The age-matched C57BL/6 mice fed with standard chow were used as normal control. Compared to the mice in HFD group, mice that received Deepure tea showed significantly reduced plasma insulin and improved insulin sensitivity. Deepure tea increased the expression of insulin receptor substrate 2 (IRS-2), which plays an important role in hepatic insulin signaling pathway. Deepure tea also led to a decrease in hepatic fatty acid synthesis and lipid accumulation, which were mediated by the downregulation of sterol regulatory element binding protein 1c (SREBP-1c), fatty acid synthesis (FAS), and acetyl-CoA carboxylase (ACC) proteins that are involved in liver lipogenesis. These results suggest that Deepure tea may be effective for protecting against insulin resistance and hepatic steatosis via modulating IRS-2 and downstream signaling SREBP-1c, FAS, and ACC.

1. Introduction

Nonalcoholic fatty liver disease (NAFLD) and insulin resistance are the main pathophysiological characteristic of metabolic syndrome [1], which has become a significant public health problem as a result of high fat diet and sedentary lifestyles [2, 3]. NAFLD, once considered benign, may progress to steatohepatitis, fibrosis, and ultimately cirrhosis [4–6]. NAFLD represents a state of lipid accumulation in hepatocytes, and its pathogenesis is associated with enhanced liver lipogenesis and hepatic insulin resistance. The liver lipogenesis can be activated by elevated plasma insulin, as seen in patients with the metabolic syndrome, type 2 diabetes, or obese individuals [4, 7].

In the liver, insulin is involved in a number of actions responsible for glucose control and lipid metabolism. Insulin receptor substrate (IRS) proteins are a family of cytoplasmic adaptor proteins that transmit signal from insulin receptor to its final biological actions through a series of intermediate effectors. Hepatic insulin signaling for these effects is mediated mainly through insulin receptor substrate 2 (IRS-2) [8, 9], rather than insulin receptor substrate 1 (IRS-1). Elevated insulin also leads to activation of the lipid biosynthetic pathway through activation of the expression and proteolytic

maturation of the transcription factor sterol regulatory element binding protein 1c (SREBP-1c) [10], thereby leading to the increased expression of fatty acid synthase (FAS) and acetyl-CoA carboxylase (ACC) in the lipogenesis pathway, resulting in steatosis. Moreover, NAFLD leads to hepatic insulin resistance by stimulating gluconeogenesis [11], and upregulated SREBP-1c may suppress IRS-2-mediated insulin signaling generating a feedforward machinery to further stimulate or worsen NAFLD [11, 12]. Thus, NAFLD and insulin resistance have a number of reciprocal relationships and can enhance each other [13, 14].

Tea is one of the most popular beverages worldwide and can be categorized into three types: nonfermented green, partially fermented oolong, and fully fermented black and Pu-erh tea [15]. Several biological functions of Pu-erh tea have been reported, such as antiobesity [16], antihyperlipidemia [17], anti-liver fat accumulation [18], and promoting skeletal muscle glucose transport [19]. Also, epigallocatechin gallate, a compound from tea, has been shown to reduce intestinal lipid absorption [20] and lower blood lipids [21]. Therefore, the mechanisms of Pu-erh tea protecting against obesity-associated disease are likely to be multifaceted. However, the study is limited so far to address the mechanism underlying the actions of Pu-erh tea.

The present study was conducted to investigate whether Deepure tea, a specific tea concentrated from Pu-erh tea, could ameliorate insulin resistance and NAFLD in high fat diet (HFD) raised mice and possible mechanisms of its action. We demonstrated that Deepure tea decreased HFD-induced hyperinsulinemia and improved diet-induced NAFLD in C57BL/6 mice. HFD markedly inhibited hepatic IRS-2 protein expression in mice, which was reversed by treatment with Deepure tea. The improved hepatic steatosis appears to be mediated through the downregulation of SREBP-1c protein level, subsequently decreasing the level of FAS and ACC, which are involved in de novo lipogenesis in the liver.

2. Materials and Methods

2.1. Materials. Deepure tea was supplied by Tasly Pharmaceutical Co. Ltd. (Tianjin, China). The raw materials were extracted from leaves of old Pu-erh tea trees, which were from Yunnan province of China. The batch number of the Deepure tea used in this experiment was 20110918. The processing of the product followed a strict quality control, and the ingredients were subjected to standardization. Deepure tea was manufactured as nanometer level powder after dynamic cycle extraction and concentrated by evaporating and spray drying.

Antibodies recognizing IRS-2 and GAPDH were from Cell Signaling Technology (Boston, MA, USA). Antibodies against SREBP-1c, FAS, and ACC were from Abcam (Cambridge, MA, USA). BCA protein assay kit was purchased from Applygen Technologies (Beijing, China). ELISA kit for LDLR of mice was purchased from Andygene (Richardson, USA). All other reagents used in our study were of analytical grade.

2.2. Animal Model and Treatment. Four-week-old male C57BL/6 mice (the animal certificate number was SCXK (Jing) 2006–2009) were purchased from Weitonglihua Animal Center, Beijing, China. The animals were housed at 21–23°C and a humidity level of 40–60%. They were exposed to a 12 h lighting cycle and allowed *ad libitum* access to water and the appointed chows. The HFD-induced mice were fed with HFD for 8 weeks, which contained 50% fat (mainly from lard), 36% carbohydrate, and 14% protein, with a total energy content of 21.0 kJ/g. In control group, aged-matched male C57BL/6 mice were fed with standard laboratory chows containing 12% fat, 62% carbohydrate, and 26% protein [22] with a total energy content of 12.6 kJ/g. The HFD-induced mice were randomly divided into two groups: HFD and Deepure tea. The animals in Deepure tea group received Deepure tea (160 mg/kg/day) orally for 14 days. The mice in HFD and control groups were given the same volume of water. All animal experiments were approved by the Beijing Municipal Ethics Committee for Laboratory Animals.

2.3. Intraperitoneal Glucose Tolerance Test (IPGTT). C57BL/6 mice were fasted for 2 h before experiment. Blood samples were collected from tail veins for determination of baseline values of blood glucose (t = 0 min). The mice were then injected intraperitoneally with glucose at 2 g/kg, and additional blood samples were collected at 15, 60, and 120 min, respectively, for glucose measurement.

2.4. Biochemical Assays. After C57BL/6 mice were fasted for 6 h, tail vein blood was collected. The samples were centrifuged at 3500 rpm for 10 min at 4°C to separate plasma. Plasma insulin levels were measured by enzyme-linked immunosorbent assay (ELISA) using an insulin ultrasensitive ELISA kit (ALPCO, Salem, NH, USA), according to the manufacturer's instruction. The concentrations of plasma triglyceride (TG) and total cholesterol (TC) were determined according to the kit instruction (Jian Cheng Biotechnology Company, Nanjing, China). Plasma glucose levels were detected to calculate the homeostasis model assessment (HOMA). HOMA-IR index = fasting blood glucose (mmol/L) × fasting plasma insulin (pmol/L)/22.5 [23]. The concentration of LDLR protein in liver tissues was assessed by ELISA kit according to the manufacturer's protocol. OD values were determined by enzyme microplate reader (Thermo Multiskan Mk3, Thermo Fisher Scientific Inc., Barrington, USA), with detection wave length of 450 nm. The LDLR level was calculated based on the standard curves.

2.5. Western Blotting. Liver tissues were lysed in sample buffer containing 62 mM Tris-HCl, pH 6.8, 0.1% SDS, 0.1 mM sodium orthovanadate, and 50 mM sodium fluoride. The protein content was determined by the BCA protein assay. Equal amounts of proteins were loaded and separated by SDS-PAGE. After electrophoresis, the proteins were transferred on membranes, after being blocked with 3% nonfat dry milk the membrane with target proteins was incubated with an antibody against IRS-2, SREBP-1c, ACC, FAS, or GAPDH overnight at 4°C. The blots were incubated with a respective HRP-conjugated second antibody, and then immunoreactive bands were revealed using an enhanced chemiluminescence

system (Applygen Technologies Inc., Beijing, China). The protein signal was quantified by scanning densitometry in the X-film by Image-Pro Plus 6.0 software (Bio-Rad, Hercules, California, USA) [24].

2.6. Hematoxylin and Eosin (HE) Staining. Liver tissue samples from each mouse were fixed in formalin saline solution (10%) and then embedded in paraffin, sliced at five micrometer thickness, and stained with HE for histological analysis under a light microscope.

2.7. Statistical Analysis. Data were expressed as means ± SEM. Student's t-test for unpaired observations was used to compare the mean values of two groups. A value of $p < 0.05$ was considered statistically significant.

3. Results

3.1. Deepure Tea Treatment Improves Hyperinsulinemia and Insulin Resistance in HFD Mice. The mice in HFD and Deepure tea groups did not show any difference in body weight but both possessed a higher body weight than those in the control group, as shown in Figure 1(a). After 6-hour fasting, the HFD mice demonstrated hypercholesterolemia, but not hypertriglyceridemia, as compared with the normal control mice (Figures 1(b) and 1(c)). Plasma TC was slightly decreased in Deepure tea groups compared to the HFD group (93.13 ± 6.799 versus 106.9 ± 5.229), but without significance.

At baseline, plasma glucose level in HFD group did not differ from that in control group but decreased by 15.3% in Deepure tea treated group with significance (Figure 1(d)). In contrast, HFD resulted in a significant increase in serum insulin, as compared with the control group, which was reduced as much as 43.5% by Deepure tea treatment (Figure 1(e)). The homeostasis model assessment (HOMA) was calculated as an index of insulin resistance. As shown in Figure 1(f), HOMA-IR index was decreased by ~54% in Deepure tea treated mice compared with HFD mice. The potential of Deepure tea treatment to improve insulin resistance was also confirmed by IPGTT (Figure 1(g)). Figure 1(h) presents the results of the plasma glucose levels detected 2 hours after glucose administration, showing a decrease by 25.1% in Deepure tea-treatment mice compared with HFD mice.

3.2. Deepure Tea Attenuates HFD-Induced Hepatic Steatosis in C57BL/6 Mice. Histological examination was conducted at the end of the experiment, and the result is illustrated in Figure 2. Strikingly, HFD led to an apparent NAFLD compared with control mice, which manifested a large number of lipid-filled vacuoles (arrowheads) in liver tissue. Impressively, liver sections from Deepure tea-treatment mice revealed an obvious reduction of lipid droplets (arrowheads), showing the potential of Deepure tea to relieve hepatic steatosis.

3.3. Deepure Tea Modulates the Expression of Genes Involved in Hepatic Insulin Signaling Pathway and Hepatic Lipid Synthesis. Insulin resistance is known showing a reduced insulin sensitivity of peripheral tissue with aberrant IRS-2 and downstream members of the insulin signaling pathway [25]. To examine whether IRS-2 expression is changed in the present setting, we assessed the IRS-2 protein in liver tissues. As an important regulator of liver insulin signaling, the expression of IRS-2 was markedly reduced in the mouse liver of the HFD group, as compared to those in normal diet mice. Significantly, mice that received Deepure tea showed evidently higher IRS-2 protein level in comparison with that in HFD mice (Figures 3(a) and 3(b)).

To gain insight into the protective mechanisms of Deepure tea against insulin resistance and hepatic steatosis in HFD-fed mice, we further examined the protein levels in hepatic tissue that are involved in insulin signaling and lipogenesis. SREBP-1c is a key transcriptional factor regulating de novo lipogenesis in liver [26]. As shown in Figures 3(c) and 3(d), HFD markedly upregulated hepatic SREBP-1c expression. Of notice, hepatic SREBP-1c protein level of the Deepure tea group was reduced by 44.7%, compared to the HFD group. Similar results were observed for the protein levels of hepatic FAS and ACC, the target gene of SREBP-1c and the key enzyme of de novo lipogenesis, which were downregulated by 25.6% (Figure 3(e)) and 65.8% (Figure 3(f)), respectively, in the Deepure tea-treatment mice, compared to the HFD group. Low density lipoprotein receptor (LDLR) plays an important role in insulin resistance [27, 28]. The level of LDLR was detected by ELISA kit. As shown in Figure 3(g), LDLR was significantly upregulated in liver tissues from HFD mice. After treatment with 160 mg/kg/day Deepure tea, the upregulation of liver LDLR induced by HFD was reduced.

4. Discussion

This study provides evidence that short-term intake of Deepure tea protects against the development of hyperinsulinemia and NAFLD in HFD mice. Histologic results clearly showed that 14-day feeding of Deepure tea at 160 mg/kg reduced dietary-induced hepatic steatosis, which was correlated with the downregulation of SREBP-1c, FAS, and ACC expression in the liver. Consistent with reduced plasma insulin, the hepatic IRS-2 expression was significantly reduced in HFD mice. Thus, the findings from our investigation suggest that Deepure tea may be a desirable food for preventing insulin resistance and ectopic lipid accumulation, especially in HFD-induced obesity.

High-energy diets are used widely in nutritional experiments as a strategy to induce obesity in animals [29]. Rodents fed a lard-based HFD are reported to exhibit visceral adiposity, dyslipidemia, hyperinsulinemia, and NAFLD [22], which are typically linked with human obesity. In line with this report, mice in the preset study were fed with high fat diet containing 50% fat, 36% carbohydrate, and 14% protein for 8 weeks and developed obesity, insulin resistance, and lipid metabolic disorder. Insulin resistance is one of the key pathogenic factors of the metabolic syndrome [30]. Impaired glucose tolerance assessed by IPGTT indicates the presence of insulin resistance and abnormality in glucose disposal [31]. The present study demonstrated that Deepure tea effectively decreased plasma insulin and ameliorated glucose tolerance

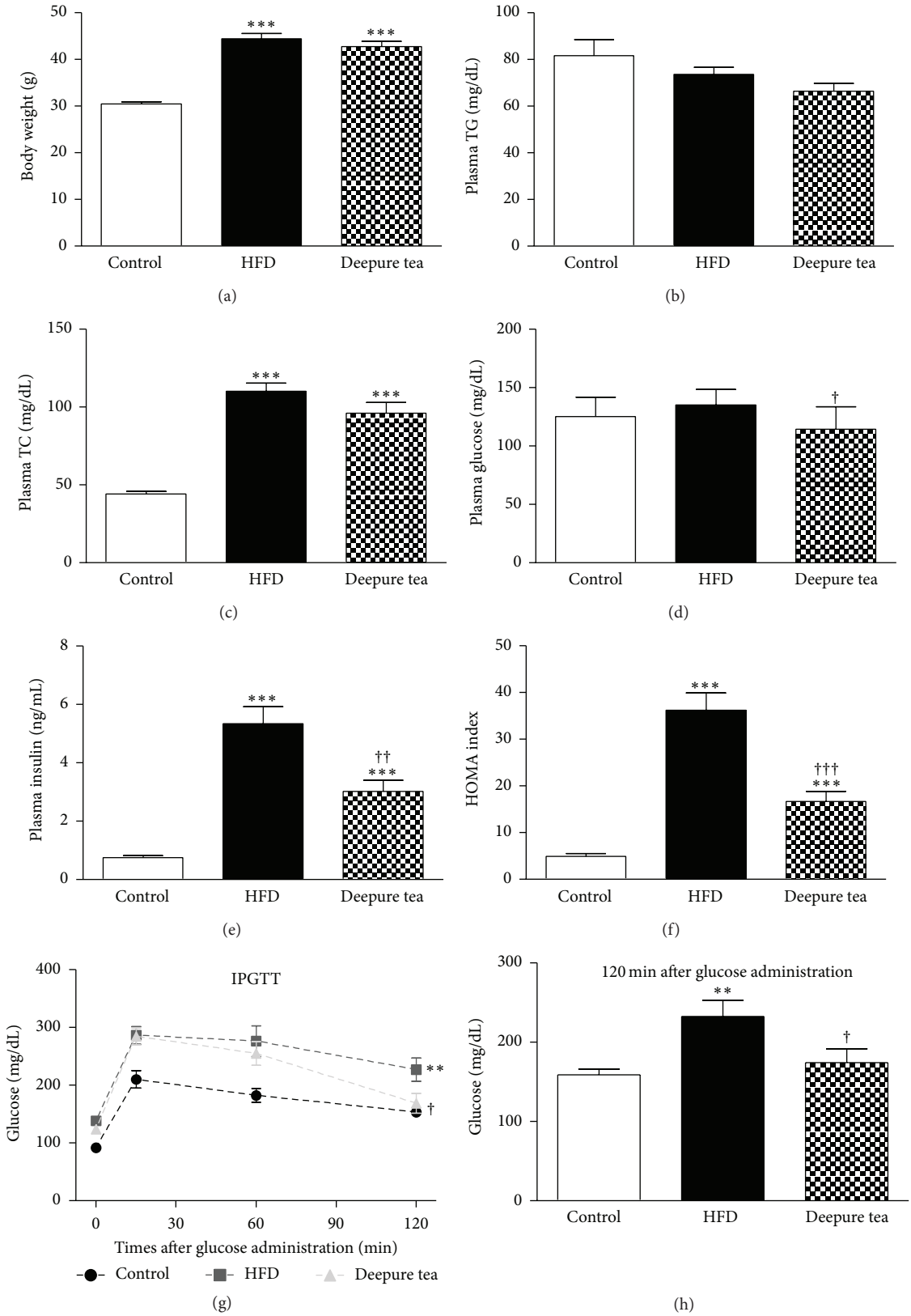

Figure 1: Deepure tea restored plasma level of insulin and improved insulin resistance in high fat diet mice. Plasma parameters were measured in the fasting state of the mice. (a) The body weight in different groups. (b)-(c) Plasma TG and TC level in different groups. (d) Plasma glucose level in different groups at baseline. (e) Plasma insulin level in different groups at baseline. (f) Insulin resistance of mice evaluated by homeostasis model assessment (HOMA) index. (g) Intraperitoneal glucose tolerance test (IPGTT). (h) Plasma glucose concentration tested 120 min after glucose administration. The number of animals included was 10 (control group), 9 (HFD group), and 8 (Deepure tea group), respectively. All experiments were performed in triplicate. Data are means ± SEM. $^{*}p < 0.05$, $^{**}p < 0.01$, and $^{***}p < 0.001$ versus control mice; $^{\dagger}p < 0.05$ and $^{\dagger\dagger}p < 0.01$ and $^{\dagger\dagger\dagger}p < 0.001$ versus HFD mice.

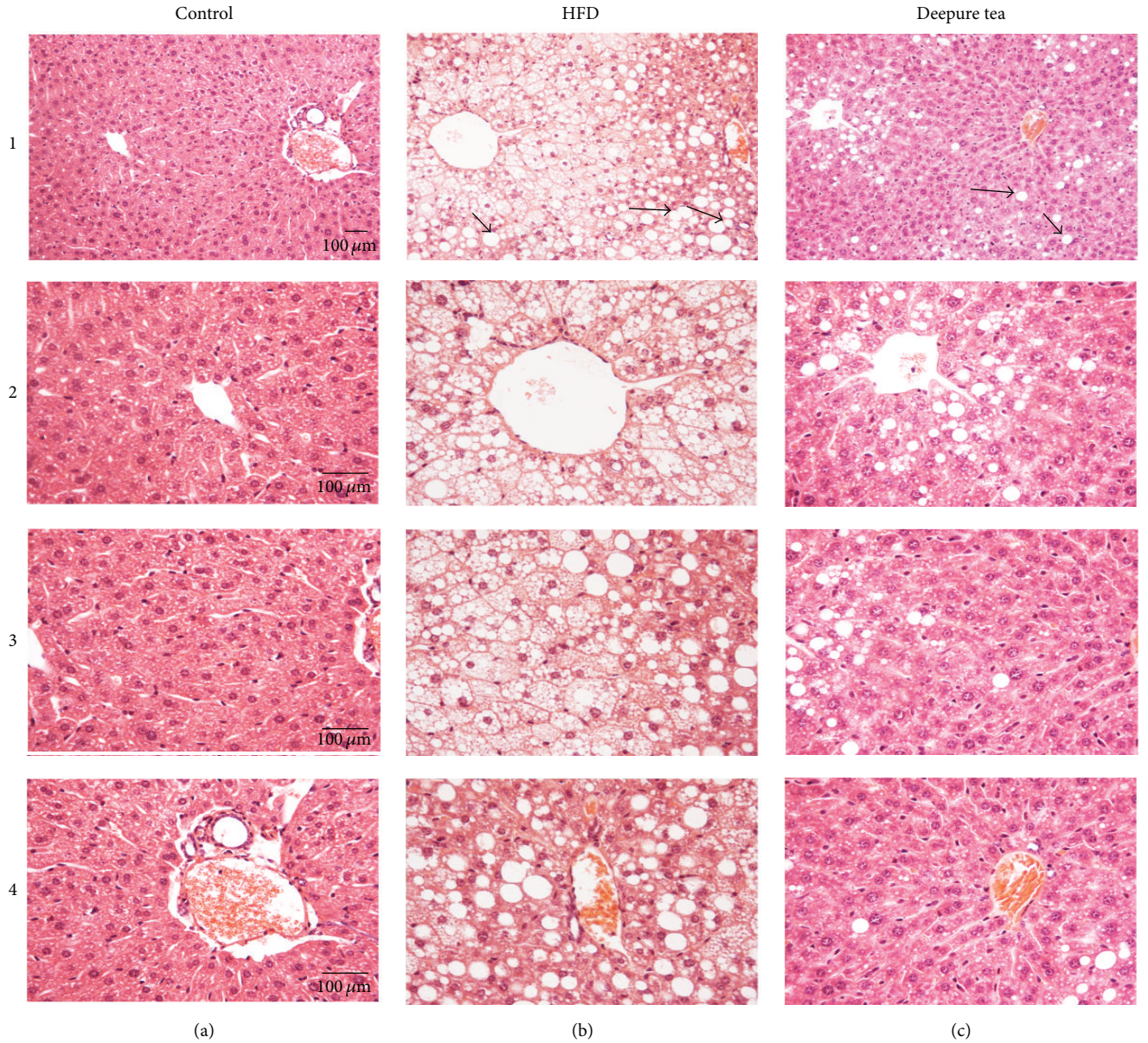

Figure 2: Deepure tea diminished nonalcoholic steatohepatitis caused by HFD in C57BL/6 mice. Representative images of liver tissues collected from the mice of control (a), HFD (b), and Deepure tea (c) group with low magnification displayed in 1 and high magnification in 2, 3, and 4 are shown. The number of mice examined in each group was 6. Bar = 100 μm.

in the high fat diet mice. A similar phenomenon has also been reported for the water extract of Pu-erh tea showing its ability to inhibit the increase in blood insulin and improve impaired glucose tolerance in db/db mice [32]. Also, we found that administration of Deepure tea for 14 days at 160 mg tea/kg body weight, a dose that is approximately equivalent to 1 g per day recommended for human, significantly repressed the elevated HOMA-IR index in HFD mice. Taken together, Deepure tea can improve insulin resistance induced by a high fat diet in C57BL/6 mice. The amount of food intake was almost the same for the mice in HFD and Deepure tea group (data not shown), and the body weight of mice did not reveal significant difference between HFD group and Deepure tea group. Plasma TC was only slightly decreased in Deepure tea group mice compared to that of the HFD group, which may result from the relatively short-term administration of Deepure tea.

Insulin resistance manifests reduced insulin sensitivity of peripheral tissue with an abnormality in the insulin signaling pathway, including IRS and other downstream molecules [33]. IRS-2 is the main mediator of hepatic insulin signaling, controlling hepatic insulin sensitivity [9]. In the present study, there was a dramatic decrease in hepatic IRS-2 in the liver of HFD mice. Deepure tea intragastrically given for 14 days could reverse the downregulation of IRS-2 protein in dietary-induced obese mice, which may be contributable to

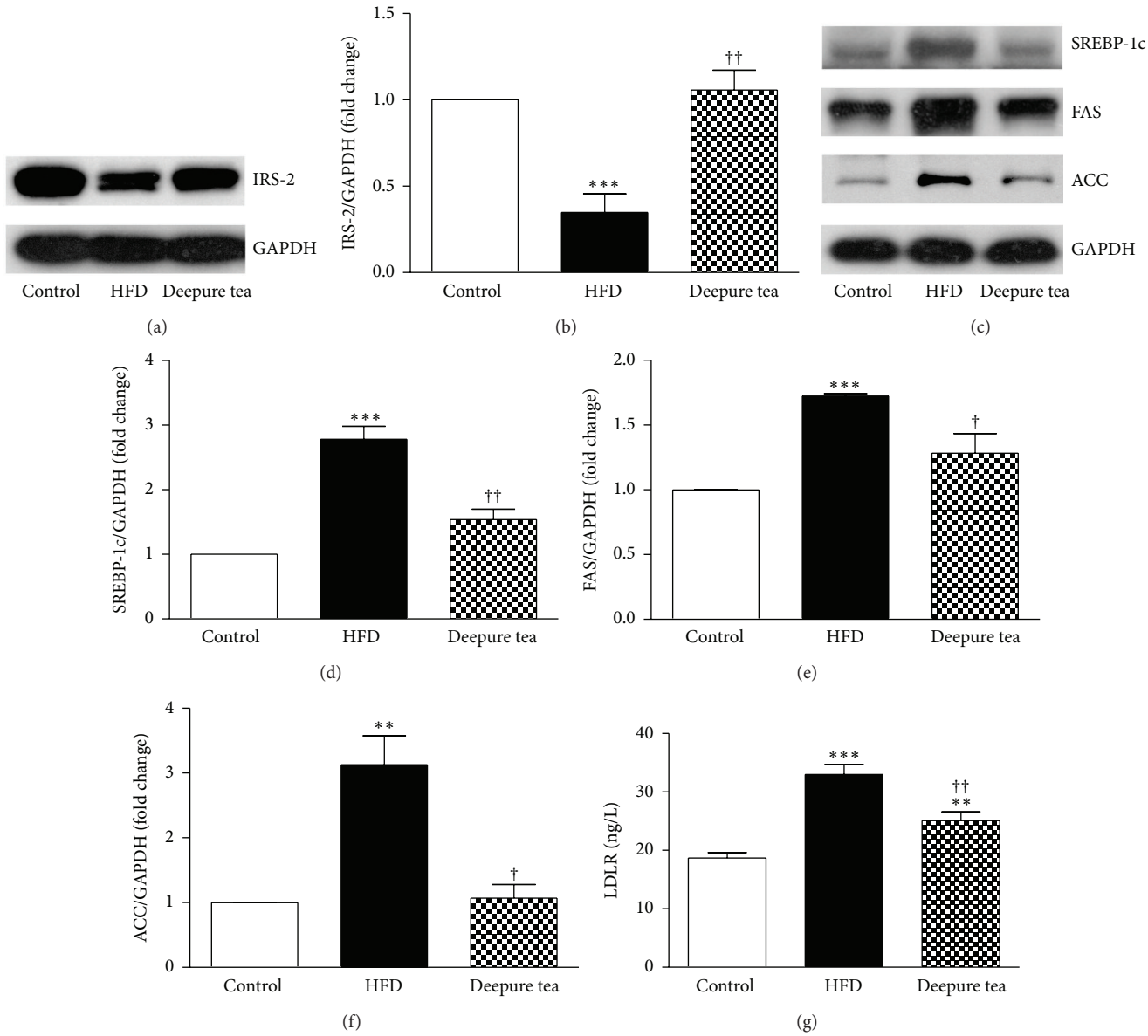

Figure 3: Deepure tea modulated the expression of genes involved in hepatic insulin signaling and lipid metabolism. (a) Representative western blot of IRS-2 expression in liver tissue of mice in different group. (b) Quantification of the western blot results of IRS-2. (c) Representative western blot of SREBP-1c, FAS, and ACC expression in liver tissue of mice in different group. (d) Quantification of the western blot results of SREBP-1c. (e) Quantification of the western blot results of FAS. (f) Quantification of the western blot results of ACC, $N = 6$. (g) LDLR levels determined by ELISA kit, $N = 8$. The results are presented as mean ± SEM of 3 experiments. $^{**}p < 0.01$ and $^{***}p < 0.001$ versus control mice; $^{\dagger}p < 0.05$ and $^{\dagger\dagger}p < 0.01$ versus HFD mice.

the improvement of hepatic insulin resistance. This result is in line with previous study showing that the water extract of Pu-erh tea can significantly increase glucose uptake by HepG2 cell [32]. Nonetheless, the present study is the first to show a possible molecular mechanism for Pu-erh tea to improve hepatic insulin resistance. However, more researches are needed to elucidate the mechanism that Deepure tea ameliorates dietary-induced hepatic insulin resistance.

Excessive intake of fatty acid will lead to fatty liver. In the present study, C57BL/6 mice fed with high fat diet displayed NAFLD, whereas after administration of Deepure tea, the lipid content in liver was significantly reduced, suggesting that the Deepure tea could significantly improve hepatic lipid accumulation.

The increased fatty acid de novo synthesis is one of the major sources of lipid accumulation in liver. The protein SREBP-1c, as a transcriptional regulator of lipid synthesis, activates genes required for de novo lipogenesis [26, 34–36]. SREBP-1c activates ACC that produces malonyl-CoA at the mitochondrial membrane and also increases the expression of FAS, which plays an important role in the lipogenesis pathway. Previously, Pu-erh tea [18], Yerba Mate tea [37],

and coffee polyphenols [38] have been shown to decrease the hepatic SREBP-1c mRNA level, resulting in the suppression of body fat accumulation. Here, we observed that the proteins of SREBP-1c, FAS, and ACC were increased impressively in the liver of high fat diet mice, which were significantly restored by treatment with Deepure tea, accompanied with an attenuation of the lipid accumulation. Deepure tea also reduced the upregulated LDLR protein induced by high fat diet. However, further investigations are required to clarify the effects of Deepure tea on the expressions of genes involved in triglyceride metabolism such as fatty acid oxidation, lipolysis, and lipid delivery.

In conclusion, this study demonstrates that short-term oral administration of Deepure tea has beneficial effects on diet-induced hyperinsulinemia and ectopic lipid accumulation. These effects are most likely mediated through modification of IRS-2 and its downstream signaling SREBP-1c, FAS, and ACC. Importantly, the dose of Deepure tea administrated in the present study was close to that which human intakes as routing. Thus, these results also suggest that regular Deepure tea consumption is conducive to maintain metabolism homeostasis.

Conflict of Interests

The authors declare that there is no conflict of interests regarding the publication of this paper.

Authors' Contribution

Jing-Na Deng and Juan Li contributed equally to this work.

Acknowledgment

This work was supported by the Production of New Medicine Program of Ministry of Science and Technology of China [2013ZX09402202].

References

[1] K. G. M. M. Alberti and P. Z. Zimmet, "Definition, diagnosis and classification of diabetes mellitus and its complications. Part 1: diagnosis and classification of diabetes mellitus provisional report of a WHO consultation," *Diabetic Medicine*, vol. 15, no. 7, pp. 539–553, 1998.

[2] J. D. Browning and J. D. Horton, "Molecular mediators of hepatic steatosis and liver injury," *The Journal of Clinical Investigation*, vol. 114, no. 2, pp. 147–152, 2004.

[3] G. Marchesini, M. Brizi, G. Blanchi et al., "Nonalcoholic fatty liver disease: a feature of the metabolic syndrome," *Diabetes*, vol. 50, no. 8, pp. 1844–1850, 2001.

[4] H. C. Masuoka and N. Chalasani, "Nonalcoholic fatty liver disease: an emerging threat to obese and diabetic individuals," *Annals of the New York Academy of Sciences*, vol. 1281, no. 1, pp. 106–122, 2013.

[5] V. Ratziu and T. Poynard, "Assessing the outcome of nonalcoholic steatohepatitis? It's time to get serious," *Hepatology*, vol. 44, no. 4, pp. 802–805, 2006.

[6] A. Kotronen and H. Yki-Järvinen, "Fatty liver: a novel component of the metabolic syndrome," *Arteriosclerosis, Thrombosis, and Vascular Biology*, vol. 28, no. 1, pp. 27–38, 2008.

[7] P. Haentjens, D. Massaad, H. Reynaert et al., "Identifying non-alcoholic fatty liver disease among asymptomatic overweight and obese individuals by clinical and biochemical characteristics," *Acta Clinica Belgica*, vol. 64, no. 6, pp. 483–493, 2009.

[8] Y. Kido, D. J. Burks, D. Withers et al., "Tissue-specific insulin resistance in mice with mutations in the insulin receptor, IRS-1, and IRS-2," *The Journal of Clinical Investigation*, vol. 105, no. 2, pp. 199–205, 2000.

[9] D. J. Withers, J. S. Gutierrez, H. Towery et al., "Disruption of IRS-2 causes type 2 diabetes in mice," *Nature*, vol. 391, no. 6670, pp. 900–904, 1998.

[10] I. Shimomura, Y. Bashmakov, S. Ikemoto, J. D. Horton, M. S. Brown, and J. L. Goldstein, "Insulin selectively increases SREBP-1c mRNA in the livers of rats with streptozotocin-induced diabetes," *Proceedings of the National Academy of Sciences of the United States of America*, vol. 96, no. 24, pp. 13656–13661, 1999.

[11] V. T. Samuel, Z.-X. Liu, X. Qu et al., "Mechanism of hepatic insulin resistance in non-alcoholic fatty liver disease," *Journal of Biological Chemistry*, vol. 279, no. 31, pp. 32345–32353, 2004.

[12] T. Ide, H. Shimano, N. Yahagi et al., "SREBPs suppress IRS-2-mediated insulin signalling in the liver," *Nature Cell Biology*, vol. 6, no. 4, pp. 351–357, 2004.

[13] M. den Boer, P. J. Voshol, F. Kuipers, L. M. Havekes, and J. A. Romijn, "Hepatic steatosis: a mediator of the metabolic syndrome. Lessons from animal models," *Arteriosclerosis, Thrombosis, and Vascular Biology*, vol. 24, no. 4, pp. 644–649, 2004.

[14] C. A. Nagle, E. L. Klett, and R. A. Coleman, "Hepatic triacylglycerol accumulation and insulin resistance," *Journal of Lipid Research*, vol. 50, supplement, pp. S74–S79, 2009.

[15] C. Cabrera, R. Artacho, and R. Giménez, "Beneficial effects of green tea—a review," *Journal of the American College of Nutrition*, vol. 25, no. 2, pp. 79–99, 2006.

[16] K. Kubota, S. Sumi, H. Tojo et al., "Improvements of mean body mass index and body weight in preobese and overweight Japanese adults with black Chinese tea (Pu-Erh) water extract," *Nutrition Research*, vol. 31, no. 6, pp. 421–428, 2011.

[17] Z.-H. Cao, D.-H. Gu, Q.-Y. Lin et al., "Effect of pu-erh tea on body fat and lipid profiles in rats with diet-induced obesity," *Phytotherapy Research*, vol. 25, no. 2, pp. 234–238, 2011.

[18] Y. Shimamura, M. Yoda, H. Sakakibara, K. Matsunaga, and S. Masuda, "Pu-erh tea suppresses diet-induced body fat accumulation in C57BL/6J mice by down-regulating SREBP-1c and related molecules," *Bioscience, Biotechnology and Biochemistry*, vol. 77, no. 7, pp. 1455–1460, 2013.

[19] X. Ma, S. Tsuda, X. Yang et al., "Pu-erh tea hot-water extract activates akt and induces insulin-independent glucose transport in rat skeletal muscle," *Journal of Medicinal Food*, vol. 16, no. 3, pp. 259–262, 2013.

[20] S. Wang, S. K. Noh, and S. I. Koo, "Epigallocatechin gallate and caffeine differentially inhibit the intestinal absorption of cholesterol and fat in ovariectomized rats," *The Journal of Nutrition*, vol. 136, no. 11, pp. 2791–2796, 2006.

[21] D. G. Raederstorff, M. F. Schlachter, V. Elste, and P. Weber, "Effect of EGCG on lipid absorption and plasma lipid levels in rats," *Journal of Nutritional Biochemistry*, vol. 14, no. 6, pp. 326–332, 2003.

[22] R. Tao, F. Ye, Y. He et al., "Improvement of high-fat-diet-induced metabolic syndrome by a compound from *Balanophora polyandra* Griff in mice," *European Journal of Pharmacology*, vol. 616, no. 1–3, pp. 328–333, 2009.

[23] D. R. Matthews, J. P. Hosker, A. S. Rudenski, B. A. Naylor, D. F. Treacher, and R. C. Turner, "Homeostasis model assessment: insulin resistance and beta-cell function from fasting plasma glucose and insulin concentrations in man," *Diabetologia*, vol. 28, no. 7, pp. 412–419, 1985.

[24] S.-Q. Lin, X.-H. Wei, P. Huang et al., "Qi Shen Yi Qi Pills prevents cardiac ischemia-reperfusion injury via energy modulation," *International Journal of Cardiology*, vol. 168, no. 2, pp. 967–974, 2013.

[25] X. J. Sun, L.-M. Wang, Y. Zhang et al., "Role of IRS-2 in insulin and cytokine signalling," *Nature*, vol. 377, no. 6545, pp. 173–177, 1995.

[26] J. D. Horton, J. L. Goldstein, and M. S. Brown, "SREBPs: activators of the complete program of cholesterol and fatty acid synthesis in the liver," *Journal of Clinical Investigation*, vol. 109, no. 9, pp. 1125–1131, 2002.

[27] S. Han, C.-P. Liang, M. Westerterp et al., "Hepatic insulin signaling regulates VLDL secretion and atherogenesis in mice," *Journal of Clinical Investigation*, vol. 119, no. 4, pp. 1029–1041, 2009.

[28] R. Streicher, J. Kotzka, D. Müller-Wieland et al., "SREBP-1 mediates activation of the low density lipoprotein receptor promoter by insulin and insulin-like growth factor-I," *The Journal of Biological Chemistry*, vol. 271, no. 12, pp. 7128–7133, 1996.

[29] J. K. Kim, M. D. Michael, S. F. Previs et al., "Redistribution of substrates to adipose tissue promotes obesity in mice with selective insulin resistance in muscle," *The Journal of Clinical Investigation*, vol. 105, no. 12, pp. 1791–1797, 2000.

[30] G. I. Shulman, "Cellular mechanisms of insulin resistance," *Journal of Clinical Investigation*, vol. 106, no. 2, pp. 171–176, 2000.

[31] M. A. Abdul-Ghani, D. Tripathy, and R. A. DeFronzo, "Contributions of beta-cell dysfunction and insulin resistance to the pathogenesis of impaired glucose tolerance and impaired fasting glucose," *Diabetes Care*, vol. 29, no. 5, pp. 1130–1139, 2006.

[32] W.-H. Du, S.-M. Peng, Z.-H. Liu, L. Shi, L.-F. Tan, and X.-Q. Zou, "Hypoglycemic effect of the water extract of Pu-erh tea," *Journal of Agricultural and Food Chemistry*, vol. 60, no. 40, pp. 10126–10132, 2012.

[33] I. Shimomura, M. Matsuda, R. E. Hammer, Y. Bashmakov, M. S. Brown, and J. L. Goldstein, "Decreased IRS-2 and increased SREBP-1c lead to mixed insulin resistance and sensitivity in livers of lipodystrophic and ob/ob mice," *Molecular Cell*, vol. 6, no. 1, pp. 77–86, 2000.

[34] H. Shimano, N. Yahagi, M. Amemiya-Kudo et al., "Sterol regulatory element-binding protein-1 as a key transcription factor for nutritional induction of lipogenic enzyme genes," *The Journal of Biological Chemistry*, vol. 274, no. 50, pp. 35832–35839, 1999.

[35] M. S. Brown and J. L. Goldstein, "The SREBP pathway: regulation of cholesterol metabolism by proteolysis of a membrane-bound transcription factor," *Cell*, vol. 89, no. 3, pp. 331–340, 1997.

[36] J. D. Horton, "Sterol regulatory element-binding proteins: transcriptional activators of lipid synthesis," *Biochemical Society Transactions*, vol. 30, no. 6, pp. 1091–1095, 2002.

[37] H. Gao, Z. Liu, W. Wan, X. Qu, and M. Chen, "Aqueous extract of yerba mate tea lowers atherosclerotic risk factors in a rat hyperlipidemia model," *Phytotherapy Research*, vol. 27, no. 8, pp. 1225–1231, 2013.

[38] T. Murase, K. Misawa, Y. Minegishi et al., "Coffee polyphenols suppress diet-induced body fat accumulation by downregulating SREBP-1c and related molecules in C57BL/6J mice," *The American Journal of Physiology—Endocrinology and Metabolism*, vol. 300, no. 1, pp. E122–E133, 2011.

Hindawi Publishing Corporation
Evidence-Based Complementary and Alternative Medicine
Volume 2015, Article ID 385976, 11 pages
http://dx.doi.org/10.1155/2015/385976

Research Article

Blackcurrant Suppresses Metabolic Syndrome Induced by High-Fructose Diet in Rats

Ji Hun Park,[1] Min Chul Kho,[1,2] Hye Yoom Kim,[1,2] You Mee Ahn,[1,2] Yun Jung Lee,[1,2] Dae Gill Kang,[1,2,3] and Ho Sub Lee[1,2,3]

[1]*Hanbang Body-Fluid Research Center, Wonkwang University, Shinyong-dong, Iksan, Jeonbuk 570-749, Republic of Korea*
[2]*College of Oriental Medicine and Professional Graduate School of Oriental Medicine, Wonkwang University, Shinyong-dong, Iksan, Jeonbuk 570-749, Republic of Korea*
[3]*Brain Korea (BK) 21 Plus Team, Professional Graduate School of Oriental Medicine, Wonkwang University, Iksan, Jeonbuk 540-749, Republic of Korea*

Correspondence should be addressed to Ho Sub Lee; host@wku.ac.kr

Received 13 May 2015; Revised 29 June 2015; Accepted 28 July 2015

Academic Editor: Abbas A. Mahdi

Increased fructose ingestion has been linked to obesity, hyperglycemia, dyslipidemia, and hypertension associated with metabolic syndrome. Blackcurrant (*Ribes nigrum*; BC) is a horticultural crop in Europe. To induce metabolic syndrome, Sprague-Dawley rats were fed 60% high-fructose diet. Treatment with BC (100 or 300 mg/kg/day for 8 weeks) significantly suppressed increased liver weight, epididymal fat weight, C-reactive protein (CRP), total bilirubin, leptin, and insulin in rats with induced metabolic syndrome. BC markedly prevented increased adipocyte size and hepatic triglyceride accumulation in rats with induced metabolic syndrome. BC suppressed oral glucose tolerance and protein expression of insulin receptor substrate-1 (IRS-1) and phosphorylated AMP-activated protein kinase (p-AMPK) in muscle. BC significantly suppressed plasma total cholesterol, triglyceride, and LDL content. BC suppressed endothelial dysfunction by inducing downregulation of endothelin-1 and adhesion molecules in the aorta. Vascular relaxation of thoracic aortic rings by sodium nitroprusside and acetylcholine was improved by BC. The present study provides evidence of the potential protective effect of BC against metabolic syndrome by demonstrating improvements in dyslipidemia, hypertension, insulin resistance, and obesity *in vivo*.

1. Introduction

Metabolic syndrome is a disease condition characterized by variable coexistence of obesity, hyperuricemia, hyperinsulinemia, hypertension, and dyslipidemia. The pathogenesis of metabolic syndrome includes multiple organs in the cardiorenal system [1]. Patients with metabolic syndrome, as defined by the National Cholesterol Education Program Adult Treatment Panel III (NCEP-ATP III), simultaneously exhibit 3 or more of the following traits: increased waist circumference, elevated blood pressure, reduced high-density lipoprotein (HDL) level, elevated triglyceride level, and hyperglycemia [2, 3].

Fructose, present in added sugars such as sucrose and high-fructose corn syrup, has been epidemiologically linked with metabolic syndrome. Increased consumption of fructose, commonly used in processed food and soft drinks, is one of the most important factors contributing to the growing prevalence of metabolic syndrome [4]. Recent findings have shown that dietary fructose accelerates metabolic disorders and induces oxidative damage [5]. A high-fructose diet induces a well-characterized metabolic syndrome, generally resulting in hyperinsulinemia, hypertension, dyslipidemia, and a low HDL level [6]. A recent study suggested that renal damage is associated with metabolic syndrome [7]. Exposure of the liver to high levels of fructose leads to rapid stimulation of lipogenesis and triglyceride accumulation, which lead to reduced insulin sensitivity and hepatic insulin resistance/glucose intolerance [8].

Blackcurrant (*Ribes nigrum*; BC) is a valuable horticultural crop in Russia, Poland, German, Scandinavia, England, New Zealand, and several Eastern European nations.

Annual worldwide production of BC is approximately 500,000 to 600,000 tons [9]. BC contains numerous physiologically active components, including vitamins, carotenoids, and flavonoids, which have antiulcer, anticonvulsion, and antidiarrhea effects, as well as protective effects against carcinomas, diabetes, and regressive disease [10, 11].

Several studies have reported that BC produces antioxidative effects. Anthocyanins from BC abrogate oxidative stress through Nrf2-mediated antioxidant mechanisms [12]. In addition, BC extract has cytoprotective and anti-inflammatory properties [13]. Moreover, BC protects against kidney stones [14]. However, the therapeutic effects of BC in subjects with metabolic disorder have not been reported. Thus, this study was designed to identify the effect of BC extract on high-fructose diet-induced metabolic syndrome in rats.

2. Methods and Materials

2.1. Plant Material and Preparation of BC Extract. BC was purchased from Gukmin Farm (Jeongeup, Korea). A voucher specimen (number HBF191) was deposited in the Herbarium of the Professional Graduate School of Oriental Medicine, Wonkwang University (Korea). BC (400 g) was boiled with 3 L of distilled water at 100°C for 2 h. The resulting extract was filtered through Whatman No. 3 filter paper and centrifuged at 990 ×g for 20 min at 4°C. The resulting supernatant was concentrated using a rotary evaporator, after which the resulting extract (63.19 g) was lyophilized using a freeze-drier and stored at −70°C until required.

2.2. Animal Experiments and Diet. All experimental procedures were carried out in accordance with the National Institute of Health Guide for the Care and Use of Laboratory Animals and were approved by the Institutional Animal Care and Utilization Committee for Medical Science of Wonkwang University (approval number: WKU 14-50). Six-week-old male Sprague-Dawley (SD) rats were obtained from Samtako (Osan, Korea) and kept in a room with automatically maintained temperature (23°C), humidity (50–60%), and light/dark cycles (12-h each) throughout the experiments. After 1 week of acclimatization, the rats were randomly divided into 4 groups (10 rats per group). The control group (Cont.) was fed a regular diet. The high-fructose (HF) diet group was fed a 60% fructose diet (Research Diet, USA). The low-dose BC group was fed 60% fructose diet with 100 mg/kg/day BC administered orally by Sonde for a period of 4 weeks. The high-dose BC group was fed 60% fructose diet with 300 mg/kg/day of BC administered orally by Sonde for a period of 4 weeks. The regular diet was composed of 50% starch, 21% protein, 4% fat, and a standard mix of vitamins and minerals. The high-fructose diet was composed of 60% fructose, 20% protein, 10% fat, and a standard mix of vitamins and minerals.

2.3. Measurement of Blood Pressure. Systolic blood pressure (SBP) was determined using noninvasive tail-cuff plethysmography and recorded with an automatic sphygmograph (MK2000; Muromachi Kikai, Tokyo, Japan). SBP was measured once per week. At least 10 determinations of SBP were made during every measurement session. Values are presented as the mean ± SEM of 8 measurements.

2.4. Estimation of Oral Glucose Tolerance. Two oral glucose tolerance tests (OGTT) were performed 2 days apart after 8 weeks of treatment. Briefly, basal blood glucose concentrations were measured after 10–12 h of overnight fasting, after which glucose (2 g/kg body weight) was immediately administered via oral gavage. Tail vein blood samples were collected 30, 60, 90, and 120 min after glucose administration.

2.5. Blood and Tissue Sampling. At the end of the experiments, the thoracic aorta and muscle were separated, rinsed with cold saline, and frozen. Plasma was obtained from coagulated blood samples by centrifugation at 3,000 rpm for 15 min at 4°C and frozen at −80°C.

2.6. Blood Parameters. Triglyceride levels in plasma were measured using commercial kits (AM 157S-K, ASAN, Korea). Levels of HDL, total cholesterol, and low-density lipoprotein (LDL) in plasma were measured using HDL and LDL assay kits (E2HL-100, Bio Assay Systems, Germany). Levels of insulin in plasma were measured using commercial kits (80-INSRT-E01, ALPCO, UK). Levels of C-reactive protein (CRP) in plasma were measured using commercial kits (557825, BD Biosciences, America). Levels of leptin in plasma were measured using commercial kits (ab100773, Abcam, UK). Levels of T-Bill and BUN in plasma were measured using commercial kits (77184, Arkray, Japan).

2.7. Preparation of Aorta and Measurement of Vascular Reactivity. The thoracic aorta was rapidly and carefully collected from each rat and placed into cold Kreb's solution (118 mM NaCl, 4.7 mM KCl, 1.1 mM $MgSO_4$, 1.2 mM KH_2PO_4, 1.5 mM CaCl, 25 mM $NaHCO_3$, 10 mM glucose, and pH 7.4). Connective tissue and fat were removed from each thoracic aorta. Each thoracic aorta was cut into rings of approximately 3 mm in length. Care was taken to protect the endothelium from accidental damage during the dissection procedure. The thoracic aortic rings were suspended in a tissue bath containing Kreb's solution at 37°C by means of 2 L-shaped stainless-steel wires inserted into the lumen and aerated with 95% O_2 and 5% CO_2. The isometric forces of the rings were measured using a Grass FT 03 force displacement transducer connected to a Model 7E polygraph recording system (Grass Technologies, Quincy, MA, USA). A passive stretch of 1 g in the thoracic aortic rings was determined to be the optimal tension for maximal responsiveness to phenylephrine (10^{-6} M). The preparations were allowed to equilibrate for approximately 1 h with the Kreb's solution replaced every 10 min. The relaxant effects of acetylcholine (ACh, 10^{-9}–10^{-6} M) and sodium nitroprusside (SNP, 10^{-10}–10^{-5} M) in the thoracic aorta rings were studied.

2.8. Western Blot Analysis in the Rat Aorta and Muscle. Thoracic aorta and muscle homogenates were prepared in ice-cold buffer containing 250 mM sucrose, 1 mM EDTA,

0.1 mM phenylmethylsulfonyl fluoride, and 20 mM potassium phosphate buffer (pH 7.6). The homogenates were centrifuged at 8,000 rpm for 10 min at 4°C, after which the resulting supernatants were centrifuged at 13,000 rpm for 5 min at 4°C to produce a cytosolic fraction for protein analysis. The recovered proteins were separated by 10% SDS-polyacrylamide gel electrophoresis and transferred to nitrocellulose membranes, which were blocked with 5% bovine serum albumin (BSA) powder in 0.05% Tween 20-Tris-buffered saline (TBS-T) for 1 h. Specific primary antibodies against ICAM-1, VCAM-1, E-selectin, eNOS, ET-1 (in aorta), AMP-activated protein kinase (AMPK), p-AMPK, and insulin receptor substrate-1 (IRS-1) (in muscle) were purchased from Santa Cruz Biotechnology, Inc. (Santa Cruz, CA, USA). The nitrocellulose membranes were incubated overnight at 4°C with protein antibodies. The blots were washed several times with TBS-T and incubated with horseradish peroxidase-conjugated secondary antibody for 1 h after which immunoreactive bands were visualized using an enhanced chemiluminescence system (Amersham, Buchinghamshire, UK). The bands were analyzed densitometrically using a Chemi-doc Image Analyzer (Bio-Rad, Hercules, CA, USA).

2.9. Hematoxylin and Eosin (H & E) and Oil Red O Staining of Aorta, Epididymal Fat, and the Liver. Thoracic aorta tissue from 5 random subjects from each group was fixed in 10% (v/v) formalin in 0.01 M phosphate-buffered saline (PBS) for 2 days, with the formalin solution changed every day to remove traces of blood. The aortic tissue samples were dehydrated and embedded in paraffin, sectioned (6 μm), and stained with H & E. Epididymal fat (from 5 random subjects from each group) and liver tissue (from 5 random subjects from each group) samples were fixed in 4% paraformaldehyde for 48 h at 4°C and incubated with 30% sucrose for 2 days. Each fat and liver sample was embedded in OCT compound (Tissue-Tek, Sakura Finetek, Torrance, CA, USA), frozen in liquid nitrogen, and stored at −80°C. Frozen sections were cut with a Shandon Cryotome SME (Thermo Electron Corporation, Pittsburg, PA, USA) and mounted on poly-L-lysine-coated slides. Epididymal fat sections were stained with H & E, whereas liver sections were stained with Oil Red O. For quantitative histopathological comparisons, each section was analyzed using Axiovision 4 Imaging/Archiving software.

2.10. Immunohistochemistry of Thoracic Aorta Tissue. Prior to immunohistochemical staining, tissue sections in paraffin were mounted on poly-L-lysine-coated slides (Fisher Scientific, Pittsburgh, PA, USA). The tissue on each slide was immunostained using Invitrogen HISOTO-STAIN-SP kits with the labeled streptavidin-biotin (LAB-SA) method. After antigen retrieval, slides were immersed in 3% hydrogen peroxide for 10 min at room temperature to block endogenous peroxidase activity and rinsed with PBS. Next, slides were incubated with 10% nonimmune goat serum for 10 min at room temperature and incubated with primary antibodies against ICAM-1, VCAM-1, ET-1, and eNOS (1 : 200; Santa Cruz, CA, USA) in humidified chambers overnight at 4°C. Next, slides were incubated with biotinylated secondary antibodies for 20 min at room temperature, followed by incubation with horseradish peroxidase-conjugated streptavidin for 20 min at room temperature. Peroxidase activity was visualized using a 3,3′-diaminobenzidine (DAB; Novex, CA) substrate-chromogen system with hematoxylin counterstaining (Zymed, CA, USA). For quantitative analysis, the average score of 10–20 randomly selected areas was calculated using NIH Image Analysis Software, ImageJ (NIH, Bethesda, MD, USA).

2.11. Statistical Analysis. All experiments were repeated at least 3 times. Results are expressed as mean ± S.D. or mean ± S.E.M. Data were analyzed using Sigmaplot 10.0 software. Student's t-test was used to determine significant differences between groups. Results of $P < 0.05$ were considered statistically significant.

3. Results

3.1. Effects of BC on Body Weight and Tissue Weights. During the experimental period, all groups showed significant increases in body weight. The body weight of the HF diet group was not significantly different from that of the control group. However, the BC1 and BC2 groups showed significantly decreased body weight in comparison with the HF diet group during the final week of the experiment.

In comparison with the control group, the HF diet group showed significantly increased liver weight, liver weight as a percentage of BW, epididymal fat pad weight, and epididymal fat pad weight as a percentage of BW. However, the BC1 and BC2 groups showed significantly reduced liver weight, liver weight as a percentage of BW, epididymal fat pad weight, and epididymal fat pad weight as a percentage of BW (Table 1).

3.2. Effects of BC on Plasma Parameters. The HF diet group showed significantly increased CRP, T-Bil, and insulin levels in comparison with those of the control group. However, the BC2 group showed significantly decreased CRP, T-Bil, and insulin in comparison with those of the HF diet group. The HF diet group showed significantly decreased leptin in comparison with that of the control group. The BC2 group showed significantly increased leptin in comparison with that of the HF diet group (Table 2).

3.3. Effects of BC on Oral Glucose Tolerance and Expression of IRS-1 and p-AMPK in Muscle. Each rat was subjected to the OGTT to measure insulin resistance. The HF diet group showed significantly increased blood glucose content 90 and 120 min after glucose administration. However, the blood glucose content of the BC2 group significantly reduced in comparison with that of the HF diet group 90 and 120 min after glucose administration.

The IRS-1 and p-AMPK protein expression levels of the HF diet group significantly decreased in comparison with those of the control group. However, the IRS-1 and p-AMPK protein expression levels in muscle tissue from the BC1 and BC2 groups reduced in comparison with those of the HF diet group (Figure 1).

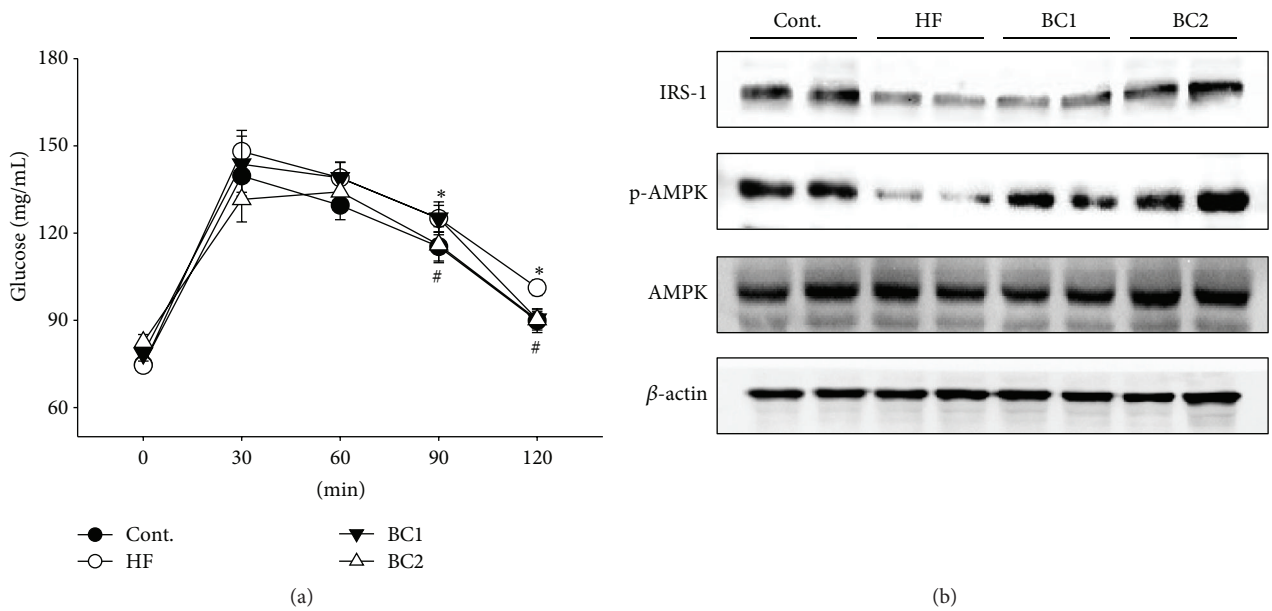

Figure 1: Effects of BC on oral glucose tolerance test (a) and the expression of IRS-1 and p-AMPK in the muscle (b). Values were expressed as mean ± S.E. ($n = 10$). $^{*}P < 0.05$ versus Cont; $^{\#}P < 0.05$ versus HF. Representative western blots of IRS-1 and p-AMPK protein levels are shown ($n = 4$). IRS-1: insulin receptor substrate 1; Cont.: control; HF: high fructose; BC1: blackcurrant 100 mg/kg/day; BC2: blackcurrant 300 mg/kg/day.

Table 1: Effects of BC on body weight, liver weight, liver weight % of BW, epididymal fat pads weight, and epididymal fat pads weight % of BW.

	Cont.	HF	BC1	BC2
Body weight (g)				
Start	227.62 ± 1.96	221.75 ± 2.64	233.79 ± 1.99	224.27 ± 2.31
Final	466.15 ± 10.75	455.14 ± 8.15	427.14 ± 10.97$^{\#}$	419.73 ± 6.6$^{\#}$
Liver weight (g)	10.9 ± 0.52	13.2 ± 0.76*	11.18 ± 0.21$^{\#}$	10.8 ± 0.23$^{\#\#}$
Liver weight % of BW	2.49 ± 0.07	2.8 ± 0.03*	2.52 ± 0.03$^{\#}$	2.54 ± 0.04$^{\#}$
Epididymal fat pads weigh (g)	6.64 ± 0.4	7.47 ± 0.46*	6.42 ± 0.55$^{\#}$	5.15 ± 0.42$^{\#}$
Epididymal fat pads weight % of BW	1.45 ± 0.05	1.74 ± 0.06*	1.38 ± 0.14$^{\#}$	1.19 ± 0.08$^{\#}$

Values were expressed as mean ± S.E. ($n = 10$). $^{*}P < 0.05$ versus Cont.; $^{\#}P < 0.05$ and $^{\#\#}P < 0.01$ versus HF. BW: body weight; Cont.: control; HF: high fructose; BC1: blackcurrant 100 mg/kg/day; BC2: blackcurrant 300 mg/kg/day.

Table 2: Effects of BC on CRP, T-Bil, leptin, and insulin.

	Cont.	HF	BC1	BC2
CRP (ng/mL)	195.62 ± 1.32	208.82 ± 5.6*	194.1 ± 2.52	193.67 ± 2.39$^{\#}$
T-Bil (mg/dL)	0.6 ± 0.03	0.72 ± 0.05*	0.63 ± 0.04	0.57 ± 0.02$^{\#}$
Leptin (pg/dL)	0.62 ± 0.03	0.45 ± 0.03*	0.53 ± 0.01	0.83 ± 0.1$^{\#\#}$
Insulin (mg/dL)	0.64 ± 0.03	1.15 ± 0.19*	0.64 ± 0.06$^{\#}$	0.62 ± 0.05$^{\#}$

Values were expressed as mean ± S.E. ($n = 10$). $^{*}P < 0.05$ versus Cont; $^{\#}P < 0.05$ and $^{\#\#}P < 0.01$ versus HF. CRP: C-reactive protein; T-Bil: total bilirubin; Cont.: control; HF: high fructose; BC1: blackcurrant 100 mg/kg/day; BC2: blackcurrant 300 mg/kg/day.

3.4. Effect of BC on the Morphology of Epididymal Fat Pads. The HF diet induced fat hypertrophy in this study. However, the adipocytes of the BC1 and BC2 groups showed significantly reduced hypertrophy in comparison with those of the HF diet group (Figure 2).

3.5. Effect of BC on Hepatic Steatosis. To investigate fat accumulation in the liver, we prepared frozen liver sections, which were stained with Oil Red O. Lipid droplets were detected in the HF diet groups. However, significantly fewer lipid droplets were counted in the BC1 and BC2 groups compared to those counted in the HF diet group (Figure 3).

3.6. Effect of BC on Lipid Metabolism Biomarker Levels. Total cholesterol, triglyceride, LDL, and HDL plasma levels were measured as biomarkers of lipid metabolism. The total cholesterol, triglyceride, and LDL levels of the HF diet group significantly increased in comparison with those of the control group. However, the total cholesterol, triglyceride,

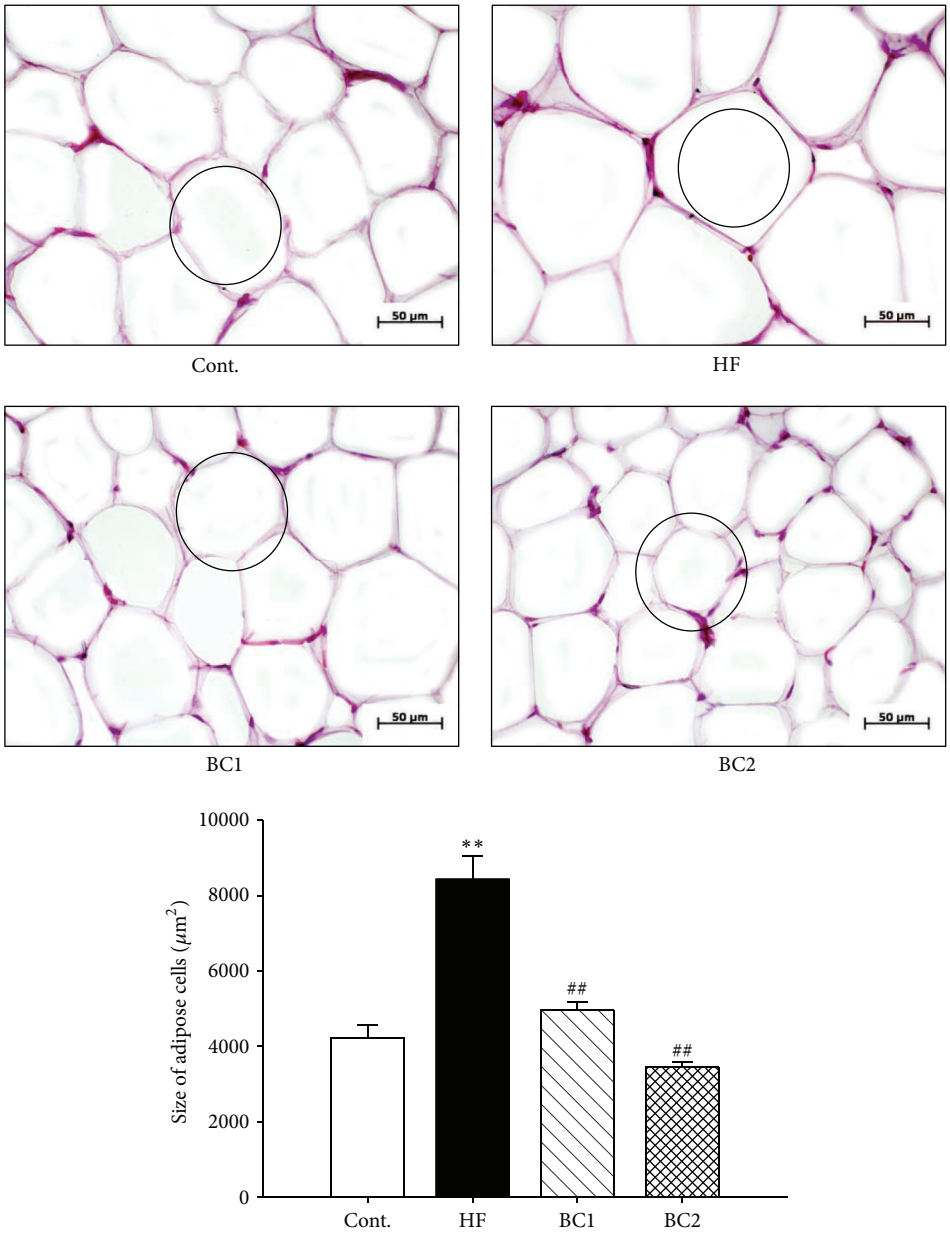

Figure 2: Effects of BC on epididymal fat pads morphology. Representative microscopic photographs in epididymal fat pads of SD rats with control diet and HF diet were stained with hematoxylin and eosin. Values were expressed as mean ± S.E. ($n = 5$). $^{**}P < 0.01$ versus Cont; $^{\#\#}P < 0.01$ versus HF. Cont.: control; HF: high fructose; BC1: blackcurrant 100 mg/kg/day; BC2: blackcurrant 300 mg/kg/day.

and LDL levels of the BC1 and BC2 groups significantly decreased in comparison with those of the HF group. There was no significant difference in the HDL level of either the HF group or the BC group (Table 3).

3.7. Effect of BC on Systolic Blood Pressure and Vascular Tension. At the beginning of the experimental feeding period, systolic blood pressure was measured by the tail-cuff technique. After 4 weeks, the systolic blood pressure of the HF diet group was significantly higher than that of the control group. The systolic blood pressure of the BC1 group was significantly lower than that of the HF diet group. The systolic blood pressure of the BC2 group was significantly lower than that of the HF diet group.

Vascular responses to SNP (1×10^{-10} to 1×10^{-7} M) and ACh (1×10^{-9} to 1×10^{-6} M) were measured in the thoracic aorta. ACh-induced relaxation of thoracic aorta rings was significantly impaired in the HF diet group in comparison with that of the other groups. SNP-induced relaxation of thoracic aorta rings was significantly impaired in the HF diet group in comparison with that of the other groups (Figure 4).

3.8. Effect of BC on the Morphology of Aorta. The tunica intima-media layer of the HF diet group showed significantly

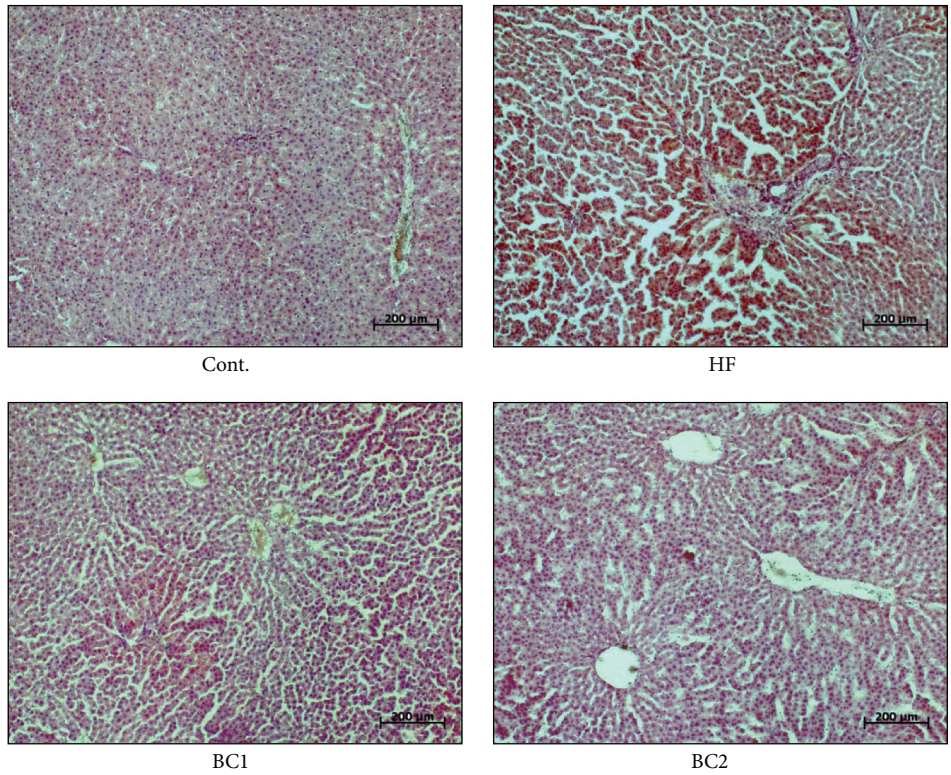

Figure 3: Effects of BC on liver morphology. Representative microscopic photographs in liver of SD rats with control diet and HF diet were stained with Oil red O ($n = 5$). Cont.: control; HF: high fructose; BC1: blackcurrant 100 mg/kg/day; BC2: blackcurrant 300 mg/kg/day.

Table 3: Lipid profile in SD rats fed HF and/or BC for 8 weeks.

	Cont.	HF	BC1	BC2
T-Cho (mg/dL)	55.36 ± 1.65	73.66 ± 3.62**	59.93 ± 3.07$^{\#}$	58.36 ± 3.76$^{\#}$
TG (mg/dL)	98.13 ± 13.43	229.66 ± 15.29**	137.32 ± 14.42$^{\#\#}$	109.38 ± 13.36$^{\#\#}$
LDL-c (mg/dL)	31.37 ± 3.73	46.76 ± 8.85*	33.32 ± 4.97$^{\#}$	34.35 ± 2.63$^{\#}$
HDL-c (mg/dL)	30.37 ± 4.8	27.49 ± 5.72	32.64 ± 5.2	35.1 ± 7.62

Values were expressed as mean ± S.E. ($n = 10$). $^{*}P < 0.05$ and $^{**}P < 0.01$ versus Cont; $^{\#}P < 0.05$ and $^{\#\#}P < 0.01$ versus HF. T-Cho: total cholesterol; TG: triglyceride; LDL-c: low-density lipoprotein; HDL-c: high-density lipoprotein; Cont.: control; HF: high fructose; BC1: blackcurrant 100 mg/kg/day; BC2: blackcurrant 300 mg/kg/day.

increased thickness in comparison with that of the control group. However, the tunica intima-media layer of the BC1 and BC2 groups showed significantly decreased thickness in comparison with that of the HF diet group (Figure 5).

3.9. Effects of BC on Expressions Levels of Adhesion Molecules, eNOS, and ET-1 in Aortic Tissue. Protein expression levels of adhesion molecules (VCAM-1, ICAM-1, and E-selectin), ET-1, and eNOS in aortic tissue were determined by western blotting. Protein levels of adhesion molecules and ET-1 increased in the HF diet group in comparison with those of the control group. However, the BC1 and BC2 groups showed decreased protein levels of adhesion molecules and ET-1 in comparison with those of the HF diet group. In addition, eNOS protein expression in the HF diet group decreased in comparison with that of the control group. However, the BC1 and BC2 groups showed increased eNOS protein expression in comparison with that of the HF group (Figure 6).

3.10. Effects of BC on Immunoreactivity of Adhesion Molecules, eNOS, and ET-1 in Aortic Tissues. Immunohistochemistry was used to evaluate expression of ET-1, ICAM-1, VCAM-1, and e-NOS in the aortic wall. ET-1, ICAM-1, and VCAM-1 protein expression levels increased in the HF diet group in comparison with those of the control group. However, the ET-1, ICAM-1, and VCAM-1 protein expression levels of the BC1 and BC2 groups decreased in comparison with those of the HF diet group. eNOS expression decreased in the HF diet group in comparison with that of the control group. However, the groups treated with BC1 and BC2 showed increased eNOS expression in comparison with that of the HF diet group (Figure 7).

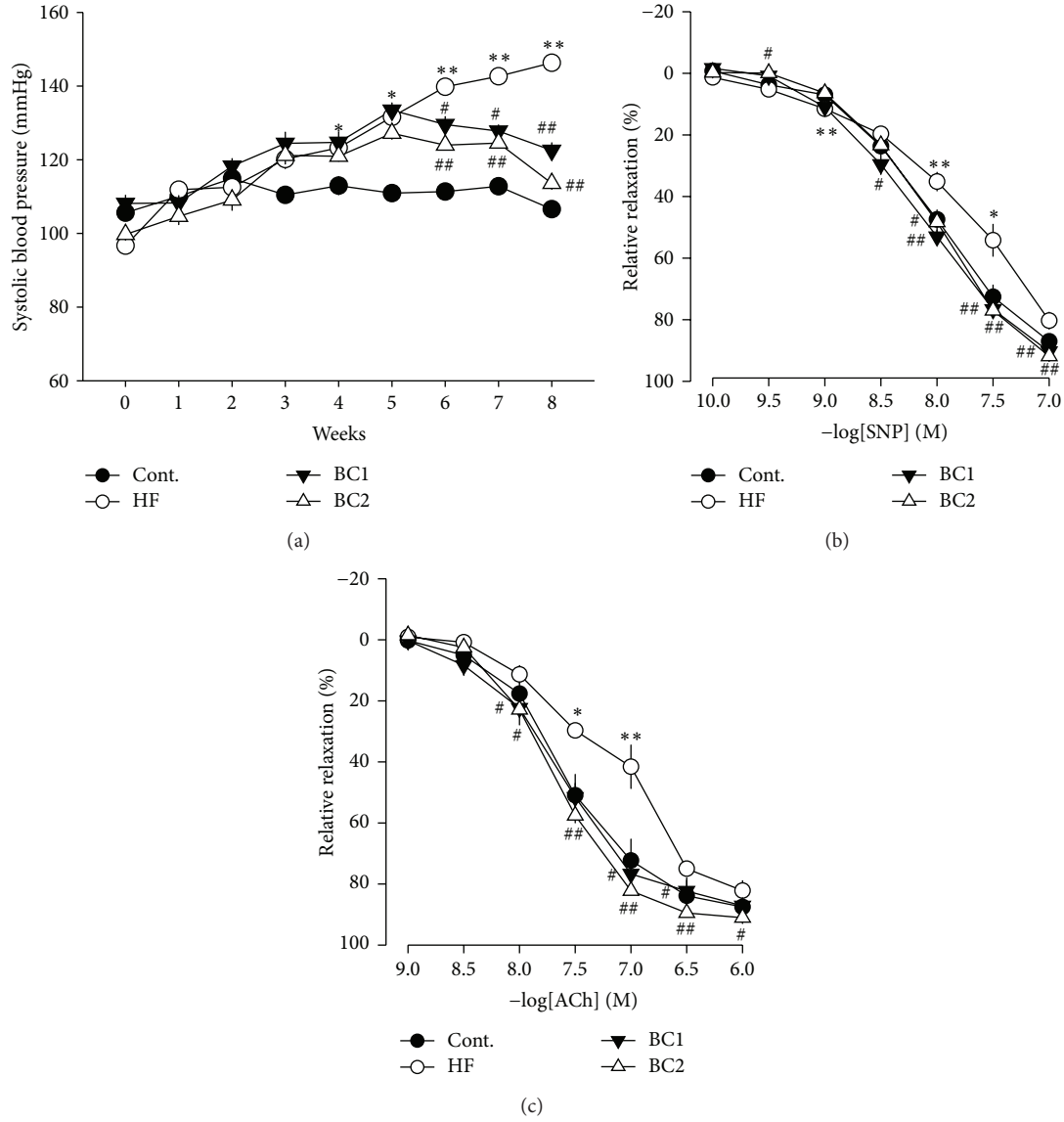

Figure 4: Effects of BC on systolic blood pressure (a), vascular tone in thoracic aorta effect of a BC on sodium nitroprusside-induced contraction in thoracic aorta (b), and effect of a BC on acetylcholine-induced relaxation in thoracic aorta (c). Values were expressed as mean ± S.E. ($n = 10$). $^{*}P < 0.05$ and $^{**}P < 0.01$ versus Cont.; $^{\#}P < 0.05$ and $^{\#\#}P < 0.01$ versus HF. SNP: sodium nitroprusside; ACh: acetylcholine; Cont.: control; HF: high fructose; BC1: blackcurrant 100 mg/kg/day; BC2: blackcurrant 300 mg/kg/day.

4. Discussion

The results of this study demonstrate that the HF diet induced metabolic syndrome with increased epididymal fat pad weight resulting from increased plasma levels of triglycerides and LDL. Treatment with BC lowered epididymal fat pad weight, triglyceride levels, and LDL levels, whereas it elevated levels of HDL, which enhances lipid metabolism. Thus, BC improves lipid metabolism by decreasing plasma levels of triglycerides and LDL. Although epididymal fat pad weight increased in response to the HF diet, the body weight of the control diet and HF diet groups was similar [15]. HF has been shown to increase hepatic lipase activity and epididymal fat hypertrophy [7, 16]. Experiments intended to measure increased body weight should be longer than the period of 8 weeks used in the present study [17]. BC reduces obesity in HF diet rats, because BC significantly decreased the HF diet-induced increase in body weight in this study. In addition, BC suppressed insulin and leptin levels [18, 19].

Because HF impairs glucose tolerance and induces obesity, dyslipidemia, and fatty liver, this study focused on the expression of AMPK in the liver and muscle [20]. HF decreased expression of IRS-1. IRS-1 deficiency causes insulin resistance. In addition, IRS-1 plays a very important role in secretion of insulin from pancreatic β-cells in the liver and muscle [21]. The BC group showed reduced IRS-1 expression in comparison with that of the HF group.

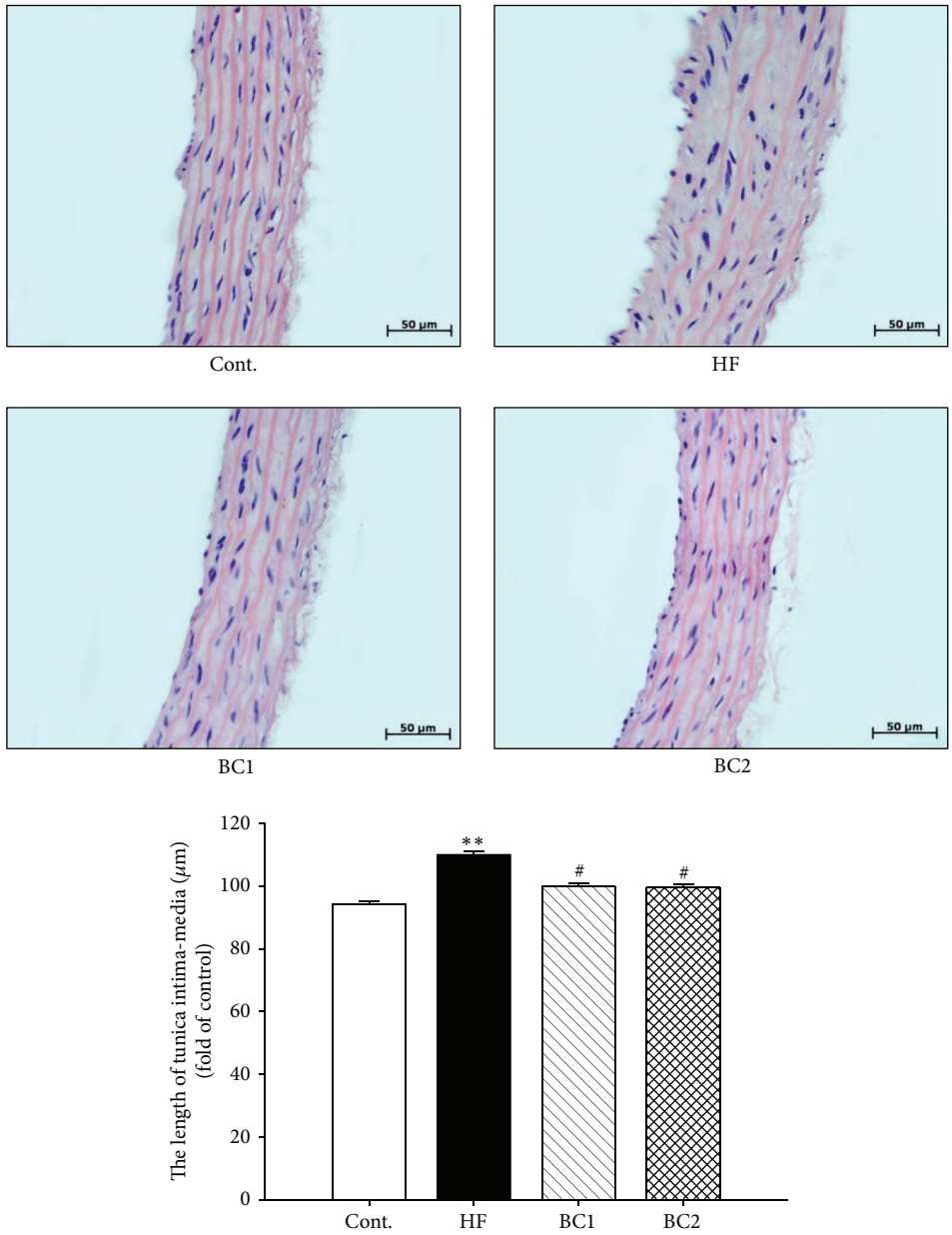

Figure 5: Effects of BC on aorta morphology. Representative microscopic photographs in aorta of SD rats with control diet and HF diet were stained with hematoxylin and eosin. Values were expressed as mean ± S.E. ($n = 5$). $^{**}P < 0.01$ versus Cont.; $^{\#}P < 0.05$ versus HF. Cont.: control; HF: high fructose; BC1: blackcurrant 100 mg/kg/day; BC2: blackcurrant 300 mg/kg/day.

In the present study, HF increased circulating levels of inflammatory marker CRP. Increased CRP is an independent risk factor for coronary artery disease [22]. Altered lipid levels induced by the HF diet were associated with aortic lesions. Histological analysis demonstrated that the endothelial layers were rougher in aortic sections from HF diet rats, which was associated with a trend towards increased development of atherosclerosis. Intima-media thickness of the thoracic aorta has been shown to correlate with prognosis and the degree of coronary artery disease [23]. BC treatment maintained smooth and soft intima endothelial layers and decreased intima-media thickness in the aortic sections of HF diet rats.

Endothelial dysfunction plays an important role in hypertension, vascular inflammation, other cardiovascular diseases, and metabolic syndrome [24, 25]. In this experimental model, expression of ET-1 and inducible adhesion molecules such as ICAM-1 and VCAM-1 in the arterial wall represented a key event in the development of atherosclerosis. BC ameliorated vascular inflammation by downregulation of ET-1, ICAM-1, VCAM-1, and E-selectin expression in the thoracic aorta. Several studies have shown that reduced blood pressure and endothelial function are related to increased eNOS reactivity, which results in increased production of NO, a strong vasodilator [26, 27]. In the present study, BC

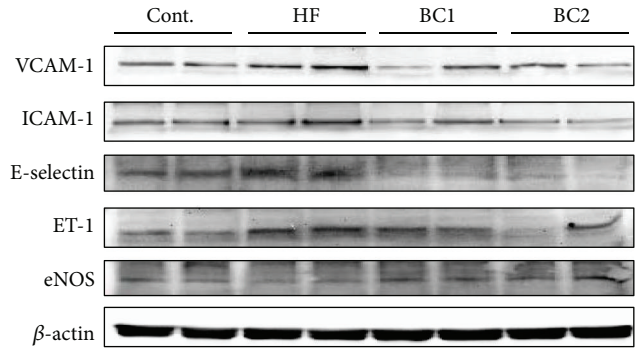

Figure 6: Effect of BC on the expression of adhesion molecules, ET-1, and eNOS in the aorta. Representative western blots of adhesion molecules, eNOS, and ET-1 protein levels are shown ($n = 5$). Cont.: control; HF: high fructose; BC1: blackcurrant 100 mg/kg/day; BC2: blackcurrant 300 mg/kg/day.

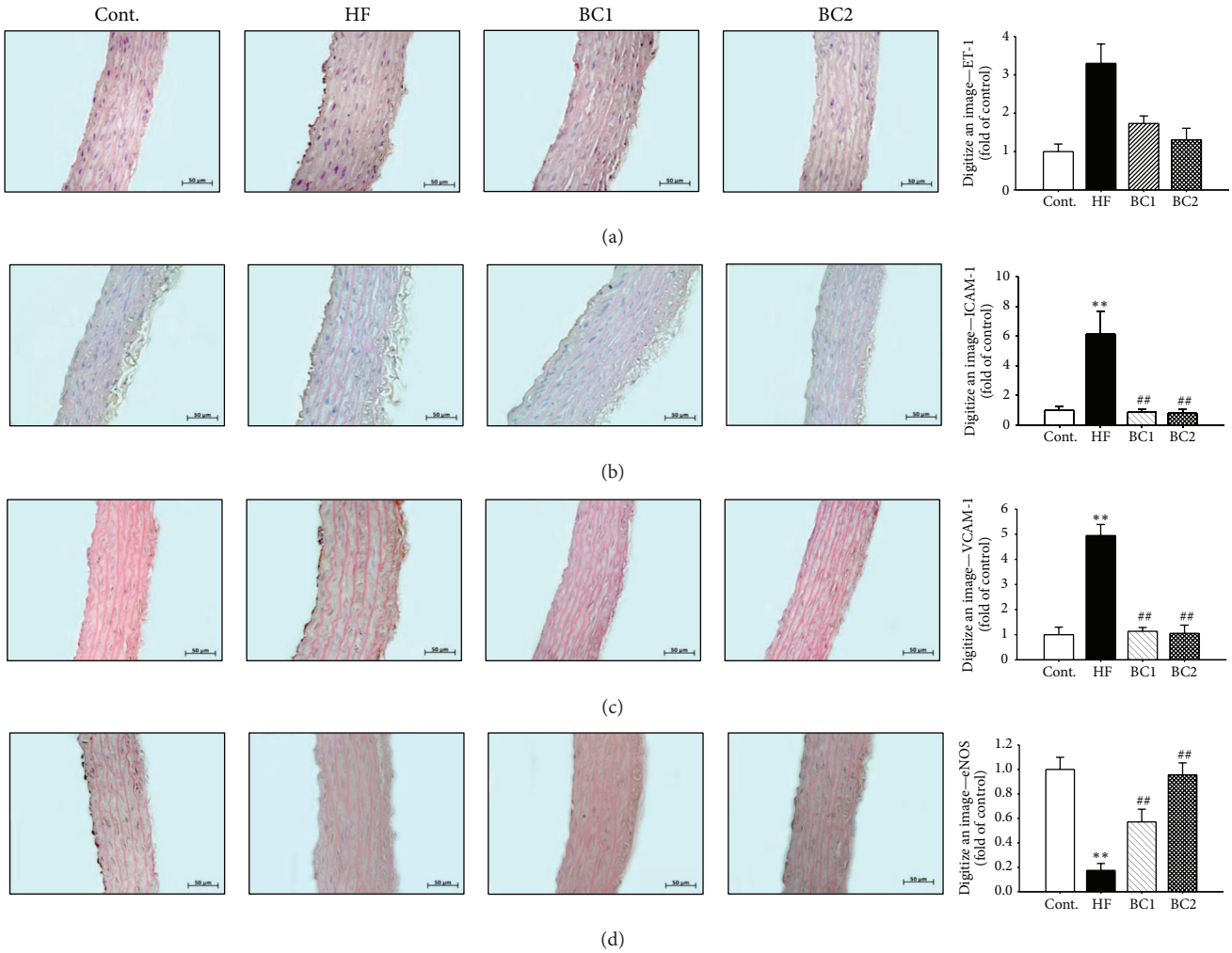

Figure 7: Effects of BC on ET-1 (a), ICAM-1 (b), VCAM-1 (c), and eNOS (d) immunoreactivity in aortic tissues. Values were expressed as mean ± S.E. ($n = 5$). $^{**}P < 0.01$ versus Cont.; $^{\#}P < 0.05$ versus HF. Cont.: control; HF: high fructose; BC1: blackcurrant 100 mg/kg/day; BC2: blackcurrant 300 mg/kg/day.

upregulated eNOS levels in the aorta and recovered HF diet-induced impairment of endothelium-dependent vasorelaxation. These results suggest that the hypotensive effect of BC is mediated by endothelium-dependent NO/cGMP signaling. The histological study revealed that BC suppressed vascular inflammation, compatible with the processes of atherosclerosis. In fact, endothelial dysfunction was initially identified as impaired vasodilation in response to specific stimuli such as ACh and bradykinin; therefore, improvement of endothelial function is predicted to regulate lipid homeostasis [28].

5. Conclusion

BC improved reduced plasma levels of biomarkers of dyslipidemia, including total cholesterol, triglycerides, and LDL. BC enhanced SNP- and ACh-induced relaxation and suppressed expression of adhesion molecules in the thoracic aorta, reduced systolic blood pressure, and reduced C-reactive protein levels. In addition, BC ameliorated insulin resistance by decreasing insulin release, improving glucose tolerance, and restoring insulin signaling by recovering IRS-1 expression in skeletal muscle tissue. In addition, BC improved obesity parameters such as leptin and adipocyte size. These results suggest that BC ameliorated dyslipidemia, hypertension, insulin resistance, and obesity in rats with HF-induced metabolic syndrome. Taken together, the results of this study demonstrate that BC may be used as a new therapeutic approach for metabolic syndrome.

Conflict of Interests

The authors declare that there is no conflict of interests regarding the publication of this paper.

Acknowledgment

This work was supported by the National Research Foundation of Korea (NRF) grant funded by the Korea government (MSIP) (2008-0062484) (NRF-2014R1A2A2A01005101).

References

[1] H. M. El-Bassossy and H. A. Shaltout, "Allopurinol alleviates hypertension and proteinuria in high fructose, high salt and high fat induced model of metabolic syndrome," *Translational Research*, vol. 165, no. 5, pp. 621–630, 2015.

[2] "Executive summary of the third report of the National Cholesterol Education Program (NCEP) expert panel on detection, evaluation, and treatment of high blood cholesterol in adults (Adult Treatment Panel III)," *The Journal of the American Medical Association*, vol. 285, pp. 2486–2497, 2001.

[3] S. M. Grundy, H. B. Brewer Jr., J. I. Cleeman, S. C. Smith Jr., and C. Lenfant, "Definition of metabolic syndrome: report of the National Heart, Lung, and Blood Institute/American Heart Association conference on scientific issues related to definition," *Circulation*, vol. 109, no. 3, pp. 433–438, 2004.

[4] R. Kumamoto, H. Uto, K. Oda et al., "Dietary fructose enhances the incidence of precancerous hepatocytes induced by administration of diethylnitrosamine in rat," *European Journal of Medical Research*, vol. 18, no. 1, article 54, 2013.

[5] P. J. Havel, "Dietary fructose: implications for dysregulation of energy homeostasis and lipid/carbohydrate metabolism," *Nutrition Reviews*, vol. 63, no. 5, pp. 133–137, 2005.

[6] H. Basciano, L. Federico, and K. Adeli, "Fructose, insulin resistance, and metabolic dyslipidemia," *Nutrition & Metabolism*, vol. 2, article 5, 2005.

[7] T. Ishimoto, M. A. Lanaspa, M. T. Le et al., "Opposing effects of fructokinase C and A isoforms on fructose-induced metabolic syndrome in mice," *Proceedings of the National Academy of Sciences of the United States of America*, vol. 109, no. 11, pp. 4320–4325, 2012.

[8] B. J. An, J. H. Kim, and O. J. Kwon, "Biological activity of Omija (*Schizandra chinensis* Baillon) extracts," *Journal of the Korean Society for Applied Biological Chemistry*, vol. 50, pp. 198–203, 2007.

[9] D. B. Shin, D. W. Lee, R. Yang, and J. A. Kim, "Antioxidative properties and flavonoids contents of matured Citrus peel extracts," *Food Science and Biotechnology*, vol. 15, pp. 357–362, 2006.

[10] H. Tilg and G. S. Hotamisligil, "Nonalcoholic fatty liver disease: cytokine-adipokine interplay and regulation of insulin resistance," *Gastroenterology*, vol. 131, no. 3, pp. 934–945, 2006.

[11] A. Bishayee, T. Mbimba, R. J. Thoppil et al., "Anthocyanin-rich black currant (*Ribes nigrum* L.) extract affords chemoprevention against diethylnitrosamine-induced hepatocellular carcinogenesis in rats," *The Journal of Nutritional Biochemistry*, vol. 22, no. 11, pp. 1035–1046, 2011.

[12] R. J. Thoppil, D. Bhatia, K. F. Barnes et al., "Black currant anthocyanins abrogate oxidative stress through Nrf2-mediated antioxidant mechanisms in a rat model of hepatocellular carcinoma," *Current Cancer Drug Targets*, vol. 12, no. 9, pp. 1244–1257, 2012.

[13] E. Ambrozewicz, A. Augustyniak, A. Gęgotek, K. Bielawska, and E. Skrzydlewska, "Black-currant protection against oxidative stress formation," *Journal of Toxicology and Environmental Health Part A: Current Issues*, vol. 76, no. 23, pp. 1293–1306, 2013.

[14] T. Keßler, B. Jansen, and A. Hesse, "Effect of blackcurrant-, cranberry- and plum juice consumption on risk factors associated with kidney stone formation," *European Journal of Clinical Nutrition*, vol. 56, no. 10, pp. 1020–1023, 2002.

[15] K. G. M. M. Alberti, R. H. Eckel, S. M. Grundy et al., "Harmonizing the metabolic syndrome: a joint interim statement of the international diabetes federation task force on epidemiology and prevention; National heart, lung, and blood institute; American heart association; World heart federation; International atherosclerosis society; And international association for the study of obesity," *Circulation*, vol. 120, no. 16, pp. 1640–1645, 2009.

[16] M. Giriş, S. Doğru-Abbasoğlu, A. Kumral, V. Olgaç, N. Koçak-Toker, and M. Uysal, "Effect of carnosine alone or combined with α-tocopherol on hepatic steatosis and oxidative stress in fructose-induced insulin-resistant rats," *Journal of Physiology and Biochemistry*, vol. 70, no. 2, pp. 385–395, 2014.

[17] S. M. Grundy, J. I. Cleeman, S. R. Daniels et al., "Diagnosis and management of the metabolic syndrome: an American Heart Association/National Heart, Lung, and Blood Institute scientific statement," *Current Opinion in Cardiology*, vol. 21, no. 1, pp. 1–6, 2006.

[18] G. M. Reaven, "Pathophysiology of insulin resistance in human disease," *Physiological Reviews*, vol. 75, no. 3, pp. 473–486, 1995.

[19] Y. Zhang, R. Proenca, M. Maffei, M. Barone, L. Leopold, and J. M. Friedman, "Positional cloning of the mouse obese gene and its human homologue," *Nature*, vol. 372, no. 6505, pp. 425–432, 1994.

[20] P. Misra and R. Chakrabarti, "The role of AMP kinase in diabetes," *Indian Journal of Medical Research*, vol. 125, no. 3, pp. 389–398, 2007.

[21] J. O. Clausen, T. Hansen, C. S. Bjorbaek et al., "Insulin resistance: interactions between obesity and a common variant of insulin receptor substrate-1," *The Lancet*, vol. 346, no. 8972, pp. 397–402, 1995.

[22] J. Danesh, J. Muir, Y.-K. Wong, M. Ward, J. R. Gallimore, and M. B. Pepys, "Risk factors for coronary heart disease and acute-phase proteins. A population-based study," *European Heart Journal*, vol. 20, no. 13, pp. 954–959, 1999.

[23] L. T. Tran, V. G. Yuen, and J. H. McNeill, "The fructose-fed rat: a review on the mechanisms of fructose-induced insulin resistance and hypertension," *Molecular and Cellular Biochemistry*, vol. 332, no. 1-2, pp. 145–159, 2009.

[24] K. Tziomalos, V. G. Athyros, A. Karagiannis, and D. P. Mikhailidis, "Endothelial dysfunction in metabolic syndrome: prevalence, pathogenesis and management," *Nutrition, Metabolism and Cardiovascular Diseases*, vol. 20, no. 2, pp. 140–146, 2010.

[25] X. Z. Chun, X. Xu, Y. Cui et al., "Increased endothelial nitric-oxide synthase expression reduces hypertension and hyperinsulinemia in fructose-treated rats," *Journal of Pharmacology and Experimental Therapeutics*, vol. 328, no. 2, pp. 610–620, 2009.

[26] M. F. Mahmoud, M. El-Nagar, and H. M. El-Bassossy, "Anti-inflammatory effect of atorvastatin on vascular reactivity and insulin resistance in fructose fed rats," *Archives of Pharmacal Research*, vol. 35, no. 1, pp. 155–162, 2012.

[27] D. H. Endemann and E. L. Schiffrin, "Nitric oxide, oxidative excess, and vascular complications of diabetes mellitus," *Current Hypertension Reports*, vol. 6, no. 2, pp. 85–89, 2004.

[28] W. J. Lee, K. L. In, S. K. Hyoun et al., "α-lipoic acid prevents endothelial dysfunction in obese rats via activation of AMP-activated protein kinase," *Arteriosclerosis, Thrombosis, and Vascular Biology*, vol. 25, no. 12, pp. 2488–2494, 2005.

Hindawi Publishing Corporation
Evidence-Based Complementary and Alternative Medicine
Volume 2015, Article ID 165457, 13 pages
http://dx.doi.org/10.1155/2015/165457

Research Article

Antioxidant and Anti-Inflammatory Activity Determination of One Hundred Kinds of Pure Chemical Compounds Using Offline and Online Screening HPLC Assay

Kwang Jin Lee, You Chang Oh, Won Kyung Cho, and Jin Yeul Ma

Korean Institute of Oriental Medicine (KIOM), KM Application Center, 70 Cheomdan-ro, Dong-gu, Daegu 701-300, Republic of Korea

Correspondence should be addressed to Jin Yeul Ma; jyma@kiom.re.kr

Received 21 April 2015; Revised 3 July 2015; Accepted 30 July 2015

Academic Editor: Abbas A. Mahdi

This study investigated the antioxidant activity of one hundred kinds of pure chemical compounds found within a number of natural substances and oriental medicinal herbs (OMH). Three different methods were used to evaluate the antioxidant activity of DPPH radical-scavenging activity, ABTS radical-scavenging activity, and online screening HPLC-ABTS assays. The results indicated that 17 compounds exhibited better inhibitory activity against ABTS radical than DPPH radical. The IC_{50} rate of a more practical substance is determined, and the ABTS assay IC_{50} values of gallic acid hydrate, (+)-catechin hydrate, caffeic acid, rutin hydrate, hyperoside, quercetin, and kaempferol compounds were 1.03 ± 0.25, 3.12 ± 0.51, 1.59 ± 0.06, 4.68 ± 1.24, 3.54 ± 0.39, 1.89 ± 0.33, and 3.70 ± 0.15 μg/mL, respectively. The ABTS assay is more sensitive to identifying the antioxidant activity since it has faster reaction kinetics and a heightened response to antioxidants. In addition, there was a very small margin of error between the results of the offline-ABTS assay and those of the online screening HPLC-ABTS assay. We also evaluated the effects of 17 compounds on the NO secretion in LPS-stimulated RAW 264.7 cells and also investigated the cytotoxicity of 17 compounds using a cell counting kit (CCK) in order to determine the optimal concentration that would provide an effective anti-inflammatory action with minimum toxicity. These results will be compiled into a database, and this method can be a powerful preselection tool for compounds intended to be studied for their potential bioactivity and antioxidant activity related to their radical-scavenging capacity.

1. Introduction

Natural substances and oriental medicinal herbs (OMH) have been traditionally administered to treat or prevent various diseases in Asia, including Korea, China, and Japan [1]. Generally OMH have very effective anticancer, anti-inflammatory, and antivirus properties [2], and researchers have reported that these natural substances also exhibit antioxidant activity. In addition, their long historical clinical practice and reliable therapeutic efficacy make them excellent sources to discover natural bioactive compounds [3]. OMH have received extensive attention for their use as drugs, functional foods, and cosmetic materials [1, 4]. An extraction solvent composed of water and ethanol is commonly used to extract the bioactive compounds from OMH with subsequent boiling and distillation to obtain useful components [5]. The chemical constituents of OMH have been shown to be composed of natural products, including triterpenes, steroids, alkaloids, flavonoids, and polysaccharides [3, 6]. During our investigation on the potential antioxidant activity of the commonly known phytochemical, one hundred kinds of pure compounds were identified. Reactive oxygen species (ROS), which originate from oxygen, are naturally produced by some enzymes as part of the metabolism within the cytoplasm [7, 8]. However, excess ROS have a fatal effect on oxygen toxicity and cellular dysfunction. In addition, excess ROS have also been linked to maladies such as cancer, stroke, Parkinson's disease, heart disease, arteriosclerosis, infection, ageing, and autoimmune disease [8, 9]. Many studies have been carried out on the antioxidant activity that eliminates ROS to obtain more conclusive information [10, 11], and OMH have been reported to contain these kinds of antioxidants: ABTS, DPPH, and lipid peroxidation inhibition. The corresponding target compounds were used to identify the

antioxidant activity, especially using DPPH or ABTS radical technique [12]. Recently, sensitive online HPLC methods (online HPLC-DPPH and online HPLC-ABTS assays) have been developed to analyse free radical-scavenging activity [5, 13]. An online system has been introduced to rapidly determine the antioxidant activity of each component in the given compounds, and online screening HPLC postcolumn assay involving DPPH or ABTS radical techniques has been developed to provide a new analysis screening technology method with which the bioactive compounds can be spectrophotometrically monitored due to the decrease in absorbance at 515 or 734 nm [14]. This new method was successfully applied to screen and identify the natural bioactivity of complex mixtures, especially for OMH [15]. In this study, we conduct DPPH and ABTS assays to screen for the antioxidant activity of one hundred kinds of pure chemical compounds, so the IC_{50} rate of a more practical substance is determined. We also evaluated the cytotoxicity of 17 compounds, including (1) (+)-catechin hydrate, (2) calycosin, (3) caffeic acid, (4) curcumin, (5) eugenol, (6) ferulic acid, (7) gallic acid hydrate, (8) hyperoside, (9) kaempferol, (10) magnolol, (11) quercetin, (12) quercetin 3-beta-D-glucoside, (13) quercitrin hydrate, (14) rutin hydrate, (15) sinapic acid, (16) vanillylacetone, and (17) L-(+)-ascorbic acid, by using a CCK assay to determine the optimal concentration that would be effective for anti-inflammatory activity with a minimum toxicity [9, 16]. In addition, the results of an online HPLC-ABTS assay of some of the compounds were compared and analysed to find a more practical approach toward the use of online screening HPLC-ABTS assays to quickly pinpoint peaks in chromatograms that correspond to bioactive compounds.

2. Experimental

2.1. Reagents and Materials. One hundred kinds of pure chemical compounds were purchased from KFDA (Korea), Daejung (Korea), Sigma (USA), Chem Faces (China), TCI (Japan), ChromaDex (USA), Fluka (USA), Wako (Japan), GlycoSyn (New Zealand, USA), Santa Cruz Biotech (USA), China Lang Chem Inc. (China), and RD Chemical (USA). The following reagents were used for radical-scavenging assays: ABTS (2,2′-azino-bis(3-ethylbenzothiazoline-6-sulfonic acid)), DPPH (2,2-diphenyl-1-picrylhydrazyl), potassium persulfate, and trifluoroacetic acid (TFA) were purchased from Sigma (USA). The HPLC-grade methanol and acetonitrile were purchased from J. T. Baker (USA). The triple distilled water was filtered with a 0.2 μm membrane filter (Advantec, Tokyo, Japan) before analysis. Materials for cell culture were obtained from Lonza (Basel, Switzerland). LPS, bovine serum albumin (BSA), and 3-(4,5-dimethylthiazol-2-yl)-2,5-diphenyltetrazolium bromide (MTT) were purchased from Sigma (St. Louis, MO, USA). Antibodies for ELISA were obtained from eBioscience (San Diego, CA, USA). The chemical structures of potentially selected compounds are shown in Figure 1.

2.2. Standard Sample Preparation. The high purity standard sample (higher than >95%) was prepared by dissolving 2 mg of each standard chemical in 20 mL of methanol and adjusting the concentration to 100 μg/mL.

2.3. Offline DPPH Assay for Antioxidant Activity Evaluation. The DPPH radical cation method [17] was modified to evaluate the free radical-scavenging effect of one hundred pure chemical compounds. The DPPH reagent was DPPH (8 mg) dissolved in MeOH (100 mL) for a solution concentration of 80 μL/mL. To determine the scavenging activity, 100 μL DPPH reagent was mixed with 100 μL of sample in a 96-well microplate and was incubated at room temperature for 30 min. After incubation, the absorbance was measured 514 nm using an ELISA reader (TECAN, Gröding, Austria), and 100% methanol was used as a control. The DPPH scavenging effect was measured using the following formula:

$$\text{Radical scavenging (\%)} = \left[\frac{(A)_{\text{control}} - (A)_{\text{sample}}}{(A)_{\text{control}}}\right] \times 100. \quad (1)$$

The IC_{50} DPPH values (the concentration of sample required for inhibition of 50% of DPPH radicals) were obtained through extrapolation from regression analysis. The antioxidant was evaluated based on this IC_{50} value.

2.4. Offline-ABTS Assay for Antioxidant Activity Evaluation. The ABTS radical cation method [17] was modified to evaluate the free radical-scavenging effect of one hundred pure chemical compounds. The ABTS reagent was prepared by mixing 5 mL of 7 mM ABTS with 88 μL of 140 mM potassium persulfate. The mixture was then kept in the dark at room temperature for 16 h to allow free radical generation and was then diluted with water (1 : 44, v/v). To determine the scavenging activity, 100 μL ABTS reagent was mixed with 100 μL of sample in a 96-well microplate and was incubated at room temperature for 6 min. After incubation, the absorbance was measured 734 nm using an ELISA reader (TECAN, Gröding, Austria), and 100% methanol was used as a control. The ABTS scavenging effect was measured using the following formula:

$$\text{Radical scavenging (\%)} = \left[\frac{(A)_{\text{control}} - (A)_{\text{sample}}}{(A)_{\text{control}}}\right] \times 100. \quad (2)$$

The IC_{50} ABTS values (the concentration of sample required for inhibition of 50% of ABTS radicals) were obtained through extrapolation from regression analysis. The antioxidant activity was evaluated based on this IC_{50} value.

2.5. Online Screening HPLC-ABTS Analysis. The online radical-scavenging activity of one hundred kinds of pure standard compounds was determined using the ABTS assay modifying the methods used by Stewart et al. [18]. A 2 mM ABTS stock solution containing 3.5 mM potassium persulfate was prepared and was kept in the dark at room temperature for 16 h to allow the completion of radical generation and

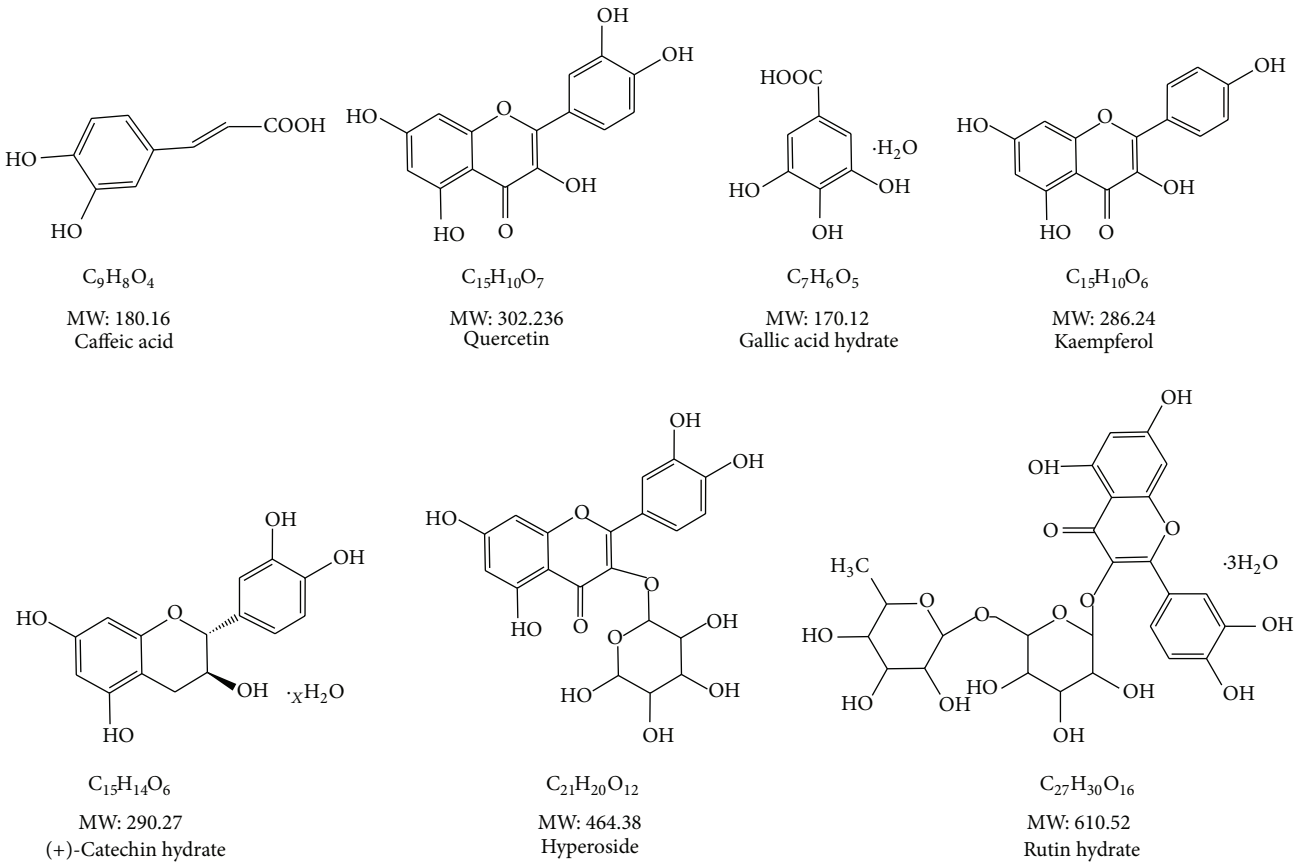

Figure 1: Chemical structure of the superior antioxidant activity compounds.

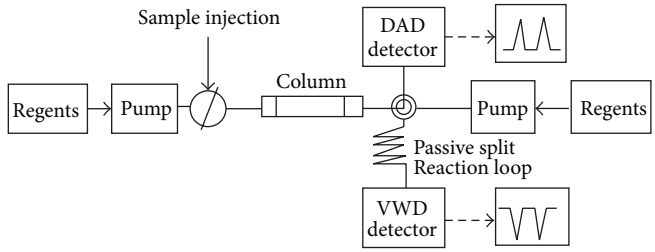

Figure 2: Schematic of online screening HPLC-ABTS system.

was then diluted with water (1 : 29, v/v). Each pure sample was injected into a Dionex Ultimate 3000 HPLC system (Thromo Scientific). The chromatographic columns used in this experiment are commercially available; this is obtained from RS-tech (0.46 × 25 cm, 5 μm, C_{18}, Daejeon, Korea). The injection volume was 10 μL, and the flow rate of the mobile phase was 1.0 mL/min. The wavelength of the UV detector was fixed at 203, 254, and 320 nm. The composition of the mobile phases was as follows: A, water/trifluoroacetic acid = 99.9/0.1, vol%, and B, acetonitrile 100%. The run time was 70 min and the solvent program was the linear gradient method (90 : 10–60 : 40, A : B vol%). Figure 2 is a schematic showing the online coupling of HPLC to a DAD (diode array detector) and the continuous flow ABTS assay. Online HPLC then arrived at a "T" piece, where ABTS was added. The ABTS flow rate was 0.5 mL/min, delivered by a Dionex Ultimate 3000 Pump. After mixing through a 1 mL loop which was maintained at 40°C, the absorbance was measured by a VIS detector at 734 nm. Data were analyzed using Chromeleon 7 software.

2.6. Cell Culture and Drug Treatment. RAW 264.7 cells were obtained from the American Type Culture Collection (ATCC, Manassas, VA, USA) and grown in RPMI 1640 medium containing 10% FBS and 100 U/mL of antibiotics sulfate. The cells were incubated in humidified 5% CO_2 atmosphere at 37°C. To stimulate the cells, the medium was changed with fresh RPMI 1640 medium and LPS (200 ng/mL) [18, 19] was added in the presence or absence of 17 compounds (1, 5, and 10 μg/mL) for 24 h.

2.7. Cell Viability Assay. Cytotoxicity was analyzed using CCK (Dojindo, Japan). 17 compounds were added to the cells and incubated for 24 hours at 37°C with 5% CO_2. 10 μL CCK solutions were added to each well and the cells were incubated for another 1 h. Then the optical density was read at 450 nm using an ELISA reader (Infinite M200, Tecan, Männedorf, Switzerland).

2.8. Measurement of NO Production. NO production was analyzed by measuring the nitrite in the supernatants of cultured macrophage cells. The cells were pretreated with 17 compounds and stimulated with LPS for 24 hours. The supernatant was mixed with the same volume of Griess reagent (1% sulfanilamide, 0.1% naphthylethylenediamine dihydrochloride, and 2.5% phosphoric acid) and incubated at room temperature (RT) for 5 min [19]. The absorbance at 570 nm was read.

2.9. Inflammatory Cytokine Determination. Cells were seeded at a density of 5×10^5 cells/mL in 24-well culture plates and pretreated with three concentrations of 17 compounds for 1 hour before LPS stimulation. ELISA plates (Nunc, Roskilde, Denmark) were coated overnight at 4°C with capture antibody diluted in coating buffer (0.1 M carbonate, pH 9.5) and then washed five times with phosphate-buffered saline (PBS) containing 0.05% Tween 20. The nonspecific protein-binding sites were blocked with assay diluent buffer (PBS containing 10% FBS, pH 7.0) for more than 1 hour. Promptly, samples and standards were added to the wells. After overnight of incubation at 4°C, the working detector solution (biotinylated detection antibody and streptavidin-HRP reagent) was added and incubated for 1 hour. Subsequently, substrate solution (tetramethylbenzidine) was added to the wells and incubated for 30 min in darkness before the reaction was stopped with stop solution (2 N H_3PO_4). The optical density was read at 450 nm [19].

2.10. Statistical Analysis. The results are expressed as mean ± SD values for the number ($n = 3$ times) of experiments. Statistical significance was compared for each treated group with the control and determined by Student's t-tests. Each experiment was repeated at least three times to yield comparable results. Values with $p < 0.01$ and $p < 0.001$ were considered significant.

3. Result and Discussion

Several researches have revealed that a variety of natural and chemical compounds from natural substance crops, fruits, vegetables, and oriental medicinal herbs (OMH) have shown high antioxidant activity after the extraction and purification processes [3]. In addition, various methods have been used to determine the antioxidant activity of natural substance crops, foods, and plant products [1, 4]. The present study used three different methods to evaluate the antioxidant activity consisting of DPPH radical-scavenging activity, ABTS radical-scavenging activity, and online screening HPLC-ABTS assays. Therefore, this work documented for the first time a comparison of the antioxidant activities of one hundred kinds of pure chemical compounds.

3.1. Offline DPPH and ABTS Assay. Antioxidant activity reportedly has an effect on various different bioactivities (whitening, anti-inflammation, and high blood pressure). The antioxidant activity of natural substances and OMH has been widely studied, and, thus, this study identifies the antioxidant activity of standard substances that have originated from various OMH in terms of their DPPH radical-scavenging activity and ABTS radical-scavenging activity. The DPPH and ABTS radical-scavenging assays offer a redox-functioned proton ion for unstable free radicals and play a critical role in stabilizing detrimental free radicals in the human body. This is generally achieved by taking advantage of the fact that unstable violet DPPH and ABTS free radicals transform to stable yellow DPPH free radicals by accepting a hydrogen ion from antioxidants. In terms of the antioxidant activity, the ability to eliminate hydroxyl radicals or superoxide radicals through a physiologic action or through oxidation is evaluated, and a high index indicates a strong antioxidant activity. Table 1 provides the results of the DPPH and ABTS radical scavenging in 100 ppm for one hundred kinds of pure standard compounds used in this study. 17 compounds among the one hundred kinds of pure standard compounds ((1) (+)-catechin hydrate, (2) calycosin, (3) caffeic acid, (4) curcumin, (5) eugenol, (6) ferulic acid, (7) gallic acid hydrate, (8) hyperoside, (9) kaempferol, (10) magnolol, (11) quercetin, (12) quercetin 3-beta-D-glucoside, (13) quercitrin, (14) rutin hydrate, (15) sinapic acid, (16) vanillylacetone, and (17) L-(+)-ascorbic acid) have an antioxidant activity of over 90%. Table 2 shows the IC_{50} rate of compounds with a strong antioxidant activity. The ABTS radical-scavenging measurement method, which is commonly used to evaluate the antioxidant activity, takes advantage of the fact that ABTS free radicals become stable by accepting a hydrogen ion from the antioxidant, losing their blue colors. Moreover, in the ABTS assay as well as in the DPPH assay, when antioxidant activity occurs, the ability to eliminate hydroxyl radicals or superoxide radicals through physiologic action or oxidation is evaluated with a high index indicating a strong antioxidant activity. Each of the DPPH and ABTS are compounds that have a proton free radical, with a characteristic absorption that decreases significantly upon exposure to proton radical scavengers. DPPH and ABTS radical-scavenging through antioxidant activity are well known to be attributable to their hydrogen-donating ability (Tables 1 and 2). The concentration of these compounds required to inhibit 50% of the radical-scavenging effect (IC_{50}) has been determined by testing a series of concentrations. In particular, the sample with (+)-catechin hydrate, caffeic acid, eugenol, gallic acid hydrate, hyperoside, quercetin, vanillylacetone, and L-(+)-ascorbic acid compounds showed the strongest activity. In addition, the 17 compounds showed better inhibitory activity against ABTS radical than the DPPH radicals. That is, the ABTS assay is more sensitive in identifying antioxidant activity because of the faster reaction kinetics, and its response to antioxidants is higher. Consequently, this study shows that the ABTS assay IC_{50} values of gallic acid hydrate, (+)-catechin

Table 1: Free radical-scavenging capacities of antioxidant activity available measured with DPPH and ABTS assay on microwell plate.

Number	Compounds names	Compounds purchased	Concentration μM (μmol/L)	Radical scavenging (%)	
				DPPH	ABTS
1	Albiflorin	Wako	208.13	−0.15 ± 0.39	0.14 ± 5.27
2	Alisol A	Wako	203.79	−0.47 ± 0.71	12.92 ± 0.86
3	Alisol B	Wako	211.55	−1.66 ± 0.23	12.78 ± 1.35
4	Amygdalin	KFDA	218.61	−0.85 ± 0.67	12.31 ± 0.03
5	Anthraquinone	Wako	480.28	0.12 ± 0.70	0.86 ± 5.12
6	Atractylenolide iii	Chem Faces	402.71	−2.07 ± 0.53	1.34 ± 8.29
7	Aucubin	Wako	288.74	−1.64 ± 0.79	1.22 ± 9.74
8	Baicalein	KFDA	370.04	95.84 ± 0.15	99.37 ± 0.12
9	Benzoic acid	Sigma	818.87	1.88 ± 0.42	3.80 ± 0.26
10	Berberine	Chem Faces	297.30	0.64 ± 0.43	84.68 ± 2.55
11	Berberine HCl	KFDA	268.95	−0.30 ± 0.30	8.74 ± 8.38
12	Caffeic acid	Sigma	555.06	95.91 ± 0.16	99.66 ± 0.24
13	Calycosin	Chem Faces	351.79	64.51 ± 0.59	99.19 ± 0.05
14	Catalpol	Wako	275.99	−2.55 ± 0.47	1.12 ± 9.62
15	Chrysin	Sigma	393.33	0.45 ± 0.53	99.13 ± 0.06
16	Cimifugin	Chem Faces	326.46	−0.89 ± 0.21	14.39 ± 1.81
17	Cinnamyl alcohol	Sigma	745.27	−0.03 ± 0.37	15.18 ± 0.75
18	cis-Inositol	Sigma	555.06	0.15 ± 0.26	0.54 ± 1.22
19	Costunolide	Sigma	430.44	2.86 ± 0.17	20.13 ± 8.74
20	Crocin	Sigma	102.36	24.43 ± 1.28	47.73 ± 0.67
21	Curcumin	Sigma	271.46	97.50 ± 0.63	99.97 ± 0.16
22	(+)-Catechin hydrate	TCI	344.51	94.50 ± 0.16	99.15 ± 0.06
23	1,8-Dihydroxy-3-methylanthraquinone	Sigma	393.33	−0.94 ± 0.54	2.09 ± 2.60
24	D-(−)-Lactic acid	Sigma	1110.12	2.51 ± 2.40	28.29 ± 0.74
25	D-(+)-Chiro-inositol	Sigma	555.06	0.49 ± 0.33	0.21 ± 0.45
26	Daidzein	Wako	393.33	0.52 ± 0.61	99.49 ± 0.49
27	Decursin	KFDA	304.54	−3.01 ± 0.91	0.97 ± 2.75
28	Decursinol	Chem Faces	406.07	−1.59 ± 1.03	15.12 ± 1.81
29	Dioscin	Sigma	115.07	−2.93 ± 1.30	0.43 ± 2.75
30	Diosgenin	Sigma	241.18	−1.38 ± 0.70	1.96 ± 9.24
31	D-Pinitol	Sigma	514.99	−2.27 ± 0.33	12.72 ± 1.85
32	6,7-Dimethylesculetin	RD Chemical	484.99	−2.74 ± 0.54	1.31 ± 0.21
33	(−)-Epicatechin	Sigma	344.51	94.51 ± 0.41	99.61 ± 0.16
34	(−)-Epigallocatechin gallate	Sigma	218.16	95.69 ± 0.14	99.51 ± 0.24
35	Eleutheroside B	Wako	268.55	−2.04 ± 1.02	1.97 ± 2.85
36	Emodin	TCI	370.04	2.20 ± 1.16	91.27 ± 1.39
37	Ephedrine-HCl	KFDA	495.81	−2.11 ± 1.52	0.00 ± 0.12
38	Ergosterol	Chem Faces	252.11	−1.65 ± 1.34	0.55 ± 9.46
39	Eugenol	Sigma	609.01	93.72 ± 0.12	99.91 ± 0.55
40	Evodiamine	KFDA	329.64	4.21 ± 1.55	40.76 ± 2.09
41	Ferulic acid	Sigma	514.99	95.12 ± 0.24	98.96 ± 0.27
42	Gallic acid hydrate	TCI	587.82	95.56 ± 0.03	101.30 ± 2.12
43	Geniposide	Chem Faces	257.49	−1.45 ± 0.90	1.22 ± 9.49
44	Genistein	TCI	370.04	−1.52 ± 0.30	98.50 ± 0.48
45	Genistin	Wako	231.28	2.23 ± 0.64	100.65 ± 0.03
46	Geraniol	Sigma	112.49	−2.43 ± 1.67	14.94 ± 0.95

Table 1: Continued.

Number	Compounds names	Compounds purchased	Concentration μM (μmol/L)	Radical scavenging (%)	
				DPPH	ABTS
47	Glabridin	Wako	308.29	42.20 ± 0.88	100.58 ± 0.04
48	Glimepiride	Sigma	203.82	−1.33 ± 0.63	7.84 ± 2.30
49	Glycyrrhetic acid	TCI	212.46	0.66 ± 0.65	10.23 ± 0.62
50	Glycyrrhizin	TCI	121.52	1.59 ± 1.96	12.36 ± 1.15
51	Gomisin A	KFDA	240.12	1.80 ± 0.28	1.74 ± 0.22
52	Gomisin N	KFDA	249.71	0.45 ± 0.51	3.80 ± 0.21
53	Hesperidin	KFDA	202.23	31.84 ± 0.37	100.21 ± 0.01
54	Hyperoside	Chem Faces	215.34	93.16 ± 0.25	99.62 ± 0.20
55	2′-Hydroxy-4′-methoxy-acetophenone	Sigma	601.76	−2.81 ± 0.28	99.73 ± 1.04
56	Icariin	TCI	147.78	3.82 ± 1.08	14.60 ± 0.12
57	Imperatorin	Chem Faces	369.99	−0.71 ± 2.31	0.74 ± 9.51
58	Isoimperatorin	Santa Cruz Biotech	369.99	0.27 ± 0.22	3.06 ± 2.17
59	Jujuboside A	Chem Faces	82.83	−1.63 ± 0.35	0.26 ± 9.74
60	Kaempferol	Chem Faces	349.36	95.02 ± 0.22	99.84 ± 0.41
61	Liquiritigenin	Chem Faces	390.24	12.26 ± 0.86	0.12 ± 0.68
62	Loganin	KFDA	256.16	2.62 ± 1.28	5.80 ± 0.62
63	Magnolol	KFDA	375.47	54.50 ± 0.12	77.74 ± 1.06
64	Mevinolin	Sigma	247.19	−0.26 ± 0.07	2.78 ± 0.69
65	Morroniside	China Lang Chem Inc.	246.08	7.11 ± 0.58	19.62 ± 1.83
66	Naringin	Sigma	172.26	3.05 ± 0.37	100.36 ± 0.05
67	Nodakenin	Chem Faces	244.86	0.68 ± 0.45	15.70 ± 1.92
68	Oleanolic acid	Wako	218.96	−0.37 ± 0.54	0.00 ± 0.12
69	Ononin	Sigma	232.34	2.23 ± 1.58	22.91 ± 1.89
70	Oxymatrine	Chem Faces	378.26	−1.63 ± 0.17	0.72 ± 8.85
71	Oxypeucedanin	Chem Faces	349.31	−0.11 ± 0.27	19.10 ± 2.38
72	Paeoniflorin	TCI	208.13	4.29 ± 1.43	22.03 ± 0.91
73	Paeonol	Sigma	601.79	0.99 ± 2.21	19.79 ± 2.35
74	Palmatine chloride hydrate	Sigma	257.82	2.57 ± 2.42	84.15 ± 2.43
75	Palmatine	Chem Faces	292.05	0.12 ± 0.23	68.05 ± 3.63
76	p-Coumaric acid	Sigma	609.16	8.89 ± 0.04	38.52 ± 0.84
77	Poncirin	KFDA	168.19	−1.44 ± 1.27	84.20 ± 3.66
78	Puerarin	Wako	240.17	9.89 ± 0.16	100.62 ± 0.06
79	Quercetin	Sigma	330.86	96.02 ± 0.08	100.18 ± 0.06
80	Quercetin 3-β-D-glucoside	Sigma	215.34	94.43 ± 0.02	99.94 ± 0.06
81	Quercitrin hydrate	Sigma	223.03	93.32 ± 0.04	99.12 ± 0.14
82	Rutaecarpine	KFDA	348.04	−1.41 ± 0.60	97.23 ± 0.63
83	Rutin hydrate	Sigma	163.79	93.57 ± 0.13	100.10 ± 0.02
84	Saikosaponin a	KFDA	128.04	−0.67 ± 0.79	16.17 ± 1.62
85	Salicylaldehyde	Sigma	818.87	2.07 ± 0.04	100.36 ± 0.05
86	Schisandrin	KFDA	231.21	−2.39 ± 0.89	10.29 ± 2.43
87	Sennoside A	KFDA	115.91	−3.09 ± 0.64	87.86 ± 3.21
88	Sequoyitol	GlycoSyn	514.99	−3.20 ± 1.37	10.28 ± 2.07
89	Sinapic acid	Fluka	445.99	94.84 ± 0.33	99.99 ± 0.23
90	Spinosin	Chem Faces	164.33	−0.96 ± 2.26	80.16 ± 2.20
91	Tetrandrine	Fluka	160.58	60.83 ± 2.11	100.28 ± 0.06

Table 1: Continued.

Number	Compounds names	Compounds purchased	Concentration μM (μmol/L)	Radical scavenging (%)	
				DPPH	ABTS
92	trans-Cinnamaldehyde	Sigma	756.66	2.83 ± 0.69	19.00 ± 1.37
93	trans-Cinnamic acid	Sigma	674.95	0.19 ± 0.15	0.02 ± 9.45
94	Uric acid	Sigma	594.85	40.37 ± 1.97	98.33 ± 0.31
95	Vanillylacetone	Sigma	514.85	93.78 ± 0.06	99.92 ± 0.24
96	Wogonin	KFDA	351.79	1.02 ± 0.51	100.57 ± 0.13
97	Wogonoside	Chem Faces	217.21	10.84 ± 0.10	98.62 ± 0.32
98	Ziyuglycoside I	Chem Faces	130.38	−1.71 ± 1.00	0.01 ± 9.85
99	Z-Ligustilide	Chem Faces	531.29	1.92 ± 0.76	68.69 ± 2.14
100	Ascorbic acid (Vitamin C)	Daejung	567.79	99.56 ± 0.89	99.89 ± 0.04

Table 2: Antioxidant activity of 17 compounds with offline DPPH and ABTS IC_{50} assay.

Number	Name	Radical- scavenging IC_{50} (μg/mL)	
		DPPH	ABTS
1	(+)-Catechin hydrate	5.25 ± 0.31	3.12 ± 0.51
2	Calycosin	61.88 ± 1.19	33.21 ± 3.59
3	Caffeic acid	4.50 ± 0.30	1.59 ± 0.06
4	Curcumin	8.89 ± 0.24	4.99 ± 0.45
5	Eugenol	5.22 ± 0.25	3.22 ± 0.45
6	Ferulic acid	9.49 ± 0.21	1.99 ± 0.12
7	Gallic acid hydrate	1.56 ± 0.38	1.03 ± 0.25
8	Hyperoside	5.44 ± 0.36	3.54 ± 0.39
9	Kaempferol	7.78 ± 0.30	3.70 ± 0.15
10	Magnolol	85.57 ± 1.40	8.37 ± 0.56
11	Quercetin	2.66 ± 0.24	1.89 ± 0.33
12	Quercetin 3-β-D-glucoside	7.05 ± 0.59	3.59 ± 0.89
13	Quercitrin hydrate	7.55 ± 0.77	4.23 ± 0.84
14	Rutin hydrate	9.72 ± 1.06	4.68 ± 1.24
15	Sinapic acid	8.26 ± 0.41	5.36 ± 0.85
16	Vanillylacetone	5.69 ± 0.00	3.45 ± 0.05
17	Ascorbic acid (Vitamin C)	3.65 ± 0.23	2.65 ± 0.46

hydrate, caffeic acid, rutin hydrate, hyperoside, quercetin, and kaempferol compounds were 1.03 ± 0.25, 3.12 ± 0.51, 1.59 ± 0.06, 4.68 ± 1.24, 3.54 ± 0.39, 1.89 ± 0.33, and 3.70 ± 0.15 μg/mL, respectively.

3.2. Online HPLC-ABTS Assay Analysis. The most popular approach utilises a relatively stable, coloured radical solution of DPPH or ABTS, which is added postcolumn to the HPLC flow. Drug, food, functional material, and plant and OMH samples are evaluated for their antioxidant capacities according to a variety of antioxidant activity test methods, such as those for ABTS [2,2′-azino-bis(3-ethylbenzothiazoline-6-sulfonic acid)] radical scavenging [20]. The HPLC analyses react postcolumn with the ABTS, and the reduction is detected as a negative peak by a VIS absorbance detector at 734 nm. The ABTS radical is much more water soluble than DPPH [13], so ABTS better shows the details of an online HPLC-ABTS assay system that analysed the 17 given compounds (Figures 3(a) and 3(b)). Combined UV (positive signals) and ABTS quenching (negative signals) chromatograms of the 17 compounds ((1) gallic acid hydrate R_t: 5.46 min, (2) (+)-catechin hydrate R_t: 9.26 min, (3) caffeic acid R_t: 11.12 min, (4) ferulic acid R_t: 15.87 min, (5) rutin hydrate R_t: 15.99 min, (6) sinapic acid R_t: 16.15 min, (7) hyperoside R_t: 16.49 min, (8) quercetin 3-beta-D-glucoside R_t: 16.82 min, (9) vanillylacetone R_t: 17.92 min, (10) quercitrin R_t: 18.90 min, (11) calycosin R_t: 23.81 min, (12) quercetin R_t: 24.31 min, (13) kaempferol R_t: 28.37 min, (14) eugenol R_t: 28.98 min, (15) curcumin R_t: 40.20 min, (16) magnolol R_t: 43.98 min, and (17) L-(+)-ascorbic acid) (not detected; L-(+)-ascorbic acid) (each concentration 100 ppm) are presented in Figure 3(a). Of these, seven compounds that showed excellent activity were further analysed. Several eluted substances were detected in the 7 compounds, including (1) gallic acid hydrate (210 nm), (2) (+)-catechin hydrate (210 nm), (3) caffeic acid (320 nm), (4) rutin hydrate (210 nm), (5) hyperoside (210 nm), (6) quercetin (210 nm), and (7) kaempferol (254 nm), which are observed as a positive signal on the UV detector (210, 254, and 320 nm). The retention times (R_t) of (1) gallic acid hydrate (R_t 5.62 min), (2) (+)-catechin hydrate (R_t 9.46 min), (3) caffeic acid (R_t 11.12 min), (4) rutin hydrate (R_t 15.86 min), (5) hyperoside (R_t 16.26 min), (6) quercetin (R_t 23.58 min), and (7) kaempferol (R_t 28.30 min) are reported in Figure 3(b). The other compounds exhibited a hydrogen-donating capacity (negative peak) towards the ABTS radical at the applied concentration. These results therefore reveal that this method can be applied for quick screening of antioxidant activity or, more precisely, of radical-scavenging activity (Table 3). This work confirms the feasibility of assessing the bioactivity of specific phytochemicals by using an online screening HPLC-ABTS assay. This method was successfully applied to screen and identify the antioxidant activity of natural substances and OMH complex mixtures [5, 15]. The results show the shape of the chromatogram by the competitive adsorption and desorption. In addition, the screening methods for the rapid activity can provide useful information in basic research on natural products chemistry and isolation analysis. It is considered that the data will only be valuable in engineering

Table 3: Simultaneous identification of antioxidant activity with online screening HPLC-ABTS assay.

Compounds	UV wavelength (nm)	Retention time (min)	Peak area (mAu)		Positive S.D.	Negative S.D.
			Positive (average)	Negative (average)		
Gallic acid hydrate	210	5.623	72.116	51.624	0.054	0.405
(+)-Catechin hydrate	210	9.463	75.974	57.981	0.076	0.328
Caffeic acid	320	11.123	108.475	57.808	0.048	0.433
Rutin hydrate	210	15.860	51.185	13.241	0.393	0.023
Hyperoside	210	16.263	80.346	15.631	0.017	0.213
Quercetin	210	23.583	109.672	22.155	0.101	0.067
Kaempferol	254	28.303	56.806	30.651	0.143	0.071

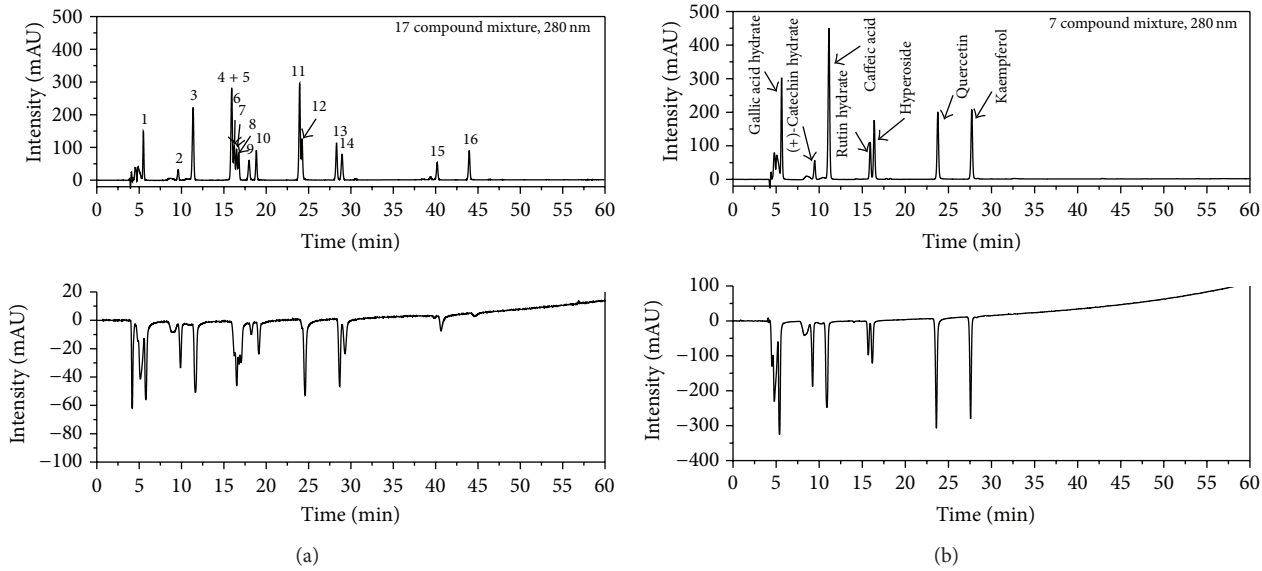

Figure 3: Identification antioxidant activity of online screening HPLC-ABTS assay ((a) simultaneous analysis of 17 compounds, (1) gallic acid hydrate, (2) (+)-catechin hydrate, (3) caffeic acid, (4) ferulic acid, (5) rutin hydrate, (6) sinapic acid, (7) hyperoside, (8) quercetin 3-β-D-glucoside, (9) vanillylacetone, (10) quercitrin hydrate, (11) calycosin, (12) quercetin, (13) kaempferol, (14) eugenol, (15) curcumin, (16) magnolol, and (17) ascorbic acid (not detected); (b) simultaneous analysis of 7 compounds).

and also very useful as functional materials and pharmaceutical materials in commercial processes.

3.3. Anti-Inflammatory Activity Screening

3.3.1. Effect of 17 Compounds on RAW 264.7 Cell Viability. We evaluated the cytotoxicity of the 17 compounds by using CCK to determine the optimal concentration that would be effective in providing anti-inflammatory activity with a minimum toxicity. As shown in Figure 4(a), kaempferol, quercetin, and curcumin show toxicity at a concentration of 10 μg/mL. Also, quercetin 3-beta-D-glucoside has a strong toxicity on macrophage viability at 5 μg/mL or more. Vanillylacetone, hyperoside, gallic acid hydrate, sinapic acid, rutin hydrate, ferulic acid, (+)-catechin hydrate, ascorbic acid, calycosin, caffeic acid, magnolol, quercitrin hydrate, and eugenol did not affect cell viability up to 10 μg/mL, indicating that these 13 compounds are not toxic to cells.

3.3.2. Effect of the 17 Compounds on NO Production in LPS-Stimulated RAW 264.7 Macrophages. We evaluated the effects of 17 compounds on NO secretion in LPS-stimulated RAW 264.7 cells. The cells were pretreated with 17 compounds at concentrations of 1, 5, and 10 μg/mL prior to LPS stimulation, and NO production was also measured. We employed 10 μM dexamethasone as a positive control, since it is widely used as an anti-inflammatory agent. As shown in Figure 4(b), vanillylacetone, gallic acid hydrate, kaempferol, quercetin, magnolol, and curcumin exhibit a strong inhibitory effect on NO secretion upon LPS stimulation. The inhibitory effects of 10 μg/mL kaempferol, quercetin, and curcumin on NO production were a result of their cytotoxicity. However, kaempferol, quercetin, and curcumin exert effective inhibition at concentrations of 1 and 5 μg/mL. In particular, magnolol strongly inhibited NO production in a dose-dependent manner without toxicity. Hyperoside, sinapic acid, rutin hydrate, ferulic acid, (+)-catechin hydrate,

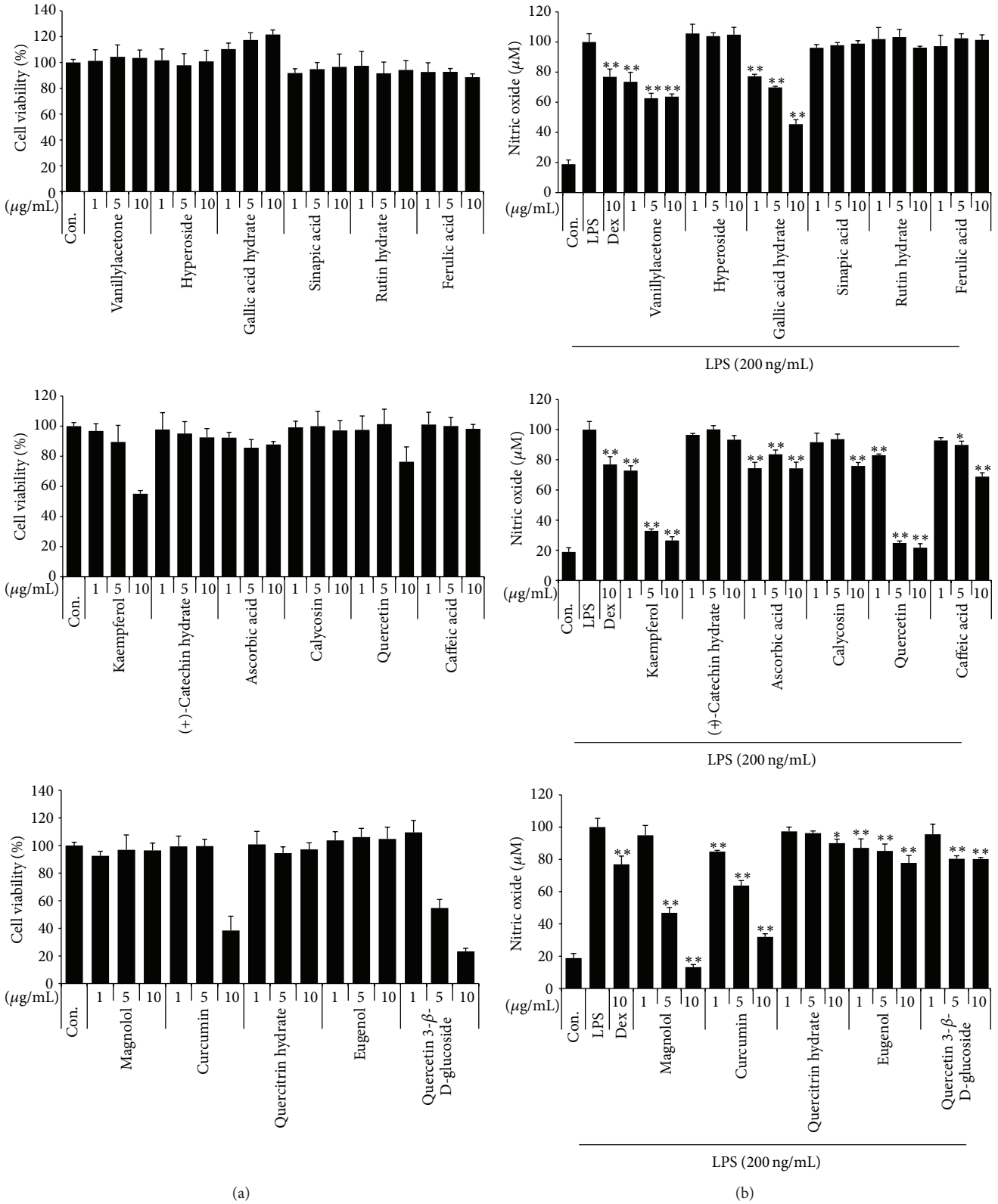

FIGURE 4: Effect of 17 compounds on (a) cell viability and LPS-induced (b) NO production in RAW 264.7 cells. RAW 264.7 cells were pretreated with 17 compounds for 1 hour before incubation with LPS for 24 hours. (a) Cytotoxicity was evaluated by a CCK. (b) The culture supernatant was analyzed for nitrite production. As a control, the cells were incubated with vehicle alone. Data shows mean ± SE values of triplicate determination from independent experiments. $^{*}p < 0.01$ and $^{**}p < 0.001$ were calculated from comparing with LPS-stimulation value.

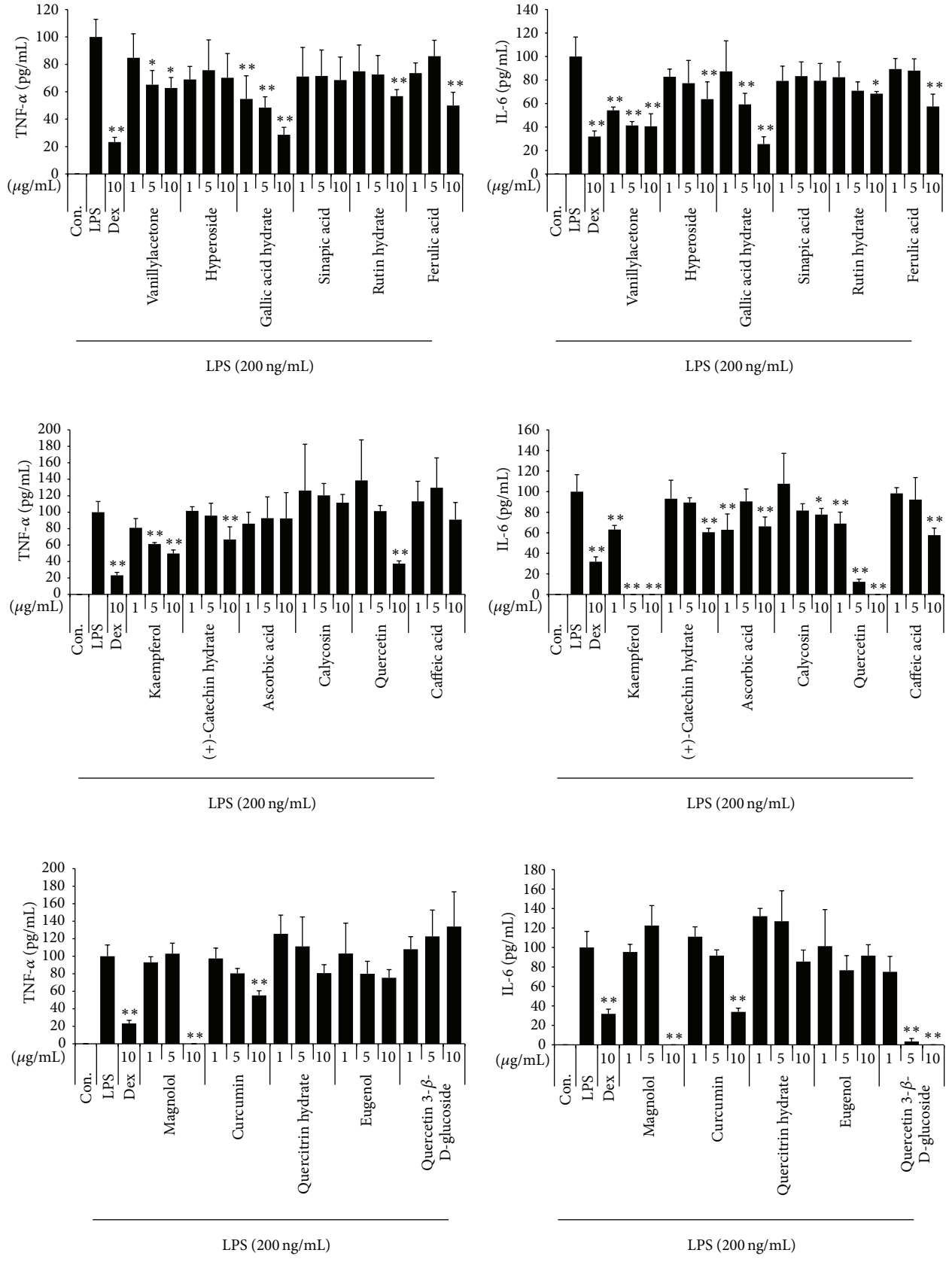

Figure 5: Continued.

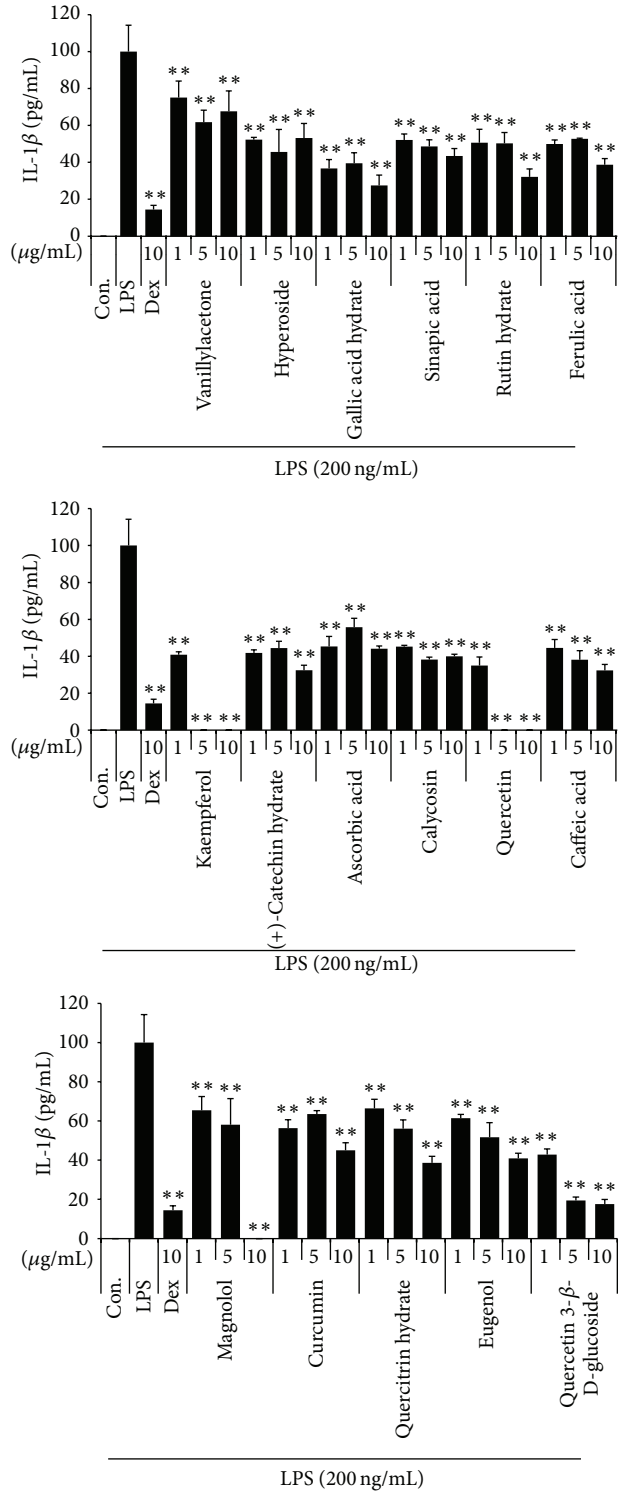

(c)

Figure 5: Effect of 17 compounds on the production of (a) TNF-α, (b) IL-6, and (c) IL-1β cytokine in macrophages. Cells were pretreated with 17 compounds for 1 hour before being incubated with LPS for 24 hours. Production of cytokines was measured by ELISA. Data shows mean ± SE values of triplicate determinations from three independent experiments. $^{*}p < 0.01$ and $^{**}p < 0.001$ were calculated from comparing with LPS-stimulation value.

ascorbic acid, calycosin, caffeic acid, quercitrin hydrate, eugenol, and quercetin 3-beta-D-glucoside do not show remarkable suppressive effects.

3.3.3. Effect of the 17 Compounds on LPS-Induced Inflammatory Cytokines Production. Next, we investigated the inhibitory effect of the 17 compounds on the production of inflammatory cytokines, including TNF-α, IL-6, and IL-1β, which are the other parameters of the inflammation. Gallic acid hydrate exerts an inhibitory effect on the TNF-α cytokine production at all concentrations in a dose-dependent manner. In addition, 5 μg/mL kaempferol and 10 μg/mL magnolol show a strong inhibitory effect (Figure 5(a)). As shown in Figure 5(b), vanillylacetone, gallic acid hydrate, kaempferol, and quercetin significantly inhibited IL-6 cytokine secretion in a statistically significant, dose-dependent manner. In addition, all of the compounds showed an inhibitory effect on IL-1β cytokine production. Gallic acid hydrate, kaempferol, quercetin, and magnolol were especially strong inhibitors of IL-1β cytokine production in a dose-dependent manner (Figure 5(c)).

4. Conclusions

This study provides a comparison of the free radical scavengers in the one hundred kinds of pure chemical compounds through an offline DPPH radical-scavenging activity assay, ABTS radical-scavenging activity assay, and an online screening HPLC-ABTS assay. Here, the IC_{50} rate of a more practical substance is determined. The results indicate that the ABTS assay IC_{50} values of gallic acid hydrate, (+)-catechin hydrate, caffeic acid, rutin hydrate, hyperoside, quercetin, and kaempferol compounds were 1.03 ± 0.25, 3.12 ± 0.51, 1.59 ± 0.06, 4.68 ± 1.24, 3.54 ± 0.39, 1.89 ± 0.33, and 3.70 ± 0.15 μg/mL, respectively. This testing methodology provided a useful tool to focus efforts on chemically active radical-scavenging compounds with high kinetic rates and allowed quick gathering of useful information related to the molecular compounds in terms of their antioxidant activity potential. In addition, there was a very small margin of error between the results of the offline-ABTS assay and those of the online screening HPLC-ABTS assay. We also evaluated the effects of 17 compounds on NO secretion in LPS-stimulated RAW 264.7 cells and the cytotoxicity of the 17 compounds using CCK to determine the optimal concentration that would be effective to provide anti-inflammatory activity with a minimum toxicity. These results will be compiled into a database, and this method can therefore be a powerful preselection tool for compounds intended to be studied for their potential bioactivity and antioxidant activity related to their radical-scavenging capacity.

Conflict of Interests

The authors declare that there is no conflict of interests regarding the publication of this paper.

Acknowledgments

This study was achieved at KM Application Center, KIOM. The authors also acknowledge the support from the Study on Drug Efficacy Enhancement Using Bioconversion for Herbal Medicines (K15280) project.

References

[1] K. Ishimaru, K. Nishikawa, T. Omoto, I. Asai, K. Yoshihira, and K. Shimomura, "Two flavone 2′-glucosides from *Scutellaria baicalensis*," *Phytochemistry*, vol. 40, no. 1, pp. 279–281, 1995.

[2] H. G. Park, S. Y. Yoon, J. Y. Choi et al., "Anticonvulsant effect of wogonin isolated from *Scutellaria baicalensis*," *European Journal of Pharmacology*, vol. 574, no. 2-3, pp. 112–119, 2007.

[3] J. H. Lee, B. W. Lee, B. Kim et al., "Changes in phenolic compounds (Isoflavones and Phenolic acids) and antioxidant properties in high-protein soybean (*Glycine max* L., cv. Saedanbaek) for different roasting conditions," *Journal of the Korean Society for Applied Biological Chemistry*, vol. 56, no. 5, pp. 605–612, 2013.

[4] X.-Y. Song, Y.-D. Li, Y.-P. Shi, L. Jin, and J. Chen, "Quality control of traditional Chinese medicines: a review," *Chinese Journal of Natural Medicines*, vol. 11, no. 6, pp. 596–607, 2013.

[5] K. J. Lee, S. D. Choi, and J. Y. Ma, "Phytochemical analysis of curcumin from turmeric by RP-HPLC," *Asian Journal of Chemistry*, vol. 25, no. 2, pp. 995–998, 2013.

[6] L.-L. Hu, Q.-Y. Ma, S.-Z. Huang et al., "Two new phenolic compounds from the fruiting bodies of *Ganoderma tropicum*," *Bulletin of the Korean Chemical Society*, vol. 34, no. 3, pp. 884–886, 2013.

[7] B. Hazra, M. D. Sarma, and U. Sanyal, "Separation methods of quinonoid constituents of plants used in Oriental traditional medicines," *Journal of Chromatography B*, vol. 812, no. 1-2, pp. 259–275, 2004.

[8] O. Adegoke and P. B. C. Forbes, "Challenges and advances in quantum dot fluorescent probes to detect reactive oxygen and nitrogen species: a review," *Analytica Chimica Acta*, vol. 862, pp. 1–13, 2015.

[9] P. S. Melo, A. P. Massarioli, C. Denny et al., "Winery by-products: extraction optimization, phenolic composition and cytotoxic evaluation to act as a new source of scavenging of reactive oxygen species," *Food Chemistry*, vol. 181, pp. 160–169, 2015.

[10] K. S. Kim, S. H. Lee, Y. S. Lee et al., "Anti-oxidant activities of the extracts from the herbs of *Artemisia apiacea*," *Journal of Ethnopharmacology*, vol. 85, no. 1, pp. 69–72, 2003.

[11] Z. Gao, K. Huang, X. Yang, and H. Xu, "Free radical scavenging and antioxidant activities of flavonoids extracted from the radix of *Scutellaria baicalensis* Georgi," *Biochimica et Biophysica Acta—General Subjects*, vol. 1472, no. 3, pp. 643–650, 1999.

[12] Y. Zhang, Q. Li, H. Xing et al., "Evaluation of antioxidant activity of ten compounds in different tea samples by means of an online HPLC-DPPH assay," *Food Research International*, vol. 53, no. 2, pp. 847–856, 2013.

[13] W. He, X. Liu, H. Xu, Y. Gong, F. Yuan, and Y. Gao, "On-line HPLC-ABTS screening and HPLC-DAD-MS/MS identification of free radical scavengers in Gardenia (*Gardenia jasminoides* Ellis) fruit extracts," *Food Chemistry*, vol. 123, no. 2, pp. 521–528, 2010.

[14] S.-Y. Shi, Y.-P. Zhang, X.-Y. Jiang et al., "Coupling HPLC to on-line, post-column (bio)chemical assays for high-resolution screening of bioactive compounds from complex mixtures," *Trends in Analytical Chemistry*, vol. 28, no. 7, pp. 865–877, 2009.

[15] K. J. Lee, N.-Y. Song, Y. C. Oh, W.-K. Cho, and J. Y. Ma, "Isolation and bioactivity analysis of ethyl acetate extract from *Acer* tegmentosum using in vitro assay and on-line screening HPLC-ABTS$^+$ system," *Journal of Analytical Methods in Chemistry*, vol. 2014, Article ID 150509, 15 pages, 2014.

[16] T. Yu, J. Lee, Y. G. Lee et al., "*In vitro* and *in vivo* anti-inflammatory effects of ethanol extract from *Acer tegmentosum*," *Journal of Ethnopharmacology*, vol. 128, no. 1, pp. 139–147, 2010.

[17] N. Pellegrini, M. Ying, and C. Rice-Evans, "Screening of dietary carotenoids and carotenoid-rich fruits extract for antioxidant activities applying 2,2′-azobis (3-ethylbenzothine-6-surfonic acid) radical cation decolorization assay," *Methods in Enzymology*, vol. 299, pp. 384–389, 1999.

[18] A. J. Stewart, W. Mullen, and A. Crozier, "On-line high-performance liquid chromatography analysis of the antioxidant activity of phenolic compounds in green and black tea," *Molecular Nutrition & Food Research*, vol. 49, no. 1, pp. 52–60, 2005.

[19] H.-J. Choi, O.-H. Kang, P.-S. Park et al., "Mume Fructus water extract inhibits pro-inflammatory mediators in lipopolysaccharide-stimulated macrophages," *Journal of Medicinal Food*, vol. 10, no. 3, pp. 460–466, 2007.

[20] A. A. Karaçelik, M. Küçük, Z. Iskefiyeli et al., "Antioxidant components of *Viburnum opulus* L. determined by on-line HPLC-UV-ABTS radical scavenging and LC-UV-ESI-MS methods," *Food Chemistry*, vol. 175, pp. 106–114, 2015.